Alfred-Wegener-Institut für Polar und Meeresforschung
Universität Potsdam, Institut für Geowissenschaften

Aquatic macrophyte-derived biomarkers as palaeolimnological proxies on the Tibetan Plateau

DISSERTATION
zur Erlangung des akademischen Grades
"doctor rerum naturalium" (Dr. rer. nat.)
in der Wissenschaftsdisziplin
Geowissenschaften / Organische Geochemie

eingereicht an der
Mathematisch-Naturwissenschaftlichen Fakultät
der Universität Potsdam

von
Bernhard Aichner

17.09.2009

Published online at the
Institutional Repository of the University of Potsdam:
URL http://opus.kobv.de/ubp/volltexte/2010/4209/
URN urn:nbn:de:kobv:517-opus-42095
http://nbn-resolving.org/urn:nbn:de:kobv:517-opus-42095

- **Betreuer der Arbeit und Erstgutachter:** Prof. Dr. Ulrike Herzschuh
  Alfred-Wegener-Intitut Potsdam / Universität Potsdam
- **Zweiter Betreuer und Gutachter:** PD Dr. Heinz Wilkes
  Helmholtz-Zentrum Potsdam – Deutsches GeoForschungsZentrum GFZ, Sektion 4.3. "Organische Geochemie" / TU Berlin
- **Dritter Gutachter:** Prof. Dr. Lorenz Schwark
  Institut für Geowissenschaften – Christian-Albrechts-Universität zu Kiel

Contents

List of Tables

List of Figures

List of Abbreviations

a.s.l.	above sea level
AMS	accelarated mass spectrometry
ASE	accelarated solvent extraction
ATR	aquatic terrigenous ratio
BIT	branched vs. isoprenoid tetraether index
cal ka BP	calibrated kilo years before present
CBT	cyclisation ratio of branched tetraethers
CSIA	compound-specific isotope analysis
EA	elementar analyser
δD_{MW}	δD of meteoric water
EC	electrical conductivity
GC	gas chromatography
GC-C-IRMS	gas chromatography/combustion/isotope ratio mass spectometry
GC-P-IRMS	gas chromatography/pyrolysis/isotope ratio mass spectometry
GC-FID	gas chromatography/flame ionisation detection
GC-MS	gas chromatography/mass spectometry
HBI	highly branched isoprenoid compound
LCA	long-chain alkenones
LC-APCI-MS	liquid chromatography / atmospheric pressure chemical ionisation/mass spectrometry
MBT	methylation index of branched tetraethers
MPLC	medium pressure liquid chromatography
NSO	compounds containing nitrogen, sulfur or oxygen
P_{ann}	mean annual precipitation
P_{aq}	proxy for aquatic macrophytes
PCC	Pearson correlation coefficient
PMI	2,6,10,15,19-pentamethylicosane
SD	standard deviation
TEX_{86}	index for tetraethers with 86 carbon atoms
TIC	total inorganic carbon
TOC	total organic carbon
TOC/TN	ratio between total organic carbon and total nitrogen

Abstract

The Tibetan Plateau is the largest elevated landmass in the world and profoundly influences atmospheric circulation patterns such as the Asian monsoon system. To be able to better predict the impact of future changes in monsoon dynamics, it is important to have detailed understanding of past climate variability. Therefore this area has been increasingly in focus of palaeoenvironmental studies. The large number of lakes on the Tibetan Plateau provides an enormous potential of climate archives and a considerable number of palaeolimnological investigations were published to date. Most of these studies applied biological, sedimentological or geochemical proxies but organic biomarkers have rarely been used. This thesis evaluates the applicability of organic biomarkers for palaeolimnological purposes on the Tibetan Plateau with a focus on aquatic macrophyte-derived biomarkers. Submerged aquatic macrophytes have to be considered to significantly influence the sediment organic matter due to their high abundance in many Tibetan lakes. They can show highly ^{13}C-enriched biomass because of their carbon metabolism and it is therefore crucial for the interpretation of δ^{13}C values in sediment cores to understand to which extent aquatic macrophytes contribute to the isotopic signal of the sediments in Tibetan lakes and in which way variations can be explained in a palaeolimnological context. Additionally, the high abundance of macrophytes makes them interesting as potential recorders of lake water δD. Hydrogen isotope analysis of biomarkers is a rapidly evolving field to reconstruct past hydrological conditions and therefore of special relevance on the Tibetan Plateau due to the direct linkage between variations of monsoon intensity and changes in regional precipitation / evaporation balances.

A set of surface sediment and aquatic macrophyte samples from the central and eastern Tibetan Plateau was analysed for composition as well as carbon and hydrogen isotopes of *n*-alkanes. It was shown how variable δ^{13}C values of bulk organic matter and leaf lipids can be in submerged macrophytes even of a single species and how strongly these parameters are affected by them in corresponding sediments. The estimated contribution of the macrophytes by means of a binary isotopic model was calculated to be up to 60% (mean: 40%) to total organic carbon (TOC) and up to 100% (mean: 66%) to mid-chain *n*-alkanes ($n\mathrm{C}_{23}$ and $n\mathrm{C}_{25}$). Examination of aliphatic lipids of submerged macrophytes revealed that those could also be a potential source of long-chain *n*-alkanes ($< n\mathrm{C}_{27}$) in lake sediments when a) experiencing episodically emergent conditions and b) possibly by transformation of unsaturated long-chain leaf lipid compounds to saturated compounds during early diagenesis. Nevertheless, since emergent and terrestrial plants contain 5-10 fold higher concentrations of *n*-alkanes, the influence of submerged macrophytes on the

long-chain lipid pool is minor. This is visible at the narrow range of δ^{13}C values of long-chain *n*-alkanes in sediment samples, which showed values typical for terrestrial C_3 plants.

Hydrogen isotopes of *n*-alkanes turned out to record δD of meteoric water, with terrestrial long-chain *n*-alkanes showing a slightly better correlation. The apparent enrichment factor between water and *n*-alkanes was in range of previously reported ones at the more humid sites, but smaller at more arid sites. This indicates an influence of evaporation and evapotranspiration on δD of source water for aquatic and terrestrial plants. The offset between δD of mid- and long-chain *n*-alkanes was close to zero in most of the samples, suggesting that lake water as well as soil- and leaf water are affected to a similar extent by evapotranspiration, which is different from previously reported assumptions.

To apply biomarkers in a palaeolimnological context, the aliphatic biomarker fraction of a sediment core from Lake Koucha (34.0° N; 97.2° E; eastern Tibetan Plateau) was analysed for concentrations, δ^{13}C and δD values of compounds. Before ca. 8 cal ka BP, the lake was dominated by aquatic macrophyte-derived mid-chain *n*-alkanes, while after 6 cal ka BP high concentrations of a C_{20} highly branched isoprenoid compound indicate a predominance of phytoplankton. Those two principally different states of the lake were linked by a transition period with high abundances of microbial and algal biomarkers (phytane, pentamethylicosane, diploptene and moretene), which were partly attributed to methanotrophic source organisms because of their depleted δ^{13}C signal ($\approx$ -60‰). δ^{13}C values were relatively constant for long-chain *n*-alkanes, while mid-chain *n*-alkanes showed variations between -23.5 to -12.6‰. Highest values were observed during the macrophyte maximum in the late glacial and during the phytoplankton maximum in the middle Holocene. Therefore, the enriched values were interpreted to be caused by carbon limitation which in turn was induced by high macrophyte and primary productivity, respectively. Hydrogen isotope signatures of mid-chain *n*-alkanes have been shown to be able to track a previously deduced episode of reduced moisture availability between ca. 10 and 7 cal ka BP, indicated by a shift towards higher δD values during that period. A depletion of deuterium at ca 1.5 cal ka BP, observed at all aquatic and terrestrial markers, might have been caused by the combined effects of lower temperatures and decreased evaporation upon δD values of meteoric water and lake water, respectively. Indications for cooler episodes at 6.0, 3.1 and 1.8 cal ka BP were gained from drops of biomarker concentrations, especially microbial-derived hopanoids, and from coincidental shifts towards lower δ^{13}C values. Those episodes correspond well with cool events reported from other locations on the Tibetan Plateau as well as in the Northern Hemisphere, and were not inferred from geochemical and biological proxies used in previous studies about Lake Koucha.

To conclude, the study of recent sediments and plants improved the understanding of factors affecting the composition and isotopic signatures of aliphatic biomarkers in sediments. Concentrations and isotopic signatures of the biomarkers in Lake Koucha could be interpreted in a palaeolimnological context and contribute to the knowledge about the

history of the lake. Aquatic macrophyte derived mid-chain *n*-alkanes were especially useful, due to their high abundance in many Tibetan Lakes and their ability to record major changes of lake productivity and palaeohydrological conditions. Therefore, they have the potential to contribute to a fuller understanding of past climate variability in this key region for atmospheric circulation systems.

Kurzfassung

Das tibetische Hochplateau ist die größte gehobene Landmasse der Erde und beeinflusst maßgeblich atmosphärische Zirkulationsmuster wie den Asiatischen Monsun. Um die Auswirkungen zukünftiger Schwankungen der Monsundynamik auf das regionale Klima besser einschätzen zu können, ist es wichtig, ein fundiertes Verständnis vergangener Klimaänderungen zu entwickeln. Daher ist das Tibetplateau in den letzten Jahren mehr und mehr in den Fokus paläoklimatischer Studien gerückt. Die große Anzahl an Seen in der Region bietet ein unerschöpfliches Klimaarchiv und viele Studien haben sich bereits mit Seesedimenten zur Klimarekonstruktion befasst. Dabei wurde in erster Linie auf biologische, sedimentologische und geochemische Parameter zurückgegriffen, wohingegen organische Biomarker recht selten benutzt wurden. Die vorliegende Arbeit untersucht die Anwendbarkeit dieser Proxies auf dem Tibetplateau in einem paläoklimatischen Kontext, wobei ein Schwerpunkt auf kutikuläre Blattwachse von Wasserpflanzen gelegt wurde. Wegen ihrer Verbreitung in tibetischen Seen ist zu erwarten, dass Wasserpflanzen einen erheblichen Beitrag zur organischen Substanz im Sediment liefern. Durch ihren speziellen Kohlenstoff-Metabolismus können aquatische Makrophyten einen im Vergleich zu Ufer- und C_3-Landpflanzen stark erhöhten δ^{13}C-Wert aufweisen. Es ist daher wichtig zu verstehen, in welchen Ausmaß Wasserpflanzen das Kohlenstoffisotopensignal von Sedimenten beeinflussen und wie Variabilitäten des δ^{13}C-Wertes in Sedimentbohrkernen paläoökologisch interpretiert werden können. In den Blattwachsen der Wasserpflanzen ist zudem die primäre Wasserstoffisotopensignatur des Seewassers gespeichert. Substanzspezifische δD-Analysen an Biomarkern wurden die letzten Jahre immer häufiger zur Rekonstruktion von Änderungen im hydrologischen Kreislauf in der Vergangenheit eingesetzt. Auf dem Tibetplateau ist dies von besonderer Relevanz, da Schwankungen der Monsunintensität direkt das Gleichgewicht zwischen Niederschlags- und Verdunstungsmenge beeinflussen.

Um den Einfluss von Wasserpflanzen auf das Sediment über einen weiten klimatischen Gradienten zu untersuchen, wurden in Oberflächensedimenten und Wasserpflanzen vom zentralen und östlichen Tibetplateau Konzentrationen sowie die Kohlen- und Wasserstoffisotopensignaturen von *n*-Alkanen untersucht. Es zeigte sich, dass die δ^{13}C-Werte (Gesamtbiomasse und *n*-Alkane) eine starke Variabilität aufweisen. Dies wirkt sich wiederum direkt auf die Sedimente aus, die ebenfalls starke Schwankungen in δ^{13}C-Werten des organischen Materials und der mittelkettigen *n*-Alkane (nC_{23} und nC_{25}) zeigen. Mit Hilfe eines binären Isotopenmodells wurde der Anteil an Makrophyten am gesamten organischen Kohlenstoff im Sediment auf maximal 60% (Mittelwert 40%) und an den mittelkettigen *n*-Alkanen auf bis zu 100% (Mittelwert 66%) geschätzt. Weiterhin wurde deutlich, dass Wasserpflan-

zen auch langkettige *n*-Alkane (> $n C_{27}$) produzieren können und außerdem ungesättigte langkettige Verbindungen aufweisen, die durch frühe Transformationsprozesse im Sediment möglicherweise zu gesättigten Verbindungen umgewandelt werden. Da Wasserpflanzen aber deutlich niedrigere Mengen an Alkanen produzieren als Ufer- und terrestrische Pflanzen, ist der Einfluss auf die langkettigen Alkane zumindest in den tibetischen Seen gering, wie die geringe Variabilität der δ^{13}C-Werte von langkettigen *n*-Alkanen gezeigt hat.

Die δD Werte der *n*-Alkane korrelierten mit den δD-Werten des Niederschlags über den gesamten klimatischen Gradienten, wobei terrestrische Alkane eine höhere Korrelation zeigten. Die scheinbare isotopische Abreicherung ("apparent enrichment factor") zwischen δD-Werten des Niederschlags und den *n*-Alkanen lag in den humiden Regionen des Untersuchungsgebietes in der Größenordnung von zuvor publizierten Daten. In den ariden Gebieten war der Faktor kleiner, was auf den Einfluss von Verdunstung und Transpiration auf die Wasserstoffisotopensignatur des See-, Boden- und Blattwassers, welches zur Biosynthese der Alkane benutzt wird, zurückgeführt werden kann. δD-Werte von mittel- und langkettigen *n*-Alkanen waren in den meisten Proben weitgehend identisch. Dies zeigt, dass Verdunstung von Seewasser sowie Verdunstung und Transpiration von Boden- und Blattwasser die Wasserstoffisotopensignatur in etwa gleichen Maßen beeinflussen.

Um die direkte Anwendbarkeit von Biomarkern in einem paläolimnologischen Kontext zu testen, wurden Proben aus einem Sedimentbohrkern des Koucha-Sees (34.0° N; 97.2° E; östliches Tibetplateau) auf Biomarkerzusammensetzung sowie deren Kohlen- und Wasserstoffisotopensignatur untersucht. Zwischen 15 und 8 kal ka v.H. (tausend Kalenderjahre vor Heute) war der See von Makrophyten dominiert, worauf hohe Anteile von mittelkettigen Alkanen hinweisen. Nach 6 kal ka v.H. deuten dagegen hohe Konzentrationen eines hochverzweigten Isoprenoids auf eine verstärkte Präsenz von Phytoplankton hin. Diese beiden prinzipiell verschiedenen Zustände des Sees wurden durch eine Übergangsepoche (ca. 8 - 6 kal ka v.H.) überbrückt. In dieser zeigen hohe Konzentrationen von Phytan, Pentamethylikosan und diversen Hopanoiden eine verstärkte mikrobielle Aktivität an, wobei Diplopten und Moreten auf Grund ihrer Kohlenstoffisotopensignatur (≈ -60‰) als methanotrophen Ursprungs interpretiert wurden. Die δ^{13}C-Werte der langkettigen *n*-Alkane zeigten über den gesamten Kern geringe Variabilität, wohingegen mittelkettige *n*-Alkane einen Bereich von -23,5 bis -12,6‰ abdecken. Die höchsten Werte wurden während des maximalen Makrophyten- und Phytoplanktonwachstums im Spätglazial bzw. im mittleren Holozän gemessen. Sie wurden daher als Anzeiger von Kohlenstofflimitierung im See gedeutet, die wiederum durch erhöhte Wasserpflanzen- und Phytoplanktonproduktivität induziert wurde.

Die δD-Werte der *n*-Alkane zeigten zwischen 15 und 10 kal ka v.H. stetig abnehmende Werte, was mit einer Steigerung der Niederschlagsmengen durch einen stärker werdenden Sommermonsun erklärt werden kann. Um ca. 9 kal ka v.H. steigen die Werte stark an, was im Einklang mit anderen Studien als Einfluss von zunehmender Evaporation auf den

δD-Wert des Seewassers gedeutet wurde. Ein Rückgang zu niedrigeren Werten um ca. 1.5 kal ka v.H. kann durch den kombinierten Effekt von fallenden Temperaturen und daraus resultierenden niedrigeren Evaporationsraten erklärt werden. Anzeichen für relative kalte Episoden bieten relativ niedrige Biomarkerkonzentrationen um ca. 6.0, 3.1 und 1.8 kal ka v.H. sowie gleichzeitige niedrige δ^{13}C-Werte. Diese kurzen Kälteperioden wurden bereits in anderen Klimaarchiven in Tibet sowie auf der nördlichen Hemisphäre belegt, konnten jedoch im Koucha-See in vorangegangenen Studien nicht durch geochemische und biologische Proxies nachgewiesen werden.

Durch Studien an rezenten Sedimenten und Pflanzenmaterial konnte das Verständnis über beeinflussende Faktoren auf die Verteilung sowie die Kohlen- und Wasserstoffisotopensignatur von Biomarkern in Sedimenten vertieft werden. Im Sedimentbohrkern konnten diese Parameter im Hinblick auf Änderungen der Produktivität und der hydrologischen Bedingungen interpretiert werden. Durch Kombination von Biomarkerkonzentrationen, δ^{13}C- und δD-Werten konnte so ein detailliertes Bild über die Entwicklung des Koucha-Sees seit dem letzten Glazial gewonnen werden. Organische Biomarker haben sich somit als geeignet erwiesen, einen Beitrag zur Klimarekonstruktion auf dem Tibetplateau zu leisten.

1 Introduction

Preface

It is widely accepted that climate change is a problem of global relevance which will have impacts on environment, economies and social relationships (IPCC report 2007, see Christensen et al., 2007). Even if a large number of scientists agree that the temporary increase of global mean temperatures is anthropogenic induced, numerous big and small scale as well as long-term and abrupt climate changes in the history of the earth have been a natural phenomenon. It is important to understand the causes and impacts of that variability to be able to make predictions about the impacts of future climate changes. To reconstruct past climates, so-called proxies are necessary. These are measurable biological, chemical or physical parameters in archives such as ice cores, speleothems or marine and lacustrine sediments, from which conclusions about past climates and environments can be drawn. The development and calibration of proxies is an ongoing process. New proxies are introduced frequently and old proxies need steady calibration, for instance if an adjustment to specific environmental conditions of a study area is necessary. This thesis focuses on the application of organic geochemical proxies, so-called biomarkers, in a key region for global atmospheric circulation systems, the Tibetan Plateau. Due to its topographic features, the Tibetan Plateau is considered as a main driving force for the Asian monsoon (Domrös and Peng, 1988) and the regional climate has been shown to react sensitively to changes in the monsoon dynamics. For a better understanding of this regional climate responses, it is necessary to obtain a detailed knowledge about past climate variability, which highlights the need for proxy data from this region.

1.1 Climatic relevance of the Tibetan Plateau

With an average altitude above 4,000 m and maximum extents from 77 to 105° E and 25 to 40° N, the Tibetan Plateau (or Tibet-Qinghai-Plateau) is the largest elevated landmass in the world. The high altitude supports the convective uplift of air-masses during the annual insolation maximum in the summer months from May until September, leading to the formation of a strong low pressure cell. Due to the pressure and temperature gradient between the Tibetan Plateau and the Indian and Pacific Ocean, moisture carrying air masses are drawn from the ocean towards the inland, resulting in relatively high precipitation amounts during summer months. In winter, the cooling of the vast Asian landmass promotes the formation of an extensive anticyclone, the so-called Mongolian and Siberian

High. Consequently, between October and April, the Tibetan Plateau experiences cold and dry conditions due to the polar air masses being delivered from the North (Domrös and Peng, 1988). This seasonal change of climate, including a change of wind directions of more than 120°, is according to the definition of Chromov (1957) a typical Monsoon climate. Hereby the system can be divided into two subsystems, the Indian monsoon and the east Asian monsoon, which have been shown to interact but to be principally independent from each other (An, 2000). The Tibetan Plateau is mainly influenced by the Indian monsoon (Ding, 1994) which delivers moisture from the Bay of Bengal to the eastern and central Tibetan Plateau and from the Arabian Sea to the western Tibetan Plateau (Domrös and Peng, 1988) (Fig. 1.1). The east Asian monsoon mainly influences the eastern margin of the Tibetan Plateau (Wang et al., 2005).

Future climate changes are suspect to go in hand with changes in monsoon intensity. This will profoundly influence the climate in the monsoonal southeast Asia and therefore the living space for more than 50% of the world's population. Detailed knowledge about past climate variations in this region can contribute to a better understanding of this complex atmospheric circulation system, which can in turn help to better predict possible impacts of future climate changes. Therefore, past monsoon dynamics have been extensively studied. A range of records (reviewed in Morill et al., 2003 and Herzschuh, 2006), including ice cores from Dunde, Guliya and Dasuopu ice caps (Thompson, 1997 and 2000), palaeosol sequences from the Chinese Loess Plateau (e.g. An et al., 1991; Chen et al., 1997; Ding and Yang 2000), speleothems from Hulu and Dongge caves (Yuan et al., 2004; Wang et al., 2008), marine sediment cores from the Arabian and Chinese Sea (Wang et al., 1999; Gupta et al., 2003; Sun et al., 2003; reviewed in Wang et al., 2005) as well as peat deposits (e.g. from Hongyuan and Hani peat bogs: Zheng et al., 2007; Seki et al., 2009) and a range of lake sediment records (e.g. from Lake Qinghai: Lister et al., 1991; Shen et al., 2005), revealed a close linkage between monsoon intensities and global climate dynamics. In the long term, the uplift of the Tibetan Plateau has been identified as the main and initial driving mechanism for the monsoon (Ding et al., 1992; Harris, 2006) while on shorter time scales, orbital-driven insolation turned out to be a major influence upon monsoon intensities, as seen for instance in the correlation between past insolation intensities and speleothem δ^{18}O-records from Dongge and Hulu caves (Yuan et al., 2004; Wang et al., 2008) which cover the last 160,000 and 224,000 years respectively. Concentrating on the last 20,000 years, numerous records inferred a maximum of monsoonal intensity during the maximum of insolation at the late glacial and the early Holocene, assuming a warmer and wetter climate and a limit of monsoon influence extending further than today.

Speleothem, loess profile and ice core records are spatially limited. In contrast, the large number of lakes in the continental realms of Asia, especially on the Tibetan Plateau, provides an enormous source for potential climate archives. There are a number of palaeoclimatic studies using lake sediments from the Tibetan Plateau and adjacent regions.

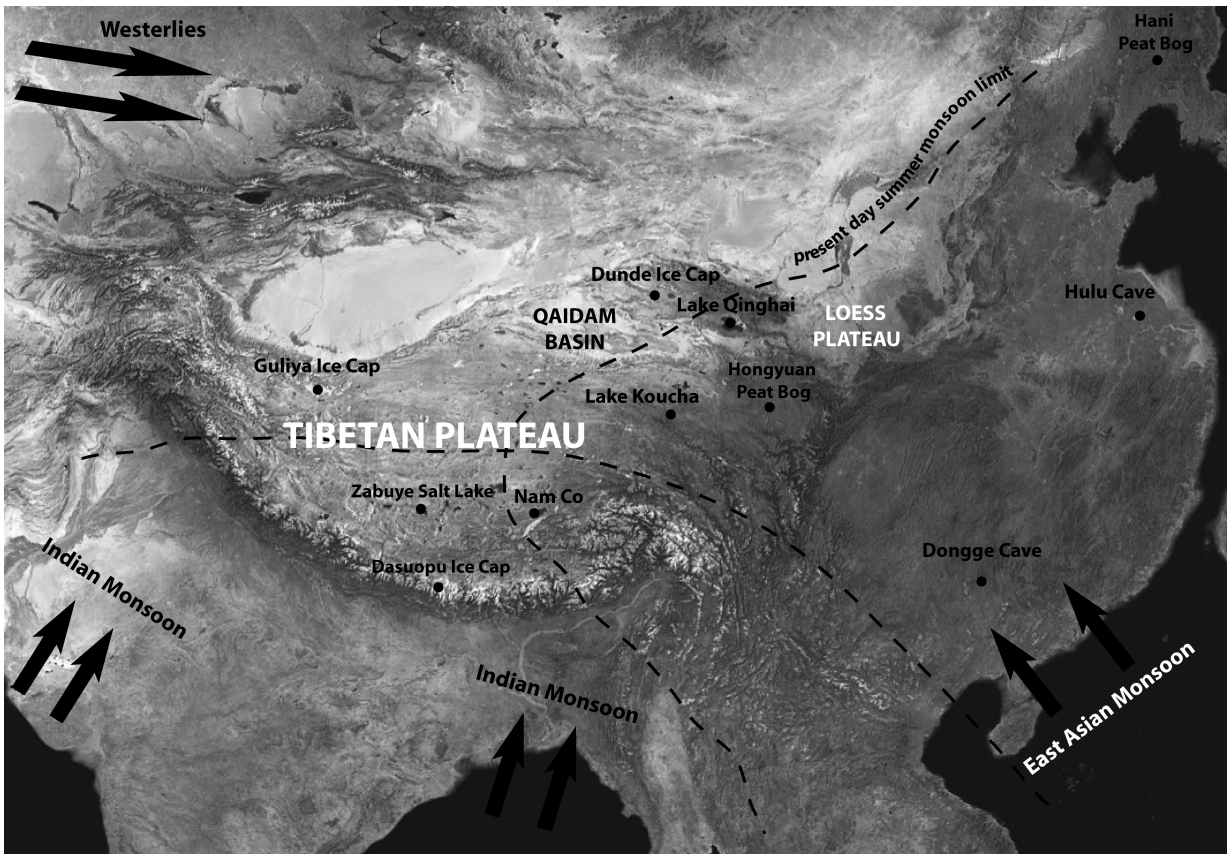

Figure 1.1: Overview map of monsoonal Asia, showing the dominant circulation systems, the present day limit of summer monsoon (after Winkler and Wang, 1993; redrawn in Morill et al., 2003 and Holmes et al., 2009) and main palaeoclimatic records referred to in the text. Map source: NASA, [http://visibleearth.nasa.gov/view_rec.php?vev1id=11656 "Blue Marble"]

These spatially highly distributed climate archives gave evidence that the late glacial and Holocene climate development was more complex and locally variable than previously assumed (He et al., 2004, Herzschuh et al., 2006). Especially, arid regions situated north and northwest to the Tibetan Plateau have obviously experienced relatively dry conditions during the early Holocene, which contrasts the assumption of a wet and humid climate during this period of maximal monsoon intensity (Herzschuh et al., 2006; Chen et al., 2008). Recently, a record from Lake Koucha (eastern Tibetan Plateau) has shown a decrease of available effective moisture during the early Holocene (Mischke et al., 2008; Herzschuh et al., 2009) and the same was inferred from the Hani peat bog record in northeastern China (Seki et al., 2009). These findings highlight the necessity for a high spatial resolution of lake sediment records in this key region for atmospheric circulations, in order to gain a full understanding of the complex system of monsoon variability.

1.2 Scientific background

1.2.1 Organic biomarkers in palaeoclimatology

Organic biomarkers are chemical fossils (Eglingon and Calvin, 1967), i.e. organic molecules derived from living organisms which can preserve in sediments over geological time scales. Most biomarkers are derived from cell membranes of prokaryotic or eukaryotic organisms and from cuticular wax layers of higher plants. While membrane lipids can mainly be considered as structural components, leaf waxes have protective functions. The synthesis of different lipids is controlled via three major pathways (Fig. 1.2), for all of which pyruvate is the main precursor (Taiz and Zeiger, 2002): the MVA (mevalonic acid) pathway leads to the formation of steroid and hopanoid compounds while isoprenoids such as phytol are formed via the MEP (methylerythritol phosphate) pathway (Chikaraishi et al. 2004b). The acetogenic pathway is relevant for fatty acid synthesis. Here, acetyl coenzyme-A (two carbon atoms) is the key component in an elongation cycle which adds successively two carbon atoms to the chain (Taiz and Zeiger, 2002). This is the reason for fatty acids (and *n*-alcohols) showing usually an even number of carbon atoms. In contrast, *n*-alkanes leave the elongation cycle by decarboxylation of the chain, resulting in odd-numbered compounds. Unbound fatty acids, *n*-alkanes and *n*-alcohols are typical components of leaf waxes, while steroid and hopanoid compounds as well as bound fatty acids are parts of cell membranes.

Information on the composition of organic biomarkers in a sediment core can significantly contribute to the understanding of the history of the respective lake and its catchment. Valuable information about the contributors to the organic matter of sediments can be obtained from these data, of which in turn potential environmental conditions can be deduced. Hereby, the most effective biomarker would have a well-defined source (Brocks and Summons, 2005), but this is only the case for a limited number of compounds. Examples for relatively specific biomarkers are botryococcenes, which are major components of the lipids of the alga *Botryococcus braunii* (Metzger and Largeau, 2005) or highly branched isoprenoids with 25 carbon atoms (C_{25} HBIs) which have up today only been identified in diatoms of the genera Rhizosolenia, Haslea, Navicula and Gyrosigma (Belt et al., 2001a and b; Sinninghe Damsté et al., 2004). Most biomarkers are semi-specific, i.e. if found in sediment cores, they indicate the presence of a specific group of organisms. For instance, the fact that the cell membranes of prokaryotic organisms contain hopanoids as rigidifiers makes this compound class indicative for the abundance of bacteria in sediments (Rohmer et al., 1984; Wakeham, 1990). Membranes of eukaryotes, in contrast, usually contain steroid compounds. Numerous sterols have been identified up to the present of which some are considered to be semi-specific for higher plants and algae (e.g. reviewed in Volkman, 1986 and Volkman, 2003). Sources of wax lipids can be distinguished by the chain-length of the lipids. Bacteria and algae have a tendency to synthesize lipid compo-

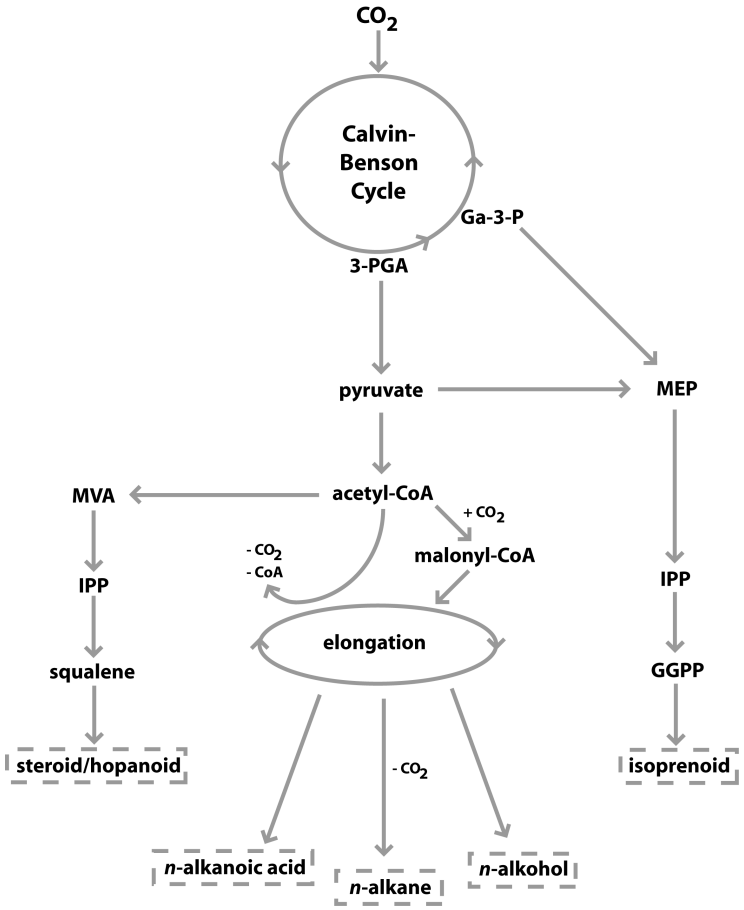

Figure 1.2: Schematic overview of lipid synthesis pathways. Abbreviations: 3-PGA: 3-phosphoglyceric acid; Ga-3-P: d-glyceraldehyde-3-phosphate; acetyl-CoA: acetyl coenzyme-A; IPP: isopentenyl pyrophosphate; MVA: mevalonic acid; MEP: 2-C-methyl-d-erythritol-4-phosphate; GGPP: geranylgeranyl pyrophosphate. Redrawn and modified after Chikaraishi et al., 2004b and Chikaraishi and Naraoka, 2007.

nents such as alkanes and fatty acids in the short-chain range, which means with 15 to 19 carbon atoms (Gelpi et al., 1970). Submerged aquatic macrophytes as well as *Sphagnum* sp. appeared to be dominated by mid-chain *n*-alkanes, especially $n\mathrm{C}_{23}$ and $n\mathrm{C}_{25}$, (Ficken et al., 2000; Baas et al., 2000), while terrestrial plants and emergent macrophytes biosynthesize preferentially long-chain homologues (Eglington and Calvin, 1967).

Beside these qualitative approaches, it has also been attempted to develop quantitative biomarker-based proxies. The dependency between the degree of unsaturation of long-chain alkenones (LCAs) derived from haptophytic algae with water temperature and salinity lead for instance to the development of the alkenone unsaturation indices (e.g. the Uk'37), which are frequently applied in the marine realm to reconstruct sea-surface temperatures (SSTs) and salinities (e.g. Volkman et al., 1980; Marlowe et al., 1984; Prahl and Wakeham, 1987; Rosell-Melé et al., 1998). LCAs have also been detected in saline as well as in some freshwater lakes (Thiel et al., 1997; Zink et al., 2001; D'Andrea and Huang, 2005) including

a range of Chinese lakes (Chu et al., 2005). However, due to uncertainties about the precise sources of LCAs in lakes as well as different physical, chemical and geological backgrounds of lacustrine environments, the extension of this proxy to these ecosystems is still under debate (Chu et al., 2005). Recently, Schouten et al. (2002) proposed another potential proxy for SST reconstruction on the basis of the number of pentacyclic moieties in archaeal ether lipids. A ratio of those ether lipids, the so-called TEX_{86} index, in globally distributed marine surface sediment samples seemed to correlate well with SSTs. The fact that samples of selected lakes fitted well in the calibration line made this proxy potentially promising for lacustrine environments. However, the contribution of soil-derived ether lipids (which could be estimated via the so-called BIT-index; Hopmans et al., 2004) could bias the TEX_{86} index which has up to now been successfully applied only in a few large lakes, as for example in Lake Tanganyika, southeast Africa (Tierney et al., 2008).

1.2.2 Carbon and hydrogen isotopes

Organic substance primarily consists of carbon and hydrogen and thus carbon and hydrogen isotopes are the major isotopes used in organic geochemistry. Isotopes are atoms of the same element (i.e. having the same numbers of protons) with differing numbers of neutrons. The primary occurring isotope of hydrogen (^{1}H) has for instance one proton and zero neutrons, while ^{2}H or D (also called deuterium) has one proton and one neutron. ^{2}H and ^{1}H are stable isotopes of hydrogen, in contrast to ^{3}H (tritium) which is unstable and susceptible to radioactive decay. The most important stable isotopes of the carbon atom are ^{12}C and ^{13}C, while ^{14}C is radioactive, and frequently applied for ^{14}C-AMS dating. Stable isotope data can be expressed in ratios (e.g. R = ^{2}H/^{1}H) but the most prevalent way of presenting the data is in delta notation, which sets the isotope ratio of a sample in relation to a standard:

$$\delta[‰] = \frac{(\mathrm{R}_{sample} - \mathrm{R}_{standard})}{\mathrm{R}_{standard}} \; x \; 1000$$

To calculate delta values for carbon isotopes (δ^{13}C), the isotopic composition of the carbon of calcite from a Belemnite from the PeeDee Formation (VPDB = +1.95‰) is referred to as a standard, while for hydrogen isotopes (δD), the standard mean of oceanic water (VSMOW = 0‰) is the common reference.

During physical, biological and chemical processes, the isotopic signal of compounds is altered due to thermodynamic (or equilibrium) and kinetic isotope effects. An example for equilibrium isotope fractionation is the isotope exchange of a compound between the liquid/dissolved and the gaseous phase. Here, the more heavy isotope tends to remain in the liquid phase (Gonfiantini, 1986) while the extent of fractionation is temperature dependent (O'Neil, 1986). In the case of the equilibrium reaction between atmospheric carbon dioxide and dissolved bicarbonate ($H^{13}CO_3^- + {}^{12}CO_2 = H^{12}CO_3^- + {}^{13}CO_2$), this

leads to an enrichment of ^{13}C of the bicarbonate compared to atmospheric CO_2 (Peters et al., 2005) which results in average $\delta^{13}C$ values of +1‰ of the first in contrast to -7‰ of the latter (Fig. 1.3). Important kinetic isotopic fractionations occur during photosynthesis. Because the lighter molecule ($^{12}CO_2$) diffuses more rapidly through the stomata and is more rapidly fixed enzymatically than the heavier molecule ($^{13}CO_2$), the biomass of plants is significantly depleted in ^{13}C compared to CO_2 (Fig. 1.3) (Farquhar et al. 1989). Another fractionation step is included during lipid synthesis, resulting in depleted values of the lipids compared to bulk biomass (Park and Epstein, 1961; Collister et al., 1994).

The degree of isotopic fractionation in plants depends on the plant type. Bulk biomass of C_3 plants, which fix CO_2 via the calvin cycle, show larger degrees of fractionation than C_4 plants, which use the so called Hatch-Slack-Cycle. As a result C_4 plants show average bulk $\delta^{13}C$ values of -13‰, while C_3 plants have average values of -27‰ (O'Leary, 1988). Aquatic plants and algae usually fix dissolved CO_2. If CO_2 supply decreases, the kinetic isotopic effect also decreases and higher amounts of $^{13}CO_2$ are assimilated leading to higher $\delta^{13}C$ values of the assimilating organism. Further, some aquatic macrophytes can switch to bicarbonate metabolism (Allen and Spence, 1981; Prins and Elzenga, 1989), for example in highly productive or highly alkaline lakes where CO_2 is limited. Due to the above mentioned ^{13}C enrichment of bicarbonate compared to CO_2, this results in higher $\delta^{13}C$ values of the aquatic macrophytes (Fig. 1.3).

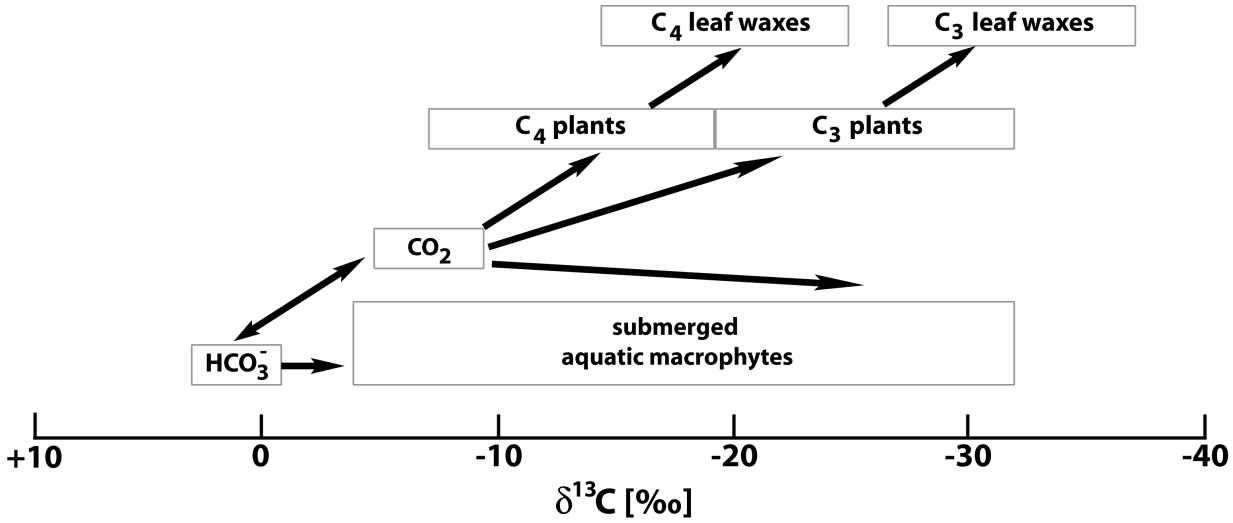

Figure 1.3: Ranges of $\delta^{13}C$ values of autotrophic organisms and their potential carbon sources. Modified from Peters et al. (2005)

The hydrogen isotope signature of water also experiences significant alteration in the water cycle. The lighter molecule (H_2O) evaporates more easily than the heavier molecule (HDO) which leads to a deuterium-depletion of the water vapour in contrast to the lake or ocean water. Those become increasingly deuterium-enriched with ongoing evaporation. This is a so-called non-equilibrium fractionation because a part of the water vapour is removed without condensation (Peters et al., 2005). In clouds, the more heavy isotopes are

preferentially condensed to rain droplets. This leads to a proceeding deuterium-depletion of the water vapour in moisture-carrying air masses, when those are transported from the ocean towards the inland (called the "continental effect"). The more it rains the more the isotopic fractionation decreases during condensation leading to lower δD values of meteoric water when rainfall intensities are higher. This process is called Rayleigh distillation (Gat, 1996) and the "amount effect" on hydrogen isotope signatures in precipitation was applied to reconstruct past precipitation amounts in palaeoclimatology (e.g. Schefuss et al., 2005).

1.2.3 Isotopes of biomarkers

The establishment of compound-specific stable isotope analyses as a routine method added a new dimension to the applications of biomarkers in palaeoclimatology. The carbon- or hydrogen isotope signal of a biomarker may give additional information about the source of organic matter and environmental conditions during sedimentation as well as biochemical processes during and after sedimentation (Hayes et al., 1990; Freeman et al., 1990).

Variations of bulk organic carbon δ^{13}C values in sediments have been frequently interpreted with respect to changes in vegetation (C_3 or C_4 input) or lake productivity (Talbot and Johannessen, 1992; Hodell and Schelske, 1998; Meyers, 2003). Carbon isotope signatures of biomarkers can help to distinguish between these effects. A shift from terrestrial C_3 to C_4 vegetation will for instance be primarily visible in terrestrial biomarkers such as long-chain aliphatic compounds or certain sterols. In contrast, changes in the aquatic milieu will be recorded by an aquatic marker, for instance short- or mid-chain *n*-alkanes. The carbon isotope signature of a compound can give further hints towards its source organism. As an example, a ^{13}C depletion of microbial biomarkers has been frequently attributed to the presence of methanotrophs (Elvert et al., 1999; Thiel et al., 1999). Biogenic methane usually carries a strongly negative δ^{13}C signal due to the large carbon-isotope fractionation during methanogenesis, and this signal is stored in the biomass of the methane consumers (Whiticar et al., 1986). Water is the only hydrogen source for plants and algae and thus the hydrogen isotope signatures of plants have been reported to reflect the isotope signature of the source water (Sternberg, 1988), which is lake water for aquatic plants and soil and meteoric water for terrestrial plants. Several authors reported similar isotopic fractionations between source water and lipids, ranging from -130 to -160‰ (Sachse et al., 2004; Huang et al., 2004; Smith and Freeman, 2006; Rao et al., 2009). Thus, the lipids of plants indirectly track the δD signal of the meteoric water. However, as illustrated in Fig. 1.4, this signal can be significantly altered by isotopic fractionations occurring during evaporation of lake, soil and leaf water, as well as by transpiration, resulting in smaller apparent isotopic fractionation between meteoric water and lipids (Leaney et al., 1985; Gonfiantini, 1986; Hou et al., 2008). In humid regions, lake water evaporation is assumed to be negligible. Therefore, aquatic lipids are supposed to be good recorders of the δD signal of meteoric water there (Sachse et al., 2004). In arid and semi-arid regions,

terrestrial lipids were proposed to be better proxies, due to a large extent of lake water evaporation which modifies the original precipitation signal (Hou et al., 2008). As a result of these dependencies and due the observed deuterium enrichment of terrestrial derived lipids in contrast to aquatic lipids in humid regions (Sachse et al., 2004), while the opposite was found for some arid regions (Mügler et al., 2008; Xie et al., 2008), the offset between δD values of terrestrial and aquatic lipids was proposed as a possible proxy for palaeohydrologic conditions (Mügler et al., 2008).

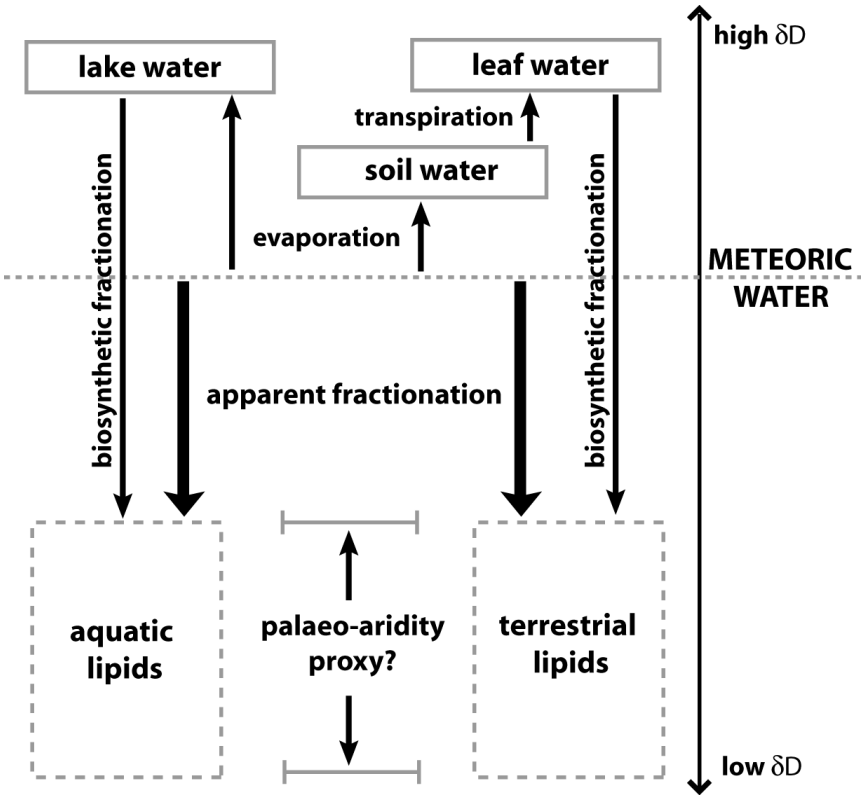

Figure 1.4: Processes influencing the δD value of the source water for aquatic and terrestrial organisms. The biosynthetic fractionation has been reported to be in the range -130 to -160‰. The δD values of the aquatic and terrestrial lipids are dependent on the extent of lake, soil and leaf water evapotranspiration. Adapted and modified from Sachse et al., 2006; Hou et al., 2008 and Mügler et al., 2008.

1.3 Biomarker studies from the Tibetan Plateau

Due to the increasing interest of palaeolimnologists in the Tibetan Plateau, a considerable number of palaeoenvironmental studies concentrating on lacustrine environments exist today (reviewed in Morrill et al., 2003; Herzschuh, 2006 or Chen et al., 2008). Most of these studies applied biological, sedimentological or geochemical proxies, but despite the vast area of the Plateau and the number of studies conducted, organic biomarkers have been used relatively seldom. Hereof, most of the studies focused on the potential

applicability of long-chain alkenones (LCAs) as temperature and salinity proxies e.g. in the saline Lake Qinghai (Li et al., 1996; Liu et al., 2006 and 2008) and in Zabuye Salt Lake (Wang and Zheng, 1998). Chu et al., 2005 evaluated LCA distributions and temperature dependence in lacustrine surface sediments mainly from eastern and central China, which also included a few lakes from the Tibetan Plateau. Another study evaluating LCAs in surface sediments concentrated on sulfate lakes mainly in Western China, but also includes one lake in the Qaidam Basin (Sun et al., 2004). Results from these studies suggest that LCAs could potentially be used to reconstruct temperature and salinity changes, but unpublished results from a surface sediment study (Anderson, A., University of Glasgow, personal communication) assume that on the Tibetan Plateau LCAs are mainly abundant in saline lakes only.

In addition, there is one study which discusses the composition and $\delta^{13}C$ values of steroid compounds in a short-core derived from Zabuye Salt Lake (Wang et al., 2004). Another one included *n*-alkane concentrations into a multi-proxy approach at Lake Luanhaizi in the Qilian Mountains (Herzschuh et al., 2005) as source indicator for sediment organic matter. Apart from the lacustrine environment, concentrations of *n*-alkanes in the Hongyuan peat deposit in the Zoîge-Basin (Zheng et al. 2007) delivered valuable information about past climate fluctuations, while leaf lipid compositions in the Ruoergai Marsh deposit (eastern Tibetan Plateau) served more to understand the diagenetic processes in the depositional environment (Duan and Ma, 2001). Recently, composition and carbon and hydrogen isotope signatures of *n*-alkanes have been analysed in a short core from Lake Qinghai (Liu et al., 2008), in a sediment core from Nam Co at the central Tibetan Plateau (Zhu et al., 2008; Mügler et al., 2009) as well as in surface sediments and terrestrial and aquatic plants in and around Nam Co (Mügler et al., 2008; Xia et al., 2008). Xia et al., (2008) also included δD values of surface sediments from lakes in the arid Qaidam Basin for comparison. The results from the first hydrogen isotope studies are promising with respect to a potential applicability of this proxy to reconstruct past hydrological conditions. This is of special relevance due to the direct linkage between variations of monsoon intensity and changes in regional precipitation / evaporation balances and emphasizes the need for further calibration studies as well as more δD data from palaeo-records.

1.4 Aims of this thesis

Even if compositional and compound-specific isotope analysis of organic biomarkers are potentially useful tools in palaeoclimatology, only very few studies applied these proxies on the Tibetan Plateau, apart from a range of alkenone studies (see above). The only organic matter based proxy which was used more frequently is $\delta^{13}C_{TOC}$. Due to the geographic setting of most Tibetan lakes in altitudes above 4000 m, the terrestrial vegetation in the lake catchments is limited to alpine steppe and meadows, which are dominated by C_3 grasses

at present (Wang, 2003). Due to the absence of C_4 vegetation, no larger fluctuations of $\delta^{13}C_{TOC}$ are to be expected from terrestrial influences. Nevertheless, changing $\delta^{13}C_{TOC}$ values have been observed in a number of lake sediment cores e.g. from Lake Qinghai (Shen et al. 2005), Lake Luanhaizi (Herzschuh et al. 2005) or Lake Koucha (Mischke et al. 2008). Mostly, those changes have been attributed to aquatic processes, for instance have decreasing $\delta^{13}C_{TOC}$ values after 6.5 cal ka BP in Lake Qinghai been interpreted as being caused by decreasing primary productivity (Shen et al. 2005). In contrast, Herzschuh et al. (2005) attributed high $\delta^{13}C_{TOC}$ values during the middle Holocene in sediments of Lake Luanhaizi to high contributions of aquatic macrophytes. A similar interpretation was given from Mischke et al. (2008) for high $\delta^{13}C_{TOC}$ values during the late glacial in Lake Koucha. Submerged macrophytes have to be considered as a profound influence upon the carbon isotope signal of sediments because of their potentially strongly ^{13}C-enriched biomass and due to the fact that many lakes on the Tibetan Plateau are rather shallow and densely populated by them. For the interpretation of $\delta^{13}C_{TOC}$ values in sediment cores, it is therefore crucial to understand to which extent aquatic macrophytes contribute to the isotopic signal of the sediments in Tibetan lakes and in which way variations can be explained in a palaeolimnological context. Additionally, the high abundance of macrophytes makes them interesting as potential recorders of lake water δD. Therefore, their lipids might contain information about palaeohydrological conditions which are a key factor of reconstructing past climate variability on the Tibetan Plateau. This is partly implied by the studies of Mügler et al. (2008 and 2009), while Xia et al. (2008) only interpreted δD values of terrestrial-derived *n*-alkanes. Generall, *n*-alkanes are useful as palaeoclimatic proxies, since they are easy to extract, purify and identify and they do not need to be derivatised for compound-specific-isotope analysis. Even if they are not taxonomically specific biomarkers, they can be roughly assigned to aquatic or terrestrial sources. Therefore, compositions and carbon and hydrogen isotope signatures of *n*-alkanes can be applied to distinguish between terrestrial and aquatic input and processes.

The principal aim of this thesis was to elucidate how organic biomarkers, and especially aquatic macrophyte-derived *n*-alkanes and their isotopic signals, can contribute to a better understanding of palaeoclimatic conditions of the Tibetan Plateau.

Special regard was given to the following questions:

1. How do aquatic macrophytes influence the composition and isotopic signal of sedimentary lipids (focusing on *n*-alkanes) in Tibetan Lakes?

2. How can variability of concentrations and $\delta^{13}C$ values of aquatic macrophyte-derived *n*-alkanes be interpreted in a palaeolimnological context, e.g. with respect to palaeoproductivity?

3. What deductions can be made from biomarker concentrations and δ^{13}C values for the history of Lake Koucha, for which significant changes of lake productivity have been previously inferred from biological and geochemical proxies?

4. Can δD values of *n*-alkanes reflect the hydrological conditions of our study region, i.e. do *n*-alkanes in sediments record the δD signal of meteoric water and how is this signal altered by evaporation and evapotranspiration effects?

5. Is there a difference between the δD signals recorded by aquatic and terrestrial biomarkers and how can potential offsets be explained?

6. Do δD values of *n*-alkanes in Lake Koucha confirm previous inferences from other proxies for changing palaeohydrological conditions, i.e. was a period of reduced moisture availability during the early Holocene recorded by the δD values of *n*-alkanes?

1.5 Thesis organisation

- **Chapter 1 - Introduction:** Gives an overview about the study region and its climatic features and about the scientific background of biomarkers and carbon and hydrogen isotopes. Furthermore, the principal aims of this thesis are highlighted.

- **Chapter 2 - Material and methods:** Gives an overview about the sample set and applied methods and a short description of the clean-up procedure of the sample extracts which is not described in more detail in the manuscripts.

- **Chapter 3 - Manuscript I:** The influence of aquatic macrophytes on stable carbon isotopic signatures of sedimentary organic matter in lakes on the Tibetan Plateau

  Authors: Bernhard Aichner[1)], Ulrike Herzschuh[1)], Heinz Wilkes[2)]

  Status: in preparation

  Aims: The variability of isotopic compositions of aquatic macrophytes (bulk and compound-specific, focusing on *n*-alkanes) and the possible influence of these variabilities on the organic matter of sediments should be evaluated. Here fore, a set of surface sediment samples and submerged and emergent macrophytes from lakes distributed across the central and eastern Tibetan Plateau was used. From the result, possible implications for palaeolimnological research shall be inferred.

- **Chapter 4 - Manuscript II:** Biomarker and compound-specific δ^{13}C evidence for changing environmental conditions and carbon limitation at Lake Koucha, eastern Tibetan Plateau

Authors: Bernhard Aichner[1)]), Heinz Wilkes[2)], Ulrike Herzschuh[1)], Steffen Mischke[3)], Chengjun Zhang[4)]

Status: accepted at Journal of Paleolimnology

Aims: The history of Lake Koucha since the late glacial was evaluated with the application of a biomarker approach by analysis of the concentration and δ^{13}C values of compounds within the aliphatic fraction of the biomarker extract. A focus was to obtain a more detailed knowledge about the contributors to the sediment organic matter than deduced from previous studies which used biological and geochemical approaches. Further, the applicability of δ^{13}C values of aquatic macrophyte-derived *n*-alkanes as a proxy for palaeo-productivity should be assessed by using a sediment core that was thoroughly interpreted using other proxies, all of which suggested significant productivity changes since the late glacial.

- **Chapter 5 - Manuscript III:** δD values of *n*-alkanes in Tibetan lake sediments and aquatic macrophytes - a surface sediment study and an application in a palaeorecord from Lake Koucha

  Authors: Bernhard Aichner[1)], Ulrike Herzschuh[1)], Heinz Wilkes[2)], Andrea Vieth[2)]

  Status: in preparation

  Aims: It was tested if δD values of *n*-alkanes in sediments and macrophytes collected over a large climatic and environmental gradient reflect the changing hydrological conditions of the study area. Further, the palaeohydrologic conditions at Lake Koucha since the late glacial should be reconstructed. Here, a focus should be set to evaluate if a period of reduced effective moisture availability, inferred from biological and geochemical proxies, is reflected in the δD values of the *n*-alkanes.

- **Chapter 6 - Synthesis:** The main results and achievements of the included manuscripts are summarised and discussed with respect to the aims highlighted in the introduction.

- **Chapter 7 - Conclusions:** The summarised results are set in a broader context and possible applications for future research are proposed.

Contribution and affiliations of co-authors

Ulrike Herzschuh[1] and Heinz Wilkes[2] are the main supervisors of this thesis, and therefore co-authors of all manuscripts. Steffen Mischke[3] drilled the sediment core of Koucha Lake, and since some of his bulk data as well as his age-model were used for manuscript II, he is co-author of that paper. Chengjun Zhang[4] is the Chinese cooperation partner from Lanzhou University and provided support during sampling and drilling of the Lake Koucha sediment core. Andrea Vieth[2] is the head of the stable isotope lab of the Organic Geochemistry

section at GFZ and was therefore included as co-author of the hydrogen isotope paper, even if not been scientifically involved. All co-authors contributed with detailed discussion, comments and revisions to initial drafts of the single manuscript.

1. Alfred Wegener Institute for Polar and Marine Research, Telegrafenberg A43, D-14473 Potsdam, Germany

2. Helmholtz Centre Potsdam GFZ German Research Centre for Geosciences, Telegrafenberg B228, D-14473 Potsdam, Germany

3. Institute of Geological Sciences, Freie Universität Berlin, Malteserstr. 74-100, D-12249 Berlin, Germany

4. Centre for Arid Environment and Paleoclimate Research, Lanzhou University, Gansu, 730000, China

2 Material and Methods

2.1 Samples and applied methods

Material for this thesis was a set of surface sediment samples and corresponding aquatic macrophytes from lakes distributed across the central and eastern Tibetan Plateau and a sediment core from Lake Koucha, eastern Tibetan Plateau. Plant samples included the species *Potamogeton pectinatus*, *Hippuris vulgaris*, *Batrachium bungei*, *Myriophyllum spicatum* and the macroalga *Chara* sp. Surface sediment and macrophyte samples have already been collected in campaigns in the years 2003, 2004 and 2006 and the sediment core was drilled in March 2003.

The applied methods were summarized in Table 2.1. Bulk parameter (TOC and TN contents and $\delta^{13}C_{TOC}$) of surface sediment samples have been analysed, while those data have already been available from the aquatic macrophytes and from the sediment core. *n*-Alkanes have been quantified by GC-FID (gas chromatography/flame ionization detection) in all samples. Additionally, highly abundant unsaturated compounds in *Potamogeton* samples, as well as hopanoid and isoprenoid compounds in the sediment core, have been qualified by GC-MS (gas chromatography/mass-spectrometry). For compound-specific isotope analysis (CSIA), GC-C-IRMS (gas chromatography/combustion/isotope-ratio mass spectrometry) was used to determine $\delta^{13}C$ values of biomarkers in the aliphatic fractions. For hydrogen isotopes, a GC-P-IRMS-system (gas chromatography/pyrolysis/isotope-ratio mass spectrometry) was used. Due to the lower sensitivity of the GC-P-IRMS system compared to the GC-C-IRMS, signal intensities were too low to determine reliable δD values in samples with little TOC or in samples of which little material was available. Detailed methodology of these methods is described in material and methods sections of the respective manuscripts.

In addition to the primary aims of this thesis, the surface sediment sample set and five selected samples from the sediment core were used to test the applicability of the TEX_{86} in our study region (see Appendix 1). Further, surface sediments and samples from a sediment core from Lake Donggi Cona (eastern Tibetan Plateau) were analysed for *n*-alkane concentrations to assess possible future applications of CSIA and high-resolution biomarker approaches in this lake (Appendix 2).

Table 2.1: Overview over the samples included in this thesis and over the applied methods

samples	number of samples	TOC / TN (EA)	$\delta^{13}C$ TOC (EA-IRMS)	*n*-alkanes (GC-FID)	biomarkers - aliphatic fraction (GC-MS)	CSIA - $\delta^{13}C$ (GC-C-IRMS) triplicate measurements	CSIA - δD (GC-P-IRMS) triplicate measurements	quantification of ether lipids (LC - APCI/MS) [a]
surface sediments	**40**	**x**	**x**	**x**		**x**	**x** *	**x**
aquatic macrophytes	**15**	**already available**	**already available**	**x**	**x** **	**x**	**x** *	
sediments (Lake Koucha sediment core)	**34**	**already available**	**already available**	**x**	**x**	**x**	**x** ***	**(x)** ****
sediments (Lake Donggi Cona; surface sediments and sediment core) [b]	37	x	x	x				

a) beyond the major scope of this thesis, the applicability of the TEX_{86} and other ether lipid ratios was tested in our study area (see Appendix A)
b) beyond the major scope of this thesis, *n*-alkane concentrations were determined in surface sediments and a sediment core from Lake Donggi Cona to assess possible future applications of CSIA or of high resolution biomarker studies in this lake (see Appendix B)

* reliable δD values could only be obtained for 16 surface sediment samples and 6 macrophyte samples
** to identify unsaturated compounds in *Potamogeton* samples
*** only 18 samples were measured for δD
**** only 5 samples were analysed

2.2 Extraction and purification of samples

7-15 grams of sediment and 0.2-1 gram of plant samples were extracted with an organic solvent [dichloromethane (DCM) / methanol (MeOH); 9:1] at 76 bar and 100 °C, using and accelerated solvent extractor (Dionex, Sunnyvale, USA). The extracts were separated in three fractions with a medium pressure liquid chromatography (MPLC) system (Radke et al., 1980; Fig. 2.1). Here for, the extracted compounds were dried under nitrogen, solved in 500µL *n*-Hexane and injected into the system. Aliphatic and aromatic compounds were separated chromatically using *n*-hexane as solvent and pre-columns filled with silicagel as well as a main column provided by the manufacturer and filled with unknown material (Radke et al. 1980) as stationary phase. More polar compounds, e.g. with functional groups containing nitrogen, sulphur or oxygen (NSO-compounds) remain on the precolumns and were washed from those later using DCM/MeOH (95:5) as solvent. The aliphatic fraction, containing *n*-alkanes, isoprenoid and hopanoid compounds, was the fraction of major interest for this thesis, while ether lipids (for TEX_{86}) were in the NSO fraction.

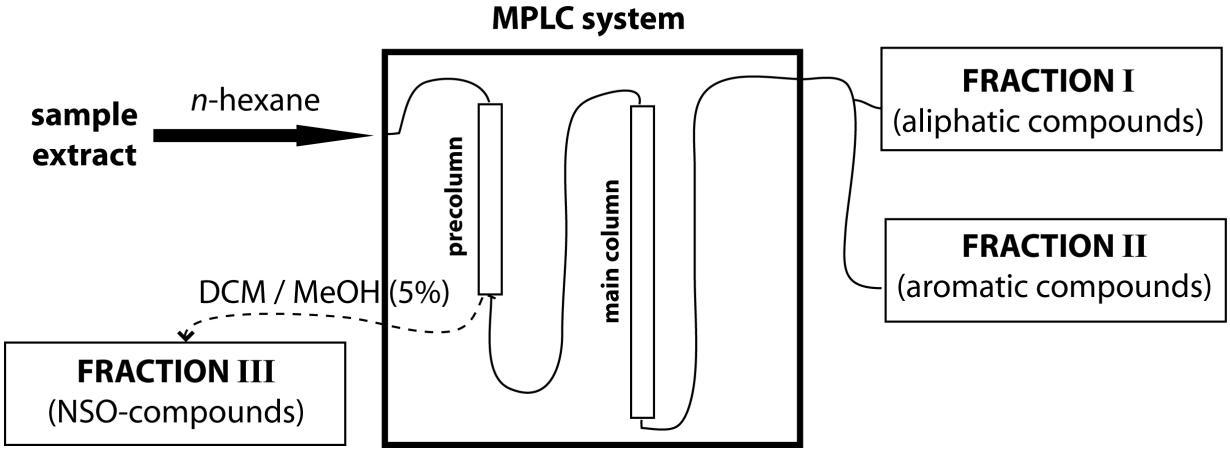

Figure 2.1: Principal functioning of a medium pressure liquid chromatography system after Radke et al., (1980). Fractions I and II are separated by a time control (aliphatic compounds elute before aromatic compounds). Fraction III is washed from the precolumn using a more polar solvent (DCM/MeOH; 95:5).

3 The influence of aquatic macrophytes on stable carbon isotopic signatures of sedimentary organic matter in lakes on the Tibetan Plateau

Abstract

We show that aquatic macrophytes beside the lipid composition and the TOC/TN ratio also influence the carbon isotope values (TOC and compound specific) of organic matter in lake sediments, a fact which is often neglected when these proxies are interpreted in palaeoenvironmental studies. A set of surface sediment samples and corresponding plants from the Tibetan Plateau provided a suitable framework for this study. This region contains many shallow lakes with a dense population of aquatic macrophytes and terrestrial influence which are typically limited to alpine non-C_4-grasses. Assessments on basis of a binary isotopic model revealed an average contribution of submerged macrophytes of up to 60% (mean: 40%) to the TOC and of up to 100% (mean: 66%) to mid-chain *n*-alkanes (C_{23} and C_{25}). Submerged aquatic macrophyte species such as *Potamogeton pectinatus* revealed typical mid-chain dominated *n*-alkane patterns in most of the samples, but also turned out to synthesize higher relative amounts of long-chain homologues within one species in more shallow lakes - possibly due to adaption to partial exposure to air. Macrophytes showed wide ranges of $\delta^{13}C$ values both in bulk organic matter (-18.1 to -5.8‰) and in *n*-alkanes (e.g. -25.2 to -13.3‰ for nC_{25} in *Potamogeton*) due to bicarbonate metabolism in the alkaline lakes. There is a highly significant correlation ($R^2 = 0.97$ for nC_{25}) between $\delta^{13}C$ values of lipids and bulk biomass in plant samples, however the offset between those two parameters has been found to increase with increasing bulk values. We assume that isotopic fractionation during lipid synthesis is enhanced if a ^{13}C enriched carbon source, like bicarbonate, is assimilated by the macrophytes. In most of the sediment samples the organic matter was found to be strongly influenced by aquatic macrophytes, with respect to TOC/TN ratios, *n*-alkane patterns, and $\delta^{13}C$ values. Wide ranges of $\delta^{13}C$ values have been observed in TOC (range -29.0 to -16.0‰) as well as in mid-chain *n*-alkanes (e.g. -34.1 to -16.6‰ for nC_{25}) while variability in long-chain *n*-alkanes (C_{27}, C_{29}, C_{31}) is relatively small. This indicates that those are only influenced minimally by submerged macrophytes. Due to the low absolute concentrations of *n*-alkanes in submerged macrophytes (39 - 150 µg/g d.w. for *Potamogeton*), compared to terrestrial or emergent plants (523 - 940 µg/g d.w. for *Hippuris vulgaris*), the effect on the isotopic signal of long-chain *n*-alkanes is minor, even when the abundance of macrophytes is high and their tendency towards producing

long-chain homologues is increased. A calibration between $\delta^{13}C$ values and limnologic parameters turned out to be difficult due to multiple influences. However, changing $\delta^{13}C$ values of plant remains, or alternatively of mid-chain *n*-alkanes, in sediment cores could be interpreted with respect to changes of primary and macrophyte productivity in lakes, while the relative contribution of aquatic macrophytes can be assessed by the *n*-alkane pattern and additionally by the offset between $\delta^{13}C$ values of TOC and of *n*-alkanes.

3.1 Introduction

Sedimentary organic matter of lakes has been used in numerous studies to reconstruct past environmental conditions. To interpret organic proxies in sediments in a lacustrine environment properly, a calibration is necessary. Hereby, a set of surface sediments can be a suitable tool. Setting up a calibration set using surface sediments is quite common in organism-based studies (Seppä and Bennett, 2003; Battarbee, 2000) but, beside the calibration of temperature related proxies such as alkenones (e.g. Zink et al., 2001; Chu et al., 2005) or ether lipids (Powers et al., 2004), such studies are relatively rare in organic geochemical approaches. Recent studies concentrated on the relation between δD values of lipids and environmental factors using lake surface sediment transects throughout North America (Huang et al., 2004) and Europe (Sachse et al., 2004).

Parameters, like bulk $\delta^{13}C$ values of organic matter in sediments, are widely used proxies in palaeolimnology. Common interpretations for observed shifts are attributed to changes of the source of the organic matter, e.g. from terrestrial C_3 to C_4 vegetation (O'Leary, 1988; Farquhar et al., 1989) and of the productivity in the lakes (Meyers, 2003). As bulk organic $\delta^{13}C$ values integrate multiple influences, compositional and compound-specific isotope analysis of lipid biomarkers, e.g. sterols, fatty acids, fatty alcohols or *n*-alkanes have been increasingly used to distinguish between different sources of organic matter in palaeolimnological studies during the last decade (e.g. Ficken et al., 1998; Schwark et al., 2002; Fuhrmann et al., 2003). Long-chain *n*-alkanes (C_{27} - C_{33}) with a strong odd-over-even predominance are usually interpreted to be of terrestrial origin. Mid-chain *n*-alkanes (C_{20} - C_{25}) were mainly assigned to aquatic macrophytes (Eglinton and Calvin, 1967; Kolattukudy et al., 1976; Huang et al., 1999; Ficken et al., 1998) but have been also detected in *Sphagnum* species (Baas et al., 2000). Bacteria, algae and fungi are supposed to produce mainly short-chain *n*-alkanes in the range of C_{14} to C_{22} (Han and Calvin, 1969; Grimalt and Albaiges, 1987), while, especially, C_{17} is considered to be a biomarker for algae and photosynthetic bacteria (Gelpi et al., 1970; Meyers, 2003). On basis of this knowledge, ratios like the aquatic-terrestrial ratio ATR (Wilkes et al., 1999) or the proxy for aquatic macrophytes P_{aq} (Ficken et al., 2000) have been developed to estimate the proportional input of algae or aquatic and terrestrial macrophyte derived organic matter. $\delta^{13}C$ values of terrestrial long-chain *n*-alkanes have been used to reconstruct input of organic matter

derived from C_3 or C_4 plants into sediments (e.g. Yamada and Ishiwatari, 1999; Huang et al., 2001; Schefuss et al., 2003; Glaser and Zech, 2005).

Up to now, there is a lack of studies examining the influence of aquatic macrophytes on the composition and isotopic signal of the sedimentary organic matter in further detail. As macrophytes contribute significantly to the TOC pool of sediments in certain environments, their isotopic shifts have to be understood before using such data as palaeolimnological proxies. $\delta^{13}C$ of aquatic macrophytes is usually in the range of C_3 plants; however, limited CO_2 availability due to high pH, alkalinity, or high CO_2 consumption at dense plant stands can lead to HCO_3^- assimilation and hence to a shift towards less negative $\delta^{13}C$ values similar to C_4 plants (Allen and Spence, 1981; Prins and Elzenga, 1989; Keeley and Sandquist, 1992). Shifts towards higher $\delta^{13}C$ values values in aquatic macrophyte derived mid-chain *n*-alkanes (C_{23} and C_{25}) in sediment cores have consequently been interpreted to be caused by limited CO_2 availability induced by water temperature, salinity, pH, enhanced productivity, low atmospheric pCO_2, or physical barriers to diffusion like ice cover (Street-Perrott et al., 2004). Mead et al. (2005) used the potential difference of $\delta^{13}C$ values between submerged and emergent/terrestrial plants for a source assessment of organic matter in sediments in combination with *n*-alkane ratios.

The Qinghai-Tibet-Plateau, in its capacity as the main driving force for the Asian monsoon, has profound influences on the atmospheric circulations and is therefore an interesting area for palaeoenvironmental research (Ruddiman and Kutzbach, 1989; Lehmkuhl and Owen, 2005). The region consists of hundreds of lakes with varying limnologic conditions, but many of them are rather shallow and densely covered by aquatic macrophytes during the short growing season. Due to the high altitude, the vegetation in the catchment areas of most of the lakes consists mainly of alpine meadows or alpine steppes. C_4 plants play a minor role in the present vegetation on the plateau (Wang, 2003). Hence, the region is ideal to test the influence of aquatic macrophytes on the lipid and isotopic composition of sediments.

The principal aims of this study are (1) to evaluate the variability of isotopic compositions of aquatic macrophytes (bulk and compound-specific, focusing on *n*-alkanes), (2) to assess how aquatic macrophytes influence the organic matter of sediments with respect to *n*-alkane compositions and isotopic values and (3) to deduce possible implications for palaeolimnological research from these results.

3.2 Study site and samples

This study is based on a set of plant and lake surface sediment samples. Surface sediment samples of lakes distributed across the eastern and central Qinghai-Tibet-Plateau (covering an area from 25.7° N to 39.2° N latitudes and 89.5° E to 102.3° E longitudes) were collected with a sediment grab during campaigns in the summers of 2003 - 2006. It was attempted

to sample the lakes at the deepest point. The 40 lakes used in our study (Fig. 3.1) were chosen to focus on the highly abundant shallow freshwater lakes but without neglecting other samples to cover the whole range of limnologic parameters with respect to altitude, lake depth, electric conductivity, and pH (Appendix 3). The altitude of the sampled lakes ranges from about 1,500 m (southeastern margin of the plateau) up to 5,133 m a.s.l.; however, most of them are from altitudes between 4,000 and 4,700 m. Typical high altitude lakes in our data set are oligotrophic, rather shallow (below 1 m) and of low salinity. There are only a few deeper lakes and a few lakes with higher salinities. The pH ranges from 7.0 to 10.7, but in 25 of the lakes, values are higher than 9. From 21 lakes, samples of the dominant submerged aquatic macrophyte *Potamogeton pectinatus* (L.) were available. Additionally in a few lakes, samples of *Myriophyllum spicatum* (4 samples), *Batrachium bungei* (3) (submerged macrophytes), *Hippuris vulgaris* (3) (emergent macrophyte), and *Chara* sp. (3) (macroalgae) were collected. All plant, algae and sediment samples were taken at the same spot, except in Lake Donggi Cona, where the plant samples were collected at the shore (0.25 m) and the sediment sample is derived from a depth beyond the limit of macrophyte growth (35 m).

All sediments and plant samples were analysed for bulk parameters (TOC, TOC/TN, $\delta^{13}C_{TOC}$). Additionally, *n*-alkane composition and $\delta^{13}C$ of *n*-alkanes were determined for all sediments and a selection of 15 plant samples. All locational, limnological, and analytical data of samples are summarized in Appendix 3. Information on pollen content and ostracod composition of the sediments are provided in Herzschuh (2007) and Mischke et al. (2007).

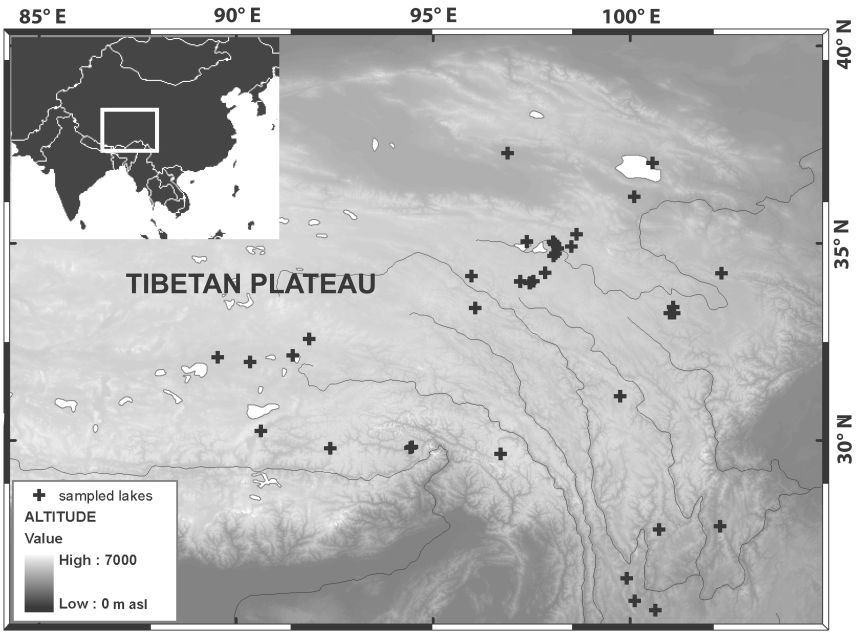

Figure 3.1: Locations of lakes sampled for surface sediments.

3.3 Methods

3.3.1 Water parameters and bulk parameters of sediments and plants

pH and salinity of the lake waters were determined with a WTW Multi 340i device (see also Mischke et al., 2007). To remove inorganic carbon, the sediments were heated at 97 °C for 3 hours after the addition of 1.3mol HCl before being measured using a Finnigan MAT Delta-S mass spectrometer equipped with a FLASH elemental analyser and a CONFLO III gas mixing system for the online determination of the carbon isotopic composition. Total organic carbon and nitrogen contents of sediments and plants were determined with a Vario el III elemental analyser (Elementar Analysensysteme GmbH, Hanau, Germany).

3.3.2 Quantification and compound-specific isotope analysis of *n*-alkanes

Samples were freeze dried and milled prior to extraction with an accelerated solvent extractor (ASE) (Dionex, Sunnyvale, USA). The extraction was performed with dichloromethane : methanol (9:1) at 76 bar and 100 °C. The aliphatic hydrocarbon fractions were isolated by liquid chromatography, using a MPLC system (Radke et al., 1980). As a quantification standard, a known amount of 5α-androstane (Sigma-Aldrich, St. Louis, USA) was added to the extract prior to MPLC. *n*-Alkanes were quantified with an Agilent 6890 GC-FID equipped with an injector heated from 40 °C to 300 °C at 700 °C/min using splitless injection and an Ultra-1 fused silica capillary column (50 m length, 0.2 mm inner diameter, 0.33 µm film thickness) using the following temperature programme: oven start temperature 40 °C, heating rate 5 °C/min to 310 °C, isotherm phase 60 min. Helium was used as a carrier gas with a constant flow of 1 ml/min. Carbon isotope ratios of the *n*-alkanes were determined with Agilent 6890N GCs, equipped with the same Ultra-1 column and coupled either to a Thermo Electron Delta V plus IRMS or to a Thermo Electron MAT253 IRMS via Combustion III interfaces (Thermo Fischer, Bremen, Germany). The injector was set to 230 °C as start temperature before heating to 300 °C at 700 °C/min. The oven was heated from 40 °C to 300 °C at a rate of 3 °C/min before a final isothermal time of 25 minutes. For quality control, a certified standard mixture of *n*-alkanes ($n\mathrm{C}_{15}$, $n\mathrm{C}_{20}$ and $n\mathrm{C}_{22}$; Chiron, Trondheim, Norway) was measured after each 10^{th} measurement. Additionally, the δ^{13}C values of the internal standard (5α-androstane) served as a control to monitor drifts during δ^{13}C analysis. The linearity range (150 mV to 10,000 mV) of the measurement system was determined with a dilution series of the same standard. Each sample was analysed in triplicate. In some cases, low abundances (in most cases of short-chain and of even-chain *n*-alkanes) resulted in signals close to the lower limit of linearity, consequently, leading to higher standard deviations. In a few samples, several compounds eluting shortly before and after $n\mathrm{C}_{17}$ prevented the determination of isotopic values of $n\mathrm{C}_{17}$ as a baseline separation of those compounds was not always possible. The

δ^{13}C values of *Chara* and *Batrachium* samples were excluded from this manuscript since these samples showed a significant hump in the elution range of mid-chain *n*-alkanes.

3.3.3 Calculations and statistics

To express *n*-alkane distributions in numbers, the aquatic/terrigenous ratio (ATR) and the proxy for submerged/floating versus emerged/terrestrial plants (P_{aq}) were used. They were calculated as follows:

$$\mathrm{ATR} = \frac{(n\mathrm{C}_{15}+ n\mathrm{C}_{17}+ n\mathrm{C}_{19})}{(n\mathrm{C}_{15}+ n\mathrm{C}_{17}+ n\mathrm{C}_{19}+ n\mathrm{C}_{27}+ n\mathrm{C}_{29}+ n\mathrm{C}_{31})} \text{ (Wilkes et al., 1999)}$$

$$\mathrm{P}_{aq} = \frac{(n\mathrm{C}_{23}+ n\mathrm{C}_{25})}{(n\mathrm{C}_{23}+ n\mathrm{C}_{25}+ n\mathrm{C}_{29}+ n\mathrm{C}_{31})} \text{ (Ficken et al., 2000)}$$

Further, a ratio of short to total *n*-alkanes was applied:

$$\text{short/total} = \frac{(\sum \text{short-chain } n\text{-alkanes})}{(\sum n\text{-alkanes})}$$

short-chain *n*-alkanes = $n\mathrm{C}_{15}$ to $n\mathrm{C}_{19}$

n-alkanes = $n\mathrm{C}_{15}$ to $n\mathrm{C}_{33}$

To express odd-over-even predominance, the carbon-preference-index (CPI) for the range $n\mathrm{C}_{23}$ to $n\mathrm{C}_{31}$ was calculated:

$$\mathrm{CPI} = 0.5 \times [\frac{(n\mathrm{C}_{23}+ n\mathrm{C}_{25}+ n\mathrm{C}_{27}+ n\mathrm{C}_{29}+ n\mathrm{C}_{31})}{(n\mathrm{C}_{22}+ n\mathrm{C}_{24}+ n\mathrm{C}_{26}+ n\mathrm{C}_{28}+ n\mathrm{C}_{30})} + \frac{(n\mathrm{C}_{23}+ n\mathrm{C}_{25}+ n\mathrm{C}_{27}+ n\mathrm{C}_{29}+ n\mathrm{C}_{31})}{(n\mathrm{C}_{24}+ n\mathrm{C}_{26}+ n\mathrm{C}_{28}+ n\mathrm{C}_{30}+ n\mathrm{C}_{32})}]$$

Cluster analysis of the *n*-alkane pattern of sediment samples was performed with the program SPSS using Ward's algorithm (Ward, 1963) as linkage rule and the squared Euclidean distance as distance measure (Everitt et al., 2001).

3.4 Results

3.4.1 Bulk parameter

Bulk δ^{13}C values of *Potamogeton* leafs showed considerable variations with -5.8‰ as a maximum and -18.1‰ as a minimum value. *Myriophyllum* and *Batrachium* plant material had values comparable to *Potamogeton* for specimens from the same sampling sites (Table 3.1 and Appendix 3). In contrast, δ^{13}C values of *Hippuris* were in the same range in all of the samples (around -26‰) and therefore up to 17‰ more depleted in ^{13}C than bulk values of submerged macrophytes from the same sites (Table 3.1). The two samples of the macroalga *Chara* sp. showed values between -16.8 and -13.1‰ and were generally less enriched in δ^{13}C than submerged plants from the corresponding sites.

Total organic carbon (TOC) contents in the sediments ranged from 0.5 to 23.7% (Appendix 3) with a mean value of 5.9% and a median of 4.4%. TOC/TN ratios ranged from

Table 3.1: Bulk parameter and δ^{13}C values of *n*-alkanes in samples of aquatic macrophytes and macroalgae

lake	species	depth [m]	pH	TOC/TN	δ^{13}C bulk [‰]	sum *n*-alkanes [µg / g d.w.]	δ^{13}C of *n*-alkanes [‰]											
							C_{19}	C_{20}	C_{21}	C_{22}	C_{23}	C_{24}	C_{25}	C_{26}	C_{27}	C_{28}	C_{29}	C_{30}	C_{31}
S-22	*Potamogeton*	2.8	9.9	12.2	-14.2	71			-19.1		-19.0	-23.4	-20.1		-21.5		-23.4		
S-22	*Myriophyllum*	2.8	9.9	16.2	-9.7	53			-22.0	-23.6	-20.1	-20.8	-21.2		-29.3				
S-22	*Chara*	2.8	9.9	13.0	-16.8	39													
S-26	*Potamogeton*	0.3	8.1	11.7	-16.6	132	-27.4		-25.0		-21.6		-23.5		-24.5		-26.9		-28.2
S-26	*Myriophyllum*	0.3	8.1	10.7	-14.3	133	-26.5	-26.2	-23.6	-24.1	-21.3	-21.6	-23.0		-27.8		-31.9		
S-26	*Hippuris*	shore	8.1	7.1	-26.4	896							-29.2		-32.6	-33.8	-32.8		-34.1
Kou-Cha	*Potamogeton*	6.0	9.8	11.1	-8.8	150	-22.1		-21.4		-17.1		-17.7		-19.8		-19.7		-24.6
Kou-Cha	*Hippuris*	shore	9.8	8.6	-25.7	523							-29.9		-33.9		-34.2		-34.5
Donggi	*Potamogeton*	0.3	7.9	21.3	-5.8	103	-24.4	-24.8	-19.2	-23.0	-13.4	-16.9	-13.3		-13.3		-15.5		-20.3
CTP-35	*Potamogeton*	2.1	9.1	8.6	-18.1	128	-25.3	-27.2	-23.0	-24.5	-22.8	-25.4	-25.2		-27.1		-27.3		-31.1
MiY-42	*Batrachium*	0.4	10.4	n.d.	-16.1	224													
MiY-42	*Hippuris*	shore	10.4	11.5	-26.5	940							-27.7		-33.4	-33.4	-33.9	-33.8	-33.5
LC-10	*Potamogeton*	0.5	7.7	29.6	-15.4	80	-24.9	-29.5	-23.8	-27.3	-22.0	-28.3	-23.4	-28.7	-23.5	-29.4	-23.0	-29.9	-26.7
CTP-20	*Potamogeton*	0.4	10.4	22.6	-7.9	39	-22.4	-28.5	-18.1	-23.3	-15.8	-20.7	-15.5	-24.1	-17.2	-24.3	-19.2		-22.5
Ga-01	*Chara*	0.8	9.7	n.d.	n.d.	74													

missing values: too low signal intensity; n.d.: no data available

4.2 to 35.9 (Appendix 3) but half of the samples have values below 10 and only 5 samples a value > 20 (mean value: 12.0, median: 9.9). $\delta^{13}C_{TOC}$ of surface sediment samples ranged from -29.0‰ to -16.0‰ (Table 3.2 and Appendix 3) and were evenly distributed (mean: -22.6‰, median -21.7).

3.4.2 *n*-Alkane patterns of plants and sediments

Fifteen samples of aquatic macrophytes were analysed for their *n*-alkane compositions. The highest total amounts of *n*-alkanes were found in the samples of the emerged macrophytes *Hippuris* (range: 523 - 940 µg/g d.w.) (Table 3.1). Absolute concentrations were significantly lower in the submerged species *Potamogeton* (39 - 150 µg/g d.w.), *Myriophyllum* (53 - 133 µg/g d.w.) and *Batrachium* (224 µg/g d.w.). Relatively low *n*-alkane concentrations were also found in the macroalgae-samples of *Chara* (39 - 74 µg/g d.w.). All *n*-alkane concentrations of plant samples are provided in Appendix 4. All samples of submerged species (*Potamogeton*, *Myriophyllum* and *Batrachium*) were dominated by odd-numbered, mid-chain *n*-alkanes, especially C_{23} and C_{25} (Fig. 3.2). *Potamogeton* samples contain relatively high abundances of unsaturated compounds in the long-chain range ($nC_{29:1}$ and $nC_{31:1}$) as shown for sample CTP-20 in Fig. 3.2b. Relatively high amounts of saturated long-chain *n*-alkanes C_{27}, C_{29} and even C_{31} were found in the *Batrachium* sample (Fig. 3.2a) and in *Potamogeton* samples from the lakes LC-10 and S-26 (Fig. 3.3a and d). The *Potamogeton* sample from lake LC-10 also contains relatively high amounts of nC_{21}.

Table 3.2: δ^{13}C values (TOC and *n*-alkanes) of sediment samples

lake	$\delta^{13}C_{TOC}$ [‰]	δ^{13}C of *n*-alkanes [‰]																		
		C_{15}	C_{16}	C_{17}	C_{18}	C_{19}	C_{20}	C_{21}	C_{22}	C_{23}	C_{24}	C_{25}	C_{26}	C_{27}	C_{28}	C_{29}	C_{30}	C_{31}	C_{32}	C_{33}
CTP-02	-20.7							-25.5		-23.1		-24.3		-28.5		-30.6		-31.9		
CTP-15	-23.5													-32.1		-33.4		-32.4		-31.9
CTP-19	-24.9									-30.9	-28.7	-32.4	-34.3	-33.5		-34.9	-33.5	-33.6		-31.4
CTP-20	-16.0									-20.4	-27.4	-22.4		-29.2	-32.5	-32.9		-34.0		
CTP-25	-21.4			-27.3				-24.7	-25.8	-24.5	-30.7	-27.8	-31.9	-28.7		-30.8		-32.8		
CTP-35	-29.0			-35.2	-27.9	-28.6	-29.1	-29.6	-29.2	-30.2	-30.0	-30.6	-32.8	-32.3	-33.7	-31.2	-32.7	-31.9		-32.0
CTP-39	-25.8							-29.4	-29.6	-28.0	-30.9	-30.0	-30.5	-31.8	-31.6	-33.0	-33.0	-32.4		-32.3
Koucha	-22.1				-31.9	-26.7	-24.8	-16.1	-19.1	-13.0		-16.6		-32.0		-30.5		-31.0		
Donggi	-24.7							-20.7		-26.5		-27.8		-35.8		-32.7		-31.9		
GA-01	-21.5					-30.5		-26.7	-27.7	-23.0	-28.5	-23.9	-29.5	-28.5	-30.2	-30.7		-32.2		
LC-02	-21.3			-23.5			-28.0	-33.1	-30.0	-24.2	-25.6	-25.7	-27.0	-26.6	-27.7	-28.9		-31.5		-29.7
LC-05	-27.0							-32.6	-37.0	-35.4	-36.0	-34.1		-33.8		-34.2	-35.3	-35.2		-35.8
LC-06	-27.1					-24.1	-24.2	-30.9	-30.7	-32.6	-30.8	-30.5	-30.8	-31.2	-31.4	-31.8	-31.6	-31.9	-32.8	-31.3
LC-10	-20.8		-28.3	-26.9						-25.3	-30.1	-25.9		-28.9		-32.2		-34.8		
MiY-21	-19.4									-26.4	-29.3	-27.0	-29.5	-28.8	-29.0	-30.2	-29.3	-30.9		
MiY-22	-18.5		-27.3					-23.7		-21.3	-27.0	-23.0	-28.0	-25.2	-28.5	-29.7	-31.4	-31.8		-31.4
MiY-28	-18.0		-28.1		-28.4					-20.8		-21.9		-26.0		-28.4		-30.3		
MiY-29	-20.6									-22.7	-28.0	-25.2	-28.9	-26.9	-28.4	-29.2	-28.4	-30.8		-31.8
MiY-30	-20.4									-22.3	-27.5	-21.5	-29.1	-25.4	-29.6	-27.9		-30.5		-31.1
MiY-35	-18.4							-23.9		-23.1		-23.8		-26.8		-29.8		-31.4		
MiY-38	-21.3									-29.1	-29.3	-28.2	-29.5	-29.3	-30.1	-31.8	-30.8	-32.6		-32.3
MiY-39	-19.3							-29.6		-25.9		-28.8		-31.5		-31.9		-33.7		
MiY-40	-19.6									-30.4		-29.7		-28.4		-30.0		-32.2		
MiY-42	-21.8			-32.8				-24.2	-24.3	-23.7	-28.2	-26.8	-30.3	-28.3	-31.1	-30.9	-29.8	-32.4		-32.3
MiY-44	-24.6			-32.1			-32.3	-31.3	-31.4	-30.9	-32.2	-31.8	-32.8	-31.8	-30.4	-32.0	-32.1	-32.2		-33.2
MiY-46	-21.6		-26.1	-31.0	-25.8					-28.3	-29.0	-28.6	-29.2	-28.3	-28.4	-30.8	-29.1	-32.2		-31.6
MiY-53	-21.4		-26.9		-28.0					-27.8	-28.9	-26.3	-28.8	-26.8	-29.6	-30.2		-32.1		
NB-01	-24.6							-32.7		-32.1		-29.6	-31.1	-31.1		-32.0		-32.9		-31.7
Qai-02	-25.9									-27.1		-28.0		-32.4		-34.5		-34.7		
Qai-06	-20.2									-17.6		-18.5		-24.2		-20.3		-22.7		
S-10	-26.2							-33.5		-31.4	-30.5	-30.7	-29.7	-31.3	-28.2	-31.9		-32.2		-32.2
S-13	-28.1						-30.0	-34.7	-37.8	-32.4	-32.0	-31.0	-30.6	-32.5	-32.8	-33.1	-33.5	-32.9	-37.1	-33.7
S-16	-27.9						-30.8	-34.8	-36.4	-32.2	-31.9	-31.8	-32.9	-32.4	-32.0	-33.3	-32.2	-33.7		-33.6
S-22	-20.0							-31.0	-32.2	-25.9	-28.7	-26.1	-29.7	-28.8	-30.3	-31.3	-30.2	-33.0		-33.4
S-26	-21.8									-27.5		-27.4		-31.3		-33.2		-32.4		
SET 15	-21.9	-31.6	-31.2		-30.5	-32.5				-31.7		-31.3		-33.3	-32.3	-32.8		-29.6		
SET 16	-18.2			-30.0	-29.0	-24.2				-25.3	-28.1	-24.3	-32.7	-26.3	-31.3	-30.6				
SET 19	-24.5	-29.8	-30.0	-33.0	-31.5	-31.4	-30.0	-33.4	-32.9	-33.6	-31.6	-28.0	-27.3	-29.3		-31.7		-31.1		-31.7
SET 21	-25.3	-29.8	-29.0	-28.1	-28.1	-27.9		-24.6	-30.5	-27.0	-28.7	-28.1	-30.9	-29.8	-29.3	-31.7		-31.6		-31.6
SET 25	-27.7	-31.8	-29.3		-30.5	-31.0	-30.5	-32.4		-32.7		-32.2		-30.7		-32.3		-31.3		-31.4

missing values: too low signal intensity; n.d.: no data available

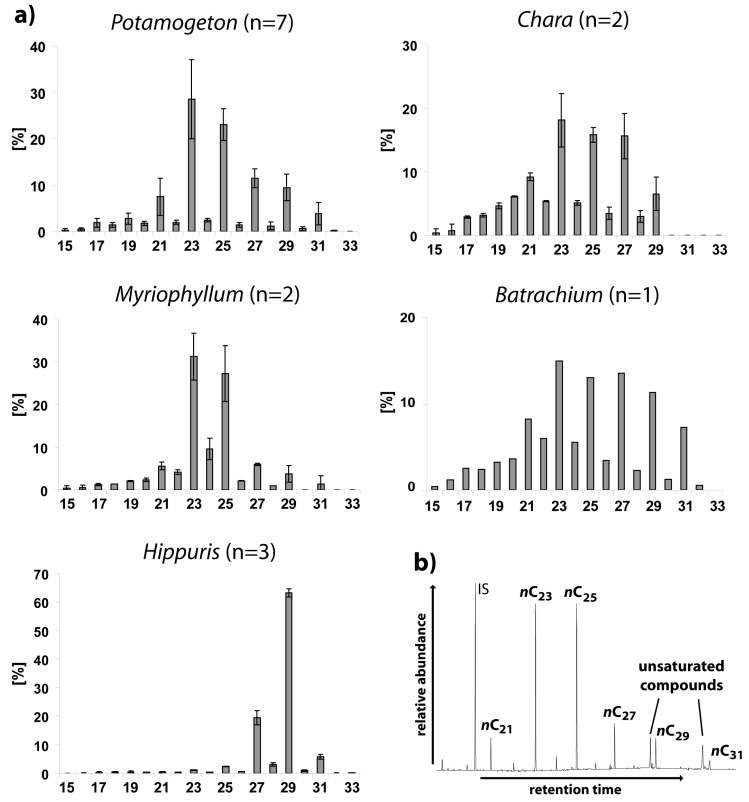

Figure 3.2: (a) Average *n*-alkane distributions (including variations) of samples from submerged macrophytes (*Potamogeton*, *Batrachium* and *Myriophyllum*), emergent macrophytes (*Hippuris*) and macroalga *Chara*. n = number of analysed samples; x-axes indicate carbon numbers. (b) GC-FID chromatogram of *Potamogeton* sample CTP-20, illustrating the high abundance of unsaturated long-chain compounds. IS = internal standard.

In the *Chara*-samples, C_{23}, C_{25}, C_{27} are also the most abundant *n*-alkanes. Lipids of the emerged species *Hippuris vulgaris* show an *n*-alkane-pattern with C_{27} and C_{29} as dominating homologues. The total amounts of *n*-alkanes (C_{15} to C_{33}) in the sediments range from 1.0 - 55.6 µg/g d.w. (Appendix 5). The sediments can be separated into four main groups by hierarchical cluster analysis according to their *n*-alkane patterns (Fig. 3.4). Type I sediments are dominated by long-chain *n*-alkanes. While sediments in cluster Ia contain mainly C_{29} and C_{31}, concentrations of mid-chain *n*-alkanes are enhanced in sediments in cluster Ib. Only a few sediment samples (type II) show relatively high abundances of short chain *n*-alkanes, especially C_{16} and C_{16}. Other sediments are dominated by mid-chain *n*-alkanes, especially C_{23} and C_{25} (type III). Samples in cluster IV contain high abundances of both mid- and long-chain *n*-alkanes, which partly show a bimodal distribution (type IVb) or slightly higher values of the long-chain homologues (IVa). Most samples show a strong odd-over-even predominance in the mid- and long-chain range (CPI_{23-31}: 4.0 - 12.6; mean 6.7, median 6.5; Appendix 3).

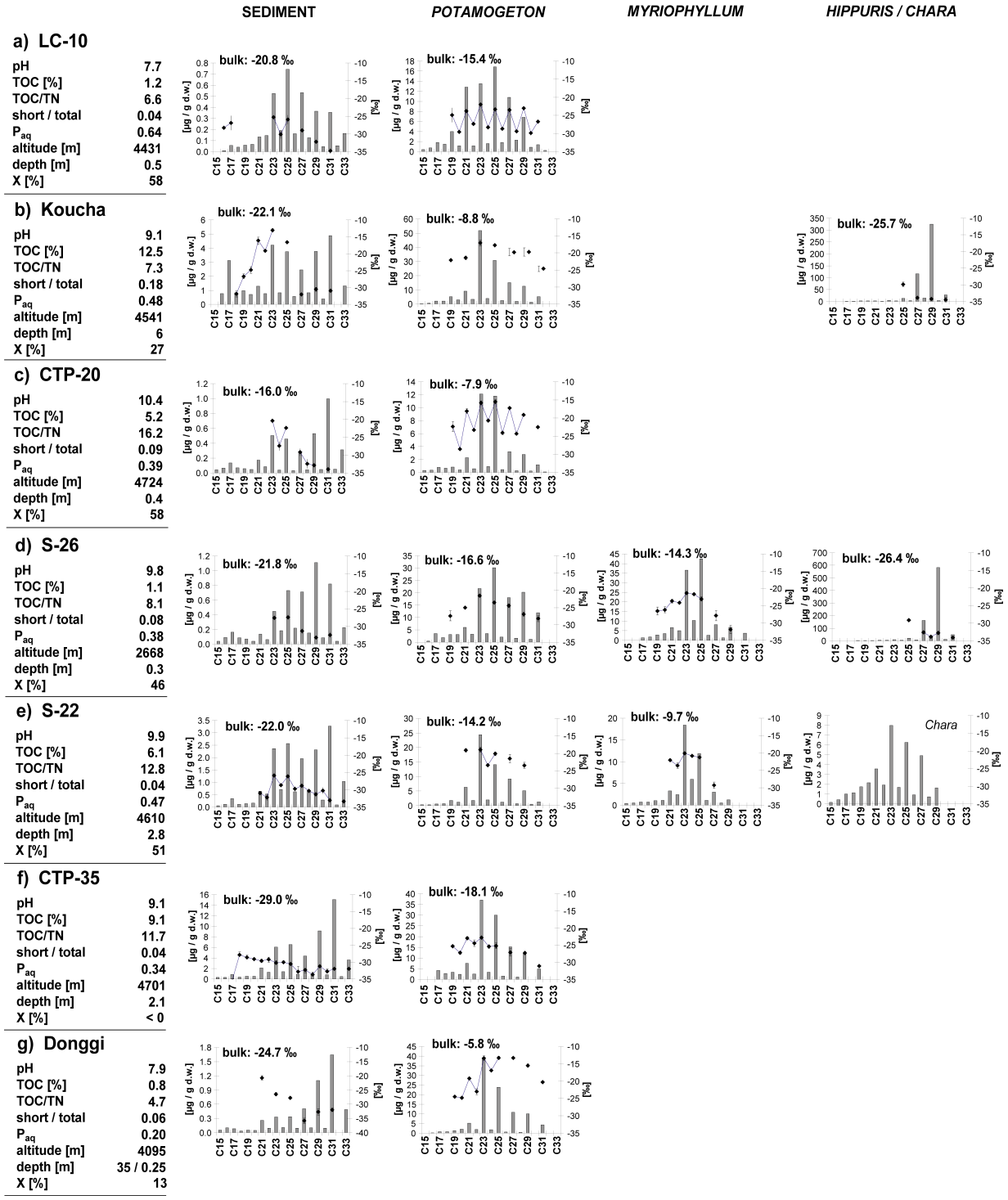

Figure 3.3: Comparison of *n*-alkane concentrations (grey bars) and carbon isotope values (black diamonds) of plants and sediments from seven lakes; x-axes indicate numbers of carbon atoms. "X" [%] is the calculated contribution of macrophytes to the sedimentary TOC (see section 3.5.3.)

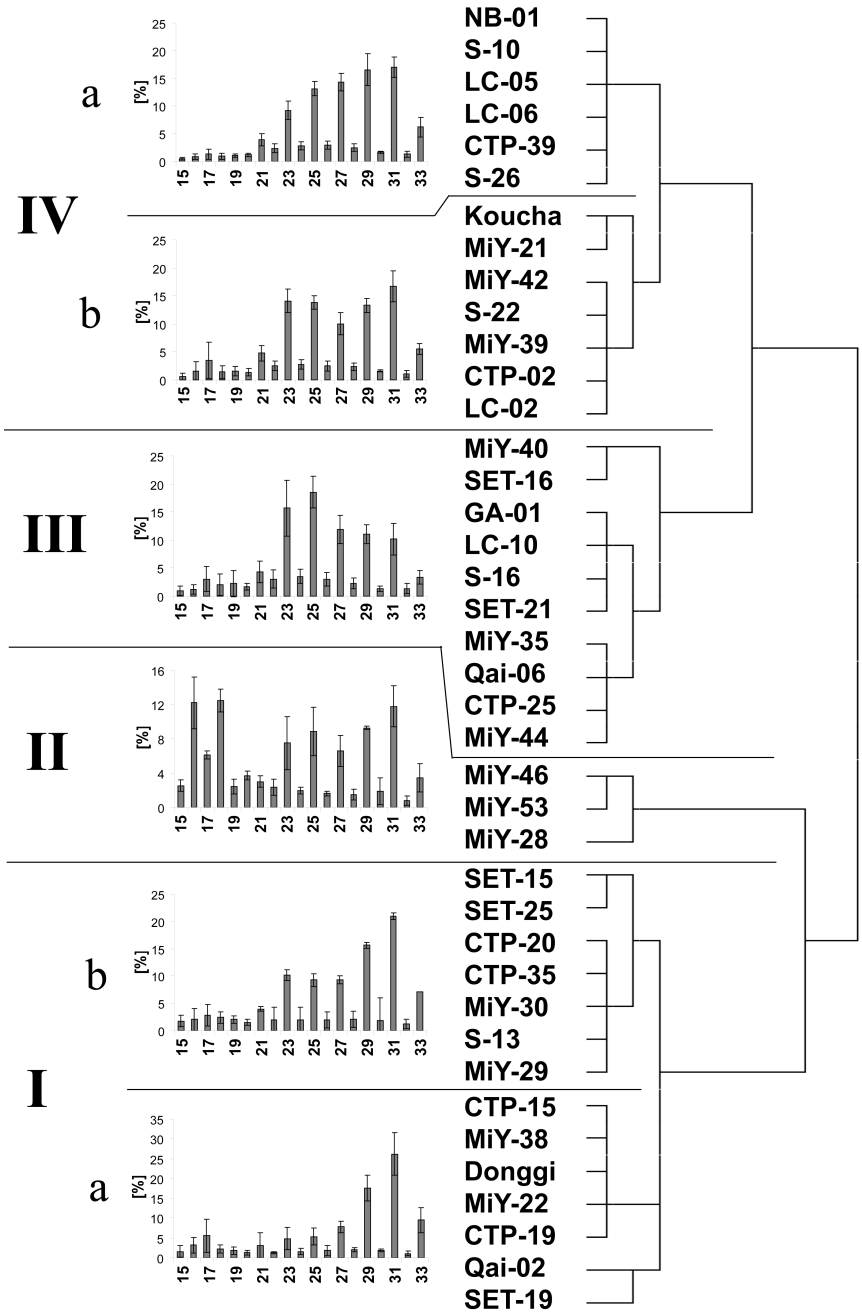

Figure 3.4: Dendrogram of sediment samples, clustered by *n*-alkane distributions. Histograms showing the average *n*-alkane distribution including standard deviation of the respective cluster; x-axes indicate carbon numbers of *n*-alkanes

3.4.3 Carbon isotopes of *n*-alkanes in plants and sediments

Generally, *n*-alkanes of plants are depleted in ^{13}C compared to the bulk biomass (Table 3.1). If samples of submerged macrophytes show relatively high bulk $\delta^{13}C$ values, shifts towards less negative values (up to -13.3‰) are also visible for the *n*-alkanes (Fig. 3.5a). This shift is most prominent for odd-numbered, mid-chain *n*-alkanes (C_{23}, C_{25} and C_{27}), but is also visible for C_{29}, C_{31} and C_{21}. Even-chain *n*-alkanes are generally more negative than odd-chain *n*-alkanes. Lipids of *Hippuris* have quite negative values for the dominant *n*-alkanes C_{27} and C_{29} ($\approx$ -33‰), compared to corresponding *Potamogeton* and *Myriophyllum* samples, but they also show a shift towards less negative values for the less abundant homologue C_{25}. $\delta^{13}C$ valuesof *n*-alkanes in most sediments show relatively little variations in the long-chain range (Fig. 3.5b). However, in a range of samples a shift towards less negative values, up to -13.0‰, is observed for mid-chain *n*-alkanes. In that case, the odd-numbered *n*-alkanes are again more enriched in ^{13}C than the even-numbered ones, resulting in a zigzag pattern. A complete list of $\delta^{13}C$ values of *n*-alkanes in sediments is provided in Table 3.2.

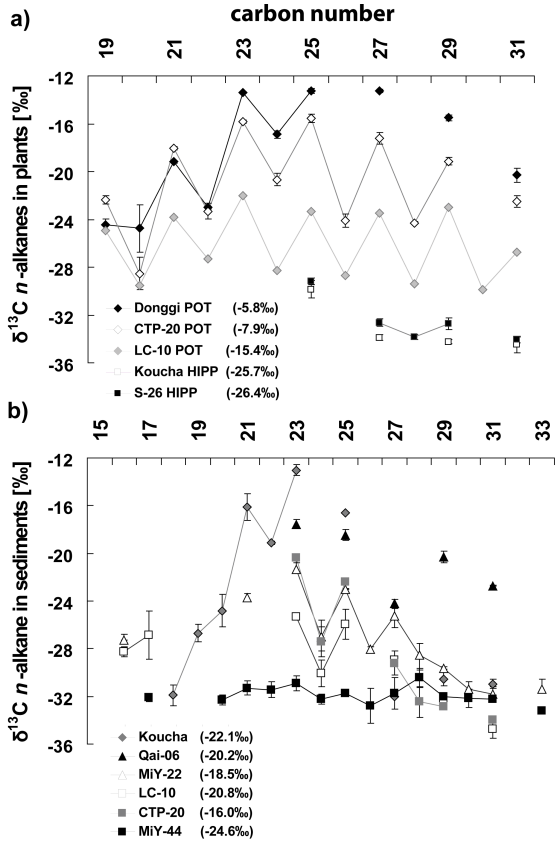

Figure 3.5: (a) $\delta^{13}C$ values of *n*-alkanes of three *Potamogeton* samples (POT, rhombuses) with differing bulk $\delta^{13}C$ values (in brackets) and of two *Hippuris* samples (HIPP, squares). (b) $\delta^{13}C$ values of six selected sediment samples illustrating the range of variability. $\delta^{13}C_{TOC}$ values in brackets.

3.5 Discussion

3.5.1 Aliphatic lipids of macrophytes

Our results confirm that submerged macrophytes (in our case *Potamogeton*, *Myriophyllum*, *Batrachium*) consist mainly of mid-chain *n*-alkanes with a maximum at C_{23} and C_{25}, in contrast to the emergent macrophyte species *Hippuris*, whose dominant *n*-alkanes are C_{27} and C_{29} (Fig. 3.2), as described by Ficken et al. (2000) and Mead et al. (2005). However, a comparison of all plant samples also shows, that the pattern can vary markedly within one species and that also long-chain *n*-alkanes C_{27}, C_{29} and C_{31} can be highly abundant in submerged plants as visible at some *Potamogeton*-samples (Fig. 3.3a and d) and the *Batrachium*-sample (Fig. 3.2).

Aquatic macrophyte samples with enhanced abundances of nC_{27} and nC_{29} appear to be characteristic for shallower lakes (Fig. 3.3a and d). In Fig. 3.6, the ratio nC_{25}/nC_{23} in relation to sample depth of submerged plants and macroalgae is plotted. All samples, except the *Potamogeton*-sample from Donggi Cona, which were derived from the shallow lakes or the shallow parts of the lakes showed significantly higher nC_{25}/nC_{23} ratios than samples derived from greater depths. Higher proportions of long-chain *n*-alkanes in plant leafs result in a thickened wax layer, which has been interpreted as a reaction to environmental influences like drought to prevent water loss in *Betula pendula* (Pedentchouk et al., 2008). Submerged plants growing at shallow spots are more exposed to environmental influences than plants in deeper parts of a lake. We hypothesize that an increasing biosynthesis of nC_{25} in favor of nC_{23} might be a first reaction of the plant to adapt to those influences e.g. to an increasing exposure to sunlight. The enhanced biosynthesis of nC_{27} and nC_{29} could be a result of partial exposure to air when the water level drops during dry episodes and the submerged plants experience emergent conditions. This could be imaginable for many of the smaller and shallower Tibetan lakes of which some fell subsequently dry. In contrast,

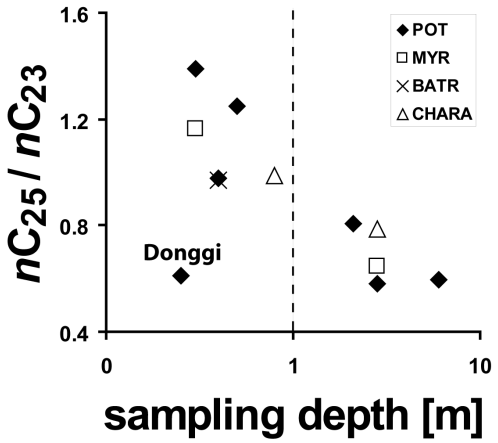

Figure 3.6: nC_{25} to nC_{23} ratio in all *Potamogeton*, *Myriophyllum*, *Chara* and *Batrachium* samples versus sample depth (logarithmic scale)

bigger lakes like Donggi Cona (maximum water depth 90 m, area 230 km²) react slower to effective moisture changes and macrophytes, even when growing in shallow parts, keep submerged throughout the year. No trend of higher total *n*-alkane concentrations at low water depths can be observed in submerged plant samples. In contrast, emergent plants contain about five- to tenfolds higher concentratins of *n*-alkanes than submerged species (Table 3.1) which is important to consider when lipid patterns of sediment samples are interpreted. Obviously, submerged species react to environmental influences with a shift towards a synthesis of long-chain homologues and not with an increased production of total lipids. Both *Chara* samples show an *n*-alkane pattern similar to submerged plants, which is in agreement with results from Nunez et al. (2002). This might be due to the fact that macroalgae like Charophyceae are, in contrast to microalgae, closely related to higher plants with respect to their lipid biosynthetic pathway (Schwender et al., 2001; Rontani and Volkman, 2003).

Another way, how submerged macrophytes could possibly contribute to long-chain *n*-alkanes in sediments, is by conversion of unsaturated long-chain compounds detected in *Potamogeton* samples (Fig. 3.2b) to saturated compounds . This has previously been hypothesised for the alga *Botryococcus braunii* A race, which produces long-chain *n*-alkenes and *n*-alkadienes (Metzger and Largeau, 2005). It was proposed, that those could be transformed to saturated compounds during early diagenesis (Lichtfouse et al., 1994; Grice et al., 1998; Chikaraishi and Naraoka, 2007; Zhang et al., 2007). The complete absence of unsaturated long-chain compounds in all of the surface sediment samples give evidence for an early transformation of those compounds.

Due to fractionation steps in biosynthesis, *n*-alkanes are usually depleted in ^{13}C in contrast to the bulk biomass of a plant (Park and Epstein, 1961; Collister et al., 1994; Chikaraishi et al., 2004). Hereby, odd-chain *n*-alkanes are often isotopically less depleted than even-chain *n*-alkanes, possibly due to different fractionation processes in the respective biosynthetic pathways, resulting in a zigzag pattern of $\delta^{13}C$ values (Fig. 3.5) (Collister et al., 1994; Canuel et al., 1997, Bi et al., 2005; Chikaraishi and Naraoka, 2007). In our *Potamogeton* samples, the $\delta^{13}C$ values of the *n*-alkanes show a good correlation with values of bulk biomass. Correlations are best for nC_{25} ($R^2 = 0.97$), nC_{23} ($R^2 = 0.95$), but are also significant for nC_{29} ($R^2 = 0.94$) and nC_{27} ($R^2 = 0.93$) and nC_{31} ($R^2 = 0.88$) (Fig. 3.7a). However, $\Delta\delta_{bulk/alkane}$ i.e. the offset between $\delta^{13}C$ of *n*-alkane and $\delta^{13}C$ of bulk biomass of the *Potamogeton* is not constant but seems to become bigger with increasing bulk $\delta^{13}C$ values (Fig. 3.7b). This is most pronounced for nC_{21} ($R^2 = 0.75$) and nC_{23} ($R^2 = 0.72$) e.g. $\Delta\delta_{bulk/alkane}$ ranges from 4.8 to 8.3 for nC_{23}. With increasing chain-length, when $\delta^{13}C$ values of odd-chain *n*-alkanes become increasingly negative (Table 3.1), this effect becomes less visible. It is known that *Potamogeton pectinatus*, *Myriophyllum spicatum*, and aquatic *Ranunculaceae* (to which *Batrachium bungei* belongs) are able to switch to HCO_3^- - uptake if CO_2 is limited (Allen and Spence, 1981; Van den Berg et al., 2002). In

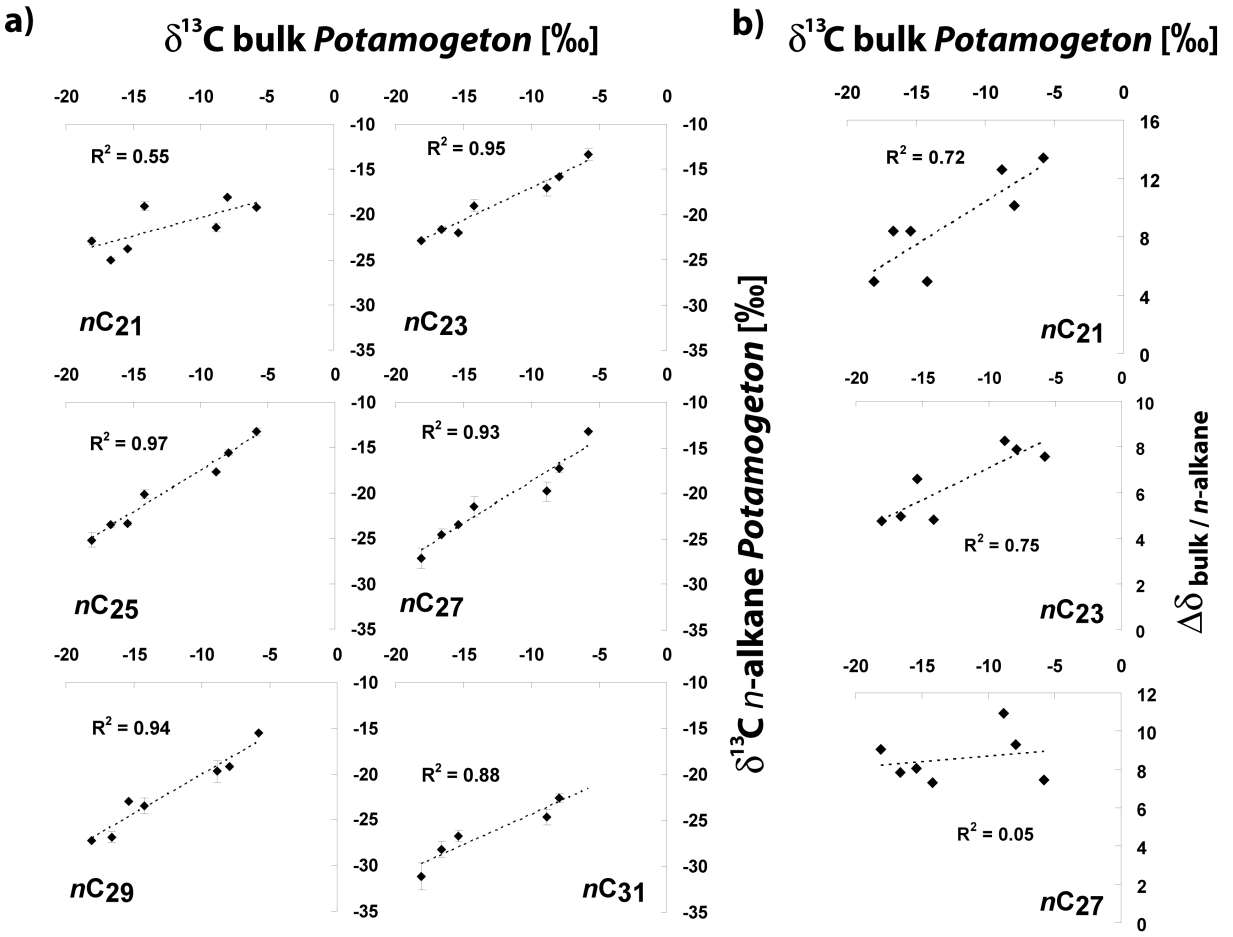

Figure 3.7: (a) Correlation between δ^{13}C values of *n*-alkanes and bulk biomass in *Potamogeton* samples. (b) $\Delta\delta_{bulk/n-alkane}$ i.e. offset between δ^{13}C values of bulk plant tissue and *n*-alkanes in *Potamogeton* correlated with bulk δ^{13}C values of *Potamogeton* samples

contrast, *Hippuris* is an obligate CO_2 user (Maberly and Spence, 1983). The δ^{13}C value of HCO_3^- is about 10‰ higher than the δ^{13}C value of dissolved CO_2 (Mook et al., 1974, Prins and Elzenga, 1989), which consequently results in a shift towards more positive δ^{13}C values of bulk biomass as well as lipids of the assimilating plants. Our results suggest an enhanced isotopic fractionation during lipid synthesis if a more ^{13}C enriched carbon source like HCO_3^- is taken up by the plant, leading to the above described increasing offsets. However, to confirm this hypothesis, the isotopic signatures of non-waxy plant compounds e.g. carbohydrates must be known.

3.5.2 *n*-Alkane pattern as an indicator for the source of sedimentary organic matter

An occasionally used proxy for the origin of the organic matter is the TOC/TN ratio. In lakes with low TOC content, the TOC/TN ratio has to be interpreted with caution as relatively high proportions of residual inorganic nitrogen could decrease the ratio (Meyers, 2003). Generally, organic material with a TOC/TN ratio <10 is considered to be of

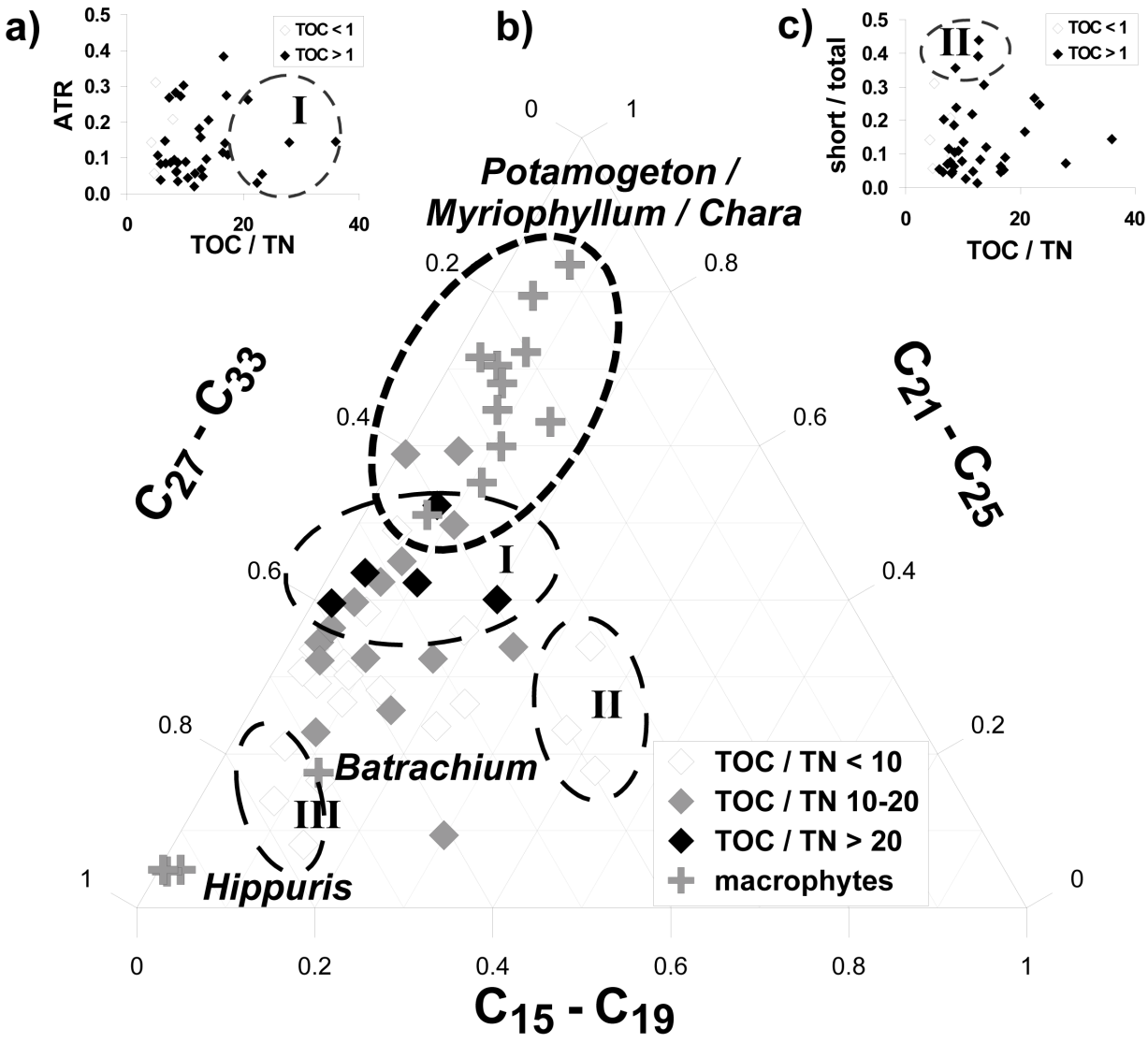

Figure 3.8: (a) Cross plot of ATR versus TOC/TN. Samples with low TOC (< 1%): open symbols. (b) Ternary diagram showing distributions of short-, mid- and long-chain *n*-alkanes in sediment and plant samples. Groups: refer to text. (c) Cross plot of short-chain to total *n*-alkane ratio versus TOC/TN.

aquatic origin (bacteria and algae), while vascular plants are postulated to have ratios >20 (Meyers and Ishiwatari, 1993). However, it is also known that the alga *Botryococcus braunii* for instance has a high TOC/TN ratio (Huang et al., 1999; Ficken et al., 2002). Aquatic macrophytes have been found to have similar or lower ratios than terrestrial plants. Cloern et al. (2002) for instance found ranges from 8.0 to 16.1 in 35 samples of submerged macrophytes from the San Francisco Bay Area. Submerged macrophyte samples from our sample set have TOC/TN ratios from 8.6 to 29.6, while emergent macrophytes range from 7.1 to 11.5 (Table 3.1).

Fig. 3.8a compares the TOC/TN ratios of our samples with the aquatic-terrestrial-ratio (ATR) calculated from the distribution of *n*-alkanes. In fact, samples with high TOC/TN

(> 20) have a low ATR (< 0.15) in four of the five relevant samples (group I). Thus, it seems that a high TOC/TN value is at least a reliable indicator for input derived from higher plants, which include aquatic macrophytes. However, the proportional input of aquatic plants, possibly enhancing the TOC/TN, remains unclear. A ternary diagram revealed the relative abundances of short- (C_{15} to C_{19}), mid- (C_{21} to C_{25}) and long-chain (C_{27} to C_{33}) *n*-alkanes in relation to the TOC/TN-ratio (Fig. 3.8b). The lipids in samples with TOC/TN > 20 (group I) are apparently not only derived from terrestrial input as the *n*-alkane pattern provides evidence for a significant macrophyte source. The group of samples with high relative concentrations of short-chain *n*-alkanes (group II; cluster II in Fig. 3.4) is clearly segregated in the diagram. In this case, the relatively high contribution of algae or bacteria to the sedimentary organic matter, deduced from the high abundance of short-chain *n*-alkanes, is supported by a low TOC/TN-ratio. On the other hand, a group of samples (III) with also low TOC/TN ratio is dominated primarily by long-chain *n*-alkanes, similar to *Batrachium* and *Hippuris*, which leads to the conclusion that emergent or submerged macrophytes reduce the TOC/TN ratio in these lakes. These results show that due to the broad possible range of TOC/TN ratios of aquatic macrophytes, this proxy may be useless in lakes with a high abundance of these contributors. However, the inclusion of the lipid pattern can help to decipher the sources of the organic matter in such cases. Additionally, when *n*-alkane ratios are used for assessing the aquatic input, bacterial even-chain *n*-alkanes and aquatic macrophyte derived mid-chain *n*-alkanes should be included into the ratio. In Fig. 3.8c, a ratio of short-chain/total *n*-alkanes is plotted versus the TOC/TN. In our case a ratio >0.35 is a reliable indicator for a more or less exclusive aquatic input. This result cannot be derived when using the ATR-ratio.

3.5.3 Contribution of aquatic macrophytes to the sedimentary organic matter

To illustrate how local conditions influence the biomarker composition and the isotopic signature of the sediments, selected lakes (Fig. 3.3) will be discussed in more detail below. Lake LC-10 is a small and shallow high altitude lake with alpine meadows in the catchment area. pH (7.7), sedimentary TOC content (1.2%), and *n*-alkane concentrations are relatively low (Fig. 3.3a). The TOC/TN ratio is also low (6.6), leading to the assumption that bacteria or algae might contribute to the TOC. This could not be confirmed from the *n*-alkane pattern, which is dominated by odd-chain C_{23} to C_{31} *n*-alkanes (low short/total; high P_{aq}). $\delta^{13}C$ values of bulk material as well as *n*-alkanes of *Potamogeton* samples are at the lower end of the range of determined values. However, the influence of the macrophytes is still visible in isotopic signatures of mid-chain *n*-alkanes, which are about 8‰ enriched in ^{13}C compared to long-chain homologues. Koucha lake (Fig. 3.3b) is deeper than lake LC-10, but the influence of the macrophytes (which are in this case highly enriched in ^{13}C) on the sediments is visible there as well. There is a distinct difference of about 15‰ between isotopic signals of mid- and long-chain *n*-alkanes. While $\delta^{13}C$ values of the former are in

the range of δ^{13}C values of the corresponding *Potamogeton* sample, the latter show values in the range of *n*-alkanes from emergent macrophytes like in the corresponding *Hippuris* sample (≈ -33‰) or in range of expected values of lipids derived from terrestrial C_3 plants (Park and Epstein, 1961; Collister et al., 1994). The high abundance of nC_{31} could be an indicator for an input of grasses (Cranwell, 1973; Schwark et al., 2002) derived from the alpine meadows in the catchment area. The step-like decrease in δ^{13}C from nC_{25} to nC_{27} is remarkable, as in other samples, e.g. the sediment sample from the already mentioned lake LC-10, a gradual decrease is observable. Lake CTP-20 (Fig. 3.3c) is another example for an observable influence of relatively enriched δ^{13}C values of macrophyte-derived organic matter on the δ^{13}C value of the sediments.

In lakes S-26 and S-22 (Fig. 3.3d and e), this shift towards higher values is less pronounced. However, the δ^{13}C values of the corresponding submerged species are comparably low for *n*-alkanes as well as for bulk material. Lake CTP-35 (Fig. 3.3f) has the lowest δ^{13}C values of bulk-material and *n*-alkanes in both plants and sediments. Lake Donggi Cona (Fig. 3.3g) is an example of a lake where the rather high bulk δ^{13}C values of the plants do not seem to influence the isotopic composition of the sediments. Lake Donggi Cona is a rather big lake (8 to 30 km) with little TOC (0.8%) and low concentrations of lipids, which is also deeper (up to 90 m) and has a lower pH (7.9) than the typical shallow lakes on the Plateau. The TOC/TN value is very low (4.7), but short chain *n*-alkanes are hardly abundant. δ^{13}C values are low for the bulk organic matter and there is only a small shift towards higher values in mid-chain *n*-alkanes even if δ^{13}C values of the submerged species found in the lake are rather high. Since relative proportions of nC_{23} and nC_{25} are low in the *n*-alkane pattern of the sediment, which is dominated by nC_{29} and nC_{31}, this leads to the assumption that the proportional contribution of the macrophytes to the sediments is also low. Keeping in mind that the sediment was sampled in a depth of 37 m below the limit of macrophyte growth, it seems that little plant material is transported to greater depths and the small amounts of lipids found in the sediment are either terrestrially derived or possibly originate from hydrocarbon producing algal species like *Botryococcus braunii*.

The *n*-alkane patterns showed in about 75% of the sediment samples high relative amounts of mid-chain *n*-alkanes (Figs. 3.3 and 3.4). The shift towards higher δ^{13}C values for these mid-chain *n*-alkanes in many lakes (Figs. 3.3 and 3.5) indicate a significant input of aquatic macrophytes to the sedimentary organic matter. The correlation between $\delta^{13}C_{TOC}$ of sediments and the corresponding 21 available *Potamogeton* samples is rather low ($R^2 = 0.38$; under the premise that the samples from Lake Donggi Cona are not included into the correlation due to there origin from different sample spots) (Fig. 3.9a). However, the influence of the water plants upon the isotopic signal of the sediments cannot be neglected since the wide range of $\delta^{13}C_{TOC}$ values in sediments cannot be explained by influence of C_4-vegetation, which is absent, or by increased primary productivity, which

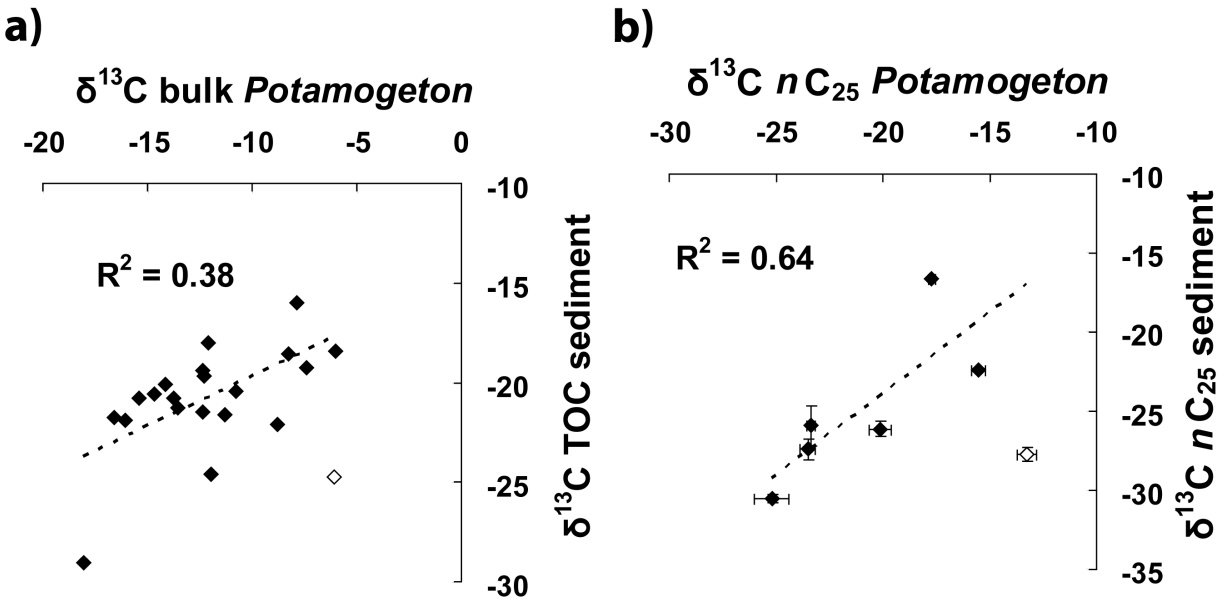

Figure 3.9: (a) Correlation between $\delta^{13}C_{TOC}$ of sediments and corresponding samples of *Potamogeton*. Sample from Donggi Cona (open symbol) is not included into the correlation. (b) Correlation between $\delta^{13}C$ values of nC_{25} in sediment and *Potamogeton* samples.

does not result in such wide ranges. When comparing $\delta^{13}C$ values of mid-chain *n*-alkanes from plants with $\delta^{13}C$ values of mid-chain *n*-alkanes from corresponding sediments, we found a fairly good correlation for nC_{25} ($R^2 = 0.64$) (Fig. 3.9b) and also nC_{23} ($R^2 = 0.64$; not shown) while correlation is much weaker for nC_{27} ($R^2 = 0.19$). Under the aspect that there are numerous other contributors to the $\delta^{13}C_{TOC}$ value and also to the nC_{23} value than *Potamogeton* (e.g. other aquatic macrophyte species, terrestrial plants, *Sphagnum* sp. and algae), it is remarkable that the trend towards higher values in sediments with corresponding ^{13}C-enriched *Potamogeton* samples is clearly visible.

Reconsidering the increasing offset between bulk $\delta^{13}C$ values and $\delta^{13}C$ values of *n*-alkanes in macrophytes (Fig. 3.7b), it is interesting that a similar trend can also be found in the sediments. In Fig. 3.10a, the offsets between $\delta^{13}C_{TOC}$ and weighted averages of $\delta^{13}C$ values of odd-chain *n*-alkanes in the range C_{21} to C_{33} in sediments are plotted versus the $\delta^{13}C_{TOC}$. Despite that there are two outliers, samples with a higher $\delta^{13}C_{TOC}$ show a tendency towards a bigger offset. We conclude that this offset might on the one hand serve as a tool for assessing the degree of bicarbonate assimilation, and on the other hand -additionally to the *n*-alkane pattern- could give a hint to the proportional input of submerged macrophytes to the sediment.

To assess the macrophyte contribution to the TOC and to the mid-chain *n*-alkanes in a quantitative manner, a simple binary isotopic model was applied:

$$\delta^{13}C_{sediment} = x \times \delta^{13}C_{macrophyte} + (1 - x) \times \delta^{13}C_{terrestrial}$$

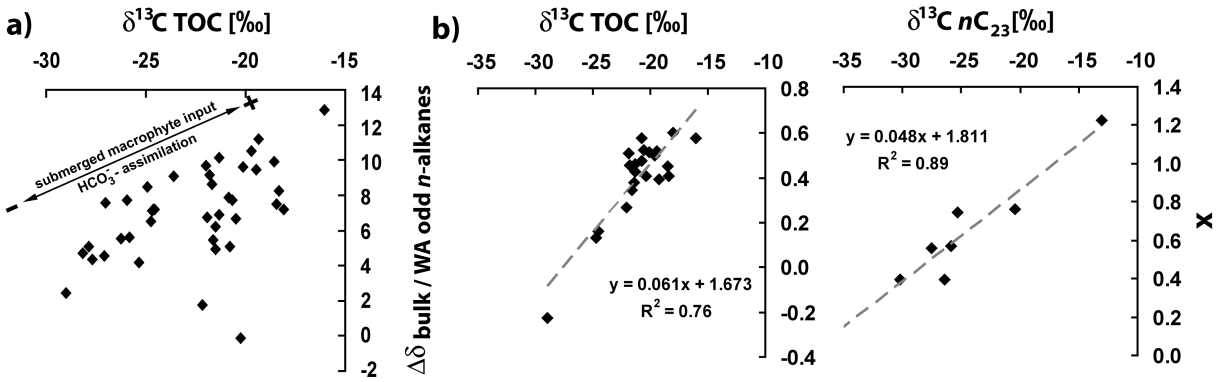

Figure 3.10: (a) Offset between $\delta^{13}C_{TOC}$ values and the weighted average (WA) of $\delta^{13}C$ values of odd-chain *n*-alkanes (C_{21} to C_{33}) in sediments in relation to $\delta^{13}C$ values. (b) Correlation between calculated contributions of aquatic macrophytes x to sediments and respective $\delta^{13}C$ values of TOC and nC_{23} in sediments

For $\delta^{13}C_{sediment}$ and $\delta^{13}C_{macrophyte}$, measured $\delta^{13}C$ values of TOC and nC_{23} can be used. For the $\delta^{13}C$ values of the plants, mean values of submerged macrophytes (see Table 3.1 and Appendix 3) were calculated, as long as available for the respective sites. For $\delta^{13}C_{terrestrial}$ a roughly estimated value for C_3-vegetation was applied, i.e. -27‰ for $\delta^{13}C_{TOC}$ and -35‰ for $\delta^{13}C_{nC_{23}}$. Then the relative contributions of the macrophytes "x" to the sediments were calculated. They range from <0 (lake CTP-35) to 58% (lake MiY-28) for TOC, (mean: 40%; median 45%), and from 40% (lakes CTP-35 and Donggi Cona) to >100% (Lake Koucha) for nC_{23} (mean: 66%; median 56%) (Fig. 3.3). This approach is simplified, but could give at least a rough estimate over absolute contributions of submerged macrophytes to the TOC and to the *n*-alkanes in sediment samples. To calculate the macrophyte contributon, isotopic data of macrophytes are necessary. However, as shown in Fig. 3.10b, there are fair correlations between calculated contributions of macrophytes and $\delta^{13}C$ values of both TOC ($R^2 = 0.76$) and nC_{23} ($R^2 = 0.89$) in sediments. This suggests, that this model could also be used to calculate macrophyte contributions for samples of which no corresponding data from plants are available, e.g. in samples from sediment cores. Therefore, in Tibetan lakes, and possibly also in other regions were C_4 vegetation is absent, the relative contribution of macrophytes to the sedimentary organic carbon and to the mid-chain *n*-alkanes could be assessed by the carbon isotope signature of sedimentary TOC and nC_{23}. Nevertheless this approach has to be considered with caution due to the isotopic heterogenity of submerged macrophyes. For example in a lake with low $\delta^{13}C$ values of TOC or mid-chain *n*-alkanes, the contribution of macrophytes could still be high, if the latter are not significantly enriched in ^{13}C. This could be the case in lakes with low or intermediate pH or in low productive lakes where carbon is not limited and bicarbonate assimilation is low.

3.5.4 Implications for palaeolimnology

The different kinds of carbon metabolism in aquatic plants result in a wide range of bulk $\delta^{13}C$ values, which also influences the carbon isotopic composition of the organic matter in sediments. The dominant carbon species in the water depends on the pH. The carbon equilibrium suggests a predominance of dissolved CO_2 until a pH of 5.4. In the range from 5.4 to 7.4, the concentration of CO_2 decreases in favor of HCO_3^- until the latter is the dominant species at pHs higher than 7.4 (Stumm and Morgan, 1981). Our sampled lakes generally show pHs in the range from 7.0 up to 10.7 (Appendix 3). Consequently bicarbonate uptake is expected to play an important role in many of these lakes. This explains a tendency to high $\delta^{13}C$ values in most of the plant samples. However, no correlation can be observed between pHs and $\delta^{13}C$ values of bulk material of *Potamogeton* samples ($R^2 = 0.001$; not shown). pHs in the lakes of which a corresponding bulk $\delta^{13}C$ value of a *Potamogeton* sample is available, range, except in two samples, from 9.1 to 10.8 and thus dissolved CO_2 is negligible and other factors than pH changes are the main driving force for varying isotopic discrimination. This could be HCO_3^--limited conditions due to high productivity at dense plant stands or variations in the isotopic signal of the assimilated HCO_3^-, which can be shifted towards higher values at conditions of increased primary productivity (Leng and Marshall, 2004). To assess the latter, $\delta^{13}C$ of the carbonate in the hardwater-lakes would have to be considered. Bulk organic carbon, covering a pH range from 7.0 to 10.8, at least shows a tendency towards lower values at pHs <8 ($R^2 = 0.32$; not shown). A better calibration is difficult due to the above mentioned reasons and due to the fact that the pH in a lake could vary up to 2 units during the day due to photosynthetic activity (Wetzel, 2001), but values are only available for the time of sampling. In Tibetan lakes with high pHs, changes of $\delta^{13}C$ values of mid-chain *n*-alkanes (like nC_{23}) throughout sediment cores are thus probably better interpreted with respect to changes in palaeoproductivity than to pH changes. In an ideal case the $\delta^{13}C_{nC23}$-curve is compared to a $\delta^{13}C_{TIC}$-curve to assess the influence of possible variations in the carbon isotope signal of the carbon source.

Bulk $\delta^{13}C$ values of plant remains in sediment cores would be the best and easiest to apply proxy to reconstruct past conditions for the plants. If no plant remains occur in the core, our results show that the $\delta^{13}C$ values of mid-chain *n*-alkanes can serve as a proxy. The relative contribution of macrophyte derived material to the sediment can additionally to the *n*-alkane pattern be estimated from $\delta^{13}C$ of TOC or mid-chain *n*-alkanes (as also shown by Mead et al., 2005) or by the offset between $\delta^{13}C$ values of *n*-alkanes and TOC.

In certain lake systems, the abundance of aquatic macrophytes might complicate the interpretation of organic geochemical proxies, especially of $\delta^{13}C_{TOC}$ of sediments. This is unlikely to be an issue for deep and big lakes, but many records from smaller lakes might be affected. On the other hand, a high abundance of macrophytes as occurring on the Tibetan Plateau make them potentially useful for applications like hydrogen isotope

analyses of mid-chain *n*-alkanes, since it is known that macrophytes can record δD values of lake waters (Huang et al., 2004; Hou et al., 2007).

Bicarbonate assimilating macrophytes occur worldwide, thus our results are not only restricted to our study site, but have to be taken into consideration also in other regions were organic proxies are used for palaeolimnological purposes. Variations of $\delta^{13}C_{TOC}$ in palaeorecords from the Tibetan Plateau could be with high probability interpreted with respect to changes in primary or macrophyte productivity due to the absence of C_4-vegetation. However, in ecosystems where C_4-plants are abundant, care should be taken when bulk organic carbon values are used and there is a suspect that aquatic macrophytes might influence the composition of the sedimentary organic matter. In this case, a biomarker approach should be applied to distinguish between the two effects.

3.6 Conclusions

Our results indicate that aquatic macrophytes provide considerable contributions to the sedimentary organic matter in certain environments (up to 60% to TOC and up to 100% to mid-chain *n*-alkanes) and profoundly influence organic matter based proxies like TOC/TN ratios and $\delta^{13}C_{TOC}$. This fact may not be neglected and might complicate the interpretation of these proxies in sediment cores, not only those derived from the Tibetan Plateau, but from all regions where aquatic macrophytes are abundant. Due to different kinds of carbon metabolism, induced by limited CO_2 availability in alkaline and/or shallow lakes with a dense macrophyte population, submerged macrophytes can have wide ranges of bulk $\delta^{13}C$ values within one species. This has an impact on the $\delta^{13}C_{TOC}$ of sediments, which has to be considered when such data are interpreted in palaeoenvironmental studies and aquatic macrophytes are abundant (or might have been abundant) in the studied lake ecosystem. In plant samples, the $\delta^{13}C$ values of *n*-alkanes directly correlate with bulk $\delta^{13}C$ values and shifts towards higher values can be seen in odd- as well as in even-chain *n*-alkanes in the chain length range of C_{21} to C_{31}. Hereby, isotopic fractionation during *n*-alkane biosynthesis in plants increases with increasing chain length and when more ^{13}C-enriched carbon sources (like HCO_3^-) are assimilated. The relatively high $\delta^{13}C$ values of *n*-alkanes in aquatic plants can be seen as well in the corresponding sediments. We found that in some cases, submerged macrophytes have a tendency to an increased production of long-chain *n*-alkanes and propose that this most likely happens in very shallow lakes were macrophytes experience emergent conditions during dry periods. *Potamogeton pectinatus* possibly also contributes to long-chain *n*-alkanes in sediments by early diagenesis of unsaturated long-chain compounds, detected in all samples of this species. Nevertheless, it seems that this contribution can be neglected as soon as the input of terrestrial or emergent macrophytes is high enough, since those plants contain five- to tenfold higher concentrations of lipids than submerged plants. Consequently, the shifts towards higher

δ^{13}C values are best visible for mid-chain *n*-alkanes, even in lakes containing macrophytes with an enhanced production of long-chain homologues. The correlation of δ^{13}C values with environmental parameters e.g. pH is difficult due to multiple other influences, but changes in the isotopic composition of plant remains or of mid-chain *n*-alkanes in sediment cores are probably best to be interpreted with respect to changes of primary or macrophyte productivity.

4 Biomarker and compound-specific δ^{13}C evidence for changing environmental conditions and carbon limitation at Lake Koucha, eastern Tibetan Plateau

Abstract

A sediment core from Lake Koucha (eastern Tibetan Plateau) was investigated using organic biomarkers and their stable carbon isotope signatures. The correlation between TOC content, total amount of aquatic macrophyte-derived *n*-alkanes (e.g. nC_{23}) and δ^{13}C values of TOC and nC_{23} indicates that Lake Koucha was macrophyte-dominated before 8 cal ka BP. Shortly after the lake turned from a saline to a freshwater system at 7.2 cal ka BP, a variety of algal and bacterial markers such as hopanoids and isoprenoids emerged, of which phytane, pentamethylicosene (PMI), moretene and diploptene are particularly abundant. Phytane and PMI show different isotopic signals (≈ -18‰ and ≈ -28‰, respectively), which indicates that they originated from different sources. Phytane may have been derived from cyanobacteria, while methanogenic archaea may be the source of PMI. The isotopic depletion of diploptene and moretene (≈ -60‰) indicates the presence of methanotrophs. After 6.1 cal ka BP, the saturated C_{20} highly branched isoprenoid (HBI) became the dominant constituent of the aliphatic hydrocarbon fraction. Such dominance has rarely been reported in lacustrine environments, and indicates a strong presence of algae (most likely diatoms) or cyanobacteria. At 4.7 cal ka BP, the appearance of an unsaturated C_{25} HBI, which is a specific biomarker for diatoms, was noted. Furthermore, the concentration of the C_{17} *n*-alkane increased in the uppermost two samples. These results suggest that the lake was phytoplankton-dominated during the last 6.1 ka. Relatively low biomarker concentrations and δ^{13}C values at 6.0, 3.1 and 1.8 cal ka BP indicate the occurrence of cool periods, which is in agreement with inferences from other locations on the Tibetan Plateau. The δ^{13}C values of nC_{23} range from -23.5 to -12.6‰, with high values at the peak of macrophyte abundance at ca. 11 cal ka BP and at the phytoplankton maximum between ca 6.1 and 2.8 cal ka BP. Thus, aquatic macrophyte-derived mid-chain *n*-alkanes have been found to be excellent indicators of carbon-limiting conditions, which lead to the assimilation of isotopically-enriched carbon species. The limitation of carbon sources could be a localized phenomenon occurring in dense plant stands (as in the older section of the core), or it may be induced by high primary productivity (as in the younger section). Since the δ^{13}C value of the inorganic carbon source may vary, the offset between the $\delta^{13}C_{nC_{23}}$ and $\delta^{13}C_{TIC}$ could serve as a more precise proxy for carbon-limiting conditions

in lacustrine environments, which could in turn be interpreted with respect to lacustrine palaeo-productivity.

4.1 Introduction

Owing to the strong control of the Tibetan Plateau on global atmospheric circulation patterns (Ruddiman and Kutzbach 1989), this area, and in particular its eastern part, has been increasingly the focus of palaeoenvironmental studies. Most of these studies have applied biological, sedimentological or geochemical proxies (Morrill et al., 2003; Wang et al., 2005; Herzschuh 2006; Chen et al., 2008). Despite the vast area of the Plateau and the number of studies conducted, organic biomarkers have seldom been used (Li et al., 1996; Wang and Zheng, 1998; Wang et al., 2004; Herzschuh et al., 2005; Liu et al., 2006, 2008; Zheng et al., 2007; Zhu et al., 2008; Mügler et al., 2009). Organic biomarkers in lake sediment records have been shown to be powerful tools for inferring past climatic and environmental conditions, especially if applied in combination with compound-specific isotope analysis (Freeman et al., 1990; Huang et al., 1999; Schouten et al., 2001, Street-Perrott et al., 2004). A range of plant-derived and/or microbial lipids may serve as specific or semi-specific biomarkers (Peters et al., 2005), and their isotopic signal may provide additional information regarding the sources of organic material and syn- and post-sedimentation processes (Hayes et al., 1990).

Hundreds of freshwater and salt lakes on the Tibetan Plateau provide an enormous source of palaeorecords. Many of these lakes are shallow and contain dense populations of aquatic macrophytes, which strongly influence the biomarker composition, e.g. the *n*-alkane pattern of sedimentary organic matter. The carbon isotope signal of many aquatic macrophyte species may exhibit a considerable range of values due to their variable carbon metabolism, which can switch from assimilation of dissolved CO_2 [CO_2(aq)] to HCO_3^- (bicarbonate) when CO_2 is limited (Allen and Spence 1981; Prins and Elzenga 1989). Bicarbonate is isotopically heavier than CO_2(aq), and consequently contributes to higher $\delta^{13}C$ values in the assimilating organism. Generally, a kinetic isotopic fractionation during carbon assimilation results in the discrimination against the heavy isotope (^{13}C). However, if demand exceeds supply, this discrimination decreases, resulting in enhanced uptake of ^{13}C (Fogel and Cifuentes, 1993; Burkhardt et al., 1999; Papadimitrou et al., 2005). In highly alkaline lakes, bicarbonate is the dominant carbon species (Stumm and Morgan, 1981), and thus a limitation will result in an enhanced uptake of ^{13}C-enriched bicarbonate and a corresponding increase in the $\delta^{13}C$ values of the consumer. This isotopic signal is then preserved in the sediments, and may be interpreted in terms of carbon-limited conditions in the lake, which can be induced by physical diffusion barriers (e.g. ice cover), high water temperature, salinity, pH, enhanced primary productivity or local carbon minima occurring in dense plant stands (Street-Perrott et al., 2004).

Lake Koucha, on the eastern Tibetan Plateau, is an alkaline lake (pH ≈ 9) with low electrical conductivity (0.502 mS/cm). The lake has been the subject of a multidisciplinary study involving bulk element, isotopic and ostracod analyses (Mischke et al., 2008) and a study of pollen (Herzschuh et al., 2009), which have provided insights into the lake and lake catchment history since the late glacial period. The data derived from these two studies suggest that, in comparison to present-day conditions, the region experienced reduced moisture availability during the early Holocene. This conclusion contradicts the general assumption that the Tibetan Plateau experienced a wet climate during this period, and has been attributed to enhanced evaporation due to higher temperatures, which may have outweighed any changes in precipitation in the semi-arid Koucha region. Mesohaline conditions between 16 and 10 cal ka BP, as well as increased salinities up to hyperhaline levels at 7.5 cal ka BP, indicate that the lake basin was closed during this period (Mischke et al., 2008). A drop in salinity, perhaps due to increased moisture availability, occurred between 7.3 and 6.5 cal ka BP, causing the lake to become an open freshwater system. This shift was accompanied by a rise in the $\delta^{13}C$ of total inorganic carbon (TIC) to +8‰. It has been suggested that a change from a macrophyte-dominated to a phytoplankton-dominated lake occurred during that time interval. At 6.6 cal ka BP, vegetation in the catchment shifted from that typical of a steppe environment to that of both alpine steppe and alpine meadow, suggesting the development of a cool and wet climate (Herzschuh et al., 2009).

The primary aims of this study were:

1. To obtain detailed knowledge about the contributors to the sediment organic matter in Lake Koucha by evaluating the concentrations and isotopic signals of biomarkers within the aliphatic fraction of the biomarker extract (containing *n*-alkanes, isoprenoid and hopanoid compounds)

2. To assess the applicability of $\delta^{13}C$ values of aquatic macrophyte-derived *n*-alkanes as a proxy for palaeo-productivity, using a sediment core that was thoroughly interpreted using other proxies, all of which suggested significant productivity changes since the late glacial.

4.2 Study site

Lake Koucha is situated on the Northeastern Tibetan Plateau (34.0° N; 97.2° E), on the southern slope of the Bayan Har mountain range, at an altitude of 4,540 m a.s.l (Fig. 4.1a). It is a freshwater lake with a maximum depth of 6.9 m and an area of 18 km². The lake is fed by several small rivers deriving from a swampy valley to the southeast. The outlet passes through another small lake 1 km north of Lake Koucha before discharging into the Yellow River (Fig. 4.1a). The relatively small catchment area (88 km²) is dominated

by alpine meadows, which are mainly composed of Kobresia. The lake itself is densely populated by aquatic macrophytes down to a depth of 4 m. *Potamogeton pectinatus* is the sole species present in the deeper part of the lake, whereas a mixture of *Potamogeton pectinatus* and *Batrachium bungei* occupies the shallower parts (Herzschuh et al., 2009).

The regional climate is monsoon-controlled. Summers are cool and wet, with moisture derived mainly from the Southeast Asian monsoon branch, which is drawn by a strong low-pressure system above the Tibetan Plateau. Winters are influenced by the Mongolian-Siberian high-pressure cell, resulting in cold and dry conditions. Data obtained from a climate station at Qingshuihe (4,415 m a.s.l., 20 km south of Lake Koucha) suggest a mean annual temperature of -4.8 °C and a mean annual precipitation of 511 mm, with most of the precipitation occurring between June and September (Fan et al., 2004).

4.3 Materials and methods

4.3.1 Core collection and chronology

A 5.6-m-long sediment core (Fig. 4.1b) was obtained from Lake Koucha in March 2003, using a Livingstone piston corer (Stitz). The lower part of the core (5.60 - 4.23 m), comprised of dark-grey loam with quartz and granite gravels, was excluded from our biomarker study. We focused on the light-grey, silty and calcareous sediments in the upper part of the core (4.23 - 0 m) with total organic carbon (TOC) contents between 5 and 25% . The results of analyses of the TOC contents, the δ^{13}C of the TOC and the TIC were published in Mischke et al. (2008). The age model was derived by linear interpolation between four dated samples of pollen concentrate and one dated sample of the alkali-soluble fraction of the bulk organic carbon (Fig. 4.1b). The age of the core top was assumed to be zero. The calendar years were calibrated from the ^{14}C years using Calib (Reimer et al., 2004). A detailed description of the bulk parameters and the age model are given in Mischke et al. (2008).

4.3.2 Biomarker extraction, analysis and quantification

Samples were freeze dried and milled prior to extraction with an accelerated solvent extractor (ASE) (Dionex, Sunnyvale, USA). The extraction was done with dichloromethane: methanol (9:1) at 76 bar and 100 °C. The aliphatic hydrocarbon fractions were isolated with liquid chromatography, using a medium pressure liquid chromatography (MPLC) system (Radke et al., 1980). As quantification standard, 5α-androstane (Sigma-Aldrich, St. Louis, USA) was added to the extracts prior to MPLC. The compounds within the aliphatic fraction were quantified using an Agilent 6890 GC-FID with an injector heated from 40 °C to 300 °C at 700 °C/min using splitless injection. For the separation of the compounds, an Ultra-1 fused silica capillary column (50 m length, 0.2 mm inner diam-

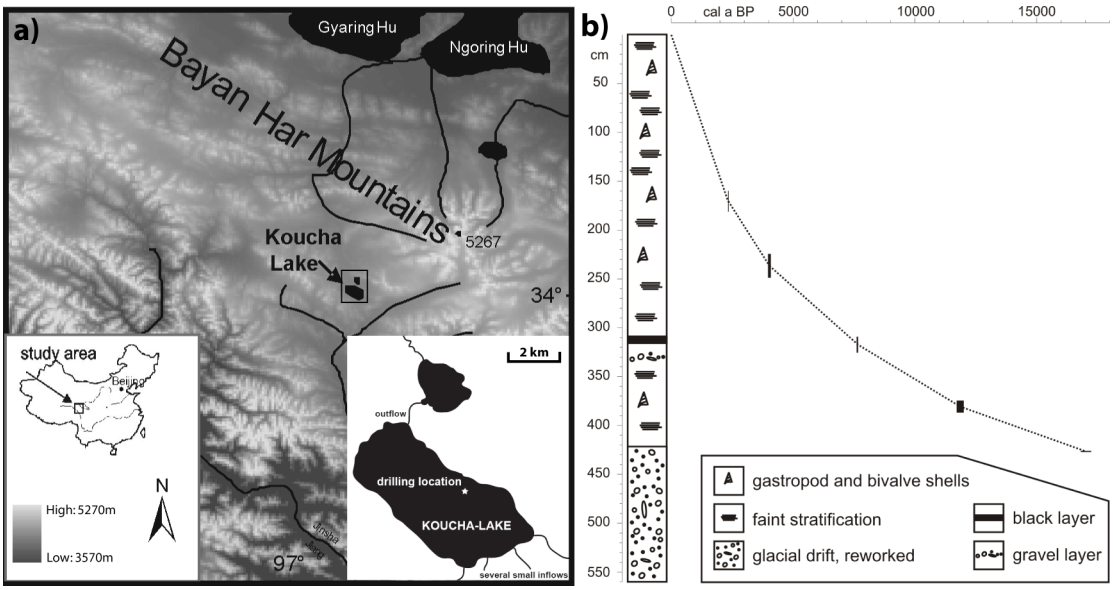

Figure 4.1: (a) Location of Lake Koucha on the eastern Tibetan Plateau. (b) Age–depth model based on a linear interpolation between ^{14}C–AMS dates of pollen extracts (uppermost four samples) and of the alkali-soluble fraction of bulk organic matter (lowermost sample). The core top was assigned an age of zero. The bar widths and lengths represent the 1σ range of the age, and the size of the sampled interval, respectively

eter, 0.33 µm film thickness) was used with the following temperature programme: an oven start temperature of 40 °C, a heating rate of 5 °C/min to 310 °C, and an isotherm phase of 60 minutes. Helium, with a constant flow rate of 1 ml/min, was used as a carrier gas. Hopanoid compounds were identified and quantified with a Thermo Electron GC-MS-system (GC: Trace GC Ultra; MS: DSQ). The GC was equipped with a PTV injector system (start temperature: 50 °C; heating rate 10 °C/sec to 300 °C; 10 min isotherm time; operated in splitless mode) and a BPX-5 column (50 m length, 0.22 mm inner diameter, 0.25 µm film thickness). The GC oven was programmed with a start temperature of 40 °C, a heating rate of 5 °C/min to 310 °C, and an isothermal phase of 60 minutes. Helium, operated with a constant flow rate of 1 ml/min, was used as a carrier gas. The mass spectrometer was operated in electron impact ionization mode. The temperature of the ion source was set to 230 °C. The scan range was 50-600 Dalton at a rate of 2.5 scans/sec.

4.3.3 Compound-specific stable isotope analysis

Carbon isotope ratios of the compounds were determined using an Agilent 6890N GC, equipped with an Ultra-1 column. The oven was heated from 40 °C to 300 °C at a rate of 3 °C/min before a final isothermal time of 25 min. The GC was coupled to a Thermo Electron Delta V plus IRMS via a Combustion III interface (Thermo Fischer, Bremen, Germany). The δ^{13}C signal of the internal standard served as a quality control for the stability of the measurement system. In addition, a certified standard mixture of *n*-alkanes

(C_{15}, C_{20} and C_{25}; Chiron, Trondheim, Norway) was analysed after every 10^{th} sample. The linearity range (150 mV to 10,000 mV) of the measurement system was determined by measuring a dilution series of the same standard mixture. Carbon isotope values were determined for the odd-numbered and most of the even-numbered *n*-alkanes in the mid- and long-chain range, as well as for isoprenoid compounds in the upper part and middle part of the core. In a few samples, some compounds (mostly even-chain *n*-alkanes) were at the lower limit of the linearity range of the GC-C-IRMS, resulting in a higher standard deviation. The concentrations of the short-chain *n*-alkanes and of all hopanoid compounds apart from diploptene and moretene were too low for accurate measurement of the $\delta^{13}C$ values. Each sample was analyzed in triplicate.

4.4 Results

4.4.1 Identification, distribution and concentration of aliphatic compounds

A range of compounds was identified in the aliphatic fraction. The characteristic fragment ions used as a basis for the identification of these compounds, as well as their most likely sources (Table 4.1), is discussed in more detail in the next section. Concentrations of all compounds are shown in Table 4.2. Throughout the core, the compounds in the aliphatic fraction show three distinct distribution patterns (Fig. 4.2), which were the basis for dividing the core into three different periods (Fig. 4.3).

In the lower part of the core (Period I; ca. 16 to 7.9 cal ka BP), the aliphatic fraction contained only *n*-alkanes in significant concentrations (Fig. 4.2c). The distribution pattern shows a strong odd-over-even predominance, and is dominated by nC_{23} and nC_{25}, which show maximum concentrations between 13 and 9 cal ka BP (Fig. 4.3). Other important homologues occurring in this period are nC_{27}, nC_{29} and nC_{31}. Short-chain *n*-alkanes and hopanoids are mainly found in very low amounts, although slightly enhanced concentrations occur between ca. 12.6 and 10.6 cal ka BP (Fig. 4.3 and Table 4.2). In the middle part of the core (period II; Fig. 4.2b), the long-chain *n*-alkanes nC_{29} and nC_{31} predominate over mid-chain *n*-alkanes. A variety of hopanoid and isoprenoid compounds were also identified. Of the latter, phytane is especially abundant. The isoprenoid compound 2,6,10,15,19-pentamethylicosane (PMI) also exhibits maximum concentrations in this part of the core. Among the hopanoids, β-C_{27} hopane, several C_{30} hopenes, $\beta\beta$-C_{29} hopane, $\beta\beta$-C_{30} hopane, $\beta\beta$-C_{31} hopane, hop-21(27)-ene and hop-22(29)-ene (diploptene) were identified (Table 4.2). The dominant hopanoid shows a mass spectrum similar to that of diploptene, which is the hopanoid with the second highest abundance in this section of the core, but has a significantly lower m/z 299 fragment ion and a higher m/z 203 fragment ion. A compound with a similar mass spectrum was identified as moret-22(29)-ene (isodiploptene) by Uemura and Ishiwatari (1995). The dominant compound in the chromatogram for the upper part of the core (6 to 0 cal ka BP) is a highly branched

Table 4.1: Molecular masses and characteristic fragment ions of identified biomarkers, as well as most likely sources of the respective biomarkers in Lake Koucha and according to the literature. See Appendix 6 for mass spectra of compounds

compound	M+	characteristic fragment ions	in Koucha Lake interpreted as a proxy for	possible sources according to literature	references
short-chain *n*-alkanes (e.g. *n*C_{17})		57, 71, 85, 99, 113,...	algal input	bacteria and algae	Gelpi et al. 1970
mid-chain *n*-alkanes (e.g. *n*C_{23} and *n*C_{25})		57, 71, 85, 99, 113,...	submerged macrophytes	submerged macrophytes	Huang et al. 1999, Ficken et al. 2000
long-chain *n*-alkanes (e.g. *n*C_{29} and *n*C_{31})		57, 71, 85, 99, 113,...	terrestrial plants and/or emergent macrophytes	terrestrial plants	Eglinton and Calvin, 1967
				emergent macrophytes	Ficken et al. 2000
				algae	Lichtfouse et al. 1994
phytane	282	183, 169, (113, 127, 197)	cyanobacteria	chlorophyll a (reducing conditions required)	Didyk et al. 1978
				ether-bound phytanyl chains of archaeal lipids	Pease et al. 1998
				sulfur-bound phytanyl chains	Koopmans et al. 1999
				methanogens	Risatti et al. 1984
				cyanobacterial mats	Kenig et al. 1995
PMI	352	239, 267, (85, 99, 113)	methanogens	bacteria, archaea	Holzer et al. 1979, Elvert et al. 1999
				methanogens	Holzer et al. 1979, Brassell et al. 1981, Schouten et al. 1997
				methanotrophs	Elvert et al. 1999, Thiel et al. 1999
C_{20} HBI	282	139/140, 168/169	phytoplankton	diatoms	Peters et al. 2005
				green algae	Rowland et al. 1985
				cyanobacterial mats	Kenig et al. 1995
				freshwater periphyton	Jaffé et al. 2001
C_{25} HBI (one degree of unsaturation)	350	266, 210	diatoms	diatoms	Belt et al. 2001a and b, Sinninghe-Damsté et al. 2004 Xu et al. 2006
hopanes		191	prokaryotes	prokaryotes	Rohmer et al. 1984, Wakeham, 1990
diploptene	410	191, 299, 395	methanotrophs	prokaryotes	Rohmer et al. 1984, Wakeham, 1990
				ferns	Ageta et al. 1983
moretene (isodiploptene)	410	191, 395	methanotrophs	unknown sources	Uemura and Ishiwatari, 1995
				methanotrophs	Blumenberg et al. 2009, Kristen et al. 2009

Table 4.2: Concentrations of biomarkers identified in Lake Koucha

period	cal a BP	cm	*n*C$_{15}$	*n*C$_{16}$	*n*C$_{17}$	*n*C$_{18}$	*n*C$_{19}$	*n*C$_{20}$	*n*C$_{21}$	*n*C$_{22}$	*n*C$_{23}$	*n*C$_{24}$	*n*C$_{25}$	*n*C$_{26}$	*n*C$_{27}$	*n*C$_{28}$	*n*C$_{29}$	*n*C$_{30}$	*n*C$_{31}$	*n*C$_{32}$	*n*C$_{33}$	C$_{30}$ HBI	C$_{25}$ HBI	phytane	PMI	β C27 hopane	C30 hopene	ββ C29 hopane	ββ C30 hopane	ββ C31 hopane	hop27 (21)ene	mor etene	diplop tene
			µg / g d.w.																					ng / g d.w.									
	0	**0**	0.0	0.8	3.1	0.8	1.0	0.7	1.3	0.8	4.2	0.8	3.8	0.6	2.5	0.8	3.8	0.4	4.9	0.0	1.3	6.1	0.85	0.0	0	394	161	99	0	64	0	0	74
	172	**23**	0.1	0.1	1.1	0.1	0.1	0.1	0.3	0.4	1.1	0.2	1.1	0.2	0.6	0.2	0.9	0.1	1.1	0.1	0.4	7.1	0.51	0.0	0	52	49	62	75	53	0	0	146
	1034	**76**	0.2	0.3	0.2	0.2	0.3	0.3	1.0	0.6	5.4	0.6	4.4	0.3	1.9	0.4	2.2	0.2	2.6	0.3	0.6	3.0	0.73	0.0	0	259	86	362	544	515	0	223	539
	1309	**96**	0.0	0.1	0.0	0.0	0.1	0.1	0.3	0.2	1.7	0.3	1.4	0.1	0.7	0.2	0.9	0.1	1.2	0.2	0.3	1.3	0.29	0.0	0	127	44	178	339	255	0	151	219
	1585	**116**	0.0	0.0	0.1	0.0	0.1	0.1	0.4	0.2	2.9	0.2	2.0	0.1	0.6	0.1	0.7	0.0	0.9	0.2	0.5	4.9	0.27	0.0	0	83	64	111	141	94	0	44	152
	1695	**124**	0.1	0.1	0.1	0.0	0.1	0.1	0.5	0.3	3.0	0.2	2.0	0.1	0.6	0.1	0.8	0.1	1.0	0.1	0.4	7.9	0.27	0.0	0	80	29	121	211	170	0	103	221
III	**1860**	**136**	0.0	0.0	0.0	0.0	0.1	0.1	0.5	0.3	2.5	0.3	2.3	0.2	0.9	0.4	0.9	0.1	1.1	0.3	0.6	4.3	0.34	0.0	0	159	127	251	304	273	0	77	293
	2135	**156**	0.0	0.0	0.1	0.1	0.1	0.1	0.7	0.5	3.8	0.6	3.5	0.4	1.8	0.7	2.5	0.2	3.1	0.3	1.0	7.0	0.33	0.0	0	330	303	527	794	713	0	286	868
	2880	**192**	0.0	0.0	0.0	0.0	0.1	0.1	0.7	0.5	3.5	0.6	3.3	0.4	1.8	0.7	2.5	0.2	3.1	0.3	1.0	12.7	0.37	0.0	0	322	349	435	707	596	0	254	655
	3188	**204**	0.0	0.0	0.0	0.0	0.1	0.1	0.3	0.1	2.1	0.2	1.5	0.1	0.6	0.2	0.7	0.1	1.0	0.1	0.4	7.3	0.15	0.0	0	109	35	152	274	236	0	0	0
	3598	**220**	0.0	0.0	0.0	0.0	0.1	0.1	0.6	0.4	3.2	0.5	3.1	0.4	1.7	0.7	2.4	0.2	2.9	0.3	0.9	7.6	0.09	0.0	0	352	119	370	546	434	0	234	501
	4752	**253**	0.0	0.0	0.1	0.0	0.1	0.1	0.5	0.4	3.3	0.5	2.6	0.3	1.2	0.3	1.7	0.2	1.8	0.1	0.5	5.7	0.18	0.0	0	244	117	291	376	327	0	0	0
	5309	**266**	0.0	0.0	0.0	0.0	0.1	0.1	0.8	0.7	4.5	0.8	4.1	0.5	2.3	0.8	3.3	0.3	3.9	0.4	1.2	17.9	0.03	0.0	0	291	129	363	375	301	0	0	116
	5681	**274**	0.0	0.0	0.0	0.0	0.0	0.0	0.2	0.2	1.1	0.2	0.9	0.1	0.3	0.1	0.3	0.0	0.3	0.1	0.1	2.4	0.00	0.0	0	65	17	77	108	113	0	0	0
	6053	**282**	0.0	0.0	0.0	0.0	0.0	0.1	0.4	0.1	2.0	0.1	1.2	0.2	0.6	0.3	0.7	0.1	1.0	0.1	0.4	9.8	0.00	0.0	0	55	24	85	101	152	0	0	0
	6425	**291**	0.0	0.0	0.0	0.0	0.1	0.2	0.8	0.7	2.8	0.6	2.7	0.3	1.4	0.7	2.2	0.2	2.6	0.2	0.7	0.4	0.00	0.1	32	439	105	224	255	189	0	86	0
II	**6796**	**299**	0.0	0.1	0.2	0.0	0.3	0.3	0.9	0.2	3.2	0.3	3.2	0.5	2.7	1.2	4.5	0.7	4.3	1.0	0.9	0.2	0.00	3.2	1109	174	60	176	209	216	74	932	492
	6982	**303**	0.0	0.0	0.1	0.0	0.1	0.1	0.4	0.3	1.3	0.3	1.3	0.2	1.0	0.4	1.9	0.1	1.6	0.0	0.2	0.1	0.00	0.4	447	135	0	0	77	110	54	109	65
	7168	**307**	0.2	0.1	0.1	0.1	0.1	0.1	0.5	0.3	0.9	0.1	0.8	0.1	0.4	0.1	0.8	0.1	0.9	0.0	0.2	0.2	0.00	0.2	22	25	0	0	0	0	0	0	0
	7916	**322**	0.0	0.0	0.1	0.1	0.2	0.1	0.3	0.2	1.2	0.1	1.2	0.1	1.1	0.1	1.4	0.0	1.5	0.0	0.2	0.1	0.00	0.3	14	24	0	0	0	14	0	0	0
	8057	**324**	0.0	0.0	0.0	0.0	0.0	0.0	0.9	0.5	4.0	0.5	3.8	0.3	2.5	0.2	2.5	0.1	1.4	0.0	0.2	0.1	0.00	0.0	0	0	0	0	0	0	0	0	0
	8340	**328**	0.0	0.0	0.0	0.0	0.0	0.1	0.4	0.3	2.1	0.3	1.8	0.2	1.2	0.1	1.4	0.1	1.3	0.1	0.3	0.0	0.00	0.0	0	0	0	0	0	0	0	0	0
	8906	**337**	0.0	0.0	0.0	0.0	0.0	0.0	0.2	0.2	1.0	0.2	0.7	0.1	0.4	0.1	0.5	0.1	0.4	0.0	0.1	0.0	0.00	0.0	0	110	0	44	50	70	0	0	0
	9189	**341**	0.0	0.0	0.0	0.0	0.1	0.1	0.9	0.8	4.6	0.8	4.1	0.3	1.8	0.2	1.9	0.1	1.5	0.0	0.3	0.1	0.00	0.1	12	54	0	0	0	0	0	0	0
	9472	**345**	0.1	0.1	0.1	0.1	0.1	0.1	0.9	0.6	5.3	0.5	4.5	0.2	1.9	0.2	2.2	0.1	1.5	0.1	0.3	0.1	0.00	0.1	23	8	0	6	5	9	0	0	0
	10037	**353**	0.0	0.0	0.0	0.0	0.0	0.1	0.4	0.2	2.9	0.3	2.4	0.1	0.9	0.1	1.1	0.1	0.8	0.0	0.2	0.1	0.00	0.0	6	36	0	0	18	32	0	0	20
I	**10603**	**362**	0.0	0.1	0.2	0.0	0.1	0.1	0.7	0.2	6.4	0.4	6.2	0.3	2.0	0.3	2.3	0.1	1.6	0.1	0.3	0.2	0.00	0.0	18	20	0	0	16	22	0	0	23
	10886	**366**	0.0	0.0	0.2	0.2	0.1	0.1	0.6	0.2	3.5	0.3	3.6	0.2	1.5	0.2	1.9	0.1	1.6	0.0	0.3	0.3	0.00	0.0	23	0	0	0	0	0	0	0	0
	11310	**372**	0.0	0.1	0.1	0.1	0.1	0.1	1.8	0.2	10.8	0.3	7.7	0.2	1.9	0.1	2.0	0.1	1.6	0.1	0.3	0.1	0.00	0.1	17	0	0	0	0	0	0	0	49
	12609	**388**	0.1	0.2	0.4	0.4	0.4	0.3	1.9	0.3	7.2	0.4	4.8	0.2	1.3	0.1	1.4	0.1	1.1	0.1	0.2	0.2	0.00	0.0	34	0	0	0	0	0	0	0	0
	12922	**391**	0.0	0.0	0.0	0.0	0.0	0.0	0.8	0.4	6.0	0.6	6.2	0.4	2.9	0.3	3.5	0.5	3.0	0.6	0.9	0.3	0.00	0.0	5	0	0	0	0	0	0	0	10
	13760	**400**	0.1	0.0	0.1	0.0	0.1	0.1	0.5	0.3	1.4	0.2	1.2	0.1	0.6	0.1	0.9	0.1	0.8	0.0	0.2	0.0	0.00	0.0	108	17	0	10	14	20	0	13	15
	14597	**408**	0.0	0.0	0.0	0.0	0.0	0.0	0.2	0.1	1.3	0.1	1.2	0.1	0.5	0.1	0.9	0.1	1.2	0.1	0.5	0.0	0.00	0.0	0	0	0	0	0	0	0	0	0
	15434	**416**	0.0	0.0	0.1	0.0	0.1	0.1	0.6	0.3	5.6	0.4	5.0	0.2	1.8	0.2	2.1	0.1	2.1	0.0	0.6	0.1	0.00	0.0	0	0	0	0	0	0	0	0	29

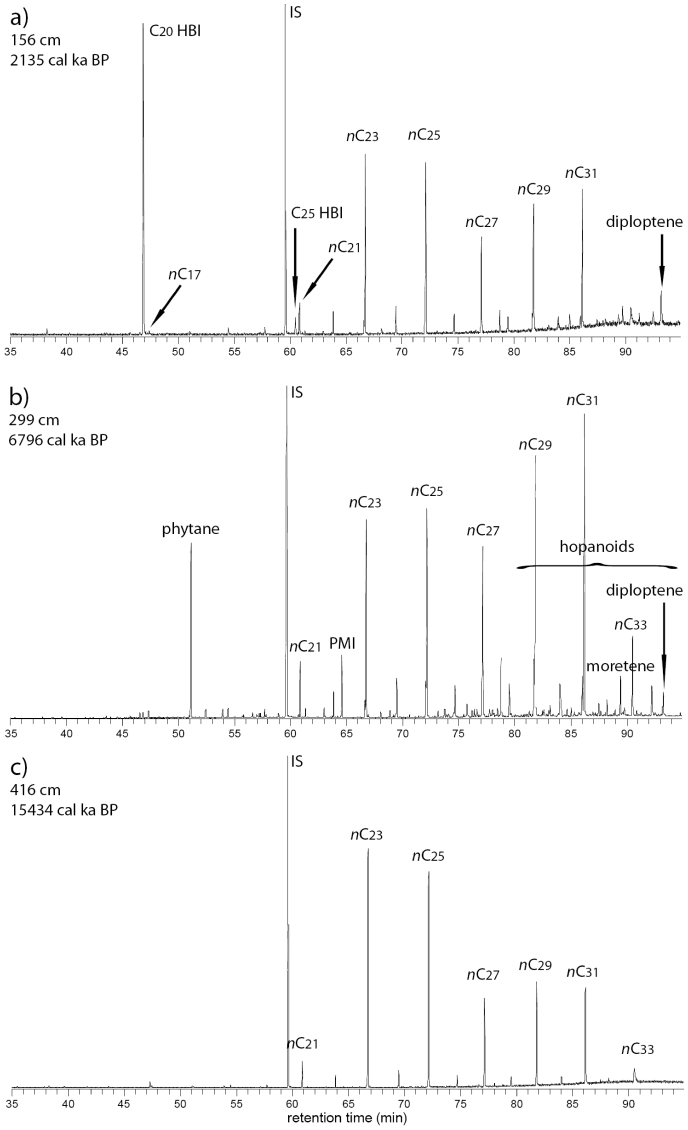

Figure 4.2: Total ion current chromatograms (GC-MS) of three sections of the core, representing period III (a) period II (b) and period I (c). Important compounds are labelled. IS = internal quantification standard

isoprenoid with 20 carbon atoms (C_{20} HBI) (Fig. 4.2a). The compound was described as 2,6,10-trimethyl-7-(3-methylbutyl)-dodecane by Yon et al. (1982) and was identified by comparing Kováts retention indices (Kováts 1958) and the mass spectrum with published data. The compound was eluted shortly after $n\mathrm{C}_{17}$ on the GC-FID (Ultra-1 column) and shortly before $n\mathrm{C}_{17}$ on the GC-MS (BPX-5 column) (Fig. 4.2a), resulting in retention indices of 1708 and 1683, respectively. These findings are in agreement with published retention indices (Rowland and Robson 1990). The mass spectrum (molecular ion m/z = 282) shows characteristic fragment ion doublets at m/z 139/140 and 168/169, and further prominent fragment ions at m/z 196/197 and 210/211. A similar spectrum was published by Dunlop and Jefferies (1985). Except in the two uppermost samples, where the $n\mathrm{C}_{17}$-alkane reaches relatively high concentrations, short-chain *n*-alkanes were either absent or

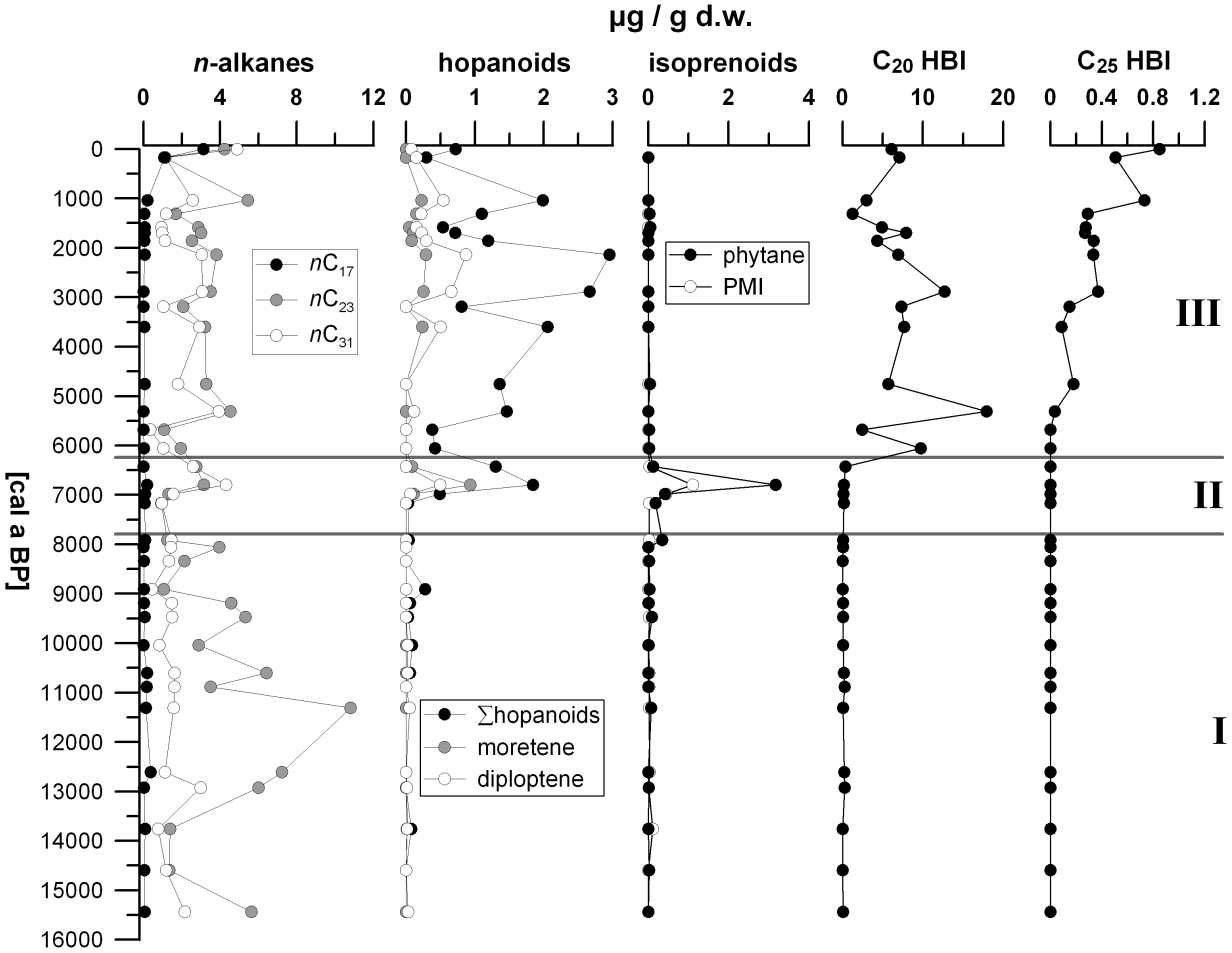

Figure 4.3: An overview of the concentrations [µg/g d.w.] of *n*-alkanes C_{17}, C_{23} and C_{31}, hopanoids, isoprenoids and HBIs versus age. The zonation is based on the distribution of the biomarkers

found in trace amounts in the top part of the core (Fig. 4.3). Careful examination of the mass spectrum on the up- and down-slope of the C_{20} HBI peak revealed that no significant amount of the C_{17}- *n*-alkane was co-eluted with this compound. A C_{25} HBI was also detected, but in lower concentrations than the C_{20} HBI. This compound was eluted shortly after nC_{21} on the GC-FID and shortly before nC_{21} on the GC-MS (Fig. 4.2a). The molecular mass (m/z = 350) indicates one degree of unsaturation. The C_{20} HBI exhibits a maximum concentration at ca. 5.3 cal ka BP, while the C_{25} HBI shows a step-like increase in concentration from 4.7 cal BP until the present day (Fig. 4.3). The *n*-alkanes in the upper part of the core show distribution patterns similar to those in the lower part, but aquatic macrophyte-derived, mid-chain *n*-alkanes do not reach concentrations as high as those seen in period I. Relatively low concentrations can be observed for the periods near 5.9 and 3.1 cal ka BP and between 1.8 and 1.3 cal ka BP. (Fig. 4.3). A similar trend is observable for concentrations of hopanoid compounds. Especially high concentrations of hopanoids were found between 2.1 and 2.9 cal ka BP. Phytane and PMI were not detected in the upper part of the core.

4.4.2 δ^{13}C values of biomarkers

The δ^{13}C values determined for all biomarkers are listed along with the standard deviations in Table 4.3. The δ^{13}C values of the mid-chain *n*-alkanes show significant variability throughout the core, e.g. from -23.5 to -11.9‰ for $n\mathrm{C}_{23}$ (Fig. 4.4). In period I, the δ^{13}C values of the mid-chain *n*-alkanes follow the trend of $\delta^{13}\mathrm{C}_{\mathrm{TOC}}$, with relatively high values between 13.7 and 9.1 cal ka BP, and relatively low values at 11.3 cal ka BP and between 8.9 and 7.1 cal ka BP. The δ^{13}C values gradually increase throughout period II and reach a maximum in period III. The long-chain *n*-alkanes are generally more depleted in ^{13}C than the mid-chain *n*-alkanes, as depletion is observed to increase with chain length. The ranges in the δ^{13}C values are less pronounced than for the mid-chain *n*-alkanes, e.g. $n\mathrm{C}_{27}$ ranges from -30.3 to -21.8‰, $n\mathrm{C}_{29}$ from -33.0 to -23.6‰ and $n\mathrm{C}_{31}$ from -35.0 to -27.5‰ (Table 4.3).

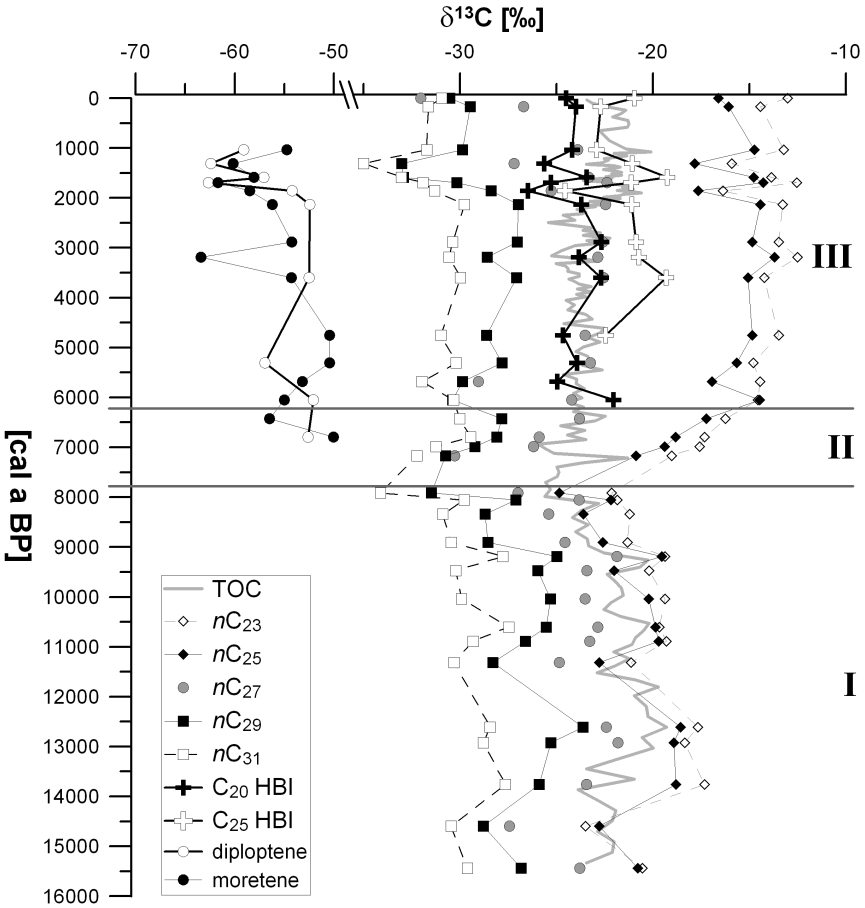

Figure 4.4: The δ^{13}C values of TOC, odd-chain *n*-alkanes, HBIs, diploptene and moretene plotted versus age

As compared to period I, period III exhibits a tendency towards lower values of $n\mathrm{C}_{29}$ and $n\mathrm{C}_{31}$ (Fig. 4.4). Together with the enriched δ^{13}C values of the mid-chain *n*-alkanes, this results in large offsets (15-19‰) between the mid- and long-chain *n*-alkanes in the upper part of the core. The values of the C_{20} HBI show comparatively little variation (-26.5

to -22.0‰), and between 6.1 and 2.1 cal ka BP are similar to $\delta^{13}C_{TOC}$, before the latter shifts to higher values around 2 cal ka BP. The C_{25} HBI is generally ≈2-4‰ less negative than the C_{20} HBI (range -24.6 to -19.4‰) (Fig. 4.4). Phytane has isotopic signatures comparable to those of the mid-chain *n*-alkanes in the same samples (-17.7 and -19.6‰), while PMI is more depleted (-28.9 and -25.9‰) (Table 4.3). Diploptene and moretene are more depleted in ^{13}C than all other compounds, having $\delta^{13}C$ values between -62.7 and -45.5‰ and -64.5 and -50.1‰, respectively (Fig. 4.4). The most negative values are found at ca. 3.1 cal ka BP and in the time interval between 2 and 1 cal ka BP, during which shifts towards more negative values can also be observed for most of the other compounds shown in Fig. 4.4.

Table 4.3: The δ^{13}C values of the biomarkers, including standard deviations

period	cal a BP	cm	*n*C$_{21}$		*n*C$_{22}$		*n*C$_{23}$		*n*C$_{24}$		*n*C$_{25}$		*n*C$_{26}$		*n*C$_{27}$		*n*C$_{28}$		*n*C$_{29}$		*n*C$_{30}$		*n*C$_{31}$		*n*C$_{33}$		C$_{20}$ HBI		C$_{25}$ HBI		phytane		PMI		diploptene		more tene	
			δ^{13}C	SD	δ^{13}C	SD	δ^{13}C	SD	δ^{13}C	SD	δ^{13}C	SD	δ^{13}C	SD	δ^{13}C	SD	δ^{13}C	SD	δ^{13}C	SD	δ^{13}C	SD	δ^{13}C	SD	δ^{13}C	SD	δ^{13}C	SD	δ^{13}C	SD	δ^{13}C	SD	δ^{13}C	SD	δ^{13}C	SD
	0	0	-16.1	1.1	-19.1	0.1	-13.0	0.5			-16.6	0.0			-32.0	0.1			-30.5	0.6			-31.0	0.4			-24.5	0.4	-21.0	0.3								
	172	23	-16.9	0.1	-22.6	0.1	-14.4	0.2	-24.8	0.3	-16.1	0.1	-30.6	1.1	-26.7	0.2	-31.1	1.3	-29.5	0.5	-32.3	0.2	-31.6	0.1			-24.0	0.3	-22.7	0.4								
	1034	76	-16.2	0.1	-21.1	0.3	-13.2	0.1	-22.9	0.2	-14.7	0.3	-28.9	0.3	-23.9	0.4	-30.8	0.7	-29.9	1.0			-31.7	1.2			-24.2	0.5	-22.9	0.9			-59.1	0.8	-54.8	1.3		
	1309	96	-20.0	1.9	-23.0	1.4	-15.9	0.3	-23.7	0.3	-17.8	0.4			-27.2	0.7	-30.9	1.7	-33.0	1.7			-35.0	2.2			-25.6	0.7	-21.1	0.5			-62.4	0.4	-60.2	1.3		
	1585	116	-15.3	0.6	-16.2	1.0	-13.9	0.2	-17.3	0.7	-14.8	0.3			-23.3	0.4	-26.5	0.1	-32.9	1.1			-33.0	0.3			-23.4	0.1	-19.3	1.4			-57.1	0.2	-58.1	0.2		
	1695	124	-13.5	0.4	-16.9	0.2	-12.6	0.7	-17.3	0.1	-14.3	0.3	-21.1	0.6	-22.4	0.2			-30.2	2.1			-31.9	1.2			-25.3	0.1	-21.1	1.0			-62.7	0.4	-61.7	1.1		
III	1860	136	-17.8	0.4			-16.4	0.1			-17.7	0.1			-25.3	0.1	-28.8	1.2	-28.4	0.5	-30.2	0.1	-31.3	0.9			-26.5	0.6	-24.6	1.0			-54.2	0.3	-58.5	1.3		
	2135	156	-16.1	0.1	-19.2	1.1	-13.3	0.1	-19.1	0.4	-14.4	0.0	-24.1	0.3	-22.4	0.3	-26.1	0.6	-27.0	0.2			-29.8	0.4			-23.7	0.1	-21.1	0.1			-52.5	1.1	-56.2	1.1		
	2880	192	-16.9	0.5	-18.9	0.2	-13.5	0.1	-19.9	0.3	-14.9	0.1	-24.7	0.4	-22.6	0.1	-25.8	0.4	-27.0	0.3			-30.4	0.4	-30.5	1.6	-22.7	0.1	-20.9	0.4			-45.5	1.0	-54.3	1.2		
	3188	204	-14.1	0.3	-19.6	0.1	-12.5	0.3	-21.3	0.5	-13.7	0.1	-26.3	0.1	-22.9	0.9	-28.6	0.3	-28.6	0.1			-30.6	0.4			-23.8	0.0	-20.7	0.7					-63.4	1.3		
	3598	220	-18.3	1.0	-19.5	0.5	-14.2	0.6	-20.2	0.8	-15.1	0.3	-24.9	1.8	-22.6	0.4	-26.0	0.2	-27.1	0.6	-26.6	0.8	-30.0	0.8	-29.7	0.3	-22.7	0.2	-19.3	0.4			-52.5	0.1	-54.3	0.4		
	4752	253	-17.4	0.1	-19.2	0.6	-13.5	0.2	-19.7	0.3	-14.8	0.2	-24.2	0.2	-23.5	0.4	-25.3	0.1	-28.6	0.2			-31.0	0.1			-24.7	0.1	-22.5	0.6					-50.5	0.6		
	5309	266	-18.8	0.1	-19.0	0.4	-14.8	0.2	-20.7	0.6	-15.7	0.3	-25.0	0.5	-23.2	0.1	-26.0	0.1	-27.8	0.3			-30.2	0.1	-30.2	0.3	-23.9	0.1					-57.0	1.2	-50.5	0.6		
	5681	274	-16.6	0.4	-17.5	0.3	-14.5	0.1	-20.0	0.6	-16.9	0.2	-29.4	1.1	-29.0	0.5	-28.6	0.4	-29.9	0.8			-32.0	0.0			-25.0	0.1							-53.2	1.1		
	6053	282	-17.0	0.9	-18.1	0.0	-14.6	1.1	-20.5	0.1	-14.5	0.5	-25.8	0.3	-24.2	1.4	-28.3	0.3	-30.4	0.3			-30.3	0.6			-22.0	0.1					-52.1	1.4	-55.0	1.3		
	6425	291	-16.4	1.4	-16.8	0.2	-16.2	0.5	-18.1	0.5	-17.2	0.5	-24.4	0.6	-23.8	0.4	-25.3	0.1	-27.8	0.2	-26.3	1.0	-30.0	0.3	-30.2	0.9									-56.5	0.3		
II	6796	299	-20.2	0.9	-25.7	0.3	-17.3	0.3	-25.6	0.2	-18.8	0.1	-27.9	0.1	-25.9	0.3	-27.8	0.1	-28.1	0.1			-29.4	0.8							-17.7	0.2	-28.9	0.1	-52.6	0.8	-50.1	0.1		
	6982	303	-20.6	1.6	-21.3	0.1	-17.6	0.2	-22.9	0.8	-19.4	0.4	-27.5	0.4	-26.2	0.2	-28.0	0.5	-29.2	0.0	-27.8	0.5	-31.2	0.2							-19.6	0.2	-25.9	0.2				
	7168	307	-21.0	0.5			-19.0	0.9	-23.5	0.2	-20.9	1.1			-30.3	1.3			-30.8	1.8			-32.2	1.9														
	7916	322	-23.5	0.3	-25.3	0.8	-22.1	1.0			-24.9	0.7			-27.0	0.8			-31.5	0.4			-34.1	0.3														
	8057	324	-22.0	0.1	-23.1	0.2	-21.8	0.1	-23.6	0.0	-22.2	0.0	-25.5	0.1	-23.8	0.2	-26.9	0.3	-27.1	0.1	-28.6	0.2	-29.8	0.2	-29.9	0.2												
	8340	328	-21.4	0.3	-22.4	0.7	-21.2	0.4	-24.8	0.9	-23.6	0.7	-28.0	0.9	-25.4	1.2	-28.9	0.2	-28.7	0.4			-30.9	0.5														
	8906	337	-21.8	0.8	-22.2	0.2	-21.3	0.5	-22.8	0.5	-22.6	0.8	-28.1	0.8	-24.6	0.5	-27.0	1.0	-28.6	0.3			-30.5	1.4														
	9189	341	-19.2	0.4	-20.4	0.2	-19.4	0.1	-20.2	0.3	-19.5	0.2	-23.8	0.4	-21.9	0.1	-26.8	0.8	-25.0	0.2			-27.8	0.5	-27.7	1.0												
	9472	345	-20.8	0.1	-22.0	0.3	-20.2	0.1	-22.1	0.5	-22.0	0.3	-26.5	0.4	-23.4	0.2	-27.8	0.7	-26.0	0.1			-30.2	0.2	-30.0	1.1												
	10037	353	-20.5	1.4	-23.5	0.5	-19.4	0.2	-22.6	0.0	-20.2	0.6	-25.8	1.8	-23.5	0.2	-28.8	0.0	-25.3	0.2			-29.9	0.3														
I	10603	362	-19.8	0.8	-23.9	0.3	-19.7	0.9	-22.3	1.0	-19.9	0.1	-25.8	1.0	-22.9	0.9	-30.2	0.4	-25.5	1.0			-27.5	0.9														
	10886	366	-20.0	0.5	-23.5	0.5	-19.3	0.3	-22.2	0.1	-19.7	0.2	-26.2	0.4	-23.3	0.2	-28.0	0.2	-26.6	0.3			-29.3	0.3	-29.5	1.0												
	11310	372	-19.5	0.7	-20.7	0.5	-21.1	0.2	-19.9	0.2	-22.8	0.3	-21.8	1.0	-24.9	0.6	-25.0	0.7	-28.3	0.9			-30.3	0.7														
	12609	388	-20.3	0.7	-21.3	1.3	-17.7	0.4	-19.6	0.5	-18.6	0.3	-20.3	0.4	-22.4	0.3	-26.4	0.1	-23.6	0.1			-28.4	1.4														
	12922	391	-19.3	0.2	-20.9	0.2	-18.4	0.3	-21.0	0.4	-18.9	0.2	-25.8	0.1	-21.8	0.3	-26.0	0.5	-25.3	0.5	-27.6	0.5	-28.8	0.5														
	13760	400	-19.7	0.8	-22.9	0.2	-17.3	0.9	-23.4	0.6	-18.8	0.4	-27.1	0.8	-23.5	0.3	-28.9	1.3	-25.9	0.8			-27.7	1.1									-26.3	0.7				
	14597	408	-23.0	0.4	-25.5	1.5	-23.5	0.6	-28.1	0.3	-22.8	0.1	-31.7	1.4	-27.4	0.7	-30.6	0.9	-28.8	0.1			-30.5	0.7	-30.2	0.1												
	15434	416	-21.2	0.5	-21.0	0.4	-20.6	0.2	-21.9	0.7	-20.8	0.5			-23.8	0.3			-26.8	0.2			-29.6	0.2	-28.4	0.2												

SD: standard deviation

4.5 Discussion

4.5.1 Organic matter sources

The potential sources of biomarkers identified in the core are summarized in Table 4.1. Bacteria and algae are an established source of short-chain *n*-alkanes (especially nC_{17}) (Gelpi et al., 1970), and their proportional input to the sediment may be assessed using the aquatic-terrestrial-ratio ATR = (nC_{15}+ nC_{17}+ nC_{19}) / (nC_{15}+ nC_{17}+ nC_{19}+ nC_{29}+ nC_{31}) (Wilkes et al., 1999). C_{23} and C_{25} *n*-alkanes in sediments have frequently been interpreted to be of submerged macrophyte origin (Huang et al., 1999; Ficken et al., 2000; Street-Perrott et al., 2004), in contrast to long-chain *n*-alkanes, which are generally thought to be derived from terrestrial plants or emergent macrophytes (Eglinton and Hamilton, 1967; Ficken et al., 2000). However, certain varieties of algae, e.g. *Botryococcus braunii*, have also been discussed as a source for long-chain *n*-alkanes in sediments (Lichtfouse et al., 1994). The proportion of submerged aquatic macrophytes relative to terrestrial plants and emergent macrophytes has been expressed using the proxy for aquatic macrophytes, P_{aq} = (nC_{23}+ nC_{25})/ (nC_{23}+ nC_{25}+ nC_{29}+ nC_{31}), by Ficken et al. (2000).

Several sources of sedimentary phytane have been discussed in the literature. Phytane is conventionally thought to occur from the diagenesis of the phytol side chain of algal and cyanobacterial chlorophyll-a under reducing conditions, via the intermediate products phytadienes and phytenes (Didyk et al., 1978). This suggested pathway has been questioned by some (Grossi et al., 1998). Archaea have also been considered as a potential source, either via the diagenetic cleavage of the ether-bound phytanyl chain of their lipid molecules (Pease et al., 1998) or even as direct producers. However, the latter hypothesis has not yet been proven (Schouten et al., 2001). Sulfur-bound phytanyl chains are also possible sources (Koopmans et al., 1999). Phytane has been reported in methanogenic microbes (Risatti et al., 1984; Venkatesan and Kaplan, 1987; Volkman et al., 1986) as well as in modern cyanobacterial mats (Kenig et al., 1995). The above possibilities, including the cleavage of larger molecules, require a certain level of sediment maturity and are therefore unlikely to be responsible for the significant phytane concentrations found in the mid-Holocene samples from Lake Koucha. Phytane is also present in crude oils, but the absence of pristane and of short-chain *n*-alkanes lacking odd-over-even predominance is an argument against sample contamination as a phytane source. In the sediments investigated in this study, the $\delta^{13}C$ values of phytane are relatively enriched and lie in the range of submerged macrophyte-derived *n*-alkanes (Table 4.3). This could be evidence for an autotrophic source organism, which often have the ability to switch to bicarbonate metabolism (Lucas and Berry, 1985). The exact origin of phytane cannot be resolved, but cyanobacteria are the possible producers.

The presence of hopanoid hydrocarbons in sediments is a sign of microbial activity, as these compounds are membrane lipids of prokaryotic organisms or represent products of

diagenetic transformations of such lipids (Rohmer et al., 1984; Wakeham, 1990; Elvert et al., 2001; Hanisch et al., 2003). Diploptene can also be derived from ferns (Ageta and Arai 1983), which are unlikely to occur in the alpine deserts and meadows of the Tibetan Plateau. Moretene has been found in marine sediments from the Black Sea (Blumenberg et al., 2009) and in several lake sediments, but high concentrations in the latter sediments have only been observed in Japanese acidotrophic lakes (Uemura and Ishiwatari 1995), in highly saline Lake Tswaing, South Africa (Kristen et al., 2009) and apparently in an hypereutrophic alkaline lagoon in Spain (Grimalt et al., 1991). The source of moretene at these localities has not yet been clarified. Due to its isotopically-depleted signal (-60.7 and -66‰), methanotrophs have been suggested as possible producers in Japanese lakes (Uemura and Ishiwatari, 1995) while a mixed community of methanotrophs and other prokaryotes was suspected to be the reason for δ^{13}C values ranging from -52.5 to -48.3‰ and -49.2 to -28.5‰ in the Black Sea and Lake Tswaing, respectively (Blumenberg et al., 2009; Kristen et al., 2009). Since moretene (-63.4 to -50.1‰) as well as diploptene (-62.7 to -45.5‰) are relatively depleted in ^{13}C in our samples, we also suspect methanotrophs to be the primary producers of both compounds in Lake Koucha.

PMI is another indicator for bacteria or archaea (Holzer et al., 1979; Elvert et al., 1999). The saturated PMI has been attributed to methanogens (Holzer et al., 1979; Brassell et al., 1981; Schouten et al., 1997) and was also postulated to be involved in methanotrophic processes due to its strongly depleted isotopic signature (< -100‰) in some sediments (Elvert et al., 1999; Thiel et al., 1999). In our samples, the δ^{13}C values of PMI are about 10‰ more negative than those of phytane (Table 4.3), making a common source unlikely. However, the δ^{13}C values are not sufficiently low for methanotrophs feeding on biogenic methane to be the most likely producers. According to Summons et al. (1998), the lipids of methanogens might be depleted in ^{13}C (as compared to the substrate) if consumption is low, in contrast to the enriched values when consumption is high (Schouten et al., 2001); in consequence, a considerable range of δ^{13}C values is possible for methanogenic lipids. We therefore conclude that methanogenic microorganisms may be the most likely source of PMI in the sediments of Lake Koucha. Sources of geogenic methane with less-depleted δ^{13}C values than those of biogenic methane cannot be ruled out in the lake area. Regardless, the strong ^{13}C depletion of diploptene and moretene indicates that methanotrophic bacteria are involved in the carbon cycle of the sediment (Summons et al., 1994; Schouten et al., 2001) and biogenic methane must therefore be present.

C_{25} HBIs have been established as specific diatom biomarkers, and have been detected in several species (Belt et al., 2001a and b; Sinninghe Damste et al., 2004; Xu et al., 2006). It has also been proposed that C_{20} HBIs are derived from diatoms, but a specific diatom producer has not yet been determined (Peters et al., 2005; Xu et al., 2006). However, C_{20} HBIs have also been identified in field samples of the green alga *Enteromorpha prolifera* (Rowland et al. 1985), in cyanobacterial mats (Kenig et al., 1995) and in freshwater

periphyton composed primarily of blue-green algae, diatoms and desmids (Jaffe et al., 2001). Thus, the presence of HBIs in sediments can generally be interpreted with respect to phytoplankton producers.

4.5.2 Development of Lake Koucha since the late glacial

The most important proxies employed in this study, including bulk data (TOC, $\delta^{13}C_{TOC}$and $\delta^{13}C_{TIC}$), and salinities inferred from the electrical conductivities (EC) of ostracod-based transfer-functions (Mischke et al., 2008), are shown versus depth in Fig. 4.5. The development of Lake Koucha is discussed with respect to the three time periods delineated from the biomarker distribution patterns (Fig. 4.2).

4.5.2.1 Period I (16 - 7.9 cal ka BP)

The *n*-alkane pattern in the lower part of the core, in which nC_{23} and nC_{25} are the predominant homologues, is typically aquatic-macrophyte derived, with some influence from terrestrial or emergent macrophytes (Eglinton and Hamilton, 1967; Kolattukudy et al., 1976; Ficken et al., 2000). Apart from one exception at ca. 12.9 cal ka BP, the concentrations of long-chain *n*-alkanes (shown for nC_{31} in Figs. 4.3 and 4.5) remain consistently low throughout period I, leading to the conclusion that terrestrial plants played a minor role during that episode. In contrast, the total amounts of macrophyte-derived *n*-alkanes (shown for nC_{23} in Figs. 4.3 and 4.5) in Lake Koucha, display a decrease at the beginning of period I and a gradual increase starting at 13.6 cal ka BP, reaching maximum values between 12.6 and 11.3 cal ka BP. The $\delta^{13}C$ values of TOC and of nC_{23} are higher in this section of the core (Figs. 4.4 and 4.5), due to the increased consumption of ^{13}C-enriched carbon sources. The concentrations of mid-chain *n*-alkanes later decrease, with minor fluctuations, to a minimum value at 7.9 cal ka BP. Assuming that *Potamogeton* species were the dominant macrophytes in period I, as is presently the case, the drop in mid-chain *n*-alkane concentrations may have been induced by rising salinities (Fig. 4.5), as both *Potamogeton* and *Batrachium* favor fresh to oligohaline conditions (Brush and Hilgartner 2000). Information regarding the possible effect of increasing salinities on the lipid concentrations and composition of aquatic macrophytes is lacking, but since the decrease of macrophyte-derived *n*-alkanes is accompanied by a drop of TOC, water plants most likely became less abundant in the second half of period I. The correlation between TOC content, concentration of macrophyte-derived lipids and $\delta^{13}C$ values throughout period I suggests that aquatic macrophytes were the dominant contributors to the Lake Koucha organic carbon pool before 8 cal ka BP. This source was likely to have been particularly important between 12.9 and 9.1 cal ka BP, when an increased ratio of mid- to long-chain *n*-alkanes (P_{aq}) is observed (Fig. 4.5). Small increases in algal biomarkers such as short-chain *n*-alkanes, resulting in a slightly higher aquatic-terrestrial-ratio (ATR) (Fig. 4.5), suggest

the presence of minor amounts of bacteria and algae at the beginning of the same period. Terrestrial organic matter input and/or emergent macrophytes most likely played a more important role only around 13 cal ka BP, when the TOC values reached the first peak and $n\mathrm{C}_{31}$ concentrations were slightly enhanced (Fig. 4.5). As terrestrial organic matter played a minor role, the fluctuations of the $\delta^{13}\mathrm{C}$ values (bulk TOC and $n\mathrm{C}_{23}$) would therefore reflect changes in autochthonous productivity, which was mainly controlled by aquatic macrophytes.

Between 12.9 and 9.1 cal ka BP, the conditions in the lake were obviously favorable for enhanced macrophyte growth. This conclusion is in agreement with the pollen-derived temperature and precipitation inferences of Herzschuh et al. (2009), who suggested that warm and semi-wet conditions occurred during this period in the catchment of Lake Koucha. Thus, the rising abundance of aquatic macrophytes was probably driven by higher insolation and temperatures during the late glacial period, starting with the Bølling/Allerød (Thompson et al., 1997). The later decline in macrophyte concentrations can be attributed to the rising salinities of Lake Koucha, which were induced by decreasing effective moisture availability during the early Holocene. In contrast, many studies inferred wet climate conditions on the Tibetan Plateau during the early Holocene (Morill et al., 2003; Wang et al., 2005; Herzschuh, 2006), but enhanced evaporation at higher temperatures may have outweighed increasing precipitation amounts in the semi-arid Lake Koucha region (Herzschuh et al., 2006 and 2009).

4.5.2.2 Period II (7.9 - 6.1 cal ka BP)

The significant change in the lacustrine system between 7.9 and 6.1 cal ka BP is also reflected in a change of the biomarker composition (Figs. 4.2b, 4.3 and 4.5). According to the interpretation of Mischke et al. (2008), the lake was very shallow and hypersaline from the end of period I until ca 7.3 cal ka BP. These authors reported the presence of a black layer with high TOC contents in this section of the core (7.6 to 7.3 cal ka BP), and speculated about possible anoxic conditions in the sediment, which may have been covered by algal and/or bacterial mats. Unfortunately, samples from this layer were not available for biomarker evaluation. However, enhanced concentrations of short-chain *n*-alkanes, resulting in a slightly increased ATR, point to increased algal productivity at least shortly before and after this period (Fig. 4.5).

After the salinity reached a maximum at about 7.2 cal ka BP (Fig. 4.5), it dropped dramatically, likely due to an increase of effective moisture availability and an opening of the lake basin. A gradual cooling toward the termination of the Holocene optimum, as reported for ca. 6.5 to 7.0 cal ka BP from the Guliya ice core on the western Tibetan Plateau (Thompson 2000), may have caused decreased evaporation rates, resulting in an increase in effective moisture availability. The salinity decreased steadily between 7 and 6 cal ka BP. This salinity change is accompanied by a rise in $\delta^{13}\mathrm{C}_{\mathrm{TIC}}$ (Fig. 4.5), which

can be explained by increased $^{13}CO_2$ or $H^{13}CO_3^-$ assimilation due to enhanced primary production (Leng and Marshall 2004). This conclusion is supported by several algal and bacterial biomarkers that show peak concentrations during that period, shown for phytane and the sum of hopanoids (Fig. 4.5), especially in a sample from 299 cm depth (6.8 cal a BP) (Fig. 4.2b). Increased input from an allochthonous source of DIC with a different isotopic signature, caused by the opening of the lake basin, may also have played a role. The $\delta^{13}C$ trend of TIC is followed by the $\delta^{13}C$ values of the mid-chain *n*-alkanes (Fig. 4.5), assuming that bicarbonate is the dominant species in the lake and therefore the major carbon source for aquatic macrophytes. The latter also became more abundant after the opening of the lake, as seen by the enhanced concentrations of nC_{23} (Fig. 4.5). The concurrent rise of long-chain *n*-alkanes can be attributed to an increased input of terrestrial material. Indeed, Cyperaceae show a maximum during that time (Herzschuh et al., 2009), but algal sources are also possible, since *Botryococcus* have been found in the respective parts of the core.

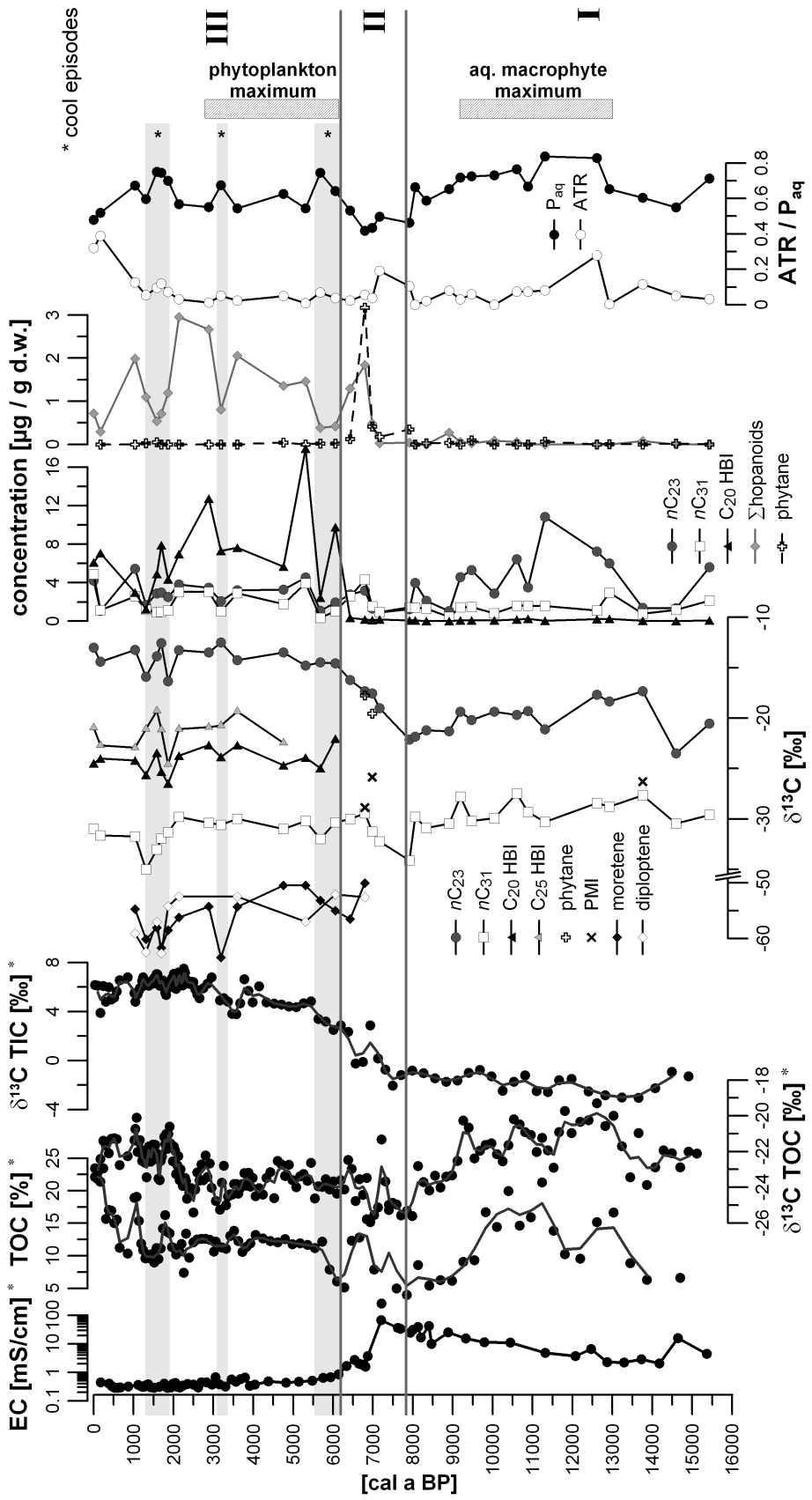

Figure 4.5: An overview of bulk sediment variables [EC (electrical conductivity), TOC, $\delta^{13}C_{TOC}$ and $\delta^{13}C_{TIC}$, *data from Mischke et al. (2008)], concentrations and $\delta^{13}C$ values of selected biomarkers, and *n*-alkane ratios P_{aq} and ATR in the Lake Koucha sediment core

4.5.2.3 Period III (6.1 - 0 cal ka BP)

The high relative abundances of bacteria, algae and macrophytes persist until 6.1 cal ka BP, when a decrease in the concentrations of many biomarkers is observed. Another significant change occurred in the lake at the same time, as revealed by the sudden appearance of phytoplankton biomarkers, especially the C_{20} HBI (Fig. 4.2b). The latter is the dominant compound in most samples from period III, and has rarely been reported from lacustrine sediments (Gomes and Azevedo 2003). A diatom-derived C_{25} HBI, which appears at 5.3 cal ka BP (Figs. 4.3 and 4.5), has considerably lower abundances. The differing distribution curves and the 2-4‰ more positive $\delta^{13}C$ values of the C_{25} HBI (Figs. 4.4 and 4.5) suggest different producers for the two types of HBIs. Interestingly, their $\delta^{13}C$ values follow the same trend, which may indicate that they had a common carbon source, but that differing carbon isotope fractionation occurred during lipid synthesis. It has been previously reported that diatoms contain lipids relatively enriched in ^{13}C, due to their tendency to grow in blooms that cause local CO_2 limitation (Deuser, 1970; Freeman et al., 1994). Throughout period I, there is a striking similarity in the concentration curves, and to some degree, $\delta^{13}C$ curves, for many compounds. For instance, low concentrations of bacterial biomarkers (hopanoids) are found between 6.1 and 5.6 cal ka BP, at 3.1 cal ka BP, and between 1.8 and 1.3 cal ka BP (Figs. 4.3 and 4.5). Similar trends can be observed for mid- and long-chain *n*-alkanes, with the latter showing a more pronounced decrease, resulting in an increased P_{aq} during the above-mentioned episodes (Fig. 4.5). A biomarker record from the Zoigê-Hongyuan peat deposit at the north-eastern edge of the Tibetan Plateau showed major climatic events, interpreted as relatively cold and dry periods, at 6.0, 4.5, 3.1 and 2.1 cal ka BP (Zheng et al., 2007). This seems to correspond well with the observed drop in biomarker concentrations in the Lake Koucha record. According to Gupta et al. (2003), periods of weak summer monsoons coincided with cold periods in the North-Atlantic region (Bond et al., 1997). Our biomarker record provides evidence that these regular events of cold and relatively dry conditions also occurred in the Koucha region during the last 6 cal ka BP, which could not be clearly inferred from geochemical, ostracod or pollen data. Even if not occurring simultaneously, phases of increased aridity during the middle Holocene have been observed at a number of lakes throughout the Tibetan Plateau (An et al., 2006; Mügler et al., 2009), including Bangong Co (Gasse et al., 1996), Nam Co (Mügler et al., 2009) and Lake Qinghai (Shen et al., 2005) in the western, central and eastern parts of the Tibetan Plateau, respectively.

The initial minimum of biomarker concentrations at 5.7 cal ka BP may still be attributed to the termination of the Holocene optimum, which led to increased moisture availability and an opening of the lake basin at ca. 7.2 cal ka BP. A further temperature decrease may have caused the collapse of all pioneer organisms, including aquatic macrophytes, bacteria and phytoplankton, which emerged shortly after the lake became a freshwater system. Zhou et al. (2007) reported maximum cooling at 5.8 cal ka BP, as inferred from

TOC contents in a sediment core from Erhai Lake on the south-eastern margin of the Tibetan Plateau, which corresponds well with the timing of low biomarker concentrations in Lake Koucha. A cold period lasting approximately from 3 to 2.5 cal ka BP has been inferred from palynological and geological evidence from several localities in southern, central and western Tibet (Wang and Fan 1987). During that episode, a shift towards lower $\delta^{13}C_{TIC}$ values occurred, which also suggests decreased productivity. The concentration of phytoplankton biomarkers, however, remained constant during that episode, and the $\delta^{13}C$ of nC_{23} does not follow the $\delta^{13}C_{TIC}$ trend. The decreases in nC_{23} and TOC concentrations are also less pronounced than at 5.7 cal ka BP.

The decrease of biomarker concentrations between 1.8 and 1.5 cal ka BP is accompanied by significantly decreased $\delta^{13}C$ values of moretene, diploptene, *n*-alkanes and HBIs (Figs. 4.3 and 4.5), suggesting a decrease of overall productivity in and around the lake. A significant change of climatic conditions, mainly attributed to a cooler climate at ca. 2 cal ka BP, was previously inferred from many other records (Shen et al., 2005; Herzschuh, 2006; Zhu et al., 2008). The $\delta^{13}C$ signals of moretene and diploptene (indicative of methanotrophic processes in the oxygenated upper part of the sediment) show the most negative values when the biomarker concentrations are low during the assumed cool periods (Fig. 4.5). The isotopic signal of methane, and consequently of methane consumers, depends primarily on the initial $\delta^{13}C$ value of the carbon source for the methane producers, on the pathway used for methanogenesis (Schaefer and Whiticar 2008) and on the degree of demand- and supply-dependent isotopic fractionation during methanogenesis and methane oxidation (Summons, 1998). The predominant pathway of methane formation in lacustrine environments is acetate fermentation, usually resulting in $\delta^{13}C$ values of methane between -65 and -50‰, which correspond to the observed values for moretene and diploptene in our samples. In contrast, methane formation through CO_2-reduction results in more depleted $\delta^{13}C$ values of the methane (-110 to -60‰) (Whiticar et al., 1986). We assume that the lower $\delta^{13}C$ signals of moretene and diploptene during cool periods simply reflect depleted ^{13}C contents of substrates utilized by the methane producers. In addition, this trend might have been enhanced due to relatively high isotopic fractionation during those times when microbial activity, including methanogenesis and methane oxidation, was generally low. A change in the community of methane-producing prokaryotes towards a higher proportion of CO_2-reducers, triggered by changing environmental conditions, cannot be ruled out, but it was beyond the scope of this study to confirm this.

As mentioned above, the concentrations of phytoplankton biomarkers (HBIs) do not clearly follow the concentration trends of the other biomarkers. The drop in the concentration of C_{20} HBI is correlated with a shift of the C_{25} HBI to higher concentrations at ca. 4.7 cal ka BP (Fig. 4.3), which most likely means that a change in the algal/diatom population occurred at that time, and that the producers of the C_{20} HBI were partly suppressed by competition from other species. Mischke et al. (2008) inferred that a minor reduction

of moisture availability occurred between 4.3 and 2.0 cal ka BP, including a short-term warming period around 2.7 cal ka BP. This climatic change could be responsible for the change in the lacustrine microbial community, even if C_{25} HBI increases at 4.7 cal ka BP. It is notable that the major increases in diatom (C_{25} HBI) abundance occur shortly after the cool periods. A shift to higher concentrations of C_{20} and C_{25} HBIs and hopanoids between 2.8 and 2.1 cal ka BP, accompanied by higher $\delta^{13}C$ values of TOC, may have been triggered by the reported short-term warming phase, which has been previously inferred from a pollen record from Lake Zigetang, central Tibetan Plateau (Herzschuh et al., 2006).

In period III, the long-chain *n*-alkanes are up to 19‰ more negative than the mid-chain *n*-alkanes. Also, they are on average 2-4‰ more depleted in ^{13}C than the long-chain *n*-alkanes in period I (Fig. 4.4). The change from steppe to tundra vegetation in the lake catchment at ca. 6.6 cal ka BP (period II), inferred from pollen data by Herzschuh et al. (2009), may have influenced the $\delta^{13}C$ signal of the long-chain *n*-alkanes. However, it is more likely that the shift was caused by the higher proportional input of terrestrial material in period III. This is in contrast to period I, in which the $\delta^{13}C$ signal of the long-chain *n*-alkanes contains a significant macrophyte component, as seen from the correlation between the curves for the mid- and long-chain *n*-alkanes (Fig. 4.4). Bicarbonate was the main carbon source for macrophytes throughout period III, as shown by the high $\delta^{13}C$ values of the mid-chain *n*-alkanes. The relatively low (-25 to -23‰) $\delta^{13}C_{TOC}$ support the assumption that macrophytes made a relatively insignificant contribution to the TOC pool, and that other organisms such as HBI producers are more important contributors, especially during the inferred phytoplankton maximum between 6.1 and 2.8 cal ka BP.

4.5.3 δ^{13}C values of aquatic macrophyte-derived *n*-alkanes as a proxy for carbon limitation

Limited CO_2 availability in lakes can lead either to enhanced uptake of ^{13}C-enriched CO_2 or to bicarbonate assimilation, which may then become limited, resulting in the uptake of ^{13}C-enriched bicarbonate (Allen and Spence, 1981; Prins and Elzenga, 1989; Fogel and Cifuentes, 1993; Burckhardt et al., 1999; Papadimitrou et al., 2005). All of these processes lead to enhanced $\delta^{13}C$ values of the assimilating organisms and, as long as these organisms are the main contributors to the TOC pool, also to higher $\delta^{13}C$ values of TOC. Considering the present high pH of Lake Koucha, uptake of [CO_2(aq)] might be of less importance, as bicarbonate is the dominant carbon species at high pH (Stumm and Morgan 1981).

Relatively high $\delta^{13}C$ values of aquatic macrophyte-derived mid-chain nC_{23} and nC_{25} alkanes were observed in period I between 13 and 9.2 cal ka BP. Although the values are low at the beginning of period II, they increase steadily and remain high throughout period III, with the exception of two excursions during the cold episode between 1.8 and 1.3 cal ka BP (Fig. 4.4). Thus, the highest values are found during the phytoplankton maximum, while values during the maximum of macrophyte growth are also relatively

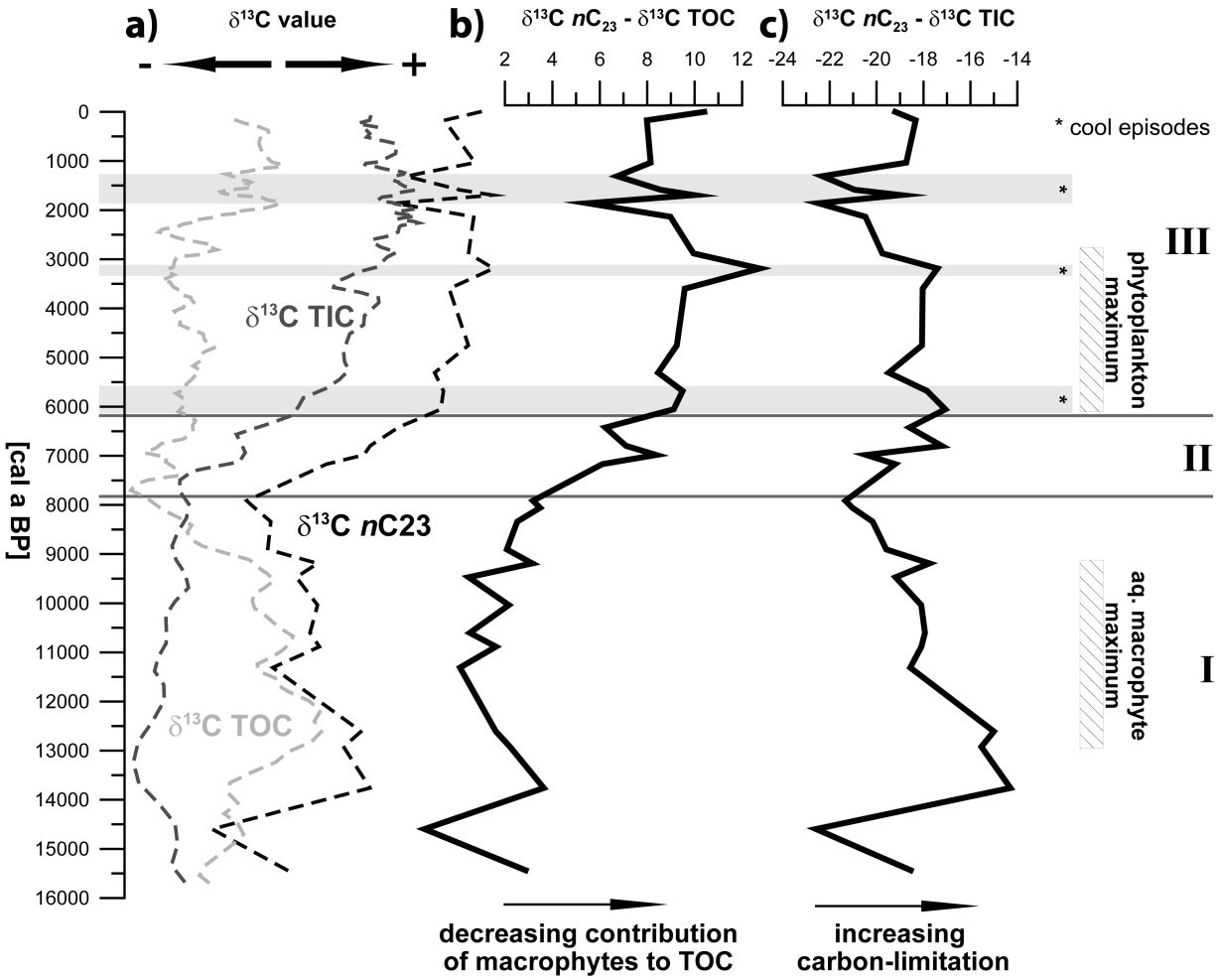

Figure 4.6: (a) Comparison of the $\delta^{13}C_{TOC}$*, $\delta^{13}C_{TOC}$* and $\delta^{13}C_{nC_{23}}$ curves (running averages). (b) The offset between $\delta^{13}C_{nC_{23}}$ and $\delta^{13}C_{TOC}$: higher values indicate a lower contribution to the organic carbon pool from aquatic macrophytes. (c) The offset between $\delta^{13}C_{nC_{23}}$ and $\delta^{13}C_{TIC}$: high values are representative of carbon-limited conditions in the lake. [* data from Mischke et al. (2008)]

high. Fig. 4.6a shows a comparison between the $\delta^{13}C$ values of TOC and TIC and $\delta^{13}C$ of the C_{23} *n*-alkane, which was chosen as a representative for aquatic macrophyte-derived biomarkers. In period I, the $\delta^{13}C$ values of nC_{23} are similar to the $\delta^{13}C$ values of TOC. This is in contrast to period II and III, in which the $\delta^{13}C$ values of nC_{23} follow the trend of increasing $\delta^{13}C_{TIC}$ and the $\delta^{13}C_{TOC}$ remains relatively low throughout the phytoplankton maximum, before increasing again at ca. 2.1 cal ka BP. Because aquatic macrophytes have been shown to be the main contributors to the TOC pool during period I, the high $\delta^{13}C$ values of nC_{23} in period I can be explained by local carbon limitation in dense plant stands in a lake where primary productivity is generally low, as indicated by low concentrations of aquatic biomarkers and low $\delta^{13}C$ values of TIC. After the transition period (II), increasing primary productivity throughout period III caused enhanced competition for carbon sources throughout the entire water column. The $\delta^{13}C$ curves for TIC and the $C_{23}n$-alkane are not completely congruent in periods II and III. Between 7.9 and 6.0 cal ka BP, $\delta^{13}C$

values of $n\mathrm{C}_{23}$ shift more strongly towards less negative values than $\delta^{13}\mathrm{C}_{\mathrm{TIC}}$, which can be explained by increased competition for bicarbonate due to increasing primary production, and a resulting enhanced uptake of ^{13}C-enriched bicarbonate. Since aquatic macrophytes contributed little to the TOC pool during this period, this shift towards positive values is not accompanied by high $\delta^{13}\mathrm{C}_{\mathrm{TOC}}$.

These findings suggest that, in addition to biomarker concentrations, comparison between the δ^{13}C curve of a particular biomarker and the δ^{13}C curve of TOC can provide valuable information regarding the contribution of the producer of that biomarker to the TOC pool. The offset between δ^{13}C of TOC and δ^{13}C of $n\mathrm{C}_{23}$ is especially low during the maximum of macrophyte growth between 13 and 9.2 cal ka BP (Fig. 4.6b). This offset then increases during period II, continuing towards high values in period III, which validates the assumption of a decreasing contribution of aquatic macrophytes to the TOC pool after 8 cal ka. This decreased contribution was only interrupted by increased input during the cold event between 1.8 and 1.3 cal ka BP.

As indicated by the $\delta^{13}\mathrm{C}_{\mathrm{TOC}}$ curve, the isotopic signature of bicarbonate assimilated by the macrophytes can exhibit strong variations. In Lake Koucha, positive δ^{13}C values of TIC up to +8‰ during episode III contribute to the high δ^{13}C values of the mid-chain *n*-alkanes. Thus, for the purpose of assessing carbon-limiting conditions, the offset between $\delta^{13}\mathrm{C}_{nC23}$ and $\delta^{13}\mathrm{C}_{\mathrm{TIC}}$ (Fig. 4.6c) may be a more precise measure than the δ^{13}C values of $n\mathrm{C}_{23}$. The largest offsets, up to -14‰, were seen in period I during the maximum growth of aquatic macrophytes (Fig. 4.6c), and in period III during the maximum growth of phytoplankton. The carbon supply for water plants increased during the cold event at 1.8 cal ka BP, due to a general decrease of lake productivity. After this event, enhanced growth of macrophytes and phytoplankton (high $n\mathrm{C}_{17}$ and C_{20} HBI, Fig. 4.3) again led to carbon-limited conditions, which persisted until the present.

The offset between the δ^{13}C values of $n\mathrm{C}_{23}$ and TIC may therefore serve as an indicator for carbon-limited conditions in lacustrine systems. Mischke et al. (2008) applied the offset between the δ^{13}C values of TOC and TIC for this purpose. However, it must be taken into account that the δ^{13}C value of TOC is influenced by multiple factors. This is also the case, albeit to a much lesser extent, for the $n\mathrm{C}_{23}$ alkane. Hence, the use of a specific biomarker, derived from autotrophic producers such as aquatic macrophytes, can provide more precise information about lacustrine carbon-limiting conditions. Plant macrofossils or pollen would be even better, but these are often not present in sufficient quantity for δ^{13}C analysis in sediment cores. Regardless, the main contributors to the organic carbon pool of the sediments must be known before the offset curves between the δ^{13}C values of biomarkers and TIC may be interpreted. This information can be obtained from the absolute concentrations of biomarkers, or alternatively by offset curves between δ^{13}C values of biomarkers and TOC, which may also help to decipher the main contributors to the TOC in different sections of a lake sediment core.

4.6 Conclusion

The quantification of biomarkers and compound-specific stable isotope analysis has provided more detailed knowledge of the contributors to the organic carbon pool in the lacustrine sediments of Lake Koucha since the late glacial period. Furthermore, the results provided new insights into the changing climatic conditions during that time. We confirmed the bulk- and ostracod-based inferences indicating that Lake Koucha was macrophyte-dominated before 8 cal ka BP, and later shifted to a phytoplankton-dominated system. Several algal and bacterial markers were found in high abundance in the transition period, including a moretene that previously had been reported only from acidic lakes, a hypertrophic alkaline lagoon, and a highly saline crater lake. The dominant constituents of the phytoplankton community after 6 cal ka BP were probably diatoms and/or cyanobacteria. The differing concentration curves for C_{20} HBI, C_{25} HBI and the C_{17} *n*-alkane suggest that several changes in the composition of the plankton population occurred during the last 6 ka. Similarly, decreases in the concentrations of bacterial and terrestrial biomarkers at ca. 6.0, 3.1 and 1.8 cal ka BP, as well as correlated trends in the $\delta^{13}C$ curves, provide evidence for cooler episodes. These episodes correspond well with cool events reported from other locations on the Tibetan Plateau, and may be attributed to reduced monsoon activity. The $\delta^{13}C$ values of aquatic macrophyte-derived *n*-alkanes were found to be a powerful tool for tracing carbon limitation in the lake, with relatively high values observed during times of maximum macrophyte and phytoplankton growth. Since the isotopic signature of the carbon source can exhibit considerable variation, the offset between $\delta^{13}C$ values of nC_{23} and TIC may provide a more precise indication of carbon limitation than the $\delta^{13}C$ value of the mid-chain *n*-alkane alone, and may therefore serve as an indicator of lake productivity. This technique may be particularly effective in lakes with abundant aquatic macrophytes, such as those in Tibet. There, the C_{23} *n*-alkane is very abundant in numerous lakes, can be attributed to a specific producer (i.e. aquatic macrophytes), and the contribution of terrestrial organic matter to the C_{23} *n*-alkane is relatively low. Furthermore, bicarbonate-assimilating macrophytes such as *Potamogeton* species occur world-wide, and thus the proxy may not be limited to our study area. In environments with a higher terrestrial input, the C_{21} *n*-alkane, which normally is not influenced significantly by terrestrial sources, could serve as an alternative. Biomarkers derived from other autotrophic organisms such as algae (e.g. short-chain *n*-alkanes) could probably also be used in certain lacustrine systems.

5 δD values of *n*-alkanes in Tibetan lake sediments and aquatic macrophytes - a surface sediment study and an application in a palaeorecord from Lake Koucha

Abstract

A set of lake surface sediment samples and aquatic macrophytes from the eastern and central Tibetan Plateau and a sediment core from Koucha Lake (northeastern Tibetan Plateau) were analysed for hydrogen isotope signals of aliphatic lipid biomarkers. Obtained δD values of *n*-alkanes could be correlated with δD values of meteoric water of summer months showing increasing Pearson correlation coefficients with increasing chain-length of the *n*-alkanes. While in the samples from more humid regions (e.g. the southeastern Tibetan Plateau) the apparent enrichment factors between meteoric water and lipids are close to those reported for other humid sites (≈-135‰ for mid-chain and ≈-125‰ for long-chain *n*-alkanes), they become smaller at sites receiving relatively little precipitation (e.g. the northeastern Tibetan Plateau or the Qaidam Basin). This might be caused by enrichment in deuterium of the source water used for lipid synthesis due to lake water evaporation and soil- and leaf water evapotranspiration. In the sediment core from Lake Koucha, decreasing δD values of all *n*-alkanes between 15 and 10 cal ka BP give evidence for increasing precipitation amounts due to an intensification of the Asian summer monsoon. Between 9 and 6.7 cal ka BP, higher δD values of mid-chain *n*-alkanes suggest enhanced evaporation of the lake water, which outweigh higher precipitation amounts because of a temperature increase during the monsoonal maximum. Only a few surface sediment samples show a significant offset between δD values of mid-chain *n*-alkanes and $n\mathrm{C}_{31}$ ($\Delta\delta_{mid-nC31}$) and no systematic dependency between this offset and environmental parameters such as mean annual precipitation was found. In contrast, in the sediment core, slight decreases of $\Delta\delta_{mid-nC31}$ between 9 and 6 cal ka BP might indicate drier conditions. Therefore, $\Delta\delta_{mid-nC31}$ can be potentially applied as a palaeoaridity proxy, but has to be interpreted critically, since it is not clear to which extent the isotopic signals of mid- and long-chain *n*-alkanes were influenced by evaporation and transpiration effects in the past.

5.1 Introduction

The Tibetan Plateau is a key region for atmospheric circulation patterns on the Northern Hemisphere due to its capacity as main driving force for the Asian monsoon system (Rud-

diman and Kutzbach, 1989) and therefore especially interesting for palaeoenvironmental research. A major point of interest of these studies centres around the reconstruction of past monsoon intensities and palaeohydrological conditions (e.g. reviewed in An et al., 2006 and Herzschuh et al., 2006). For this purpose, stable isotope ratios of the water molecule ($^{18}O/^{16}O$ and D/H), stored in the frozen water of ice cores (e.g. Dansgaard et al., 1993), in carbonates of speleothems (Wang et al., 2001; Yuan et al., 2004) or in sedimentary deposits such as ostracod shells (e.g. Schwalb, 2003), carbonates (Morinaga et al., 1993) or organic biomarkers (Sauer et al., 2001), have been shown to be promising proxies. On the Tibetan Plateau a large number of lakes provide an extensive source of sedimentary records which have been subject to a range of studies, that mostly focused on biological, sedimentological or inorganic geochemical proxies (cf. reviews by Morrill et al., 2003; Wang et al., 2005; Herzschuh, 2006; Chen et al., 2008), while studies including organic biomarkers are relatively rare.

In lipid molecules such as *n*-alkanes, the hydrogen atom is covalently bound to the carbon atom and therefore not exchangeable, leading to a long-term preservation of the hydrogen isotope ratio in the sediment (Schimmelmann et al., 1999). Hydrogen isotope ratios of lipid biomarkers derived from terrestrial or aquatic organisms have been frequently used to reconstruct relative variations of past precipitation amounts (e.g. Schefuß et al., 2005), benefiting from the fact, that with increasing amount of precipitation the meteoric water gets increasingly depleted in deuterium due to Rayleigh distillation (Gat, 1996). Beside this so-called amount effect, other factors like temperature, altitude, latitude and continentality (i.e. distance from the ocean) influence the isotopic composition of the rain water (Dansgaard, 1964; Rozanski et al., 1992). Since the 1960s the stable isotope composition of rain water is monitored and recorded world-wide by the Global Network for Isotopes in Precipitation (GNIP). Today, these data are available for each point of the world via web-resources e.g. from the International Atomic Energy Agency (IAEA, 2001) or the Online Isotope Precipitation Calculator (OIPC, Bowen and Revenaugh, 2003) which uses models on basis of latitude, longitude, altitude, and interpolated values from climate stations for the calculation of isotope values (Bowen and Revenaugh, 2003). To reconstruct past δD values of precipitation it is necessary to identify compounds in the sediment which record the isotopic signal of the water assimilated by the source organisms of the biomarker. Good correlations between the δD values of the source water and the δD values of lipids from aquatic organisms (e.g. the C_{17} *n*-alkane) have for instance been inferred from transect studies in humid regions like Northern America (Huang et al., 2004) and Europe (Sachse et al., 2004) revealing an average isotopic fractionation of -160‰ between the source water and the lipids. This was consistent with findings from Sessions et al. (1999) and Chikaraishi and Naraoka (2003) who reported similar isotopic fractionations for *n*-alkanes in seaweeds. Broader ranges and generally smaller isotopic fractionations were found for lipids of terrestrial plants or terrestrially derived

lipids in sediments such as long-chain *n*-alkanes or long-chain fatty acids (Chikaraishi and Naraoka, 2003; Yang and Huang, 2003; Chikaraishi et al., 2004a and b; Sachse et al., 2004 and 2006; Smith and Freeman, 2006). For example, a surface soil study along a North-South transect at the Chinese east coast recently revealed isotopic fractionations of -140‰ to -130‰ between δD of meteoric water (δD_{MW}) and long-chain *n*-alkanes (Rao et al., 2009). This was attributed to varying deuterium enrichment of soil and leaf water due to evaporation and transpiration effects (depending on temperature, relative humidity and leaf morphology) (Sachse et al., 2006) as well as varying isotopic fractionations for different kinds of vegetation types and even for different lipids within the same species, depending on the respective biosynthetic pathway (Sessions, 2006; Pedentchouk et al., 2008). In arid regions, the δD signal of the lake water could be significantly enriched by evaporation effects, compared to the original δD signal of the meteoric water. Hence, terrestrially derived biomarkers have been proposed to be more suitable proxies for meteoric water δD in arid environments (Hou et al., 2008). This assumption implicates, that in arid regions the influence of evapotranspiration upon the δD signal of source water for terrestrial plants is minor compared to the extensive enrichment of lake water δD. On the other hand, it has been shown, that evapotranspiration indeed significantly influences the δD signal of terrestrial leaf waxes in arid regions (Smith and Freeman, 2006), but the relative extent of both effects has so far not been quantified. Mügler et al. (2008) found on average 60‰ more negative δD values in terrestrial plants and sedimentary long-chain *n*-alkanes (nC$_{29}$ and nC$_{31}$) compared to aquatic plants and sedimentary mid-chain *n*-alkanes (nC$_{23}$ and nC$_{25}$) in lakes situated on the relatively arid central Tibetan Plateau. Since long-chain *n*-alkanes in humid regions in contrast have been found to be more enriched in δD than mid-chain *n*-alkanes, they concluded, that the offset between δD values of mid- and long-chain *n*-alkanes ($\Delta\delta_{mid-long}$) might serve as a proxy for hydroclimatic characteristics of a lake site in terms of humid or arid climate conditions (Mügler et al., 2008).

Surface sediment studies are a possible way to test the applicability of a proxy by comparing the proxy data with environmental parameters. Another possibility is to compare the data of the respective proxy with more established proxies e.g. using a sediment core. Recently, a surface sediment study using a small number of lakes from the central and northern Tibetan Plateau inferred a good relationship between δD_{MW} and δD of terrestrially derived *n*-alkanes, while the isotopic fractionation between both was found to be relatively small (- 95 to -41‰) which was explained by strong soil and leaf water evapotranspiration (Xia et al., 2008). However, this study covered only a small range of environmental conditions (mean annual precipitation ranging from 95 to 379 mm) and aquatic biomarkers were not considered. It has been shown, that sedimentary organic matter in most of the Tibetan lakes is strongly influenced by biomarkers derived from aquatic macrophytes (e.g. mid-chain *n*-alkanes) due to the high abundance of these organisms in the Tibetan lakes (manuscript I). Thus the first aim of this study was to evaluate δD values of

n-alkanes in surface sediments and additionally of samples from emergent and submerged macrophytes, which cover a broad climatic gradient. A main focus was to evaluate the difference between δD values of aquatic macrophyte derived mid-chain and terrestrially derived long-chain *n*-alkanes. Secondly, the δD values of *n*-alkanes in a sediment core from Lake Koucha, situated on the eastern Tibetan Plateau, were determined. Geochemical, palynological and biological proxies revealed a significant decrease of the effective moisture availability in the lake catchment area during the early Holocene (Herzschuh et al., 2009; Mischke et al., 2008). This was explained by an insolation-driven intensification of the monsoon which lead to higher precipitation amounts but also to higher temperatures. Consequently, an enhanced evaporation could possibly have outweighed the higher precipitation resulting in a lower net availability of moisture (Herzschuh, 2006; Herzschuh et al., 2009). In this study, we investigated whether aquatic macrophyte derived mid-chain *n*-alkanes, terrestrial long-chain *n*-alkanes or the offset between δD values of both is able to record this period of decreased available moisture availability.

5.2 Study site

5.2.1 The Tibetan Plateau

The Tibetan Plateau, with an average altitude above 4,000 m and a maximum extent from 77° E to 105° E and 25° N to 40° N, is the largest elevated landmass in the world. In this study we concentrated on the eastern and central Tibetan Plateau covering an area from 25.9° N to 37.4° N latitudes and 89.5° E to 100.5° E longitudes (Fig. 5.1a). The study area is monsoon influenced, resulting in most of the precipitation occurring during summer months (Fan et al., 2004). The influence of the monsoon decreases from southeast to northwest. Therefore, the southeastern margin of the plateau receives higher annual precipitation (P_{ann}), which ranges from ca 600 to 1,500 mm, than the central and northeastern Tibetan Plateau (ca 300-500 mm) (Table 5.1). Precipitation is very low in the Qaidam Basin (P_{ann}< 50 mm), a dry basin situated between the Kunlun Shan and Qilian Shan mountain ranges at the northern margin of the Tibetan Plateau. The altitude in our study area varies between ca 1,900 and 5,100 m. Conifer and broad-leaf forests are only found in altitudes up to 4,000 m in the more warm and humid south and up to ca 3,000 m at the north-eastern and eastern margin of the plateau. In higher altitudes, the vegetation consists of alpine steppes and meadows (mostly dominated by *Artemisia* and *Kobresia*). Sparse desert vegetation (mainly Chenopodiaceae) covers the Qaidam Basin.

5.2.2 Lake Koucha

Lake Koucha is situated on the northeastern Tibetan Plateau (34.0° N; 97.2° E), on the southern slope of the Bayan Har mountain range, in an altitude of 4,540 m a.s.l (Fig.

Table 5.1: Location parameter and δD values of *n*-alkanes of surface sediment and aquatic macrophyte samples

region	sample code	sample type	Latitude [°]	Longitude [°]	Altitude [m]	P_{ann} [mm] *	T_{July} [°C] *	TOC [%] ***	$\delta^{13}C_{TOC}$ [‰] ***	EC [mS / cm] ***	pH ***	sampling depth [m]	$n C_{17}$ δD [‰]	SD	$n C_{19}$ δD [‰]	SD	$n C_{21}$ δD [‰]	SD	$n C_{23}$ δD [‰]	SD	$n C_{25}$ δD [‰]	SD	$n C_{27}$ δD [‰]	SD	$n C_{29}$ δD [‰]	SD	$n C_{31}$ δD [‰]	SD	$\delta D_{mw\ ann.\ mean}$ [‰] ****	$\delta D_{mw\ august}$ [‰] ****	95% confidence interval ****
Qaidam	**Qai-07**	sediment	37.463	95.577	3174	43	15.8	0.3	-21.7	130.30	8.4	0.3																	-81	-83	4
Basin	**Qai-06**	sediment	37.288	96.887	2812	65	18.1	7.3	-20.2	1.05	8.5	6.8							-113	3	-114	5							-74	-80	15
	Qai-02	sediment	37.036	100.576	3205	312	11.1	11.5	-25.9	41.30	9.2	7.0											-135	2	-150	6	-173	2	-78	-80	15
	Donggi	sediment	35.227	98.650	4095	304 **	n.d.	0.8	-24.7	0.70	7.9	37.0							-175 a		-166	9	-158	13	-162	12	-168	4	-92	-96	17
		Potamogeton										0.3							-166	4	-157	8	-157	2							
	MiY-35	sediment	34.742	98.112	4241	388	8.2	13.1	-18.4	1.81	10.2	0.2							-158	4	-154	6			-169	4	-176	7	-95	-100	17
north	**MiY-46**	sediment	34.679	98.064	4233	356	8.2	2.9	-21.6	0.59	10.8	0.5													-188	5	-188	3	-95	-100	17
eastern	**CTP-35**	sediment	34.158	95.977	4701	370	5.2	9.1	-29.0	0.65	9.1	2.1							-207	1	-207	1	-191	3	-188	5	-188	3	-105	-113	12
Tibetan	**MiY-42**	sediment	34.030	97.545	4617	389	5.1	13.2	-21.8	0.21	10.4	0.5							-182	1	-185	4	-176	2	-189	13	-186	1	-102	-109	15
Plateau		*Hippuris*																					-176	2	-191	1	-178	3			
		sediment																	-176	8	-183	3	-169	2	-180	5	-176	5			
	Koucha	*Potamogeton*	34.024	97.220	4541	511 ***	8 ***	12.5	-22.1	0.50	9.1	6.0							-174 a		-165 a								-102	-109	15
		Hippuris																					-175	4	-182	3					
	MiY-39	sediment	33.990	97.455	4581	366	5.4	10.4	-19.3	1.85	10.5	0.4							-210	2	-210	2	-199	5	-205	4	-212	1	-102	-109	15
central	**CTP-25**	sediment	32.572	91.857	5133	540	6.0	6.8	-21.4	0.20	8.5	0.4							-174	5	-176	1							-121	-138	18
Tibetan	**CTP-20**	sediment	32.098	89.528	4724	488	9.2	5.2	-16.0	0.23	10.4	0.4							-206	3	-199	4	-187	1	-194	1	-210	1	-116	-135	17
Plateau		*Potamogeton*																	-198	6	-195	0									
south	**LC-06**	sediment	29.825	94.456	4132	1408	8.2	4.9	-27.1	0.01	7.0	23.0							-245	1	-244	2	-237	2	-232	0	-228	1	-103	-124	13
eastern	**LC-05**	sediment	29.813	94.433	4050	1413	8.2	1.4	-27.0	0.01	8.0	38.0							-232	2	-236	2	-229	4	-230	2	-232	0	-102	-123	13
Tibetan	**LC-10**	sediment	29.654	96.716	4431	1073	7.1	1.2	-20.8	0.11	7.7	0.5							-197	1	-192	4	-186	4	-193	2	-220	6	-104	-119	12
Plateau		*Potamogeton*															-185	10													
	SET-16	sediment	25.918	100.118	1967	685	20.3	23.7	-18.2	0.21	9.0	5.0	-181	4	-191	6			-172	2	-172	3	-168	2	-172	1	-178	8	-68	-81	4

*: data from Böhner, 2006
**: data from Madoi climate station (Chinese Central Meteorological Office, 1984); source: Dietze et al. (in review)
***: data from Mischke et al. 2008
****: data from online isotope precipitation calculator (OIPC), Bowen and Revenaugh, 2003

SD = standard deviation
$\delta D_{mw} = \delta D_{meteoric\ water}$, EC = electrical conductivity
a: only one measurement available
n.d.: no data available

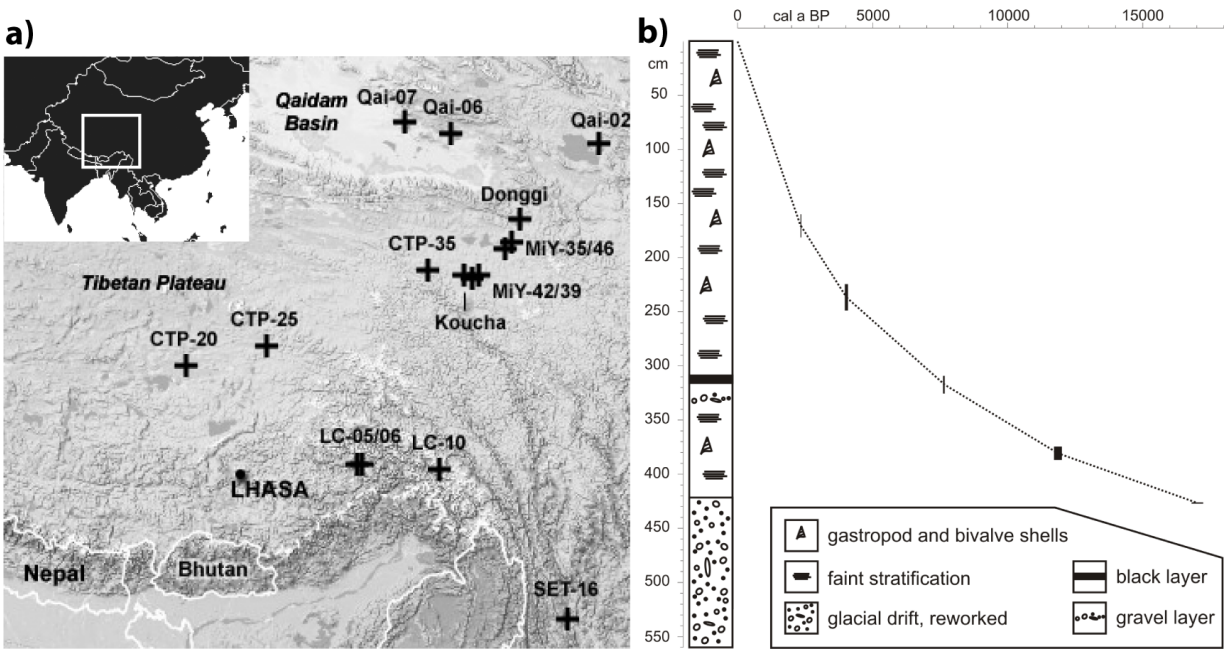

Figure 5.1: (a) Study area with location of the lakes sampled for surface sediments. *Potamogeton* samples were derived from lakes LC-10, CTP-20, Koucha and Donggi Cona. *Hippuris* samples were from lakes MiY-42 and Koucha. (b) Age-depth model of the Lake Koucha sediment core based on a linear interpolation between ^{14}C-AMS dates of pollen extracts (uppermost four samples) and of the alkali-soluble fraction of bulk organic matter (lowermost sample). The core top was assigned an age of zero. The bar widths and lengths represent the 1σ range and the sampled interval, respectively.

5.1b). It is a freshwater lake with a maximum depth of 6.9 m and an area of 18 km². Data obtained from a climate station at Qingshuihe (4,415 m a.s.l., 20 km south of Lake Koucha) suggest a mean annual temperature of -4.8 °C and a mean annual precipitation of 511 mm, with most of the precipitation occurring between June and September (Fan et al, 2004). The lake is fed by several small streams deriving from a swampy valley to the south-east; the outlet passes through another small lake 1 km north of Lake Koucha before discharging into the Yellow River. The relatively small catchment area (88 km²) is dominated by alpine meadows, which are mainly composed of *Kobresia*. The lake itself is densely populated by aquatic macrophytes, mainly *Potamogeton pectinatus*, down to a depth of 4 m (Herzschuh et al., 2009).

5.3 Samples

5.3.1 Surface sediment and macrophyte samples

Surface sediment samples of lakes chosen for this study represent four different regions of our study area: the Qaidam Basin, the northeastern, the central and the southeastern Tibetan Plateau (Fig 5.1). Basic information of all sampled lakes is summarised in Table

5.1. The Qaidam Basin is represented by lakes Qai-06 and Qai-07 while lake Qai-02 is located more to the east, close to Lake Qinghai. Qai-07 and Qai-02 are the only lakes in our set with relatively high salinities. Lakes at the northeastern Tibetan Plateau (Qai-02, MiY-35, MiY-39, MiY-42, MiY-46, Donggi Cona, Koucha and CTP-35) are all situated in high altitude (>4 000 m) and so are lakes at the central Tibetan Plateau (CTP-20 and CTP-25; >4,700 m). On the southeastern Tibetan Plateau, the lakes LC-05, LC-06 and LC-10 represent high altitude examples with high P_{ann} (<1,000 mm) while lake SET-16 is situated on the southeastern slope of the Plateau in lower altitude (1,967 m) and receives less precipitation (685 mm) (Table 5.1). Most of the lakes in our sample set, except LC-05, LC-06 and Donggi Cona, are shallow (mean depth: 7.5 m; median depth: 0.5 m) and have neutral to high pHs (range 7.0 to 10.8) (Table 5.1). In addition to the sediment samples, samples of aquatic macrophytes from lakes LC-10, MiY-42, CTP-20, Koucha and Donggi Cona, have been analysed. *Potamogeton pectinatus* is the dominant submerged aquatic macrophyte species in Tibetan lakes, while the emergent species *Hippuris vulgaris* occurs frequently at the shore lines.

5.3.2 Sediment core from Lake Koucha

A 5.6 m-long sediment core (Fig. 5.1b) was obtained from Lake Koucha in March 2003, using a Livingstone piston corer (Stitz). The lower part of the core (5.60 - 4.23 m), comprised of dark-grey loam with quartz and granite gravels and with low TOC content, was excluded from our study. We focused on the light-grey silty and calcareous sediments in the upper part of the core (4.23 - 0 m) with total organic carbon (TOC) contents between 5 and 25‰. The same section of the core was already subject to a biomarker study, including compound-specific carbon isotope analysis (Aichner et al., in press; manuscript II), while pollen, ostracod and geochemical data were published in Herzschuh et al. (2009) and (Mischke et al. (2008).

5.3.3 Biomarker distributions in sediment and macrophyte samples

The *n*-alkane patterns in the Tibetan surface sediment and corresponding macrophyte samples have been extensively described in Aichner et al. (manuscript I), and the biomarker distributions in the sediment core from Lake Koucha were discussed in Aichner et al. (in press; manuscript II). Briefly, as expected from the literature, submerged macrophyte samples are dominated by mid-chain *n*-alkanes C_{23} and C_{25} while emergent macrophyte samples consist of nC_{27} and nC_{29} (Fig. 5.2a) (Ficken et al., 2000). The absolute concentrations of *n*-alkanes are five- to tenfold higher in emergent than in submerged species. The *n*-alkane pattern of the surface samples is dominated by mid-chain *n*-alkanes from submerged macrophyes and/or long-chain *n*-alkanes derived from emergent macrophytes or terrestrial vegetation. In contrast, short-chain homologues are found in significant amounts

in a few samples only (Fig 5.2). In the Lake Koucha sediment core, the mid-chain *n*-alkanes are predominant especially in the lower part of the core (16 to 7.9 cal ka BP). In the middle part (7.9 to 6.1 cal ka BP) long-chain *n*-alkanes and algal and bacterial biomarkers (e.g., phytane and pentamethylicosane) are more abundant (Fig 5.3; Aichner et al., in press; manuscript II). In the upper part of the core (6.1 to 0 cal ka BP), mid-chain *n*-alkanes show relatively high abundances, but the dominant compound in most of the samples is a highly branched isoprenoid compound with 20 carbon atoms (C_{20} HBI), indicative for phytoplankton input (Jaffé et al., 2001).

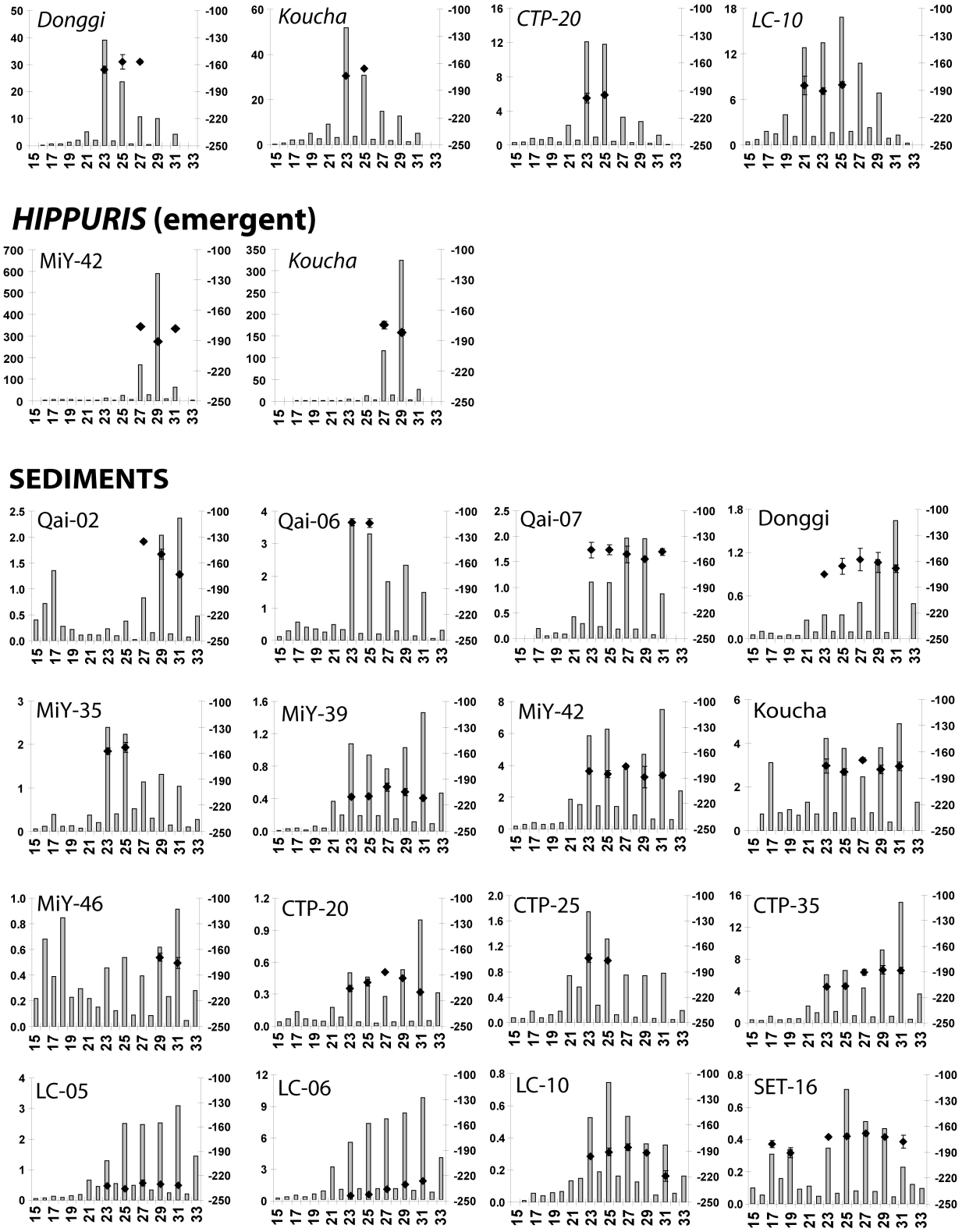

Figure 5.2: *n*-Alkane concentrations in µg/g dry weight (left y-axes, grey bars) and δD values of *n*-alkanes (right y-axes, black diamonds) in *Potamogeton*, *Hippuris* and surface sediment samples

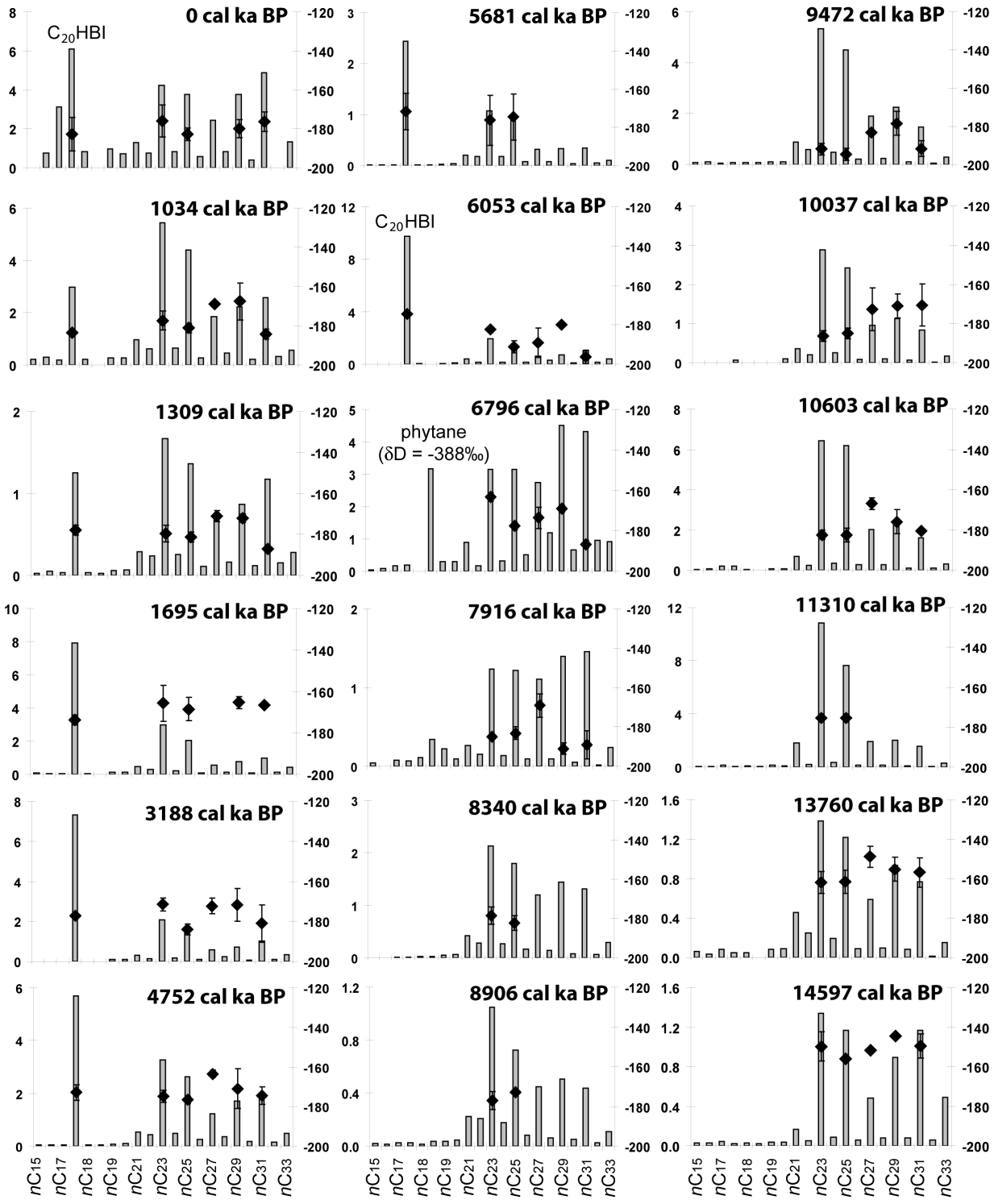

Figure 5.3: *n*-Alkane concentrations in µg/g dry weight (left y-axes, grey bars) and δD values of *n*-alkanes (right y-axes, black diamonds) in samples from the Lake Koucha sediment core

5.4 Methods

5.4.1 Chronology of the sediment core

Surface sediment and plant samples were collected with a sediment grabber during campaigns in the summers between 2003 and 2006. The standard methods used for determination of water and bulk parameters of sediments and plants were described in Mischke et al. (2007). The age model of the Lake Koucha sediment core was derived by linear interpolation between four dated samples of pollen concentrate and one dated sample of the alkali-soluble fraction of the bulk organic carbon (Fig. 5.1b). The age of the core-top was assumed to be zero. The calendar years were calibrated from the ^{14}C years using Calib (Reimer et al., 2004). A detailed description of the age model and the determination of the bulk parameters are given in Mischke et al. (2008).

5.4.2 Biomarker extraction, analysis and quantification

Biomarker quantification methods were described in detail in Aichner et al. (in press; manuscript II). Briefly, the freeze dried and milled samples were extracted with an accelerated solvent extractor (ASE) (Dionex, Sunnyvale, USA) using dichloromethane : methanol (9:1) at 76 bar and 100 °C. The aliphatic hydrocarbon fractions were isolated using a medium pressure liquid chromatography (MPLC) system (Radke et al., 1980). As quantification standard, 5α-androstane (Sigma-Aldrich, St. Louis, USA) was added to the extracts prior to MPLC. The individual compounds of the aliphatic fraction were quantified using an Agilent 6890 GC-FID with an injector heated from 40 °C to 300 °C at 700 °C/min using splitless injection. For the separation of the compounds, an Ultra-1 fused silica capillary column (50 m length, 0.2 mm inner diameter, 0.33 µm film thickness) was used with the following temperature programme: an oven start temperature of 40 °C, a heating rate of 5 °C/min to 310 °C, and an isotherm phase of 60 minutes. Helium with a constant flow rate of 1 ml/min was used as a carrier gas.

5.4.3 Compound-specific hydrogen isotope analysis

Hydrogen isotope ratios of the compounds were measured by GC-P-IRMS (gas chromatography-pyrolysis-isotope-ratio mass spectrometry). The GC-P-IRMS system consisted of a GC unit (6890N, Agilent Technology, USA) connected to a GC-C/TC III combustion device coupled via open split to a Delta V Plus mass spectrometer (ThermoFisher Scientific, Germany). Saturated hydrocarbons were separated on a fused silica capillary column (HP Ultra 1, 50 m x 0.2 mm ID, 0.33 µm FT, Agilent Technology, USA). Saturated fractions have been injected to the programmable temperature vaporisation inlet (PTV, Agilent Technology, USA) with a septumless head, working in split/splitless mode. The injector was held at a split ratio of 1:2 and an initial temperature of 230 °C. With injection, the

injector was heated to 300 °C at a programmed rate of 700 °C min^{-1} and held at this temperature for the rest of the analysis time. Individual hydrocarbons were separated on a fused silica capillary column (HP Ultra 1, 50 m x 0.2 mm ID, 0.33 µm FT, Agilent Technology, USA). The GC oven temperature was set to 40 °C and kept for 2 min. After that the temperature increased to 300 °C at a rate of 4 °C/min followed by an isothermal time of 45 min. Helium, set to a flow rate of 1.0 ml min^{-1}, was used as carrier gas. After passing the GC, hydrocarbons were reduced to H_2 and elemental carbon in the pyrolysis reactor held at 1450 °C. H_2 was transferred on line to the mass spectrometer to determine hydrogen isotope ratios. All saturated fractions were measured in triplicate. A mixture of *n*-alkanes (C_{17}, C_{19}, C_{21}, C_{23} and C_{25}; Schimmelmann, Bloomington, USA) with certified isotopic composition was used as external standard for calibration of the reference gas. In addition, the δD signal of the internal standard served as a quality control for the stability of the system. The H_3^+-factor was determined daily by measuring 10 reference gas peaks with increasing amplitude (1,000 to 10,000 mV). This factor had an average value of 2.60 ± 0.03 ppm/nA. In surface sediment and plant samples, hydrogen isotope values could be determined for most of the odd-numbered *n*-alkanes in the mid- and long-chain range. Additionally, δD values of highly abundant isoprenoid compounds could be measured in the upper and middle part of the Lake Koucha sediment core. Only peaks with abundances within the linearity range of the measurement system (1,000 to 10,000 mV) were used for this study.

5.4.4 Precipitation model

Site-specific climate information on T_{july}, and P_{ann} were obtained from Böhner (2006). A comprehensive description of the methods used is given in Böhner (2004 and 2005). The empirical database comprises temperature and precipitation records from more than 400 climate stations in Central Asia, but the density of climate stations on the western Tibetan Plateau is low. Temperature and precipitation layers having a resolution 1 × 1 km were estimated by statistical downscaling, namely large-scale circulation modes (represented by general circulation model predictor variables) were related to the corresponding local variations of single weather variables (observed at one or a set of meteorological stations) using multivariate statistical analyses.

5.4.5 Calculations

The isotopic fractionations (or apparent enrichment factors) between δD values of lipid compounds and δD values of meteoric water were calculated as follows:

$$\epsilon_{compound/water} = 1000 \times [\frac{(\delta D_{compound} + 1000)}{(\delta D_{water} + 1000)} - 1]$$

5.5 Results

5.5.1 δD values of *n*-alkanes in surface sediment and plant samples

In surface sediment and aquatic macrophyte samples, reliable δD values could be obtained for predominant odd-chain *n*-alkanes. In contrast, even-chain *n*-alkanes were too low in abundance for δD analysis. All measured δD values of *n*-alkanes are listed in Table 5.1 and are visualized together with the *n*-alkane patterns in Fig. 5.2. Average δD values of mid-chain and long-chain *n*-alkanes in sediments ranged from -245 to -114‰ and from -231 to -148‰, respectively. In most of the samples, relatively little variations were visible in δD values of the individual *n*-alkanes. Exceptions are sample Qai-02 (which showed an offset of about -45‰ between $n\mathrm{C}_{27}$ and $n\mathrm{C}_{31}$), sample CTP-35 (long-chain *n*-alkanes show an enrichment of 20‰ compared to mid-chain *n*-alkanes), sample LC-06 (slightly increasing δD values with increasing chain length) and sample LC-10 ($n\mathrm{C}_{31}$ is about 25‰ more depleted in deuterium than the other *n*-alkanes). δD values of *n*-alkanes in submerged and emergent macrophytes were in the same range as values from the corresponding sediment samples (Fig. 5.4 and Table 5.1). Generally, *n*-alkanes showed slightly higher δD values in submerged macrophytes than in sediments, however, the offset was smaller than 10‰, with the exception of $n\mathrm{C}_{25}$ in Koucha samples (offset: 17‰).

5.5.2 δD values of biomarkers in samples from Lake Koucha sediment core

δD values of most of the odd-chain *n*-alkanes in the mid- and long-chain range ($n\mathrm{C}_{25}$ to $n\mathrm{C}_{31}$) could be obtained for the samples from the Lake Koucha sediment core. In four samples (from 5.7, 8.3, 8.9 and 11.3 cal ka BP; see Table 5.2 and Fig. 5.3), the abundance of the long-chain homologues was too low for accurate δD determination. δD values of the *n*-alkanes varied about 40‰ throughout the core e.g. ranging from -192 to -150‰ for $n\mathrm{C}_{23}$ or from -196 to -150‰ for $n\mathrm{C}_{31}$ (Table 5.2). Additionally, in the upper part of the core, δD values of the C_{20} HBI have been obtained, which show a variability of 12‰ (ranging from -184 to -172‰) and do not differ significantly from δD values of *n*-alkanes in the same section of the core (Table 5.2 and Fig. 5.3). Phytane, which is highly abundant in the sample from 299 cm depth (6.8 cal a BP) is much more depleted in deuterium than all other compounds, showing a δD value of -388‰.

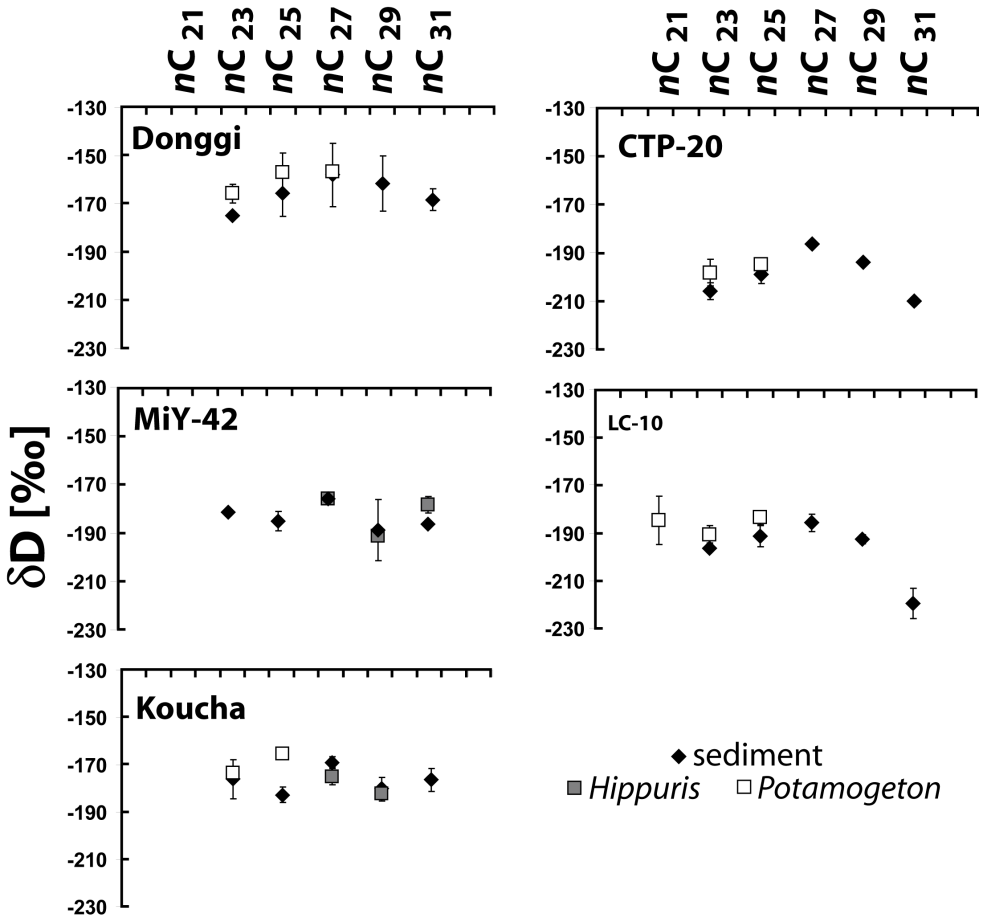

Figure 5.4: Comparison of δD values of *n*-alkanes from emergent macrophytes (*Hippuris*) and submerged macrophytes (*Potamogeton*) with δD values of *n*-alkanes in corresponding sediments in lakes Donggi Cona, MiY-42, Koucha, CTP-20 and LC-10.

Table 5.2: δD values and concentrations of compounds in the sediment core from Lake Koucha

age	depth	*n*C$_{23}$			*n*C$_{25}$			*n*C$_{27}$			*n*C$_{29}$			*n*C$_{31}$			C$_{20}$ HBI			phytane			*n*C$_{17}$	*n*C$_{23}$	*n*C$_{25}$	*n*C$_{27}$	*n*C$_{29}$	*n*C$_{31}$	*n*C$_{33}$	C$_{20}$ HBI	phytane
[cal a BP]	[cm]	δD [‰]	SD		δD [‰]	SD		δD [‰]	SD		δD [‰]	SD		δD [‰]	SD		δD [‰]	SD		δD [‰]	SD		[µg / g d.w.]								
0	0	-176	8		-183	3					-180	5		-176	5		-183	9					3.1	4.2	3.8	2.5	3.8	4.9	1.3	6.1	0.0
1034	76	-177	5		-181	2		-169	1		-168	10		-184	3		-184	1					0.2	5.4	4.4	1.9	2.2	2.6	0.6	3.0	0.0
1309	96	-180	4		-181	2		-171	3		-172	1		-187	1		-178	2					0.0	1.7	1.4	0.7	0.9	1.2	0.3	1.3	0.0
1695	124	-166	9		-169	6					-165	3		-166	1		-174	2					0.1	3.0	2.0	0.6	0.8	1.0	0.4	7.9	0.0
3188	204	-172	3		-184	3		-172	4		-172	8		-181	9		-177	1					0.0	2.1	1.5	0.6	0.7	1.0	0.4	7.3	0.0
4752	253	-175	3		-177	2		-164	2		-171	10		-175	4		-173	4					0.1	3.3	2.6	1.2	1.7	1.8	0.5	5.7	0.0
5681	274	-176	13		-175	12											-172	10					0.0	1.1	0.9	0.3	0.3	0.3	0.1	2.4	0.0
6053	282	-182	1		-191	3		-189	7		-180	1		-196	3		-175	0					0.0	2.0	1.2	0.6	0.7	1.0	0.4	9.8	0.0
6796	299	-163	2		-178	2		-174	5		-169	2		-187	2					-388	21		0.2	3.2	3.2	2.7	4.5	4.3	0.9	0.2	3.2
7916	322	-185	1		-183	3		-169	6		-191	3		-189	7								0.1	1.2	1.2	1.1	1.4	1.5	0.2	0.1	0.3
8340	328	-179	4		-182	4																	0.0	2.1	1.8	1.2	1.4	1.3	0.3	0.0	0.0
8906	337	-177	5		-173	2																	0.0	1.0	0.7	0.4	0.5	0.4	0.1	0.0	0.0
9472	345	-192	3		-195	3		-183	1		-178	6		-192	4								0.1	5.3	4.5	1.9	2.2	1.5	0.3	0.1	0.1
10037	353	-186	3		-185	3		-173	11		-171	6		-171	11								0.0	2.9	2.4	0.9	1.1	0.8	0.2	0.1	0.0
10603	362	-182	2		-183	3		-167	3		-176	6		-180	1								0.2	6.4	6.2	2.0	2.3	1.6	0.3	0.2	0.0
11310	372	-175	2		-175	2																	0.1	10.8	7.7	1.9	2.0	1.6	0.3	0.1	0.1
13760	400	-162	6		-162	6		-149	5		-155	6		-157	7								0.1	1.4	1.2	0.6	0.9	0.8	0.2	0.0	0.0
14597	408	-150	7		-156			-152			-145	1		-150	6								0.0	1.3	1.2	0.5	0.9	1.2	0.5	0.0	0.0

5.6 Discussion

5.6.1 Do *n*-alkanes record the δD signal of meteoric water?

Sternberg (1988) found that bulk lipids of submerged aquatic macrophytes record δD of meteoric water, since the original δD signal of the lake water is not altered by transpiration. As aquatic macrophytes are highly abundant in Tibetan lakes, they are potential candidates as recorders for δD of lake water in our study region. However, it has to be considered that the Tibetan Plateau is a relatively arid region. Thus, the δD values of the lake water are most likely affected by evaporation effects and consequently be more enriched in deuterium than the original meteoric water (Gat, 1996). Due to this fact, Hou et al. (2008) proposed terrestrially derived biomarkers to be better proxies for δD of precipitation in arid regions. Nevertheless, a study consisting of surface sediment samples from five Tibetan lakes showed a good correlation between δD of the aquatic macrophyte derived C_{25} *n*-alkane (and also of nC_{27}, nC_{29} and nC_{31}) and δD of meteoric water (Xia et al., 2008).

Table 5.3: Pearson correlation coefficients (r) between δD values of *n*-alkanes in sediments and plants and δD values of meteoric water

		δD meteoric water												
		Jan	Feb	Mar	Apr	May	June	July	Aug	Sep	Oct	Nov	Dec	annual mean
δD compound	*n* C_{23} SEDIMENT	-0.30	-0.18	0.17	-0.05	0.26	0.48	0.63	**0.68**	**0.72**	0.50	0.02	-0.19	0.56
	n C_{25} SEDIMENT	-0.23	-0.12	0.22	0.01	0.31	0.51	0.64	**0.68**	**0.71**	0.53	0.08	-0.13	0.58
	n C_{27} SEDIMENT	-0.21	-0.07	0.29	0.04	0.35	0.57	0.71	**0.79**	**0.80**	0.62	0.12	-0.08	0.65
	n C_{29} SEDIMENT	-0.20	-0.06	0.30	0.05	0.35	0.57	**0.71**	**0.81**	**0.82**	0.64	0.13	-0.07	0.66
	n C_{31} SEDIMENT	-0.25	-0.10	0.28	0.02	0.34	0.58	**0.73**	**0.84**	**0.85**	0.64	0.10	-0.11	0.68
	average mid-chain SED	-0.31	-0.18	0.18	-0.05	0.27	0.49	0.64	**0.70**	**0.74**	0.51	0.02	-0.19	0.57
	average long-chain SED	-0.37	-0.21	0.16	-0.11	0.23	0.49	**0.66**	**0.80**	**0.84**	0.57	-0.03	-0.23	0.60

bold and black numbers: correlation is significant at the 99% level (p<0.01)
bold and grey numbers: correlation is significant at the 95% level (p<0.05)

Table 5.3 shows Pearson correlation coefficients (PCCs) of δD values of *n*-alkanes (from macrophytes and sediments) versus δD_{MW} (calculated with OIPC, Bowen and Revenaugh, 2003). Significant correlations ($p < 0.01$) were determined for δD values of sedimentary *n*-alkanes versus $\delta D_{MW-August}$ and $\delta D_{MW-September}$. For $\delta D_{MW-annualmean}$, the correlations were still significant ($p < 0.05$) . This suggests that *n*-alkanes in fact record the precipitation signal on a mean annual basis and especially the signal of summer precipitation. A similar tendency seems to exist for δD values of *n*-alkanes in aquatic macrophytes, but no correlations coefficients have been calculated due to the low number of samples. It is not surprising that the best correlation is found for δD_{MW} of the summer months, since the region is influenced by the monsoon, with maximum precipitation occurring between June and September (Fan et al., 2004). Generally, PCCs increase with chain-length, suggest-

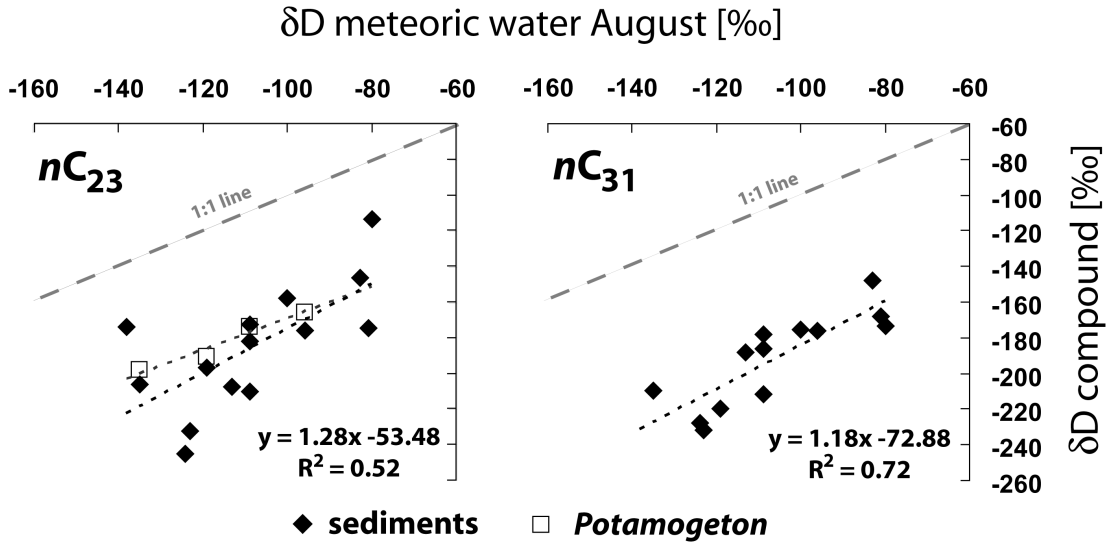

Figure 5.5: δD values of $n\mathrm{C}_{23}$ and $n\mathrm{C}_{31}$ in sediments and *Potamogeton* plotted over δD values of meteoric water from August (data taken from OIPC, Bowen and Revenaugh, 2003)

ing long-chain *n*-alkanes to be better recorders of $\delta\mathrm{D}_{MW}$ than mid-chain *n*-alkanes (Table 5.3 and Fig. 5.5). In a previous study we have assumed that submerged macrophytes can produce significant amounts of long-chain *n*-alkanes in very shallow lakes (Aichner et al., manuscript I). Additionally, from the *n*-alkane patterns (Fig. 5.2) and from the hydrogen isotope signals (Fig. 5.4) of the sediments we see an obvious contribution of emergent macrophytes. Emergent macrophytes depend on the same water source as submerged macrophytes, but are susceptible to transpirational water loss. Thus, lipids would be expected to be deuterium-enriched in emergent macrophytes in contrast to submerged macrophytes. At least in Lake Koucha this is not the case (Fig. 5.4), so the alteration of the δD signal through transpiration is either minor or this effect is diluted by unknown differences of biosynthetic isotopic fractionation of the two species. Generally, it can be said, that the proportional contribution of aquatic organisms to aliphatic lipid compounds in sediments decreases with increasing chain-length of the *n*-alkanes pre-assuming that potential algal contributors of long-chain *n*-alkanes like *Botryococcus braunii* A race (Metzger et al., 1986; Lichtfouse et al., 1994) are of minor importance. This suggests that the C_{31} *n*-alkane is probably a more suitable recorder of the precipitation signal than the C_{27} *n*-alkane, the C_{29} *n*-alkane or a mean value of long-chain *n*-alkanes, since this compound is least influenced by aquatic organisms. On the other hand, using an average δD value of long-chain *n*-alkanes as proxy in a sediment core can possibly integrate the effect of changing terrestrial vegetation on the δD value of single *n*-alkanes as proposed by Hou et al. (2007).

5.6.2 δD values of *n*-alkanes as indicators for precipitation amounts

Water vapor becomes increasingly depleted in deuterium when air masses move landwards (Dansgaard, 1964; Gat, 1996) and precipitation amounts decrease. This can be seen in our southernmost six sediment samples (SET-16, LC-10, LC-05, LC-06, CTP-20 and CTP-25) which show a gradual decrease of meteoric δD values from the southeast to the northwest (see Fig 5.1a and Table 5.1). Lakes located more to the north (MiY-group, CTP-35, Koucha, Donggi and Qai-group) receive less precipitation, are situated in gradually decreasing altitude, and are exposed to higher temperatures, which results in increasing δD values with increasing latitude. There is a fair correlation ($R^2 = 0.84$; $p < 0.01$) between precipitation amount and the latitude (Fig. 5.6a), when not considering the sample from lake SET-16 which is situated in much lower altitude and faces higher temperature than all other studied lakes. As a result from these dependencies, we related the observed δD values of the *n*-alkanes of the surface sediment samples with latitude and with precipitation amounts, yielding significant correlations on the 99% confidence level ($R^2 = 0.86$; as shown for $n\mathrm{C}_{31}$ in Fig. 5.6b as well as $R^2 = 0.59$ for $n\mathrm{C}_{23}$ and 0.65 for $n\mathrm{C}_{31}$ as shown in Fig. 5c). Hence, we found higher δD values in areas with low precipitation (high latitude) like the strong continental Qaidam Basin or in areas of relatively low altitude with relatively high temperatures like lake SET-16. Low δD values were found in regions with high precipitation (low latitude) such as high altitude areas of the southeastern Tibetan Plateau (LC-05/06/10) (Fig. 5.6c).

5.6.3 Apparent enrichment factors between source water and lipids

Recently, Xia et al. (2008) found relatively small apparent enrichment factors between meteoric water and long-chain *n*-alkanes in a transect of five Tibetan lakes, inferring an enhanced evaporation from soil and evapotranspiration from leaves on the arid Tibetan Plateau compared to more humid regions. No systematic relationship between hydrologic parameters (e.g., mean annual precipitation or mean annual relative humidity) and the fractionation factor has been found in that study, however, the sampled lakes cover a comparably small gradient of mostly arid conditions (e.g. P_{ann} ranging from 95 to 379 mm). In contrast, our sample set covers a broader hydrological range, from relatively humid conditions on the southeastern Tibetan Plateau to extremely arid conditions in the Qaidam Basin. Fig. 5.7a shows apparent enrichment factors ϵ between $\delta\mathrm{D}_{MW-August}$ and average δD values of mid-chain *n*-alkanes ($n\mathrm{C}_{23}$ and $n\mathrm{C}_{25}$) and the C_{31} *n*-alkane in our samples. Enrichment factors for mid-chain *n*-alkanes and $n\mathrm{C}_{31}$ at the most humid sites are $\approx$ -135‰ and $\approx$ -125‰, respectively, which is close to previously reported values for aquatic and terrestrial biomarkes in Europe, North America and eastern China (Sachse et al., 2004; Huang et al., 2004; Rao et al., 2009).

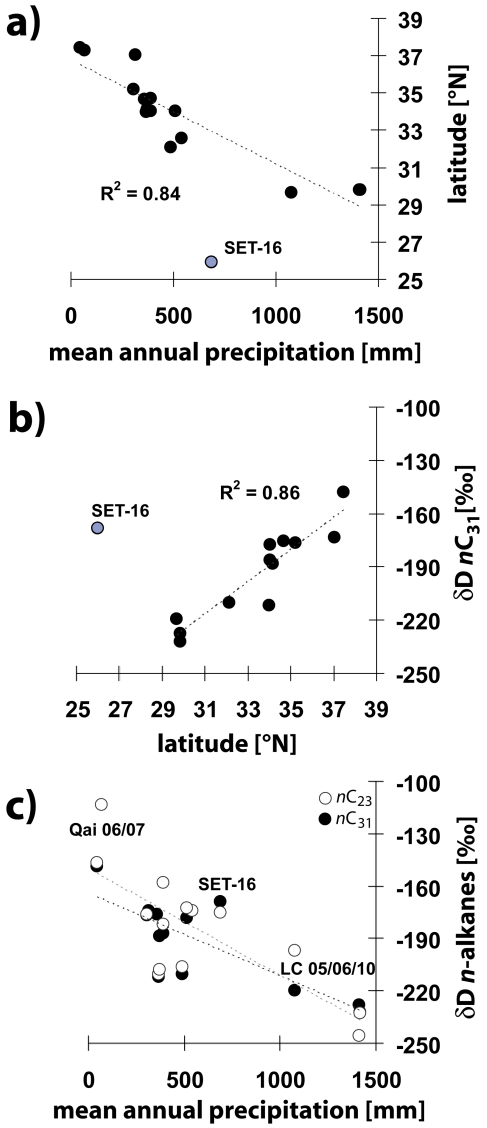

Figure 5.6: (a) Correlation between mean annual precipitation and latitude in our study area. (b) Correlation between δD values of $n\mathrm{C}_{31}$ and latitude. (c) Relationship between δD values of $n\mathrm{C}_{23}$ and $n\mathrm{C}_{31}$ and precipitation amounts

In contrast, there is a tendency of smaller fractionation factors at sites receiving less precipitation amounts. A similar relationship has been found by Smith and Freeman (2006) who analysed δD signals of long-chain n-alkanes from grasses collected in the Great Plains, USA, along a precipitation gradient ranging from 233 to 718 mm/a. This relationship can be observed for mid- as well as for long-chain n-alkanes. The data of Xia et al. (2008), with fractionation factors ranging from -95 to -41‰ are consistent with our results. Xia et al. (2008) interpreted their analysed n-alkanes ($n\mathrm{C}_{25}$, $n\mathrm{C}_{27}$, $n\mathrm{C}_{29}$ and $n\mathrm{C}_{31}$) to be of terrestrial origin. Recently, we have shown that aquatic macrophytes profoundly influence the sedimentary organic matter of lakes on the Tibetan Plateau (Aichner et al., manuscript I). Thus we would interpret at least $n\mathrm{C}_{25}$ to be definitively of aquatic origin, while $n\mathrm{C}_{27}$ and $n\mathrm{C}_{29}$ might be influenced by macrophytes as well, and only $n\mathrm{C}_{31}$ is a more or less

reliable proxy for terrestrial vegetation (see above). As a consequence, we attribute the decreasing apparent fractionation factors found for mid-chain *n*-alkanes at more arid sites to an increase of the lake water δD due to lake water evaporation.

Evapotranspirational effects could be a reason for the low fractionation factors of $n\mathrm{C}_{31}$, as proposed by Xia et al. (2008). This would mean that lake water evaporation and soil and leaf water evapotranspiration would occur at a more or less similar extent. This becomes clearer, when calculating the δD offset between mid-chain *n*-alkanes and $n\mathrm{C}_{31}$. As depicted in Fig. 5.7b and also visible in Fig. 5.2, this offset is close to zero for most of the samples. Only in lakes LC-06 and CTP-35 the δD of $n\mathrm{C}_{31}$ is significantly higher than δD of mid-chain *n*-alkanes while only in lake LC-10 it has a considerably more negative value. This is in contrast to data reported from the Tibetan Plateau before. Mügler et al. (2008) found more negative values (in average -68‰ on average) for long-chain compared to mid-chain *n*-alkanes in Lakes Nam Co and Co Jiana on the central Tibetan Plateau. In the data set of Xia et al. (2008), the differences between $n\mathrm{C}_{25}$ and $n\mathrm{C}_{31}$ range from -9 to -34‰, with the highest offset also visible for Nam Co. Lake KLK in the paper of Xia et al. (2008), is identical with our lake Qai-06, and we found δD values for mid-chain *n*-alkanes (-114‰ for $n\mathrm{C}_{25}$) in the same range (-104‰ for $n\mathrm{C}_{25}$), while we did not evaluate the long-chain *n*-alkanes from this sample due to low signal intensity. In Lake XQ, which corresponds to our lake Qai-07, we found similar values of $n\mathrm{C}_{31}$ (-139‰: reported by Xia et al.; -148‰: our results). However, they observed higher values for mid-chain *n*-alkanes (e.g. -118‰ for $n\mathrm{C}_{25}$) compared to values (-146‰) resulting in discrepancies up to -28‰.

Mügler et al. (2008) proposed the offset between mid- and long-chain *n*-alkanes as a proxy for assessing the hydroclimatic characteristics of a lake, with arid conditions indicated by depleted δD values of long-chain compared to mid-chain *n*-alkanes and humid condition *vice versa*. This presumes that δD enrichment of soil and leaf water δD is outweighed by lake water evaporation. Our sample set, covering a wide range of environmental conditions, however, indicates that this is not the case for the Tibetan Plateau and the two effects show similar extents in most of the studied lakes. Changes of the terrestrial vegetation throughout our study area and resulting different isotopic fractionations between the source water and the lipids might also have influenced the δD signal of the sedimentary long-chain *n*-alkanes. Nevertheless, the correlation between $\epsilon_{nC31/MW}$ and P_{ann} suggests increasing evapotranspiration to be the main driving force behind the isotopic signals of long-chain *n*-alkanes. Precise data about mean annual evaporation or relative humidity at the respective sites are not available, but higher evaporation rates at sites receiving little rainfall is plausible, especially in the Qaidam Basin where temperatures are relatively high (Table 5.1).

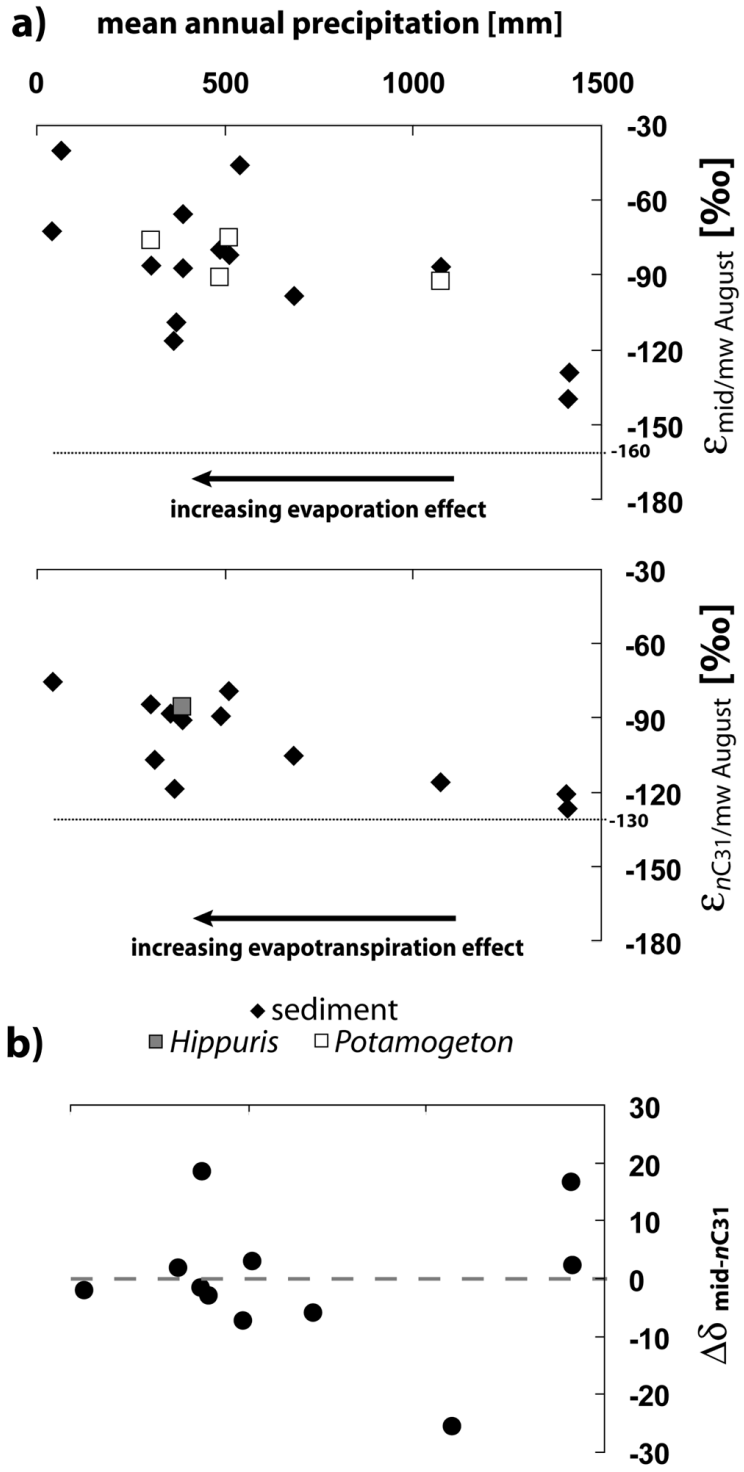

Figure 5.7: (a) Apparent enrichment factors (ϵ) between δD values of mid-chain n-alkanes (=mean value of $n\mathrm{C}_{23}$ and $n\mathrm{C}_{25}$) and δD values of $n\mathrm{C}_{31}$ with δD values of meteoric water (August). Dashed lines indicate average enrichment factors reported for aquatic and terrestrial plants from humid regions (e.g. Sachse et al., 2004; Huang et al., 2004 and Rao et al., 2009). (b) Offsets between δD values of mid-chain n-alkanes and $n\mathrm{C}_{31}$ ($\Delta\delta_{mid-nC31}$) in sediment samples.

5.6.4 δD of biomarkers in a sediment core from Lake Koucha

The past hydroclimatic condition in the Lake Koucha catchment have been recently reconstructed using pollen and ostracod transfer functions (Mischke et al., 2008; Herzschuh et al., 2009), while the changing biomarker compositions since the late glacial and carbon isotope signatures of biomarkers have been described in Aichner et al. (in press; manuscript II). Fig. 5.8 shows a depth plot of the δD values of the *n*-alkanes together with relevant parameters from the studies mentioned above. A reconstruction of palaeo-conductivity, based on an ostracod transfer function (Mischke et al., 2007) gave evidence for the hydrologic states of Lake Koucha: the electrical conductivity was intermediate during the late glacial, it was high between 10 and 7.3 cal ka BP and a shift to freshwater conditions occurred at 7.3 cal ka BP (Fig. 5.8; Mischke et al., 2008). Pollen-based reconstructed quantitative precipitation amounts infer a steady decrease of precipitation from the late glacial to the early Holocene (Fig. 5.8; Herzschuh et al., 2009), which is in phase with an increase of monsoonal intensity in southern and eastern Asia (Thompson, 1997; Wang et al., 2005; Herzschuh et al., 2006). Then, between ca 9.8 and 7.5 cal ka BP, a drop of precipitation amounts was reconstructed, co-occurring with the increasing salinities in the lake. While most records from the Asian Monsoon realm and many records from the Tibetan Plateau infer warm and wet conditions during the early and the mid-Holocene, some have also shown the opposite trend with comparably dry conditions during that period (see Morill et al., 2003; Wang et al., 2005 or Herzschuh et al., 2006 for reviews). Those records have been derived mainly from arid regions like the northern Tibetan foreland or the Qaidam Basin, and a suggested explanation was, that increasing evaporation may have outweighed the increasing precipitation amounts during the monsoonal maximum, resulting in a decrease of effective moisture availability at those sites.

δD values of all *n*-alkanes in samples from Lake Koucha show a trend towards lower values from 15 to 10 cal ka BP, which probably reflects the increase of precipitation amounts in phase with the late glacial strengthening of the monsoon. At ca 9 cal ka BP a shift towards higher δD values is observable for mid-chain *n*-alkanes. This gives evidence for either a reduction of precipitation amounts or an increased enrichment of lake water δD due to enhanced lake water evaporation. The increase of salinity might additionally have contributed to an isotopic enrichment of the lake water (Sachse and Sachs, 2008). Relatively high δD values between 10 and 7 cal ka BP were recently reported from $n\mathrm{C}_{27}$ in the Hani peat bog in northeastern China (Seki et al., 2009). The authors of this study suggested that most likely evaporation exceeded precipitation during the early Holocene, which is in agreement with the interpretation of our data with respect to humidity changes. δD values of long-chain *n*-alkanes are lacking for the timing of the shift due to low signal intensity. Available data from the assumed period of reduced effective moisture do not seem to show a significant shift towards higher values (Fig. 5.8).

At ca 1.5 cal ka BP, the δD values of all biomarkers, including the phytoplankton derived C_{20} HBI (Rowland et al., 1990; Kenig et al., 1995), show a co-occurring shift towards more negative values. Between 1.8 and 1.3 cal ka BP, a cool event was inferred from a drop of concentrations and carbon isotope signatures of biomarkers (Aichner et al., in press; manuscript II). This event was reported from a range of records on the Tibetan Plateau (e.g. Shen et al., 2005; Herzschuh 2006; Zhu et al., 2008) including a record from a peat deposit in the relatively close Zoîge-Basin (Zheng et al., 2007) which suggested cold and dry conditions during this episode. Liu et al. (2008) found a 12‰ depletion of δD values of the nC$_{28}$ fatty acid at ca 1.5 cal ka BP in a short core from Lake Qinghai, which is about the same extent of depletion as observed for the n-alkanes in Lake Koucha. They set this drop in phase with the so-called Dark Ages Cool Period but also argued that temperature and precipitation changes could not explain this shift alone and that a change of moisture source must have occurred. However, an intensification of the summer monsoon during that cool period as proposed by Liu et al. (2008) is not in agreement with inferences from other studies (e.g. Gupta et al., 2003). We rather suppose that on the contrary a weakening of the monsoon and consequently increased influence of the Westerlies could have decreased δD of precipitation. Meteoric water above central Asia is relatively strongly depleted in deuterium due to the continental effect (Bowen and Revenaugh, 2003). Higher relative amounts of moisture delivered by the Westerlies could therefore possibly result in lower δD of meteoric water. The offset between δD values of mid-chain n-alkanes and nC$_{31}$ ($\Delta\delta_{mid-nC31}$) in the Lake Koucha sediment core is hard to evaluate, because δD values of long-chain n-alkanes are missing in key sections of the core due to low signal intensity. In most of the available samples, the offset is close to zero. However, a decrease of $\Delta\delta_{mid-nC31}$ between 10 and 7 cal ka BP could be interpreted to be induced by aridification, which would be an example for a possible applicability of this proxy as proposed by Mügler et al. (2008). However, this decrease is not very pronounced (max.: -17‰) and should probably not be overvalued. A slightly decreased offset between δD_{nC27} and δD_{nC31} was also observed by Seki et al. (2009) during the same period in Hani peat bog. Generally, the offset proxy is neglecting the fact, that in arid regions not only the lake water is enriched in deuterium, but evapotranspiration also alters the hydrogen isotope signal of leaf and soil water. It must also be taken into account that a number of factors (e.g. size and morphology of the lake catchment, composition of the vegetation and morphology of the plants, hydrology i.e. abundance of inflows and outflows, seasonality of the recorded signal) influence as to which extent both effects are occurring. In a sediment core from a single lake, the variability of these factors is minimized compared to the larger number of lakes considered in a surface sediment transect study. Then, changes in the evaporation/precipitation balance could actually result in differences between δD values of aquatic and terrestrial biomarkers. Therefore, the offset might be applicable as a palaeoaridity proxy but should in any case be interpreted with caution.

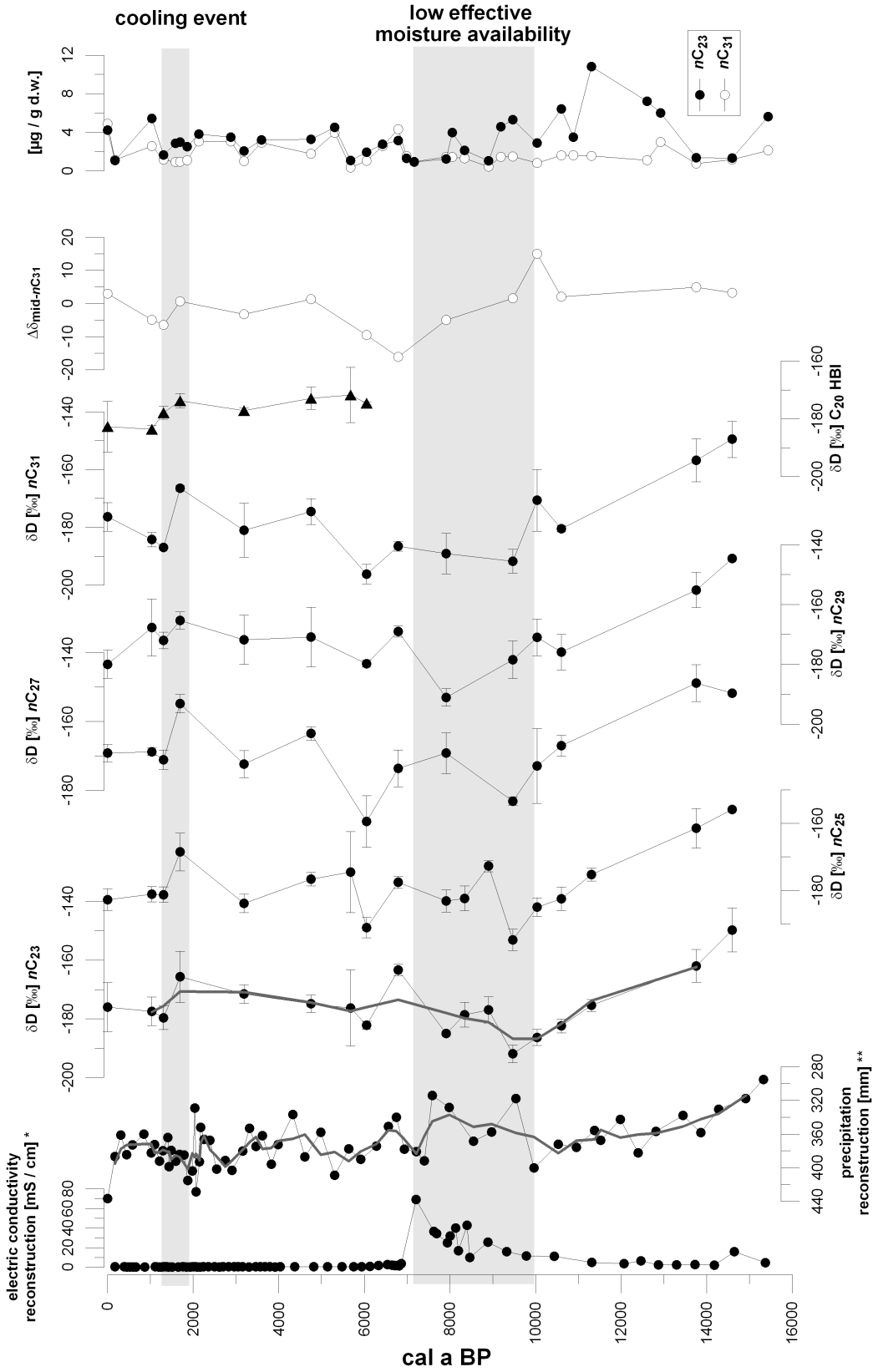

Figure 5.8: Depth plot from Lake Koucha sediment core showing reconstructed electrical conductivities (* from Mischke et al., 2008), reconstructed precipitation amounts (** from Herzschuh et al., 2009) as well as δD values of n-alkanes and offsets between δD valuesof mid-chain n-alkanes and $n\mathrm{C}_{31}$ ($\Delta\delta_{mid-nC31}$).

5.7 Conclusion

Our set of surface sediment samples from 16 lakes covering a wide hydrological gradient on the eastern Tibetan Plateau indicate, that the δD value of summer precipitation is recorded by lipid components, with long-chain *n*-alkanes showing the most significant correlation. Apparent fractionation factors between source water and lipids are smaller at sites receiving little precipitation for both mid- and long-chain *n*-alkanes. This suggests that aquatic macrophytes assimilate lake water relatively enriched in deuterium due to increased lake water evaporation and that increased leaf and soil water evapotranspiration leads to higher δD values for water used by terrestrial plants. Comparing δD values of mid- and long-chain *n*-alkanes revealed, that both effects occur to a similar extent at most sites, reducing its proxy value for palaeoaridity. On the other hand, there are indications for an applicapility of the proxy from results from the Lake Koucha sediment core. Mid-chain *n*-alkanes turned out to be good indicators for palaeohydrologic conditions. Relatively high δD values of mid-chain *n*-alkanes indicated an increase of lake water evaporation during the early Holocene, which is in good agreement with interpretations derived from biological and geochemical proxies.

6 Synthesis

6.1 Aquatic macrophytes as contributors to sediment organic matter in Tibetan lakes

The evaluation of *n*-alkane patterns and carbon and hydrogen isotope signatures of surface sediments and submerged and emergent macrophytes from the eastern and central Tibetan Plateau revealed that aquatic macrophytes can be considered as a major contributor to the sedimentary organic matter in Tibetan lakes (manuscript I). Firstly, the generally accepted assumption that cuticular leaf waxes of submerged macrophytes mainly consist of mid-chain *n*-alkanes ($n\mathrm{C}_{23}$ and $n\mathrm{C}_{25}$), while emergent species synthesise preferentially long-chain homologues ($n\mathrm{C}_{29}$ and $n\mathrm{C}_{31}$) (Ficken et al., 2000), could be confirmed by analysing the *n*-alkane composition of plant samples collected across the eastern and central Tibetan Plateau. Secondly, our observations indicate that aquatic macrophytes can also have a tendency to produce higher proportions of long-chain lipids in more shallow lakes, probably as a reaction to increased exposure to environmental influences such as sunlight or occasional ambient conditions. Thirdly, *Potamogeton pectinatus* samples showed high abundances of unsaturated compounds in the long-chain range, especially $n\mathrm{C}_{29:1}$ and $n\mathrm{C}_{31:1}$. These compounds were not found in the corresponding sediments and may have been transformed to saturated compounds during early diagenesis and therefore might have contributed to the pool of long-chain *n*-alkanes in sediments (as similarly proposed for lipids derived from *Botryococcus braunii* A race; Metzger and Largeau, 2005; Zhang et al., 2007). Nevertheless, the strong abundance of mid-chain *n*-alkanes in the sediment samples gives evidence for a high contribution of submerged macrophytes to the sediments, especially when taken into account that submerged macrophytes produce significantly lower concentrations of leaf waxes compared to emergent species and terrestrial plants.

Due to the fact that C_4 vegetation play a minor role (Wang, 2003) in the catchments of the examined lakes, variations of $\delta^{13}\mathrm{C}$ values of TOC and *n*-alkanes in sediments can mainly be attributed to aquatic processes. In a number of studies, variations in the $\delta^{13}\mathrm{C}_{\mathrm{TOC}}$ have been interpreted to be caused by changes in primary productivity (e.g. Hollander and McKenzie, 1991; Brenner et al., 1999). It is also known that aquatic macrophytes can be considerably enriched in $^{13}\mathrm{C}$ due to their ability to switch to bicarbonate metabolism (Allen and Spence, 1981; Prins and Elzenga, 1989). In fact, the bulk biomass and the lipids of our analysed submerged macrophyte samples show large ranges of $\delta^{13}\mathrm{C}$ values,

covering and even exceeding the whole range of possible values known for terrestrial C_3 and C_4 plants (Fig. 6.1a). This certainly has an impact onto the sediments and therefore the large variation of $\delta^{13}C$ values of TOC in sediments of Tibetan lakes was mainly attributed to the influence of submerged macrophytes. This assumption can be consolidated when considering the strongly enriched $\delta^{13}C$ values of mid-chain *n*-alkanes in many of the sediment samples (Fig. 6.1b), while long-chain homologues show more or less similar values in the range typical for terrestrial C_3 plants. An algal contribution to the bulk sediment is also possible, but at least the aliphatic fraction of the sediment extract did not show significant abundances of typical algal biomarkers in most of the samples. Similar δD values in sedimentary *n*-alkanes and corresponding plants are a further argument for the high contribution of macrophytes to the sedimentary lipid pool, which is however weakened by the fact that terrestrial and aquatic derived *n*-alkanes do not show significantly different δD values in our analysed samples (manuscript III).

To assess the degree of macrophyte input to the sediment without considering *n*-alkane concentrations or ratios, $\delta^{13}C$ values of lipids (e.g. aquatic macrophyte derived mid-chain *n*-alkanes or the weighted average of $\delta^{13}C$ values) and $\delta^{13}C_{TOC}$ were compared. With this approach, the contribution of aquatic macrophytes to TOC was estimated in the Lake Koucha sediment core (manuscript II). To present a simple proxy, here the $\delta^{13}C_{TOC}$ curve was compared with the $\delta^{13}C_{nC_{23}}$ curve (taking the weighted average of $\delta^{13}C$ of lipids would have obtained a similar curve). The offset between the two $\delta^{13}C$ values is lower in the older part of the core, suggesting a higher contribution of macrophytes, and higher in the younger part, suggesting a lower contribution (Fig. 6.2). This is in agreement with inferences from the composition of the aliphatic fraction of the biomarker extract which is dominated by macrophyte-derived mid-chain *n*-alkanes in the older and a phytoplankton-derived C_{20} HBI in the younger part of the sediment core. To quantify the input of aquatic macrophytes to the sediments, a simple binary isotopic model was used (manuscript I). Due to the isotopic heterogeneity of submerged macrophytes this is only possible for recent sediment samples, for which $\delta^{13}C$ values are available from corresponding plant samples. This is a very simplified approach, but suitable to get a rough idea about the degree of macrophyte input which turned out to be 30-50% for bulk sediments and 60-70% for mid-chain *n*-alkanes in most of the samples.

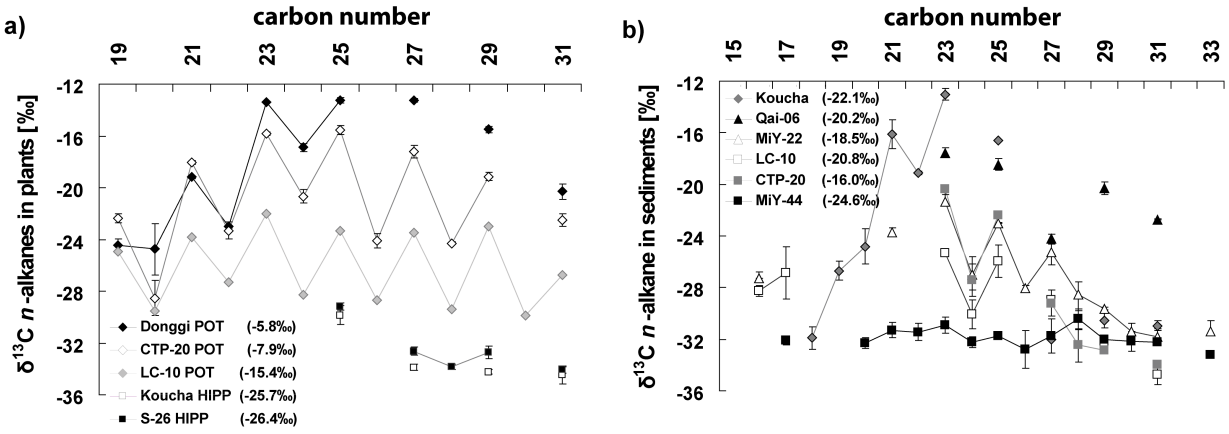

Figure 6.1: (a) δ^{13}C values of *n*-alkanes of three *Potamogeton* samples with differing bulk δ^{13}C values (in brackets) and of two *Hippuris* samples (HIPP, squares). (b) δ^{13}C values of six selected sediment samples illustrating the range of variations. δ^{13}C values of bulk plant material and of TOC in brackets.

6.2 Aquatic macrophyte-derived *n*-alkanes as proxies in palaeolimnology

6.2.1 δ^{13}C of *n*-alkanes

The variation of δ^{13}C values of mid-chain *n*-alkanes in the Lake Koucha sediment core illustrates how principally different states of the lake ecosystem can influence the carbon isotope signals of aquatic biomarkers, which in case of nC_{23} in Lake Koucha range from -23.5 to -12.6‰ (manuscript II). The first state was a closed lacustrine system with gradually rising salinities and with high abundances of macrophytes and low primary productivity lasting from the late glacial until ca 7.3 cal ka BP. The second state was a phytoplankton dominated freshwater system which lasts until present days. Relatively high δ^{13}C values of nC_{23} could be observed during the maximum of macrophyte growth in the late glacial and during almost the whole period dominated by phytoplankton in the middle and late Holocene. The high values could therefore be explained by carbon limitation, similar to the interpretation of Street-Perrott et al. (2004) which interpreted shifts towards higher δ^{13}C values of mid-chain *n*-alkanes in several African lakes to be also induced by carbon limitation. In case of Lake Koucha, the carbon limitation can be attributed to two different causes (Fig. 6.2). During the maximum of macrophyte abundance, carbon limited conditions occurred only in dense plant stands, while in the water column carbon supply exceeded the demand, as can be inferred from low $\delta^{13}C_{TIC}$ values. This is in contrast to the phytoplankton maximum, when high primary productivity and high demand for carbon sources possibly decreased the supply throughout the water column which resulted in high δ^{13}C values of TIC due to a reduced isotopic discrimination during photosynthesis (Leng and Marshall, 2004). This signal is then recorded by autotrophic aquatic organisms such as submerged macrophytes which assimilate inorganic carbon sources. In this case,

the carbon isotope signal of the macrophyte derived *n*-alkanes indirectly reflects a general carbon limitation in the lake. To get a more precise measure about carbon supply for the macrophytes, a comparison of $\delta^{13}C_{nC_{23}}$ and $\delta^{13}C_{TIC}$ curves was proposed as an estimate (Fig. 6.2). This eliminates the influence of the isotopic heterogenity of the carbon source upon the $\delta^{13}C$ signal of macrophytes and therefore reflects the demand and supply-driven isotopic fractionation during carbon assimilation. Based on this assumption, carbon limitation in Lake Koucha was highest during the aquatic macrophyte maximum in the late glacial and during the phytoplankton maximum in the middle Holocene.

$\delta^{13}C$ values of mid-chain *n*-alkanes can therefore be used to a) assess the contribution of aquatic macrophytes to the sedimentary organic matter and b) track conditions of carbon limitation. Since the carbon isotopic signatures of the inorganic carbon sources can show considerable variations, a comparison with $\delta^{13}C_{TIC}$ might give a more precise estimate of carbon limiting conditions for macrophytes.

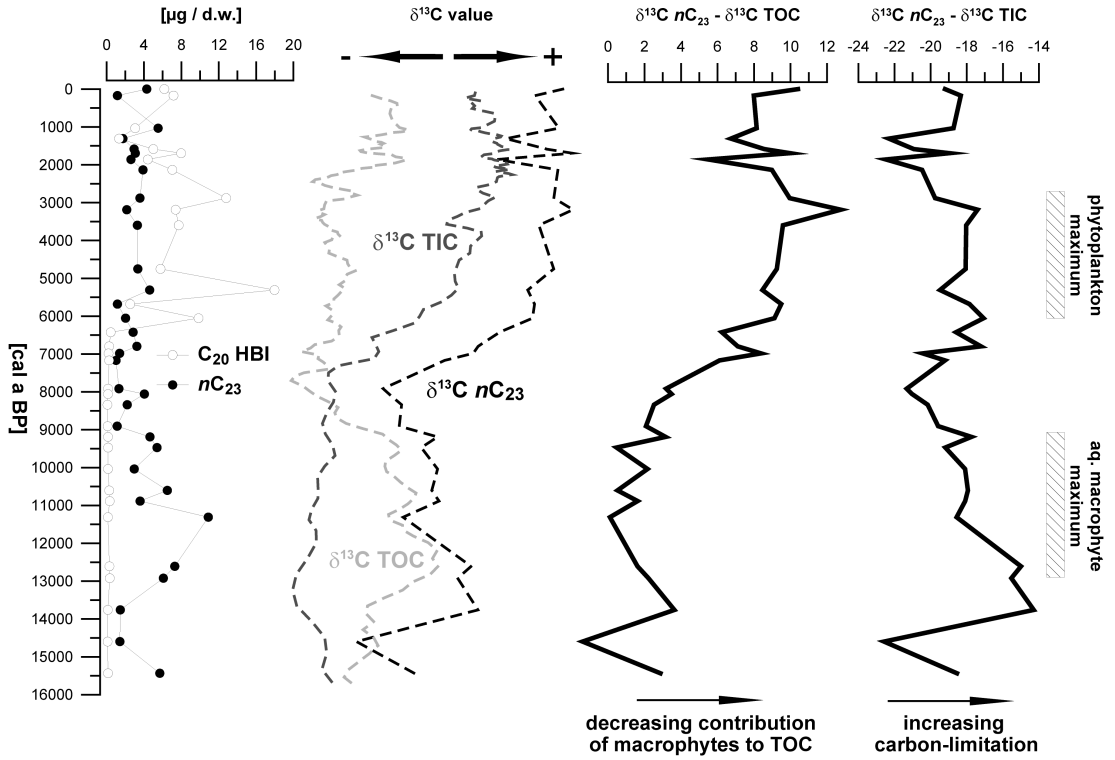

Figure 6.2: Concentrations of biomarkers for submerged macrophytes (nC_{23}) and phytoplankton (C_{20} HBI) and comparison between $\delta^{13}C$ values of nC_{23}, TOC and TIC in the Lake Koucha sediment core.

6.2.2 δD of *n*-alkanes

A surface sediment study with samples covering a large climatic gradient showed that mid-chain *n*-alkanes of macrophyte origin indeed reflect the trend of changing hydrogen isotopic signals of the meteoric water at the respective sites (Fig. 6.3a; manuscript III). However, better correlations were found for terrestrial derived long-chain *n*-alkanes. This

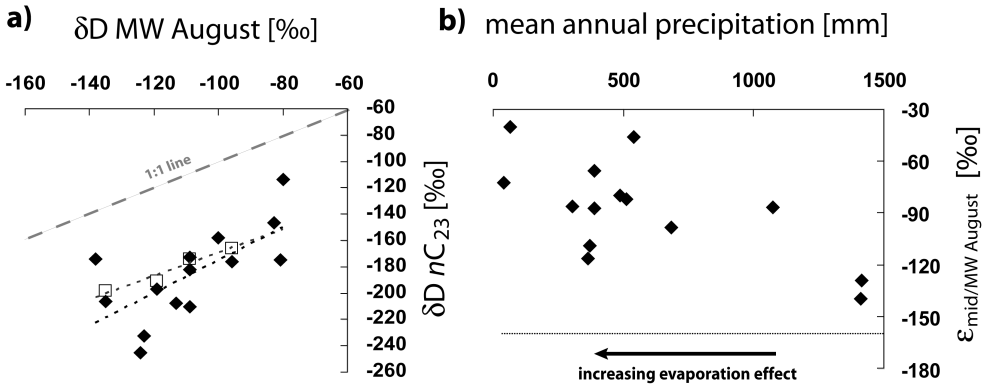

Figure 6.3: (a) δD values of $n\mathrm{C}_{23}$ in sediments (diamonds) and *Potamogeton* (squares) plotted over δD values of meteoric water from August (data taken from OIPC, Bowen and Revenaugh, 2003). (b) Apparent enrichment factors (ϵ) between δD values of mid-chain n-alkanes and δD values of meteoric water (August). Dashed line indicates enrichment factors reported for humid sites (Sachse et al. 2004; Huang et al. 2004)

can be explained by variations in the evaporational alteration of the hydrogen isotope signal of the lake waters, i.e. the source water for submerged macrophytes, while the impact of evapotranspiration on the source water for terrestrial plants is increasing relatively constantly from the humid to the arid regions. It becomes clear that evaporation and evapotranspiration plays a role when plotting the isotopic fractionation between meteoric water and n-alkanes versus mean annual precipitation of the respective sites. While apparent fractionation factors were in range of previously reported ones at humid sites (Sachse et al., 2004; Huang et al., 2004), significantly lower apparent fractionations were calculated for the more arid sites (Fig. 6.3b). The fact that evaporation enhances the δD signal of the lake water and therefore prevents a precise recovery of the meteoric δD signal by determining δD of aquatic n-alkanes is not necessarily detrimental. It can be beneficial when a reconstruction of the general palaeohydrological state is required, i.e. if it is of interest whether conditions were more arid or more humid. This was shown by means of the example of Lake Koucha for which changing hydrological conditions have been previously inferred from biological and geochemical proxies. Of special interest is a period during the early Holocene for which reconstructions of electrical conductivity and precipitation, using ostracod and pollen transfer functions, suggested increasing evaporation during the early Holocene monsoonal maximum which might have outweighed the increasing precipitation amounts, leading to a net decrease of available moisture (Mischke et al. 2008; Herzschuh et al. 2009). This increase of evaporation was recorded by δD values of mid-chain n-alkanes in the Lake Koucha sediment core (Fig. 6.4) which show a shift towards higher values at ca 9 cal ka BP. Generally, the δD curve of $n\mathrm{C}_{23}$ throughout the Lake Koucha sediment core resembles the precipitation reconstruction curve derived from a pollen transfer function, despite the first being an aquatic and the second being a terrestrial proxy. However, the

δD values of mid-chain n-alkanes indicate the shift towards more arid conditions with an approximate delay of 500 years compared to the precipitation reconstruction (Fig. 6.4). It is difficult to assess to which extent the δD signal of meteoric water is affected by the opposing effects of rising temperatures and precipitation amounts during the early Holocene, i.e. at which point the temperature effect outweighs the precipitation effect, leading to an increase of δD of meteoric water. Additionally, a delayed response of the lake water δD signal to changes in effective moisture compared to the composition of the terrestrial vegetation is likely. The latter react immediately to environmental and climatic changes while a significant change of the water balance is probably necessary until an overall change of δD of lake water is observable.

At ca. 1.5 cal ka BP, a drop of δD values, which has also been observed at hydrogen isotope signatures of fatty acids in Lake Qinghai (Liu et al., 2008), indicates cooler conditions inferred from concentrations and δ^{13}C values of biomarkers (see below). The depletion might directly reflect the combined effects of lower temperatures and reduced evaporation upon δD values of meteoric water and lake water and the increased contribution of moisture delivered from the Westerlies during a period of decreased monsoon intensity.

In contrast to previous studies (Xia et al., 2008; Mügler et al., 2008), we did not find significant differences of δD values of mid- and long-chain n-alkanes in most of our Tibetan surface sediment samples, which speaks against an applicability of this offset as a proxy for palaeohydrologic conditions. However, a slight decrease of this offset is observable in the Lake Koucha sediment core, indicating more arid conditions during the early Holocene, which would be in agreement with inferences from all other data for this period. It was hypothesised, that over a large climatic gradient the extent of evaporation and evapotranspiration might be more or less balanced. In contrast, if the climatic conditions change on a specific location, this could actually lead to minor differences between the two effects, resulting in an offset between δD values of aquatic and terrestrial biomarkers, as proposed by Mügler et al. (2008)

It can be concluded that aquatic macrophyte-derived mid-chain n-alkanes might be less suitable to record δD_{MW} compared to terrestrial n-alkanes. However, they can track changes of effective moisture and could therefore contribute to the understanding of past hydrological conditions. The offset between δD of mid- and long-chain n-alkanes might be applicable as a palaeoaridity-proxy but should be interpreted with caution.

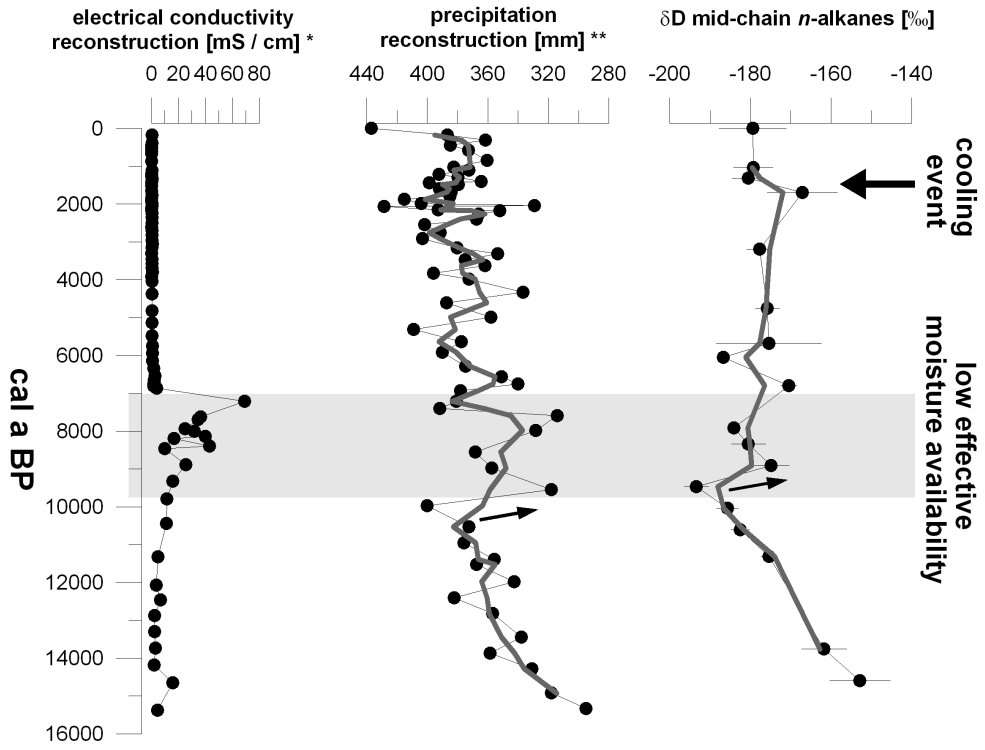

Figure 6.4: Comparison between proxies indicating decreased effective moisture (shaded area) at Lake Koucha during the early Holocene. Electrical conductivity reconstruction base on ostracod transfer function (* data from Mischke et al. 2008). Precipitation reconstruction base on pollen transfer function (** data from Herzschuh et al. 2009). Arrows indicate timing of effective moisture decrease

6.2.3 *n*-Alkane distribution and concentrations

The distribution pattern of *n*-alkanes in lakes was frequently used to assess the proportional contribution of aquatic or of different terrestrial sources (e.g. Ficken et al., 1998; Schwark et al., 2002; Fuhrmann et al., 2003). An evaluation of *n*-alkane patterns in surface samples of Donggi Cona, northeastern Tibetan Plateau, revealed that the *n*-alkane composition can be rather homogenous even in a relatively large and deep lake (Aichner, unpublished results; see Appendix 2 for more information), and that biomarker distributions in a sediment core can therefore be representative for the whole lake. The concentrations of $n\mathrm{C}_{23}$ in Lake Koucha start to increase around 13.5 cal ka BP (Fig. 6.5). This is in phase with an amelioration of the climate in course of the start of the Bølling/Allerød period, for which an intensification of the summer monsoon was inferred from ice core (Thompson, 1997) and many other records. A similar increase of $n\mathrm{C}_{23}$ can be observed in a sediment core from Lake Donggi Cona (Aichner, unpublished results; Appendix 2), which is situated 185 km northeast of Lake Koucha. The $n\mathrm{C}_{23}$ concentrations in Lake Koucha drop at ca 11 cal ka BP. This drop was indirectly triggered by a reduction of effective moisture and a resulting increase of salinity. In Lake Donggi Cona, the concentrations decrease more gradually from 10 cal ka BP on, until reaching minimum values at ca 6 cal ka BP. Even

if the nC_{23} concentrations are ten fold lower in Donggi Cona, both lakes show a maximum of nC_{23} concentrations approximately during the late glacial insolation maximum (Berger and Loutre, 1991). The reason for the rise of macrophytes might be attributed to the relatively high insolation and consequently temperatures which might have favoured macrophyte growth. The decline of nC_{23} in Lake Donggi Cona probably reflects the decrease of insolation. Whether the Donggi Cona region did experience reduced moisture availability similar to Lake Koucha cannot be inferred from nC_{23} concentrations alone. First results from biological and geochemical proxies do not suggest this (Diekmann, B., AWI Potsdam; Mischke, S., FU Berlin; personal communication). δD anlaysis of n-alkane could provide more evidence but it is a challenge to apply this proxy in Donggi Cona, due to the very low concentrations of mid-chain n-alkanes which request a large amount of sample material. Unfortunately there are no n-alkane concentration data of other lakes available for comparison in order to confirm that macrophytes had optimal growth conditions during the late glacial/early Holocene insolation maximum. The Nam Co n-alkane record reaches back until 7.2 cal ka BP (Mügler et al., 2009) and a sediment record from Lake Luanhaizi covers the last 45 ka, but only five biomarker data points from the late glacial and Holocene are included in this study and two dating points provide only a poorly calibrated age-model for this period (Herzschuh et al., 2005). This emphasises the need for more biomarker records from the region.

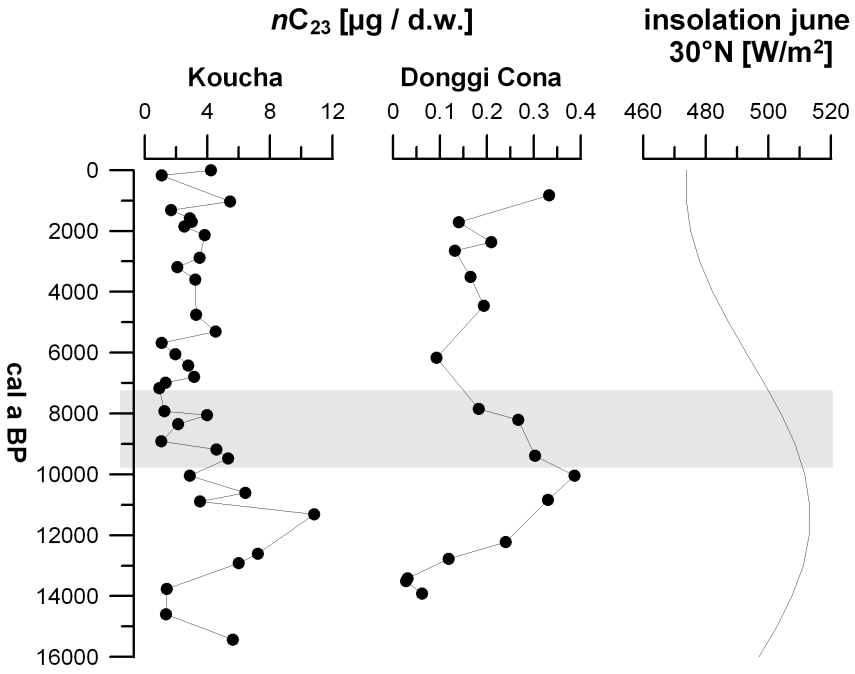

Figure 6.5: Comparison of nC_{23} concentrations in sediment cores from Lake Koucha and Lake Donggi Cona. See Appendix 2 for details about the Donggi Cona record. Insolation data are from Berger and Loutre, 1991. Shaded area indicates period of reduced effective moisture at Lake Koucha.

6.3 Development of Lake Koucha since the late glacial inferred from biomarker proxies

In a sediment core from Lake Koucha, three clearly different periods could be distinguished on basis of the biomarker distribution in the aliphatic fraction of the sediment extract (manuscript II; Fig. 6.6). Before 7.9 cal ka BP, the dominance of $n\mathrm{C}_{23}$ and $n\mathrm{C}_{25}$ suggest that the lake was dominated primarily by aquatic macrophytes (period I). From 6.1 cal ka BP on, highly branched isoprenoid compounds (C_{20} and C_{25} HBIs) give evidence for a phytoplankton dominated lake (period III). These interpretations are in agreement with previous inferences from Mischke et al. (2008) on basis of geochemical data, especially $\delta^{13}\mathrm{C}_{\mathrm{TOC}}$ and $\delta^{13}\mathrm{C}_{\mathrm{TIC}}$.

Period I: The correlation between TOC, $\delta^{13}\mathrm{C}_{\mathrm{TOC}}$ and $\delta^{13}\mathrm{C}_{nC23}$ curves during period I suggest aquatic macrophytes mainly influencing the composition and isotopic signal of the sediment organic matter, with higher $\delta^{13}\mathrm{C}$ values being caused by carbon limitation at dense plant stands (see section above). $\delta\mathrm{D}$ values of mid- and long-chain *n*-alkanes suggest increasingly humid conditions between 15 and 9 cal ka BP, before a shift towards higher values was interpreted with respect to enhanced evaporation. A further evidence for more arid conditions during that episode come from the slightly decreasing offset between $\delta\mathrm{D}$ values of mid-chain *n*-alkanes and $n\mathrm{C}_{31}$, even if it must be taken into account that $\delta^{13}\mathrm{C}$ values of $n\mathrm{C}_{31}$could not be obtained for all samples.

Period II: Biomarker data revealed that the above mentioned two principally different states of the lake were linked by a transition period (period II) between 7.9 and 6.1 cal ka BP. While no samples for biomarker analysis were available from a black layer (7.9 to 7.4 cal ka BP), which was attributed to algal mats by Mischke et al. (2008), several isoprenoid and hopanoid compounds indicate a strong presence of algae and bacteria between 7.3 and 6.1 cal ka BP, especially in a sample from 6.8 cal ka BP. The dominating isoprenoids (phytane and PMI) in this sample have been attributed to specific sources due to their isotopic signature. Phytane, which carries a similar isotopic signature as $n\mathrm{C}_{25}$ (-17.7‰), could be derived from chlorophyll of waterplants. However, the high concentration in this section of the core rather suggests this compound to be derived from a specific producer than to be a product of diagenic alteration of bigger molecules. The isotopic signal suggests an autotrophic precursor and cyanobacteria are among the most likely sources. PMI has been related to microbes involved in the methane cycle (Holzer et al., 1979; Brassell et al., 1981; Elvert et al., 1999; Thiel et al., 1999). Since the PMI in Lake Koucha shows no strong depletion of $^{13}\mathrm{C}$ (-28‰), this compound was attributed to methanogenic sources. In contrast, methanotrophic sources have been postulated for the dominating hopanoid compounds, diploptene and moretene (isodiploptene), which showed $\delta^{13}\mathrm{C}$ values between -63 and -45‰.

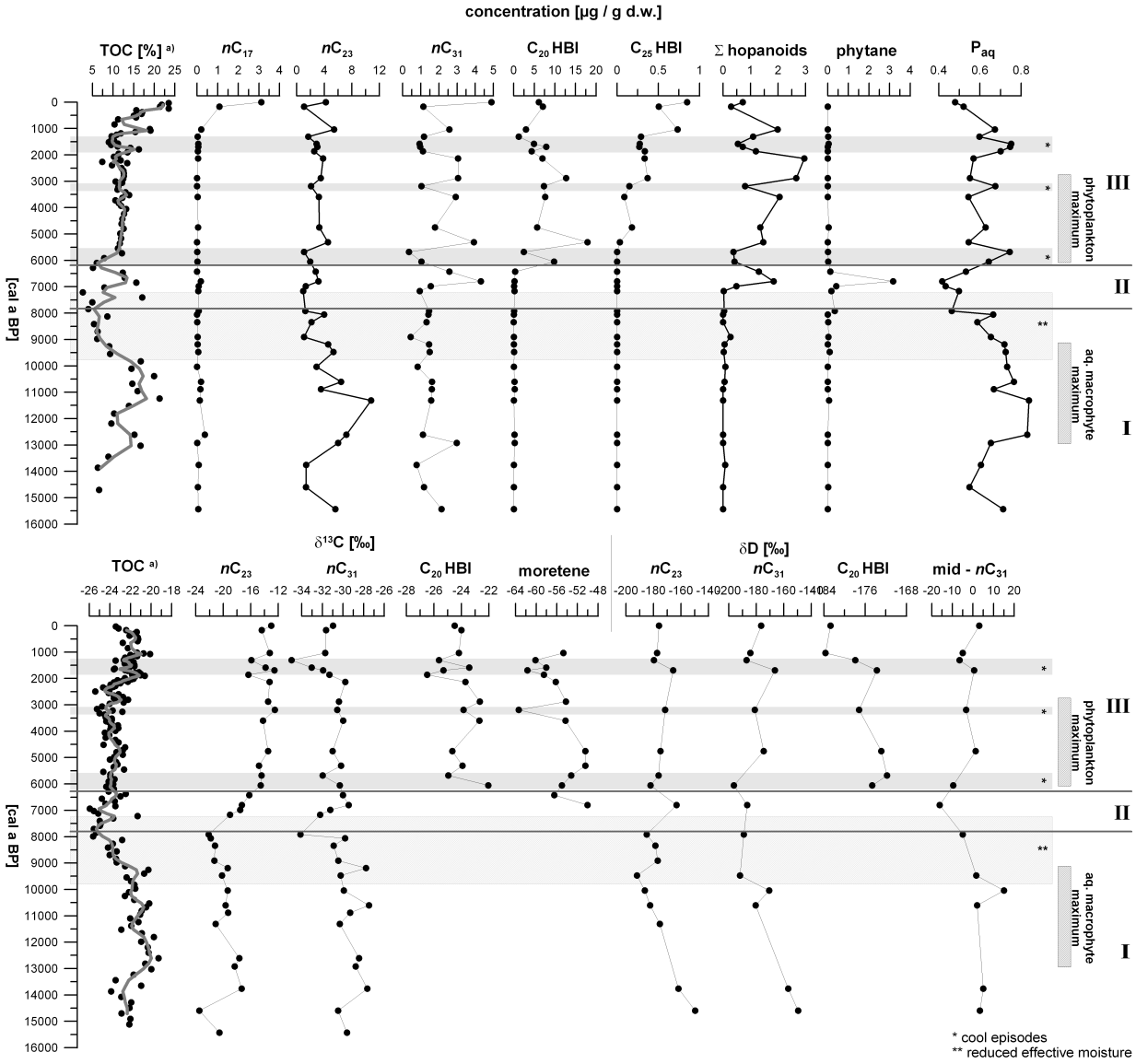

Figure 6.6: Overview about organic matter related parameters determined in the sediment core from Lake Koucha, such as concentrations, δ^{13}C and δD values of biomarkers. TOC-contents and $\delta^{13}C_{TOC}$ $^{(a)}$ are from Mischke et al. 2008. Shaded areas indicate cool episodes during the mid- and late Holocene and a period of reduced effective moisture during the early Holocene. Zonation of the core was according to biomarker distributions.

Period III: Variations of δ^{13}C values and concentrations of biomarkers turned out to be major indicators for climate variability during period III. Relatively low values of moretene, diploptene, C_{20} and C_{25} HBIs and *n*-alkanes have been found in the periods 6.0 to 5.6 cal ka BP, around 3.1 cal ka BP and 1.8 to 1.3 cal ka BP. During the same episodes, pronounced decreases of biomarker concentrations, especially of hopanoids and long-chain *n*-alkanes, are visible. These indicators of low microbial activity and terrestrially organic matter input can be interpreted with respect to a cooling in the Lake Koucha area. Submerged

plants were comparably less affected than terrestrial plants, visible at high P_{aq} during those episodes. This is plausible, since terrestrial vegetation in this high altitude might react more sensitively to minor changes of environmental conditions than macrophyes protected by the water column.

The most pronounced temperature decrease most likely was the episode between 1.8 to 1.3 cal ka BP. Here, even a shift towards lower $\delta^{13}C_{TIC}$ values (reflected in $\delta^{13}C_{nC_{23}}$) can be observed and indicates a general decrease of lake productivity. A deuterium depletion of *n*-alkanes and of the C_{20} HBI at ca. 1.5 kal ca BP could be attributed to the combined effect of lower temperatures and increased influence of the Westerlies upon the δD values of the meteoric water. The assumed cool episodes are in phase with similar events reported from other climate archives in monsoonal Asia, such as marine cores from the Arabian Sea (Gupta et al. 2003), the Hongyuan peat bog (Hong et al., 2003; Zheng et al., 2007), speleothems from Dongge Cave (Wang et al., 2005), palaeosols (Yu et al., 2006) and lake sediments (Shen et al., 2005; Herzschuh, 2006; Zhou et al., 2007; Selvaraj et al. 2008; Zhu et al., 2008) and were interpreted as slight weakening of the summer monsoon, co-occurring with major climatic events on the Northern Hemisphere (Bond et al., 1997 and 2001). A number of trigger mechanisms were discussed for these regular events, but a satisfying theory does not yet exist.

The examination of the biomarker contribution revealed interesting details about the composition of the phytoplankton. The C_{20} HBI showed highest concentration in the first half of period III. This compound has to be considered as a general phytoplankton biomarker, because even if attributed mainly to diatoms, no distinct diatomal producer has yet been identified, and in the mean time it was found also in green algae and periphyton (Rowland et al., 1985; Kenig et al., 1995; Jaffé et al., 2001). In contrast, the C_{25} HBI is a specific diatom biomarker, identified in several species (Belt et al., 2001a and b; Sinninghe-Damsté et al., 2004). This compound shows a step-like increase of concentrations throughout period III, with most pronounced increases shortly after the assumed cool episodes, indicating that diatoms benefit mostly from the climate ameliorations. In the uppermost two samples the appearance of the C_{17} *n*-alkane, another algal marker which was not found throughout the whole core, gives evidence for another change in the phytoplankton community.

A detailed knowledge of about the contributors to the sediment organic matter could be obtained from biomarker compositions in the Lake Koucha sediment core. Concentrations and isotopic signatures of the biomarkers could be interpreted with respect to changes in lake productivity, palaeohydrological conditions and climate and therefore contributed to the understanding of the history of Lake Koucha.

7 Conclusion

Organic biomarkers extracted from lake sediments turned out to be excellent proxies for the reconstruction of past climatic and environmental conditions on the Tibetan Plateau. Aquatic macrophyte derived biomarkers were especially useful due to their high abundance in many Tibetan Lakes and their ability to record major changes of lake productivity and palaeohydrological conditions.

For the first time it was shown in a systematic study how variable δ^{13}C values of bulk organic matter and lipids can be in submerged macrophytes of a single species, how profoundly these parameters are affected in corresponding sediments of lakes with a high abundance of aquatic macrophytes and how the resulting fluctuations of δ^{13}C values of mid-chain *n*-alkanes in sediments can be interpreted in a palaeolimnologic context. In a sediment core from Lake Koucha, high δ^{13}C values of nC_{23} have been shown to reflect episodes of increased carbon limitation which were partly induced by high primary productivity and partly by enhanced macrophyte growth. Further, it was proposed how the extent of submerged macrophyte input to the sediment could be - beside the *n*-alkane composition - assessed from the carbon isotope signature of sedimentary organic matter. Examination of aliphatic lipids of submerged macrophytes revealed that those could be a potential source of long-chain *n*-alkanes in lake sediments. Macrophytes turned out to produce higher proportions of long-chain homologues when experiencing episodically emergent conditions and contain partly high amount of unsaturated long-chain compounds which could be transformed to saturated compounds during early diagenesis. Nevertheless, the relatively narrow range of δ^{13}C values of long-chain *n*-alkanes in sediments indicate that a significant contribution of submerged macrophytes can be excluded at least in our examined lakes, possibly due to the relatively low concentrations of lipids in biomass of submerged plants compared to emergent and terrestrial plants.

New insights about the history of Lake Koucha were gained from biomarker data in the Lake Koucha sediment core. Indications for cooler episodes were gained from regular drops of biomarker concentrations and from similar shifts towards lower δ^{13}C values. Those episodes correspond well with cool events reported from other locations on the Tibetan Plateau and were not inferred from geochemical and biological proxies used in previous studies.

Hydrogen isotope analysis of biomarkers is a rapidly evolving field to reconstruct past variations in the hydrological state but many processes leading to variations of δD values of biomarkers are not yet completely understood. The data set δD values derived from *n*-alkanes in surface sediment samples used in this study is the first one which covers the

whole climatic gradient of the region and therefore important for the interpretation of δD data in sediment cores. It was shown that both aquatic and terrestrially derived n-alkanes record the δD values of summer precipitation, with the latter showing a slightly better correlation. The effect of evaporation and transpiration upon the source water for lipid synthesis was revealed by generally smaller apparent fractionation factors between lipids and meteoric water at more arid sites. Analog fractionation factors were calculated for mid- and long-chain n-alkanes in most of the samples. This assumes that δD of terrestrial lipids are similarly affected by evapotranspirational effects as aquatic lipids by evaporation effects, which contrasts hypotheses from other studies. δD of $n\mathrm{C}_{23}$ recorded the episode of reduced effective moisture at Koucha Lake. The general resemblance between δD curves in the sediment core and a precipitation reconstruction curve derived from a pollen transfer function highlights the usefulness of these proxies in reconstructing palaeohydrological conditions.

Valuable information about monsoon intensities can probably also be obtained from changes in biomarker concentrations. Results from Lake Koucha and Lake Donggi Cona assume that macrophyte derived biomarkers show maximum concentrations during the late glacial / early Holocene monsoonal maximum. In case of Lake Koucha, even the decrease of effective moisture is visible at a decrease of the concentration of mid-chain n-alkanes, indirectly induced by the rising salinities. Nevertheless, interpreting concentration curves of mid-chain n-alkanes with respect to changing monsoon intensities is a vague hypothesis which needs further evidence from other records. It is also likely that the high insolation is the main driving force for the enhanced macrophytes growth and that other resulting factors such as higher temperatures and lake level changes due to fluctuations in the precipitation/evaporation ratio are of minor importance.

In this thesis, the data points of the examined sediment core from Lake Koucha are of relatively low time resolution. There are indications from the Lake Koucha sediment core that biomarkers can give evidence for short-term climate fluctuations, and therefore it is promising to apply these proxies in high resolution. The sediment core from Donggi Cona (see Appendix 2) is a candidate for a high resolution study to monitor potential late glacial and Holocene short-term climate fluctuations. This core would also be interesting for an evaluation of δD values of n-alkanes to see if the Donggi Cona region also experienced reduced moisture availability during the early Holocene. TOC-contents show a drop between 10 and 8.5 cal ka BP (Fig. 7.1) which might be induced by a decrease of effective moisture. A similar occurring drop in a sediment core from Lake Qinghai was attributed to the 8.2 ka event, however, Yu and Kelts (2002) also argued on basis of a multi-proxy study that increased evaporation prevented a rise of the lake level during the early Holocene. The n-alkane concentrations are low in the core from Donggi Cona which could complicate δD analysis, but fatty acids, which were not subject of this thesis, could

serve as an alternative, since those compounds usually show higher concentrations than *n*-alkanes in sediments.

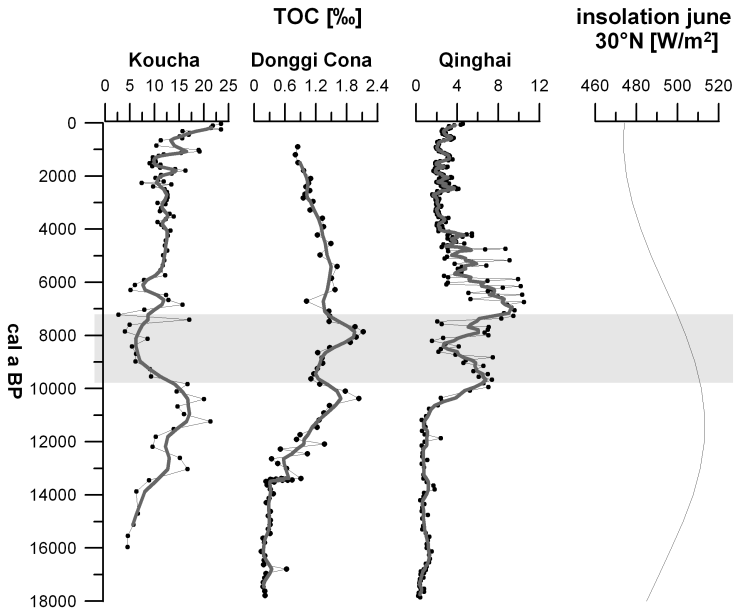

Figure 7.1: Comparison of TOC-contents in the lakes Koucha, Donggi Cona and Qinghai (data from Shen et al., 2005). Insolation data from Berger and Loutre (1991). Shaded area indicates episode of low effective moisture at Lake Koucha.

Generally, there is a need for more palaeo-records from the Tibetan Plateau, especially from the up to now poorly explored central and western parts. As shown in this thesis, biomarker based proxies have - alone or as part of multi proxy studies - the potential to contribute to the understanding of past climate and environmental changes and should therefore be increasingly applied in this key region for global atmospheric circulation patterns.

References

Ageta, H. and Arai, Y. (1983) Fern constituents: pentacyclic triterpenoids isolated from *Polypodium niponicum* and *P. formosamum*. Phytochemistry 22, 1801-1808.

Allen, E.D. and Spence, D.H.N. (1981) The differential ability of aquatic plants to utilize the inorganic carbon supply in fresh water. New Phytologist 87(2), 269-283.

An, C.B., Feng, Z.D. and Barton, L. (2006) Dry or humid? Mid-Holocene humidity changes in arid and semi-arid China. Quaternary Science Reviews 25, 351-361.

An, Z. (2000) The history and variability of the East Asian paleomonsoon climate. Quaternary Science Reviews 19, 171-187.

An, Z., Kukla, G.J., Porter, S. and Xiao, J. (1991) Magnetic susceptibility evidence of monsoon variation on the Loess Plateau of Central China during the last 130,000 years. Quaternary Research 36, 29-36.

Baas, M., Pancost, R., Geel, B. Van and Sinninghe Damste, J.S. (2000) A comparative study of lipids in Sphagnum species. Organic Geochemistry 31, 535-541.

Battarbee, R.W. (2000) Palaeolimnological approaches to climate change, with special regard to the biological record. Quaternary Science Reviews 19, 107-124.

Belt, S.T., Massé, G., Allard, W.G., Robert, J.M. and Rowland, S.J. (2001a) Identification of a C_{25} highly branched isoprenoid triene in the freshwater diatom Navicula sclesvicensis. Organic Geochemistry 32, 1169-1172.

Belt, S.T., Massé, G., Allard, W.G., Robert, J.M. and Rowland, S.J. (2001b) C_{25} highly branched isoprenoid alkenes in planktonic diatoms of the Pleurosigma genus. Organic Geochemistry 32, 1271-1275.

Berger, A. and Loutre, M.F. (1991) Insolation values for the climate of the last 10 million years. Quaternary Science Reviews 10, 297-317.

Bi, X., Sheng, G., Liu, X., Li, C. and Fu, J. (2005) Molecular and carbon and hydrogen isotopic composition of *n*-alkanes in plant leaf waxes. Organic Geochemistry 36, 1405-1417.

Blumenberg, M., Seifert, R., Kasten, S., Bahlmann, E. and Michaelis, W. (2009) Euphotic zone bacterioplankton sources major sedimentary bacteriohopanepolyols in the Holocene Black Sea. Geochimica et Cosmochimica Acta 73, 750-766.

Böhner, J. (2004): Climate Spatial Prediction and Environmental Modelling by Means of Terrain Analyses, Process Parameterisation and Remote Sensing. - Habilitationsschrift an der Fakultät für Geowissenschaften und Geographie der Georg-August-Universität Göttingen, 294 S. [Geogr. Inst. Univ. Göttingen, unveröff.].

Böhner, J. (2005): Advancements and new approaches in Climate Spatial Prediction and Environmental Modelling. - Arbeitsberichte des Geographischen Instituts der HU zu Berlin 109, 49-90.

Böhner, J. (2006): General climatic controls and topoclimatic variations in Central and High Asia. - BOREAS 35 2/2006, 279-295.

Bond, G., Showers, W., Cheseby, M., Lotti, R., Almasi, P., deMenocal, P., Priore, P., Cullen, H., Haydas, I. and Bonani, G. (1997) A pervasive millennial-scale cycle in North Atlantic Holocene and Glacial climates. Science 278, 1257-1266.

Bond, G., Kromer, B., Beer, J., Muscheler, R., Evans, M.N., Showers, W., Hoffmann, S., Lotti-Bond, R., Hajdas, I. and Bonani, G. (2001) Persistent solar influence on the North Atlantic climate during the Holocene. Science 294, 2130-2136.

Bowen, G.J. and Revenaugh J. (2003) Interpolating the isotopic composition of modern meteoric precipitation. Water Resources Research 39, 1299-1311.

Brassell, S.C., Wardroper, A.M.K., Thomson, I.D., Maxwell, J.R. and Eglinton, G. (1981). Specific acyclic isoprenoids as biological markers of methanogenic bacteria in marine sediments. Nature 290, 693-696.

Brenner, M., Whitmore, T.J., Curtis, J.H., Hodell, D.A. and Schelske, C.L. (1999) Stable isotope (^{13}C and $\delta^{15}N$) signatures of sedimented organic matter as indicators of historic lake trophic state. Journal of Paleolimnology 22, 205-221.

Brocks, J.J. and Summons, R.E. (2005) Sedimentary Hydrocarbons, Biomarkers for Early Life. In: Treatise on Geochemistry, Volume 8; Biogeochemistry. p. 63-115 Eds: Heinrich D. Holland and Karl K. Turekian ; Volumeed: W. H. Schlesinger; Elsevier Science, Cambridge, MA, USA

Brush, G.S. and Hilgartner, W.B. (2000) Paleoecology of submerged macrophytes in the upper Chesapeake Bay. Ecol Monogr 70, 645- 667.

Burkhardt, S., Riebesell, U. and Zondervan, I. (1999) Effects of growth rate, CO_2 concentration and cell size on the stable carbon isotope fractionation in marine phytoplankton. Geochimica et Cosmochimica Acta 63, 3729-3741.

Canuel, E.A., Freeman, K.H. and Wakeham, S.G. (1997) Isotopic composition of lipid biomarker compounds in estuarine plants and surface sediments. Limnology and Oceanography 42, 1570-1583.

Chen, F., Yu, Z., Yang, M., Ito, E., Wang, S., Madsen, D.B., Huang, X., Zhao, Y., Sato, T., Birks, H.J.B., Boomer, I., Chen, J., An, C. and Wünnemann, B. (2008) Holocene moisture evolution in arid central Asia and its out-of-phase relationship with Asian monsoon history. Quaternary Science Reviews 27, 351-364.

Chen, F., Bloemendal, J., Wang, J.M., Li, J. and Oldfield, F. (1997) Highresolution multiproxy climate records from Chinese Loess: Evidence for rapid climate changes over the last 75 kyr BP. Palaeogeography, Palaeoclimatology, Palaeoecology 130, 323-335.

Chikaraishi, Y. and Naraoka, H. (2003) Compound-specific delta D-delta C-13 analyses of *n*-alkanes extracted from terrestrial and aquatic plants. Phytochemistry, 63, 361-371.

Chikaraishi, Y. and Naraoka, H. (2007) δ^{13}C and δD relationships among three n-alkyl compound classes (*n*-alkanoic acid, *n*-alkane and *n*-alkanol) of terrestrial higher plants. Organic Geochemistry 38, 198-215.

Chikaraishi, Y., Naraoka, H. and Poulson, S.R. (2004a) Carbon and hydrogen isotopic fractionation during lipid biosynthesis in a higher plant (*Cryptomeria japonica*). Phytochemistry 65, 323-330.

Chikaraishi, Y., Naraoka, H. and Poulson, S.R. (2004b) Hydrogen and carbon isotopic fractionations of lipid biosynthesis among terrestrial (C3, C4 and CAM) and aquatic plants. Phytochemistry 65, 1369-1381.

Christensen, J.H., Hewitson, B., Busuioc, A., Chen, A., Gao, X., Held, I., Jones, R., Kolli, R.K., Kwon, W.-T., Laprise, R., Magaña Rueda, V., Mearns, L., Menéndez, C.G., Räisänen, J., Rinke, A., Sarr, A. and Whetton, P., (2007) Regional Climate Projections. In: Solomon, S., Qin, D., Manning, M., Chen, Z., Marquis, M., Averyt, K.B., Tignor M., Miller, H.L., (eds.), Climate Change 2007. The Physical Science Basis. Contribution of working group I to the fourth assessment report of the Intergovernmental Panel on Climate Change. Cambridge University Press, Cambridge, United Kingdom and New York, NY, USA, 847-940.

Chromov, S. P. (1957) Die geographische Verbreitung der Monsune. Petermanns Geographische Mitteilungen 101, 234-237.

Chu, G.Q., Sun, Q., Li, S.Q., Zheng, M.P., Jia, X.X., Lu, C.F., Liu, J.Q. and Liu, T.S. (2005) Long-chain alkenone distributions and temperature dependence in lacustrine surface sediments from China. Geochimica et Cosmochimica Acta 69, 4985-5003.

Cloern, J.E., Canuel, E.A. and Harris, D. (2002) Stable carbon and nitrogen isotope composition of aquatic and terrestrial plants of the San Francisco Bay estuarine system. Limnology and Oceanography 47, 713-729.

Collister, J.W., Rieley, G., Stern, B., Eglinton, G. and Fry, B. (1994) Compound-specific δ^{13}C analysis of leaf lipids from plants with different carbon dioxide metabolism. Organic Geochemistry 21, 619-627.

Cranwell, P.A., 1973. Chain-length distribution of *n*-alkanes from lake sediments in relation to post-glacial environmental change. Freshwater Biology 3, 259-265.

Dansgaard, W. (1964). Stable isotopes in precipitation. Tellus 16, 436-468.

Dansgaard, W., Johnsen, S.J., Clausen, H.B., Dahl-Jensen, D., Gundestrup, N.S., Hammer, C.U., Hvidberg, C.S., Steffensen, J.P., Sveinbjornsdottir, A.E., Jouzel, J. and Bond, G.C. (1993) Evidence for general instability of past climate from a 250-kyr ice-core record. Nature 364, 218-220.

D'Andrea W.J. and Huang Y. (2005) Long-chain alkenones in Greenland lake sediments: Low δ^{13}C valuesand exceptional abundance. Organic Geochemistry 36, 1234-1241.

Deuser, W.G. (1970) Isotopic evidence for diminishing supply for available carbon during diatom bloom in the Black Sea. Nature 225, 1069-1071.

Didyk, B.M., Simoneit, B., Brassell, S. and Eglinton, G. (1978) Organic geochemical indicators of palaeoenvironmental conditions of sedimentation. Nature 272, 216-222.

Dietze, E., Wünnemann, B., Diekmann, B., Hartmann, K., Aichner, B., Herzschuh, U., IJmker, J., Jin, H., Kopsch, C., Lehmkul, F., Li, S., Mischke, S., Opitz, S., Yan, S., Stauch, G. Basin morphology and seismic stratigraphy of Lake Donggi Cona, north-eastern Tibetan Plateau, China. Quaternary International, in review

Ding, Y. (1994) Monsoons over China. Kluwer, Dordrecht, 419 pp.

Ding, Z.L., Rutter, N.W., Han, J.T. and Liu, T.S. (1992) A coupled environmental system formed at about 2.5Ma over East Asia. Palaeogeography Palaeoclimatology Palaeoecology 94, 223-242.

Ding Z.L. and Yang S.L. (2000) C3/C4 vegetation evolution over the last 7.0 Myr in the Chinese Loess Plateau: evidence from pedogenic carbonate ^{13}C. Palaeogeography, Palaeoclimatology, Palaeoecology 160, 291-299.

Domrös, M. and Peng, G. (1988) The climate of China. Springer Verlag Berlin, Heidelberg, 361pp.

Duan, Y. and Ma, L. (2001) Lipid geochemistry in a sediment core from Ruoergai Marsh deposit (Eastern Qinghai-Tibet plateau, China). Organic Geochemistry 32, 1429-1442.

Dunlop, R.W. and Jefferies, P.R. (1985) Hydrocarbons of the hypersaline basins of Shark Bay, Western Australia. Organic Geochemistry 8, 313-320.

Eglinton, G. and Calvin, M. (1967) Chemical fossils. Scientific American 216, 32-43.

Eglinton, G. and Hamilton, R.J. (1967) Leaf epicuticular waxes. Science 156, 1322-1335.

Elvert, M., Suess, E., and Whiticar, M.J. (1999) Anaerobic methane oxidation associated with marine gas hydrates: Superlight C-isotopes from saturated and unsaturated C_{20} and C_{25} irregular isoprenoids. Naturwissenschaften 86: 295-300.

Elvert, M., Whiticar, M.J. and Suess, E. (2001) Diploptene in varved sediments of Saanich Inlet: indicator of increasing bacterial activity under anaerobic conditions during the Holocene. Marine Geology 174, 371-383

Everitt, B.S., Landau, S. and Leese, M. (2001) Cluster Analysis (4th edition). Arnold Publishers. London

Fan, P., Wang, D. and Qi, R. (2004) Analysis on climatic feature and its change in source region of the Yellow River. Journal of Qinghai University 22, 19-24.

Farquhar, G.D., Ehleringer, J.R. and Hubick, K.T. (1989) Carbon isotope discrimination and photosynthesis. Annual Review of Plant Physiology and Plant Molecular Biology 40, 503-537.

Ficken, K.J., Li, B., Swain, D.L. and Eglinton, G. (2000) An *n*-alkane proxy for the sedimentary input of submerged/floating freshwater aquatic macrophytes. Organic Geochemistry 31, 745-749.

Ficken, K.J., Street-Perrott, F.A., Perrott, R.A., Swain, D.L., Olago, D.O. and Eglinton, G. (1998) Glacial/interglacial variations in carbon cycling revealed by molecular and isotope stratigraphy of Lake Nkunga, Mt. Kenya, East Africa. Organic Geochemistry 29, 1701-1719.

Ficken, K.J., Wooller, M.J., Swain, D.L., Street-Perrott, F.A. and Eglinton, G. (2002) Reconstruction of a subalpine grass-dominated ecosystem, Lake Rutundu, Mount Kenya: a novel multi-proxy approach. Palaeogeogr. Palaeoclimatol. Palaeoecol. 177, 137-149.

Fogel, M.L. and Cifuentes, L.A. (1993) Isotope fractionation during primary production. In: Organic geochemistry: Principles and applications. (eds. Engel MH and Macko SA) Plenum press. p 73-98

Freeman, K.H., Hayes, J.M., Trendel, J.M. and Albrecht, P. (1990) Evidence from GC-MS carbon isotopic measurements for multiple origins of sedimentary hydrocarbons. Nature 353, 627-644.

Freeman, K.H., Wakeham, S.G. and Hayes, J.M. (1994) Predictive isotopic biogeochemistry: hydrocarbons from anoxic marine basins. Organic Geochemistry 21, 629-644.

Fuhrmann, A., Mingram, J., Lucke, A., Lu, H.Y., Horsfield, B., Liu, J.Q., Negendank, J.F.W., Schleser, G.H. and Wilkes, H. (2003) Variations in organic matter composition in sediments from Lake Huguang Maar (Huguangyan), South China during the last 68 ka: implications for environmental and climatic change. Organic Geochemistry 34, 1497-1515.

Gasse, F., Fontes, J.C., VanCampo, E. and Wei, K. (1996) Holocene environmental changes in Bangong Co basin (western Tibet). 4. Discussion and conclusions. Palaeogeography Palaeoclimatology Palaeoecology 120, 79-92.

Gat, J.R., (1996) Oxygen and hydrogen isotopes in the hydrologic cycle. Annual Review of Earth and Planetary Sciences, 24, 225-262.

Gelpi, E., H. Schneider, Mann J. and Oró J. (1970) Hydrocarbons of geochemical significance in microscopic algae. Phytochemistry 9, 603-612.

Glaser, B. and Zech, W. (2005) Reconstruction of climate and landscape changes in a high mountain lake catchment in the Gorkha Himal, Nepal during the Late Glacial and Holocene as deduced from radiocarbon and compound-specific stable isotope analysis of terrestrial, aquatic and microbial biomarkers. Organic Geochemistry 36, 1086-1098.

Gonfiantini, R. (1986) Environmental isotopes in Lake studies. In: P. Fritz, J.C. Fontes (eds.), HAndbook of Environmental Isotope Geochemistry. Elsevier, Amsterdam, pp. 113-163.

Gomes, A. and Azevedo, D. (2003) Aliphatic and aromatic hydrocarbons in tropical recent sediments of Campos dos Goytacazes, RJ, Brazil. Journal of the Brazilian Chemical Society 14, 358-368.

Grice, K., Schouten, S., Nissenbaum, A., Charrach, J. and Sinninghe Damsté, J.S. (1998) A remarkable paradox: Sulfurised freshwater algal (*Botryococcus braunii*) lipids in an ancient hypersaline euxinic ecosystem. Organic Geochemistry 28, 195-216.

Grimalt, J. and Albaiges, J. (1987) Sources and occurrence of C_{12}-C_{22} *n*-alkane distributions with even carbon-number preference in sedimentary environments. Geochimica et Cosmochimica Acta 51, 1379-1384.

Grimalt, J., Yruela, I., Saiz-Jimenez, C., Toja, J., DeLeeuw, J.W. and Albaiges, J. (1991) Sedimentary lipid biogeochemistry of an hypereutrophic alkaline lagoon. Geochimica et Cosmochimica Acta 55, 2555-2577.

Grossi, V., Hirschler, A., Raphel, D., Rontani, J.F., De Leeuw, J.W. and Bertrand, J.C. (1998) Biotransformation pathways of phytol in recent anoxic sediments. Organic Geochemistry 29, 845-861.

Gupta, A., Anderson, D.M. and Overpeck, J.T. (2003) Abrupt changes in the Asian southwest monsoon during the Holocene and their links to the North Atlantic Ocean. Nature 421, 354-357.

Han, J. and Calvin, M. (1969) Hydrocarbon distribution of algae and bacteria, and microbiological activity in sediments. Proceedings of the National academy of Sciences of the United States of America 64, 436-443.

Hanisch, S., Ariztegui, D. and Puttmann, W. (2003) The biomarker record of Lake Albano, central Italy-implications for Holocene aquatic system response to environmental change. Organic Geochemistry 34, 1223-1235.

Harris, N. (2006). The elevation history of the Tibetan Plateau and its implications for the Asian monsoon. Palaeogeography, Palaeoclimatology, Palaeoecology 241, 4-15.

Hayes, J.M., Freemann, K.H., Popp, B.N. and Hoham, C.H. (1990) Compound-specific isotopic analyses: A novel tool for reconstruction of ancient biogeochemical processes. Organic Geochemistry 16, 1115-1128.

He, Y., Theakstone, W.H., Zhang, Z., Zhang D., Yao, T., Chen, T., Shen Y. and Pang H. (2004) Asynchronous Holocene climatic change across China. Quaternary Research 61, 52-63.

Herzschuh, U. (2006) Palaeo-moisture evolution at the margins of the Asian monsoon during the last 50 ka. Quaternary Science Reviews 25, 163-178.

Herzschuh, U. (2007) Reliability of pollen ratios for environmental reconstructions on the Tibetan Plateau. Journal of Biogeography 34, 1265-1273.

Herzschuh, U., Kramer, A., Mischke, S. and Zhang, C. (2009) Quantitative climate and vegetation trends since the late glacial on the northeastern Tibetan Plateau deduced from Koucha Lake pollen spectra. Quaternary Research 71: 162-171.

Herzschuh, U., Winter, K., Wünnemann, B. and Li, S. (2006) A general cooling trend on the central Tibetan Plateau throughout the Holocene recorded by Lake Zigetang pollen spectra. Quaternary International 154-155, 113-121.

Herzschuh, U., Zhang, C., Mischke, S., Herzschuh, R., Mohammadi, F., Mingram, B., Kürschner, H. and Riedel, F. (2005) A late Quaternary lake record from the Qilian Mountains (NW China): evolution of the primary production and the water depth reconstructed from macrofossil, pollen, biomarker, and isotope data. Global and Planetary Change 46, 361-379.

Hodell, D.A. and Schelske, C.L. (1998) Production, sedimentation, and isotopic composition of organic matter in Lake Ontario. Limnology and Oceanography 43, 200Ű214.

Hollander, D.J. and Mackenzie, J.A. (1991) CO_2 control on carbon-isotope fractionation during aqueous photosynthesis: a paleo-pCO_2 barometer. Geology 19, 929-932.

Holmes, J.A., Cook, E.R. and Yang, B. (2009) Climate change over the past 2000 years in Western China. Quaternary International 194, 91-107.

Holzer, G., Oro, J. and Tornabene, T.G. (1979) Gas chromatography-mass spectrometric analysis of neutral lipids from methanogenic and thermoacidophilic bacteria. Journal of Chromatography 186, 795-809.

Hong, Y.T., Hong, B., Lin, Q.H., Zhu, Y.X., Shibata, Y., Hirota, M., Uchida, M., Leng, X.T., Jiang, H.B., Xua, H., Wang, H. and Yi, L. (2003) Correlation between Indian Ocean summer monsoon and North Atlantic climate during the Holocene. Earth and Planetary Science Letters 211, 371-380.

Hopmans, E.C., Weijers, J.W.H., SchefuSS, E., Herfort, L., Sinninghe Damsté, J.S., Schouten, S. (2004) A novel proxy for terrestrial organic matter in sediments based on branched and isoprenoid tetraether lipids. Earth and Planetary Science Letters 224, 107-116.

Hou, J., D'Andrea, W.J., MacDonald, D. and Huang, Y. (2007). Hydrogen isotopic variability in leaf waxes among terrestrial and aquatic plants around Blood Pond, Massachusetts (USA). Organic Geochemistry 38, 977-984.

Hou, J., D'Andrea, W.J. and Huang, Y., (2008) Can sedimentary leaf waxes record D/H ratios of continental precipitation? Field, model, and experimental assessments. Geochimica et Cosmochimica Acta, 72, 3503-3517.

Hou, J., Huang, Y., Oswald, W.W., Foster, D.R. and Shuman, B. (2007) Centennial-scale compound-specific hydrogen isotope record of Late Pleistocene - Holocene climate transition from southern New England. Geophysical Research Letter 34, L19706

Huang, Y.S., Shuman, B., Wang, Y. and Webb, T. (2004) Hydrogen isotope ratios of individual lipids in lake sediments as novel tracers of climatic and environmental change: a surface sediment test. Journal of Paleolimnology. 31(3), 363-375.

Huang, Y.S., Street-Perrott, F.A., Perrot, R.A., Metzger, P. and Eglinton, G. (1999) Glacial-interglacial environmental changes inferred from molecular and compound-specific delta C-13 analyses of sediments from Sacred Lake, Mt. Kenya. Geochimica et Cosmochimica Acta 63, 1383-1404.

Huang, Y.S., Street-Perrott, F.A., Metcalfe, S.E., Brenner M., Moreland, M. and Freeman K.H. (2001) Climate change as the dominant control on glacial-interglacial variations in C_3 and C_4 plant abundance. Science 293, 1647-1651.

IAEA, 2001. GNIP maps and animations. International Atomic Energy Agency, Vienna. Accessible at http://isohis.iaea.org.

Jaffé, R., Mead, R., Hernandez, M.E., Peralba, M.C. and DiGuida, O.A. (2001) Origin and transport of sedimentary organic matter in two subtropical estuaries: a comparative, biomarker-based study. Organic Geochemistry 32, 507-526.

Keeley, J.E. and Sandquist, D.R. (1992) Carbon: freshwater plants. Plant, Cell and Environment 15, 1021-1035.

Kenig, F., Sinninghe Damsté, J.S., Kock-van Dalen, A.C., Rijpstra, W.I.C., Huc, A.Y. and de Leeuw, J.W. (1995) Occurrence and origin of mono-, di-, and trimethylalkanes in modern and Holocene cyanobacterial mats from Abu Dhabi, United Arab Emirates. Geochimica et Cosmochimica Acta 59, 2999-3015.

Kolattukudy, P.E., Croteau, R. and Buckner, J. S. (1976) Biochemistry of plant waxes. In: Chemistry and biochemistry of natural waxes (ed. P. E. Kolattukudy). Elsevier, Amsterdam. pp. 289-347.

Koopmans, M.P., Rijpstra, W.I.C, Klapwijk, M.M., de Leeuw, J.W., Lewan, M.D. and Sinninghe Damsté, J.S. (1999) A thermal and chemical degradation approach to decipher pristane and phytane precursors in sedimentary organic matter. Organic Geochemistry 30, 1089-1104.

Kovats, E. (1958) Gas-chromatographic characterisation of organic compounds. Part 1. Retention indexes of aliphatic halides, alcohols, aldehydes and ketones. Helv Chim Acta 41, 1915-1932.

Kristen, I., Wilkes, H., Vieth, A., Zink, K.G., Plessen, B., Thorpe, J. and Oberhänsli H (2009) Biomarker and stable carbon isotope analyses of sedimentary organic matter

from Lake Tswaing: Evidence for deglacial wetness and early Holocene drought from South Africa. Journal of Paleolimnology. in review

Leaney, F.W., Osmond, C.B., Allison, G.B. and Ziegler, H. (1985) Hydrogen-Isotope Composition of Leaf Water in C-3 and C-4 Plants - Its Relationship to the Hydrogen-Isotope Composition of Dry-Matter. Planta 164, 215-220.

Lehmkuhl, F. and Owen, L.A. (2005) Late quaternary glaciation of Tibet and the bordering mountains: a review. Boreas 34, 87-100.

Leng, M.J. and Marshall, J.D. (2004) Palaeoclimate interpretation of stable isotope data from lake sediment archives. Quaternary Science Reviews 23, 811-831.

Li, J.G., Philip, R.P., Pu, F. and Allen, J. (1996) Long-chain alkenones in Qinghai lake sediments. Geochimica et Cosmochimica Acta 60, 235-241.

Lichtfouse, E., Derenne, S., Mariotti, A. and Largeau, C. (1994) Possible algal origin of long chain odd *n*-alkanes in immature sediments as revealed by distributions and carbon isotope ratios. Organic Geochemistry 22, 1023-1027.

Liu, Z.H., Henderson, A.C.G. and Huang, Y. (2006) Alkenone-based reconstruction of late-Holocene surface temperature and salinity changes in Lake Qinghai, China. Geophysical Research Letters 33, L09707

Liu, Z.H., Henderson, A.C.G. and Huang, Y.S. (2008) Regional moisture source changes inferred from Late Holocene stable isotope records. Advances in Atmospheric Sciences 25, 1021-1028.

Lister, G.S., Kelts, K., Chen, K.Z., Yu, J.Q. and Niessen, F. (1991) Lake Qinghai, China: closed-basin lake levels and the oxygen isotope record for ostracoda since the last Pleistocene. Palaeogeography, Palaeoclimatology, Palaeoecology 84, 141-162.

Lucas, W.J. and Berry, J.A. (1985) Inorganic carbon transport in aquatic photosynthetic organisms. Physiologia Plantarum 65, 539-543.

Maberly, S.C. and Spence, D.H. (1983) Photosynthetic inorganic carbon use by freshwater plants. The Journal of Ecology 71, 705-724.

Marlowe, I.T., Brassell, S.C., Eglinton, G. and Green, J.C. (1984) Long chain unsaturated ketones and esters in living algae and marine sediments. Organic Geochemistry 6, 135-141.

Mead, R., Xu, Y., Chong, J. and Jaffe, R. (2005) Sediment and soil organic matter source assessment as revealed by the molecular distribution and carbon isotopic composition of *n*-alkanes. Organic Geochemistry 36, 363-370.

Metzger P., Templier J., Largeau C. and Casadevall E. (1986) An n-alkatriene and some *n*-alkadienes from the A Race of the green alga *Botryococcus braunii*. Phytochemistry 25, 1869-1872.

Metzger, P. and Largeau, C. (2005) *Botryococcus braunii*: a rich source for hydrocarbons and related ether lipids. Applied Microbiology and Biotechnology 66, 486-496.

Meyers, P.A. (2003) Applications of Organic Geochemistry to paleolimnological reconstructions: a summary of examples from the Laurentian Great Lakes. Organic Geochemistry 34, 261-289.

Meyers, P.A. and Ishiwatari, R. (1993) Lacustrine Organic Geochemistry - an overview of indicators of organic matter sources and diagenesis in lake sediments. Organic Geochemistry 20, 867-900.

Mischke, S., Herzschuh, U. Massmann, G. and Zhang, C. (2007) An ostracod-conductivity transfer function for Tibetan lakes. Journal of Paleolimnology 38, 509-524.

Mischke, S., Kramer, M., Zhang, C., Shang, H., Herzschuh, U. and Erzinger, J. (2008) Reduced early Holocene moisture availability in the Bayan Har Mountains, northeastern Tibetan Plateau, inferred from a multi-proxy lake record. Palaeogeography Palaeoclimatology Palaeoecology 267, 59-76.

Mook, W.G., Bommerson, J.C. and Staverman, W.H. (1974) Carbon isotope fractionation between dissolved bicarbonate and gaseous carbon dioxide. Earth and Planetary Science Letters 22, 169-176.

Morill, C., Overpeck, J.T. and Cole, J.E. (2003) A synthesis of abrupt changes in the Asian summer monsoon since the last deglaciation. Holocene 13, 465-476.

Morinaga, H., Itota, C., Isezaki, N., Goto, H., Yaskawa, K., Kusakabe, M., Liu, J., Gu, Z., Yuan, B. and Cong, S., 1993. Oxygen-18 and carbon-13 records for the last 14,000 years from lacustrine carbonates of siling-co (lake) in the qinghai-tibetan plateau. Geophysical Research Letters 20, 2909-2912.

Mügler, I., Sachse, D., Werner, M., Xu, B., Wu, G., Yao, T. and Gleixner, G. (2008) Effect of lake evaporation on δD values of lacustrine *n*-alkanes: A comparison of Nam Co (Tibetan Plateau) and Holzmaar (Germany). Organic Geochemistry 39, 711-729.

Mügler, I., Gleixner, G., Mäusbacher, R., Daut, G., Schütt, B., Berking, J., Schwalb, A., Schwark, L., Xu, B., Yao, T., Zhu, L. and Yi, C. (2009) A multi-proxy approach to reconstruct hydrological changes and Holocene climate development of Nam Co, Central Tibet. Journal of Paleolimnology, DOI 10.1007/s10933-009-9357-0

Nuñez, R., Spiro, B., Pentecost, A., Kim A. and Coletta, P. (2002) Organo-geochemical and stable isotope indicators of environmental change in a marl lake, Malham Tarn, North Yorkshire, UK, Journal of Paleolimnology 28, 403-417.

O'Leary, M. (1988) Carbon isotopes in photosynthesis: fractionation techniques may reveal new aspects of carbon dynamics in plants. BioScience 38(5), 328-335.

O'Neil, J.R. (1986) Theoretical and experimental aspects of isotopic fractionation. Mineralogical Society of America Reviews in Mineralogy 16, 1-40.

Papadimitrou. S., Kennedy, H., Kennedy, D.P. and Borum, J. (2005) Seasonal and spatial variation in the organic carbon and nitrogen concentration and their stable isotopic composition in Zostera marina (Denmark). Limnology and Oceanography 50, 1084-1095.

Park, R. and Epstein, S. (1961) Metabolic fractionation of C13 and C12 in plants. Plant Physiology 36, 133-138.

Pease, T.K., Van Vleet, E.S., Barre, J.S. and Dickins, H.D. (1998) Simulated degradation of glyceryl ethers by hydrous and flash pyrolysis. Organic Geochemistry 29, 979-988.

Pedentchouk, N., Sumner, W., Tipple, B., Pagani, M. (2008) δ^{13}Cand δD compositions of n-alkanes from modern angiosperms and conifers: An experimental set up in central Washington State, USA. Organic Geochemistry 39, 1066-1071.

Peters, K.E., Walters, C.C. and Moldowan, J.M. (2005) The Biomarker Guide, Volume 1 and 2: Biomarkers and Isotopes in the Petroleum Exploration and Earth History. Cambridge University Press, Cambridge

Powers, L.A., Werne, J.P., Johnson, T.C., Hopmans, E.C., Damste, J.S.S. and Schouten, S., (2004) Crenarchaeotal membrane lipids in lake sediments: A new paleotemperature proxy for continental paleoclimate reconstruction? Geology 32, 613-616.

Prahl F.G. and Wakeham S.G. (1987) Calibration of unsaturation patterns in long-chain ketone compositions for paleotemperature assessment. Nature 341, 434-437.

Prins, H.B.A. and Elzenga, J.T.M. (1989) Bicarbonate utilization: function and mechanism. Aquatic Botanx 34, 59-83.

Radke, M., Willsch, H. and Welte, D.H. (1980) Preparative hydrocarbon group type determination by automated medium pressure liquid chromatography. Analytical Chemistry 52, 406-411.

Rao, Z., Zhu, Z., Jia, G., Henderson, A.C.G., Xue, Q. and Wang, S. (2009) Compound specific δD values of long chain *n*-alkanes derived from terrestrial higher plants are indicative of the δD of meteoric waters: Evidence from surface soils in eastern China. Organic Geochemistry 40, 922-930.

Reimer, P.J., Baillie, M.G.L., Bard, E., Bayliss, A., Beck, J.W., Bertrand, C.H.J., Blackwell, P.G., Buck, C.E., Burr, G.S., Cutler, K.B., Damon, P.E., Edwards, R.L., Fairbanks, R.G., Friedrich, M., Guilderson, T.P., Hogg, A.G., Hughen, K.A., Kromer, B., McCormac, G., Manning, S., Bronk Ramsey, C., Reimer, R.W., Plicht, J.V.D. and Weyhenmeyer, C.E. (2004) IntCal04 terrestrial radiocarbon age calibration, 0-26 cal kyr BP. Radiocarbon 46, 1029-1058.

Risatti, J.B., Rowland, S.J., Yon, D.A. and Maxwell, J.R. (1984) Stereochemical studies of acyclic isoprenoids-XII. Lipids of methanogenic bacteria and possible contributions to sediments. Organic Geochemistry 6, 93-103.

Rohmer, M., Bouvier-Nave, P. and Ourisson, G. (1984) Distribution of hopanoid triterpenes in prokaryotes. Journal of General Microbiology 130, 1137- 1150.

Rontani, J.F. and Volkman, J.K. (2003) Phytol degradation products as biogeochemical tracers in aquatic environments. Organic Geochemistry 34, 1-35.

Rosell-Melé, A. (1998). Interhemispheric appraisal of the value of alkenone indices as temperature and salinity proxies in high-latitude locations. Paleoceanography 13, 694-703.

Rowland, S.J., Yon, D.A., Lewis, C.A. and Maxwell, J.R. (1985) Occurrence of 2,6,10-trimethyl-7-(3-methylbutyl) dodecane and related hydrocarbons in the green alga Enteromorpha prolifera and sediments. Organic Geochemistry 8, 207-13.

Rowland, S.J. and Robson, J.N. (1990) The widespread occurrence of highly branched acyclic C_{20}, C_{25} and C_{30} hydrocarbons in recent sediments and biota-a review. Marine Environment Research 30, 191-216.

Rozanski, K., L. Araguds-Araguds and R. Gonfiantini (1992) Relation between long-term trends of $^{18}0$ isotope composition of precipitation and climate. Science 258, 981-985.

Ruddiman, W. F. and Kutzbach, J. E. (1989) Forcing of Late Cenozoic Northern Hemisphere climate by plateau uplift in southern Asia and the America west. Journal of Geophysical Research 94, 409-427.

Sachse, D., Radke, J. and Gleixner, G. (2004) Hydrogen isotope ratios of recent lacustrine sedimentary *n*-alkanes record modern climate variability. Geochimica et Cosmochimica Acta 68, 4877-4889.

Sachse, D., Radke, J. and Gleixner, G. (2006) δD values of individual n-alkanes from terrestrial plants along a climatic gradient - Implications for the sedimentary biomarker record. Organic Geochemistry 37, 469-483.

Sachse, D. and Sachs, J. (2008) Inverse relationship between D/H fractionation in cyanobacterial lipids and salinity in Christmas Island saline ponds. Geochimica et Cosmochimica Acta 72, 793-806.

Sauer, P.E., Eglinton, T.I., Hayes, J.M., Schimmelmann, A. and Sessions, A.L. (2001) Compound-specific D/H ratios of lipid biomarkers from sediments as a proxy for environmental and climatic conditions. Geochimica et Cosmochimica Acta 65, 213-222.

Schaefer, H. and Whiticar, M.J. (2008) Potential glacial-interglacial changes in stable carbon isotope ratios of methane sources and sink fractionation. Global Biogeochemical Cycles 22, GB1001

Schefuß, E., Schouten, S. and Jansen, J.H.F. and Sinninghe Damste, J.S. (2003) African vegetation controlled by tropical sea surface temperatures in the mid-Pleistocene period. Nature 422, 418-421.

Schefuß, E., Schouten, S. and Schneider, R.R. (2005) Climatic controls on central African hydrology during the past 20,000 years. Nature 437, 1003-1006.

Schimmelmann, A., Lewan, M.D. and Wintsch, R.P. (1999) D/H isotope ratios of kerogen, bitumen, oil, and water in hydrous pyrolysis of source rocks containing kerogen types I, II, and III. Geochimica et Cosmochimica Acta 63, 3751-3766.

Schouten, S., Hopmans E. C., Schefuß, E. C. and Sinninghe Damste, J.S. (2002) Distributional variations in marine crenarchaeotal membrane lipids: a new tool for reconstructing ancient sea water temperatures? Earth and Planetary Science Letters 204, 265 - 274.

Schouten, S., Rijpstra, W.I.C., Kok, M., Hopmans, E.C., Summons, R.E., Volkman, J.K. and Sinninghe-Damsté, J.S. (2001) Molecular organic tracers of biogeochemical processes in a saline meromictic lake (Ace Lake). Geochimica et Cosmochimica Acta 65, 1629-1640.

Schouten, S., van der Maarel, M.J.E.C., Huber, R. and Sinninghe Damsté, J.S. (1997) 2,6,10,15,19-pentamethylicosenes in *Methanolobus bombayensis*, a marine methanogenic archaeon and *Methanosarcina mazei*. Organic Geochemistry 26, 409-414.

Schwalb, A. (2003) Lacustrine ostracodes as stable isotope recorders of late-glacial and Holocene environmental dynamics and climate. Journal of Paleolimnology 29, 267-351.

Schwark, L., Zink, K. and Lechterbeck, J., (2002) Reconstruction of postglacial to early Holocene vegetation history in terrestrial Central Europe via cuticular lipid biomarkers and pollen records from lake sediments. Geology 30, 463-466.

Schwender, J., Gemunden C. and Lichtenthaler, H.K. (2001) Chlorophyta exclusively use the 1-deoxyxylulose 5-phosphate/2-C-methylerythritol 4-phosphate pathway for the biosynthesis of isoprenoids. Planta 212, 416-423.

Seki, O., Meyers, P.A., Kawamura, K., Zheng, Y. and Zhou, W. (2009) Hydrogen isotopic ratios of plant wax *n*-alkanes in a peat bog deposited in northeast China during the last 16 kyr. Organic Geochemistry 40, 671-677.

Selvaraj, K., Chen, C.T.A. and Lou, J.Y. (2008) Holocene weak summer East Asian monsoon intervals in subtropical Taiwan and their global synchronicity. Climate of the Past Discussions 4, 929-953.

Seppä, H. and Bennett, K. (2003) Quaternary pollen analysis: recent progress in palaeoecology and palaeoclimatology. Progress in Physical Geography 27, 548-579.

Sessions, A.L., Burgoyne, T.W., Schimmelmann, A. and Hayes, J.M. (1999). Fractionation of hydrogen isotopes in lipid biosynthesis. Organic Geochemistry 30, 1193-1200.

Sessions, A.L. (2006) Seasonal changes in D/H fractionation accompanying lipid biosynthesis in Spartina alterniflora. Geochimica et Cosmochimica Acta 70, 2153-2162.

Shen, J., Liu, X.Q., Wang, S.M. and Matsumoto, R. (2005) Palaeoclimatic changes in the Qinghai Lake area during the last 18,000 years. Quaternary International 136, 131-140.

Sinninghe-Damsté, J., Muyzer, G., Abbas, B., Rampen, S.W., Massé, G., Allard, W.G., Belt, S.T., Robert, J.M., Rowland, S.J., Moldowan, J.M., Barbanti, S.M., Fago, F.J., Denisevich, P., Dahl, J., Trindade, L.A.F. and Schouten, S. (2004) The rise of the Rhizosolenid diatoms. Science 304, 584-587.

Smith F. A. and Freeman K. H. (2006) Influence of physiology and climate on δD of leaf wax *n*-alkanes from C_3 and C_4 grasses. Geochimica Cosmochimica Acta 70, 1172-1187.

Sternberg, L.D.S.L. (1988) D/H ratios of environmental water recorded by D/H ratios of plant lipids. Nature 333, 59-61.

Street-Perrott, F.A., Ficken, K.J., Huang, Y.S. and Eglinton, G. (2004) Late quaternary changes in carbon cycling on Mt. Kenya, East Africa: an overview of the delta C-13 record in lacustrine organic matter. Quaternary Science Reviews 23, 861-879.

Stumm, W. and Morgan J.J. (1981) Aquatic chemistry : an introduction emphasizing chemical equilibria in natural waters. 2nd Edition, Wiley, New York

Summons, R.E., Franzmann, P.D. and Nichols, P.D. (1998) Carbon isotopic fractionation associated with methylotrophic methanogenesis. Organic Geochemistry 28, 465-475.

Summons, R.E., Jahnke, L.J., Roksandic, Z. (1994) Carbon isotopic fractionation in lipids from methanotrophic bacteria: relevance for interpretation of the geochemical record of biomarkers. Geochimica et Cosmochimica Acta 58, 2853-2863.

Sun, X.J., Luo, Y, Huang, F., Tian, J. and Wang, P. (2003). Deep-sea pollen from the South China Sea: Pleistocene indicators of East Asian monsoon. Marine Geology, 201, 97-118.

Sun, Q., Chu, G.Q., Li, S.Q., Lu, C.F. and Zheng, M.P. (2004) Long-chain alkenones in sulfate lakes and paleoclimatic implications, Chinese Science Bulletin 49, 2082-2086.

Taiz, L. and Zeiger. E. (2002) Plant physiology. (3rd Edition). Eds.: Sinauer. Sinauer Associates, Massachussets, USA

Talbot, M.R. and Johannessen, T. (1992) A high resolution palaeoclimatic record for the last 27,500 years in tropical West Africa from the carbon and nitrogen isotopic composition of lacustrine organic matter. Earth and Planetary Science Letters 110, 23-37.

Tierney, J.E., Russell, J.M, Huang, Y., Sinninghe Damsté, J.S., Hopmans, E.C. and Cohen, A.S. (2008) Northern Hemisphere controls on tropical Southeast African climate during the past 60,000 years. Science 322, 252-255.

Thiel, V., Jenisch, A., Landmann, G., Reimer, A., and Michaelis, W. (1997) Unusual distributions of long-chain alkenones and tetrahymanol from the highly alkaline Lake Van, Turkey. Geochimica et Cosmochimica Acta 61, 2053-2064.

Thiel, V., Peckmann, J., Seifert, R., Wehrung, P., Reitner, J. and Michaelis, W. (1999) Highly isotopically depleted isoprenoids: Molecular markers for ancient methane venting. Geochimica et Cosmochimica Acta 63, 3959-3966.

Thompson, L.G., Yao, T., Davis, M.E., Henderson, K.A., Mosley-Thompson, E., Lin, P., Beer, J., Synal, H.A., Cole-Dai, J. and Bolzan, J.F. (1997) Tropical climate instability: the last glacial cycle from a Qinghai-Tibetan ice core. Science 276, 1821-1825.

Thompson, L.G. (2000) Ice core evidence for climate change in the Tropics: implications for our future. Quaternary Science Reviews 19, 19-35.

Uemura, H. and Ishiwatari, R.(1995) Identification of unusual 17β(H)-moret-22(29)-ene in lake sediments. Organic Geochemistry 23, 675-680.

Van den Berg, M., Coops, H., Simons, J. and Pilon, J. (2002) A comparative study of the use of inorganic carbon resources by Chara aspera and Potamogeton pectinatus. Aquatic Botany 72, 219-233.

Venkatesan, M.I. and Kaplan, I.R. (1987) Organic geochemistry of Antarctic marine sediments, Part I. Bransfield Strait. Marine Chemistry 21, 347-75.

Volkman J. K. (1986) A review of sterol markers for marine and terrigenous organic matter. Organic Geochemistry 9, 83-99.

Volkman J. K. (2003) Sterols in microorganisms. Applied Microbiology and Biotechnology 60, 496-506.

Volkman, J.K., Allen, D.I., Stevenson, P.L. and Burton, H.R. (1986) Bacterial and algal hydrocarbons in sediments from a saline Antarctic Lake, Ace Lake. Organic Geochemistry 10, 671-681.

Volkman, J. K., Eglinton, G., Corner, E. D. S. and Forsberg, T. E. V. (1980) Long-chain alkenes and alkenones in the marine coccolithophorid *Emiliania huxleyi*. Phytochemistry 19, 2619-2622.

Wakeham, S.G. (1990) Algal and bacterial hydrocarbons in particulate matter and interfacial sediment of the Cariaco Trench. Geochimica et Cosmochimica Acta 54, 1325-1336.

Wang, F.B. and Fan, C.Y. (1987) Climatic changes in the Qinghai-Xizang (Tibetan) region of China during the Holocene. Quaternary Research 28, 50-60.

Wang, L., Sarntheim, M., Erlenkeuser, H., Grimalt, J., Grootes, P., Heilig, S., Ivanova, E., Kienast, M., Pelejero, C. and Pflaumann, U. (1999) East Asian monsoon climate during the Late Pleistocene: high resolution sediment records from the South China Sea. Marine Geology 156, 245-284.

Wang, P., Clemens, S., Beaufort, L., Braconnot, P., Ganssen, G., Jian, Z., Kershaw, P. and Sarthein, M (2005) Evolution and variability of the Asian monsoon system: state of the art and outstanding issues. Quaternary Science Reviews 24, 595-629.

Wang, R., Brassel, S.C., Scarpitta, S.C., Zheng, M.P., Zhang, S.C., Hayde, P.R. and Muench, L.M. (2004) Steroids in sediments from Zabuye Salt Lake, western Tibet: diagenetic, ecological or climatic signals? Organic Geochemistry 35, 157-168.

Wang, R. and Zheng, M. (1998) Occurence and environmental significance of long-chain alkenones in Tibetan Zabuye Salt Lake, S.W. China. International Journal of Salt Lake Research 6, 281-302.

Wang, R.Z. (2003) C4 plants in the vegetation of Tibet, China: their natural occurrence and altitude distribution pattern. Photosynthetica 41, 21-26.

Wang, Y. J., Cheng H., Edwards R. L., An Z. S., Wu J. Y., Shen C. C. and Dorale J. A. (2001) A high-resolution absolute-dated late Pleistocene monsoon record from Hulu Cave, China. Science 294, 2345-2348.

Wang, Y., Cheng, H., Edwards, L., Kong, X., Shao, X., Chen, S., Wu, J., Jiang, X., Wang, X. and An, Z. (2008) Millenial- and orbital-scale changes in the East Asian monsoon over the past 220,000 years. Nature 451, 1090-1093.

Ward, J.H. (1963). Hierarchical Grouping to optimize an objective function. Journal of the American Statistical Association 58, 236-244.

Wetzel, R.G. (2001) Limnology - Lake and River Ecosystems. 3rd Edition, Academic Press. San Diego, California

Whiticar, M.J., Faber, E. and Schoell, M. (1986) Biogenic methane formation in marine and freshwater environments: CO2 reduction vs. acetate fermentation - Isotope evidence. Geochimica et Cosmochimica Acta 50: 693-709.

Winkler, M.G. and Wang, P.K. (1993) The late Quaternary vegetation and climate of China. In Wright, H.E., editor, Global climates since the last glacial maximum, Minneapolis: University of Minnesota Press, 221-61.

Wilkes, H., Ramrath A. and Negendank, J.F.W. (1999). Organic geochemical evidence for environmental changes since 34,000 yrs BP from Lago di Mezzano, central Italy. Journal of Paleolimnology 22, 349-365.

Xia, Z.H., Xu, B.Q., Mügler, I., Wu, G.J., Gleixner G., Sachse, D. and Zhu, L.P. (2008) Hydrogen isotope ratios of terrigenous *n*-alkanes in lacustrine surface sediment of the Tibetan Plateau record the precipitation signal. Geochemical Journal 42, 331-338.

Xu, Y., Jaffé, R., Wachnicka, A. and Gaiser, E.E. (2006) Occurrence of C_{25} highly branched isoprenoids (HBIs) in Florida Bay: paleoenvironmental indicators of diatom-derived organic matter inputs. Organic Geochemistry 37, 847-859.

Yamada, K. and Ishiwatari, R. (1999) Carbon isotopic compositions of long-chain *n*-alkanes in the Japan Sea sediments: implications for paleoenvironmental changes over the past 85 kyr. Organic Geochemistry 30, 367-377.

Yang, H. and Huang, Y.S. (2003) Preservation of lipid hydrogen isotope ratios in Miocene lacustrine sediments and plant fossils at Clarkia, northern ID, USA. Organic Geochemistry 34, 413-423.

Yon, D.A., Ryback, G. and Maxwell, J.R. (1982) 2,6,10-trimethyl-7-(3 methylbutyl)dodecane, a novel sedimentary biological marker compound. Tetrahedron Letters 23, 2143-2146.

Yu, J.Q. and Kelts, K.R. (2002) Abrupt changes in climatic conditions across the late-glacial /Holocene transition on the N. E. Tibet-Qinghai Plateau: evidence from Lake Qinghai, China. Journal of Paleolimnology 28, 195Ű206.

Yu, Y., Yang, T., Li, J., Liu, J., An, C., Liu, X., Fan, Z., Lu, Z., Li, Y. and Su, X. (2006) Millennial-scale Holocene climate variability in the NW China drylands and links to the tropical Pacific and the North Atlantic. Palaeogeography, Palaeoclimatology, Palaeoecology, 233, 149-162.

Yuan D. X., Cheng H., Edwards R. L., Dykoski C. A., Kelly M. J., Zhang M., Qing J., Lin Y., Wang Y., Wu J., Dorale J. A., An Z. S. and Cai Y. (2004) Timing, during, and transitions of last interglacial Asian monsoon. Science 304, 575-578.

Zhang, Z., Metzger, P. and Sachs, J.P. (2007) Biomarker evidence for the co-occurrence of three races (A, B and L) of *Botryococcus braunii* in El Junco Lake, Galapagos. Organic Geochemistry 38, 1459-1478.

Zheng, Y., Zhou, W., Meyers, P.A. and Xie, S. (2007) Lipid biomarkers in the Zoige-Hongyuan peat deposit: indicators of Holocene climate changes in West China. Organic Geochemistry 38, 1927-1940.

Zhou, J., Wang, S., Yang, G. and Xiao, H. (2007) Younger Dryas event and cold events in early-mid Holocene: record from the sediment of Erhai Lake. Advances in Climate Change Research 3 (Suppl.), 41-44.

Zhu, L., Wu, Y., Wang, J., Lin, X., Ju, J., Xie, M., Li, M., Mäusbacher, R., Schwalb, A. and Daut, G. (2008) Environmental changes since 8.4 ka reflected in the lacustrine core sediments from Nam Co, central Tibetan plateau, China. Holocene 18, 831-839

Zink, K.G., Leythaeuser, D., Melkonian, M. and Schwark, L. (2001) Temperature dependency of long-chain alkenone distributions in recent to fossil limnic sediments and in lake waters. Geochimica et Cosmochimica Acta 65, 253-265.

A Appendix

A.1 Testing a possible applicability of the TEX_{86} in Tibet

Due to the large climatic gradient of the surface sample set it was tested if the TEX_{86} (for explanation see introduction page 6) could be applied on the Tibetan Plateau. Therefore NSO fractions of surface sediment samples were analysed for GDGTs (glycerol-diphytanyl-glycerol-tetraethers) using an LC/APCI-MS system, operated in selected ion monitoring (SIM) mode. Ether lipids, necessary to calculate the TEX_{86}, were found in most of the samples, but attempts to reconstruct surface temperatures applying the TEX_{86} index, were not successful. First of all, the signal to noise ratio of the target compounds was rather low, making a precise quantification difficult. Additionally high concentrations of branched isoprenoid ether lipids (as shown at BIT indices > 0.9 in 90% of all samples) indicate a high input of ether lipids from soils, which most likely bias the TEX_{86}. Calculating temperatures from this TEX_{86} values obtained for the surface samples and samples from Koucha Lake therefore resulted in unrealistic high temperatures. The drawn conclusions were: (a) temperatures are too low in most of Tibetan lakes to obtain a strong enough signal of aquatic ether lipids; (b) input of ether lipids from soils is too high to obtain a reliable TEX_{86} ratio, and the proxy therefore is hardly applicable in our study region.

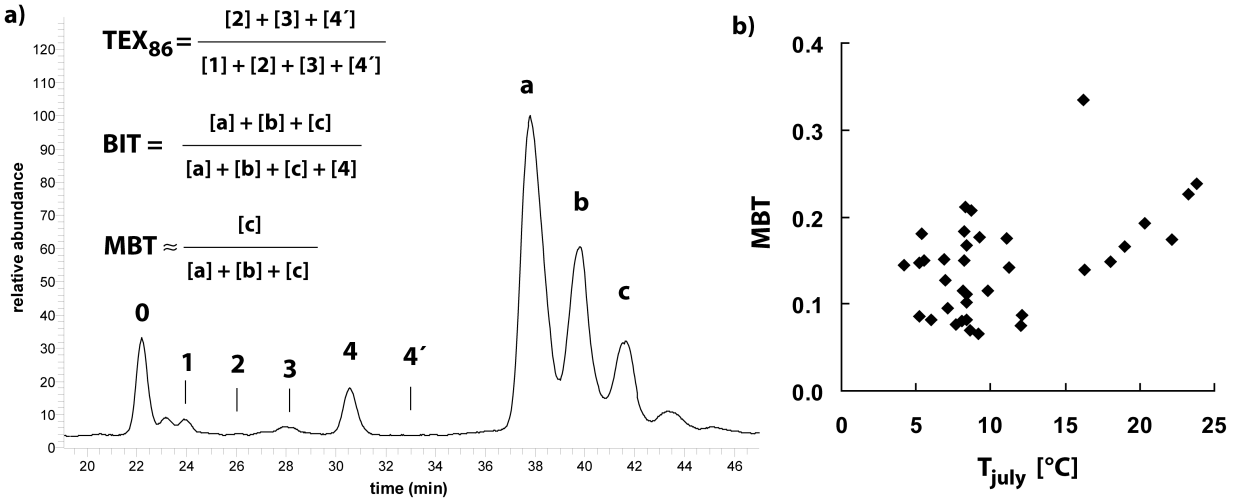

Figure A.1: (a) LC-MS chromatogram of a surface sediment sample from the Tibetan Plateau, showing ether lipids relevant for calculation of the TEX_{86}, the BIT and the MBT (Hopmans et al., 2002; Schouten et al., 2002; Sinninghe-Damsté et al., 2002; Weijers et al., 2007). (b) A simplified MBT plotted against T_{july}

New ether lipid-based proxies such as the methylation index of branched tetraethers (MBT) and the cyclisation ratio of the branched tetraethers (CBT) were proposed in course of this thesis, but additional compounds necessary to calculate these ratios have not yet been included in the SIM-modus while measuring our samples. However, the MBT ratio can also be assessed by using a simplified ratio as shown in Fig. A.1. If plotted versus T_{july} [°C], MBT values are scattering in the low temperature range, but a temperature dependence is observable at higher temperatures (T_{july} >15 °C; SET and Qai samples). Hence, the MBT ratio was not considered to be a promising temperature proxy for Lake Koucha as well as for other high-altitude lakes on the central or northeastern Tibetan Plateau. However, it could be potentially calibrated for warmer regions such as the southeastern slope of the Tibetan Plateau or the Qaidam Basin. The pattern of the compounds "a", "b" and "c", which are dominated by compound "a" in Tibetan lakes, is different from reported ether lipid distribution in soils (Weijers et al., 2007), which show a dominance of compound "c". However, it is similar to the distribution of ether lipids in New Zealand lakes (Zink, K., GNS New Zealand, personal communication). This could be evidence for different source organisms of branched ether lipids in lakes and soils.

References:

Hopmans E, Weijers J, Schefuß E, Herfort L, Sinninghe Damsté J, Schouten S (2002) A novel proxy for terrestrial organic matter in sediments based on branched and isoprenoid tetraether lipids. Earth Planet. Sci. Lett. 224, 107 - 116.

Schouten S, Hopmans E, Schefuß E, Sinninghe Damsté J (2002) Distributional variations in marine crenarchaeotal membrane lipids: a new tool for reconstructing ancient sea water temperatures? Earth Planet. Sci. Lett. 204, 265 - 274.

Sinninghe Damsté J, Schouten S, Hopmans E, van Duin A, Geenevasen J (2002) Crenarchaeol: the characteristic core glycerol dibiphytanyl glycerol tetraether membrane lipid of cosmopolitan pelagic crenarchaeota. J. Lipid Res. 43, 1641 - 1651.

Weijers J, Schouten S, van den Donker J, Hopmans E, Sinninghe Damsté (2007) Environmental controls on bacterial tetraether membrane lipid distribution in soils. Geochim. Cosmochim. Acta 71, 703-713.

A.2 *n*-Alkane concentrations in surface sediments and in a sediment core from Lake Donggi Cona, eastern Tibetan Plateau

Introduction

In this short draft, results from a first evaluation of bulk organic matter data and *n*-alkane concentrations in surface samples and a sediment core from Lake Donggi Cona are presented. Even if Lake Donggi Cona was not a major focus of this thesis, the data are important to unterstand spatial distribution of lipid patterns within a larger lake and serve as a comparison for the data from Lake Koucha. Both of these aspects were taken up in the synthesis of this dissertation.

Regional setting

Lake Donggi Cona is situated on the northeastern margin of the Tibetan Plateau (35° 18' N, 98° 32' E, 4,090 m a.s.l.) and close to the present day summer monsoon limit (An et al., 2001). According to data from a climate station ca 50 km southeast of the lake, mean annual precipitation and air temperatures are 304 mm and -4.1 °C, respectively (Dietze et al., in review). It is an oligotrophic freshwater lake (specific conductivity 0.635 mS/cm) with oxygen supply down to the lake bottom and a mean pH of 8.6 (Mischke et al., 2009), with ice-cover from November to April and without distinct stratification due to full circulation (Dietze et al., in review). The lake, which has a maximum depth of 90 m, is fed by a perennial inflow from the northwestern shore (Fig. A.2) and some seasonal inflows from the north, east and south. An outflow channel at the western shore, which is controlled by a gauge station, discharges the lake towards the Qaidam Basin. The vegetation in the lake catchment consists mainly of alpine meadows dominated by Kobresia, Artemisia, and Poaceae (Kürschner et al., 2005) and a few *Salix* sp. growing on dunes on the alluvial plane in the east (Dietze et al., in review).

Materials and core chronology

Surface sediments samples where taken in summer 2006 with a sediment grabber (Fig. A.2). The sediment core PG1790 was drilled from ice-cover at 35° 20' N, 98° 26' W and in 35 m water depth (Fig A1) in February 2007 using an UWITEC coring system. The obtained core was 4.84 m long, with the upper 10 cm been lost during recovery. ^{14}C-AMS dating of TOC of the topmost sample of a short-core obtained from a position close to the PG1790 site yielded an age of 1983 years. A preliminary age model was derived from ^{14}C-AMS dating of thirteen samples throughout core PG1790, by correcting the ages of a potential reservoir effect of 1983 years before calibrating with CALIB (online version 5.1.beta, Reimer et al., 2004).

Results and discussion

n-Alkanes in surface sediments

Despite the large size of the lake, the *n*-alkanes show similar distribution patterns in almost all surface samples derived from different depths throughout the lake (Fig. A.2). A clear dominance

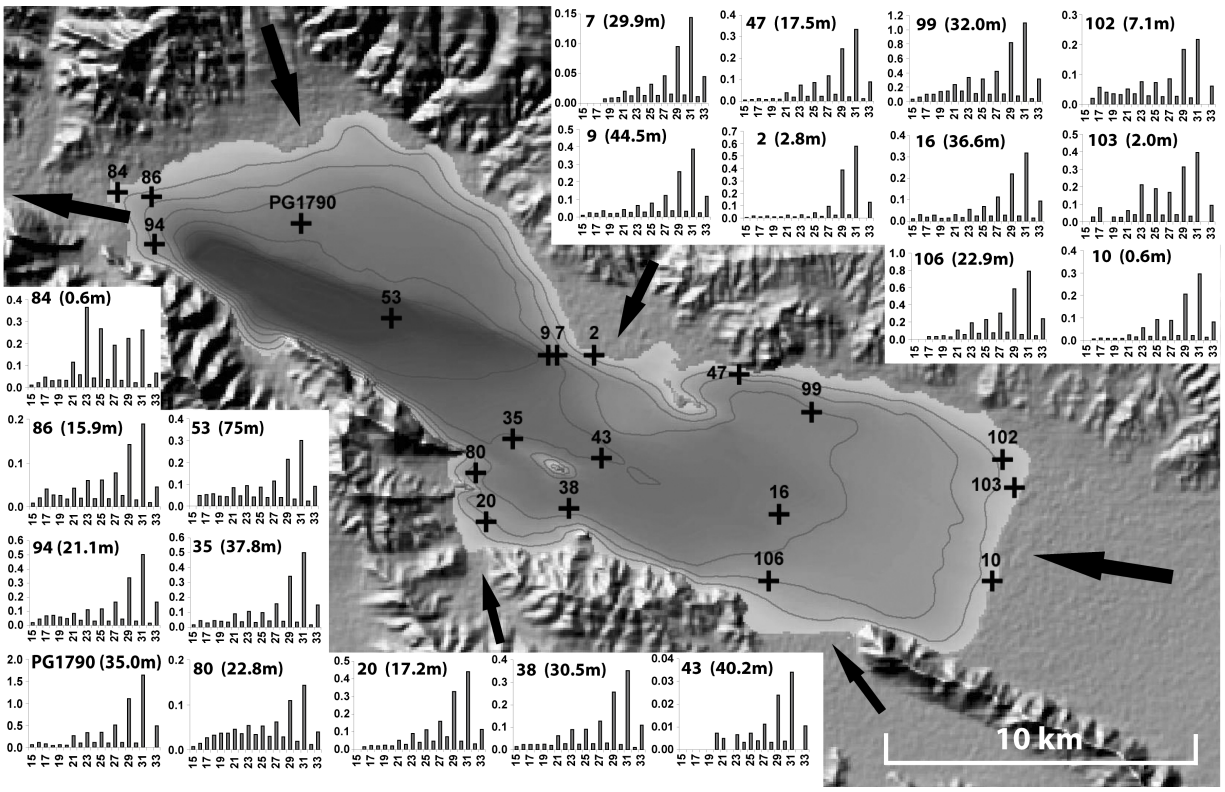

Figure A.2: *n*-Alkane patterns of surface samples and the top sample of sediment core PG1790 from Lake Donggi Cona and their respective depths and location in the lake. X-axes of histograms indicate carbon number of *n*-alkanes, y-axes show concentrations in µg/g d.w. Arrows in the map indicate inflows and outflows. The single perennial inflow enters the lake from the northwest. Distances between isobaths are 10 meters.

of long-chain *n*-alkanes nC_{29} and nC_{31} can be seen in all samples, except sample 84, which is situated in a depth of 0.6m close to the outflow and dominated by mid-chain *n*-alkanes nC_{23} and nC_{25}. The concentrations of *n*-alkanes range from 0.12 - 5.55 µg/g TOC (median: 1.37 µg/g d.w.). The *n*-alkane pattern probably reflects the vegetation around the lake which is dominated by alpine meadows. It is rather surprising that no higher concentrations of mid-chain *n*-alkanes were found, at least in samples from the shallower parts of the lakes, since aquatic macrophytes can be found in depths up to 30 meters (observations at field-trip in the year 2006). The submerged macrophyte vegetation consists mainly of *Chara* sp., and in the more shallow parts additionally of *Potamogeton pectinatus*. Samples of *Chara* sp. analysed for *n*-alkane concentrations contain very little concentrations of *n*-alkanes (manuscript I) and it is known that terrestrial plants and also emergent macrophytes produce 5 to 10 fold higher amounts of lipids than submerged macrophytes (manuscript I). Considering the very low concentrations of all *n*-alkanes in the lake, concentrations of terrestrial lipids might therefore easily exceed the concentrations of aquatic lipids. It has to be clarified by means of other proxies (e.g. organic petrology, pollen data or evaluation of other biomarker fractions of the sediment extract) whether the long-chain *n*-alkanes actually derived from terrestrial vegetation or from other sources such as *Botryococcus braunii* A race (Metzger and Largeau, 2005). The results indicate that lakes

as large as Donggi Cona can show similar *n*-alkane patterns throughout their sediment surface. This gives evidence that core PG1790 is representative for the whole lake with respect to the distribution pattern of *n*-alkanes and possibly of other biomarker groups.

Bulk proxies and *n*-alkanes in sediment core PG1790

Determined bulk parameter and *n*-alkane concentrations of samples from Lake Donggi Cona were presented in Fig. A.3. TOC and TN contents and *n*-alkane concentrations were low before ca. 13 cal ka BP, afterwards they gradually increased. Maximum TOC contents of ca 2% were reached at ca 10 cal ka BP and 8.2 cal ka BP. After the second maximum, the values dropped and especially after 6 cal ka BP gradually decreased to values below 1%. Total nitrogen contents show a more or less steady increase from values below the detection limit up to ca 0.2% at core top, only interrupted by a shift to slightly lower contents between ca. 4.5 and 2.0 cal ka BP. The concentration curve of the *n*-alkanes follows a similar trend. The *n*-alkane pattern is mostly dominated by long-chain homologues throughout the core. Only in two samples from the late glacial (ca 13 to 12 cal ka BP) mid-chain *n*-alkanes show higher abundances than long-chain homologues ($P_{aq} > 0.5$). The steady increase of long-chain *n*-alkanes while mid-chain *n*-alkanes dropped to lower concentrations after 10 cal ka BP, consequently leaded to a constant decrease of Paq since the early Holocene until ca 4.5 cal ka BP. The concentration curves of TOC and mid-chain *n*-alkanes with high values during the late glacial and early Holocene, possibly reflect the climate optimum during the early Holocene monsoon maximum. However, a TOC maximum during the 8.2 ka event is surprising. Evidence for this event comes from $\delta^{13}C_{TOC}$, which showed a drop of ca. 3‰ at ca. 8.5 cal ka BP. Generally, $\delta^{13}C_{TOC}$ varied within a relatively small range (-26 to -22‰) throughout the whole core and especially from ca 8 cal ka BP on, the values remained more or less stable at ca. -25‰.

It is not clear from the composition of the aliphatic fraction what the main factors influencing the TOC content from the late glacial to the present are. Significant amounts of short-chain *n*-alkanes, isoprenoid or hopanoid compounds, which could provide information about algal or microbial contributors to the organic matter, were not discovered. However, relatively high amounts of unsaturated nC_{23} and nC_{25} compounds (discussed below) were found in almost all samples in the core. The TOC content in Lake Donggi Cona might be controlled by biomass derived from aquatic macrophytes and other unknown contributors. Possibly, allochthonous lipids from the terrestrial realm are washed into the lake and therefore only enhance the lipid pool but not the bulk organic matter pool. However, as mentioned above, it has to be clarified, whether the increasing concentration of long-chain *n*-alkanes towards the top of the core represents a terrestrial signal. The low TOC/TN ratios in the upper part of the core would indicate the predominance of algae (Meyers, 2003), but TOC/TN ratios of the alga *Botryococcos braunii*, which are a possible source of long-chain *n*-alkanes have been reported to show relatively high TOC/TN ratios (Huang et al., 1999). Emergent macrophytes are also likely contributors to the sediments. Those have been shown to contain high concentrations of lipids while their TOC/TN ratio is relatively low (manuscript I). Nevertheless, due to the very low concentrations and the

more or less constant decrease of TN, the TOC/TN ratio reflects the TOC curve throughout the core and therefore should not been overvalued.

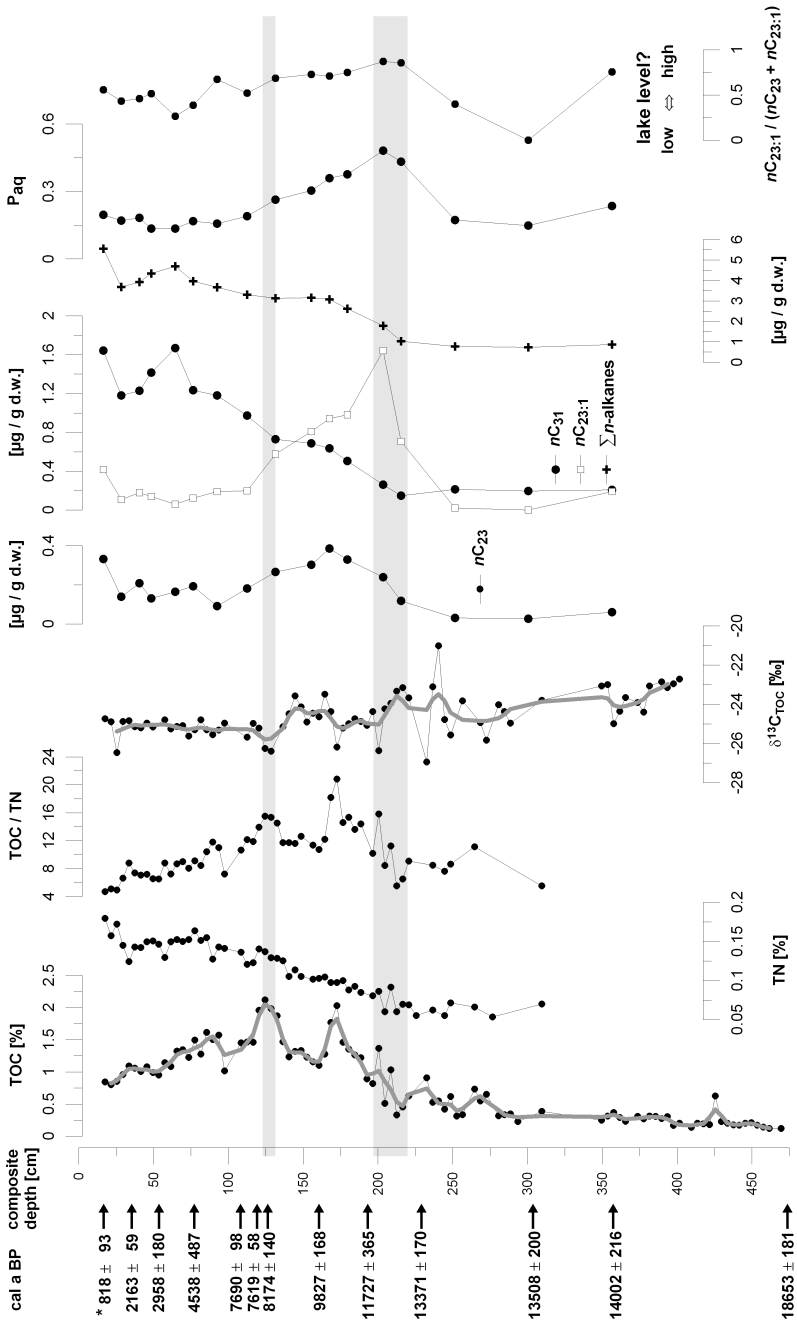

Figure A.3: Depth plot of bulk parameter, *n*-alkane and *n*-alkene concentrations and -ratios in sediment core PG1790 from Lake Donggi Cona. Note the different scales of concentrations of mid- and long-chain *n*-alkanes. Ages result from ^{14}C-AMS dating of TOC (except *: NaOH-soluble fraction). The ages were corrected for a potential reservoir effect of 1983 years (deduced from ^{14}C AMS dating of the uppermost sample of a short core). Shaded areas indicate timing of the Younger Dryas period and of the 8.2 ka event.

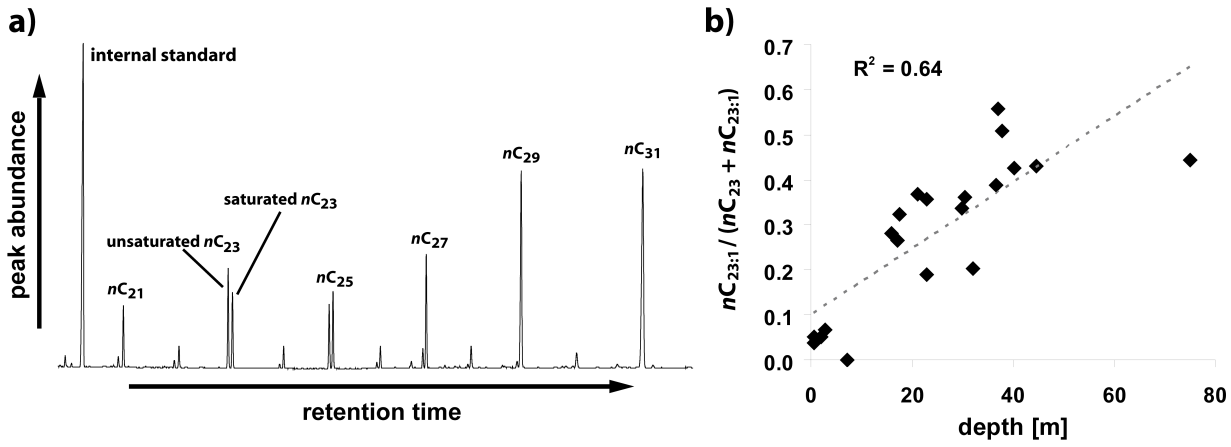

Figure A.4: (a) GC-FID chromatogram of a surface sample from location PG1790 showing the dominating *n*-alkanes and the highly abundant unsaturated compounds in the mid-chain range (C_{23} and C_{25} *n*-alkenes). (b) Ratios of unsaturated ($nC_{23:1}$) to saturated (nC_{23}) compound vs. sample depths

Unsaturated mid-chain compounds in lake Donggi Cona

All surface sediment and almost all sediment core samples show high abundances of unsaturated compounds, especially nC_{23} and nC_{25} *n*-alkenes (Fig. A.4a). The source of these compounds is unclear. In all known cases, higher abundances of unsaturated compounds in lakes were attributed to reeds and peats (Giger and Schaffner, 1977; Cardoso et al., 1983; Cranwell et al., 1987; Duan and Ma, 2001), sources which can be excluded for Lake Donggi Cona. Recently, Scherf and Rullkötter (2009) found odd-numbered unsaturated mid-chain compounds in microbial mats. Some algal species are also known to synthesize *n*-alkenes in the range C_{21} to C_{27} (Gelpi et al., 1970), which could be a possible source for these compounds in Donggi Cona sediments. Submerged macrophyte sources must also be taken into consideration. *Potamogeton* turned out to be a potential source of long-chain *n*-alkenes; however, the latter have never been detected in one of the corresponding sediments (manuscript I). It cannot be excluded that *Chara* sp., which are dominant in Donggi Cona, also synthesize unsaturated compounds under some circumstances but the *Chara* samples analysed from 0.8 and 2.8m water depths (manuscript I) did not show significant *n*-alkene concentrations. The ratio between the unsaturated and corresponding saturated compound (as shown for $nC_{23:1}$ / (nC_{23} + $nC_{23:1}$) in Fig. A.4b) is higher in surface samples derived from deeper parts of the lake. This does not necessarily imply that this ratio could be applied to assess lake level fluctuations when plotted for samples of a sediment core, especially as long as the source of the unsaturated compounds is not known. In Fig. A.3, this ratio is plotted versus age for the PG1790 sediment core and it can be seen that higher ratios were obtained during the late glacial and early Holocene. A higher lake level during the monsoonal maximum, when precipitation amounts were probably higher might be plausible. Nevertheless, the curve of this potential proxy should be compared with established proxies for lake level fluctuations such as ostracods (Mischke et al., 2009), and early results from these proxies do not seem to be in agreement with our data (Mischke, S., FU Berlin, personal communication). Further information

about previous lake level highstands is expected from dating results of terraces above the present day lake level.

Conclusion

First results from Lake Donggi Cona indicate a connection between the late glacial/early Holocene monsoon maximum and TOC contents as well as concentrations of mid-chain *n*-alkanes. A drop of TOC contents during the early Holocene might be attributed to a decrease of effective moisture, similar to Lake Koucha. This could be evaluated by the determination of δD values of $n\mathrm{C}_{23}$. However, low concentrations of mid-chain compounds probably will make it difficult to obtain reliable δD values throughout the core and fatty acids might be a good alternative, since these compounds usually are higher concentrated in sediments than *n*-alkanes. Concentrations of long-chain *n*-alkanes, which are the dominating homologues in almost all analysed samples, steadily increase from ca 13.0 cal ka until present days and it has to be clarified using other proxies, whether this rise can be attributed to an aquatic or a terrestrial source. A higher sample resolution of biomarker data is necessary to monitor short-term fluctuations. Further, the potential applicability of unsaturated compounds in the mid-chain range as a proxy for lake level fluctuations has to be tested by a comparison with inferences from established proxies.

References:

Cardoso JN, Gaskell SJ, Quirk MM, Eglinton G (1983). Hydrocarbons and fatty acid distributions in Rostherne Lake sediment (England). Chem. Geol. 38: 107-128.

Cranwell PA, Eglinton G, Robinson N (1987) Lipids of aquatic organisms as potential contributors to lacustrine sediments II. Org. Geochem. 11: 513-527

Dietze E, Wünnemann B, Diekmann B, Hartmann K, Aichner B, Herzschuh U, IJmker J, Jin H, Kopsch C, Lehmkul F, Li S, Mischke S, Opitz S, Yan S, Stauch G. Basin morphology and seismic stratigraphy of Lake Donggi Cona, north-eastern Tibetan Plateau, China. Quat. Int. in review

Duan Y, Ma L (2001). Lipid geochemistry in a sediment core from Ruoergai Marsh deposit (Eastern Qinghai-Tibet plateau, China). Org. Geochem 32: 1429-1442

Giger W, Schaffner C.(1977) Aliphatic, olefinic, and aromatic hydrocarbons in recent sediments of a highly eutrophic lake. In Advances in Organic Geochemistry 1975 (Edited by Campos R. and Goni J.), pp. 375-390. Enadimsa, Madrid.

Huang Y, Street-Perrott FA, Perrot RA, Metzger P, Eglinton G (1999) Glacial-interglacial environmental changes inferred from molecular and compound-specific δ^{13}C analyses of sediments from Sacred Lake, Mt. Kenya. Geochim. Cosmochim. Acta 63, 1383-1404.

Kürschner H, Herzschuh U, Wagner D (2005) Phytosociological studies in the northeastern Qinghai-Xizang Plateau (NW China) - A first contribution to the subalpine scrub and alpine meadow vegetation. Botanische Jahrbücher der Systematik 126, 273-315.

Meyers P (2003) Applications of Organic Geochemistry to paleolimnological reconstructions: a summary of examples from the Laurentian Great Lakes. Org. Geochem. 34, 261-289.

Mischke S, Bößneck U, Diekmann B, Herzschuh U, Jin H, Kramer A, Wünnemann, B, Zhang C (2009) Quantitative relationship between water-depth and sub-fossil ostracod assemblages in Lake Donggi Cona, Qinghai Province, China. J. Paleolimn. Online first (DOI 10.1007/s10933-009-9355-2).

Scherf AK, Rullkötter J (2009) Biogeochemistry of high salinity microbial mats – Part 1: Lipid composition of microbial mats across intertidal flats of Abu Dhabi, United Arab Emirates. Org. Geochem 40, 1018-1028

A.3 Parameter of lakes sampled for surface sediments

	location parameter			limnologic parameter			sediment parameter						plant parameter				
lake	altitude [m]	latitude [°N]	longitude [°E]	depth [m]	pH	el. conductivity [mS cm^{-1}]	TOC [%]	TOC/TN	ATR	P_{aq}	CPI (n_{23}-nC_{31})	$\delta^{13}C_{TOC}$ sediment [‰]	δ^{13}C bulk *Potamogeton* [‰]	δ^{13}C bulk *Myriophyllum* [‰]	δ^{13}C bulk *Batrachium* [‰]	δ^{13}C bulk *Hippuris* [‰]	δ^{13}C bulk *Charaphyceae* [‰]
CTP-02	4607	30.23	90.63	0.5	10.7	0.36	4.7	17.3	0.15	0.56	7.6	-20.7	-13.8	n.a.	n.a.	n.a.	n.a.
CTP-15	4637	31.99	90.35	0.5	9.6	9.06	1.2	8.8	0.10	0.15	6.4	-23.5	n.a.	n.a.	n.a.	n.a.	n.a.
CTP-19	4616	32.15	91.44	0.6	10.4	0.35	0.6	4.2	0.16	0.08	8.3	-24.9	n.a.	n.a.	n.a.	n.a.	n.a.
CTP-20	4724	32.10	89.53	0.4	10.4	0.23	5.2	16.5	0.13	0.39	12.5	-16.0	-7.9	n.a.	n.a.	n.a.	n.a.
CTP-25	5133	32.57	91.86	0.4	8.5	0.20	6.8	16.8	0.20	0.67	6.7	-21.4	n.a.	n.a.	n.a.	n.a.	n.a.
CTP-35	4701	34.16	95.98	2.1	9.1	0.65	9.1	11.7	0.07	0.34	8.6	-29.0	-18.1	n.a.	n.a.	n.a.	n.a.
CTP-39	4545	34.04	97.22	0.3	8.4	0.35	3.3	13.0	0.07	0.41	5.4	-25.8	n.a.	n.a.	n.a.	n.a.	n.a.
Koucha	4541	34.02	97.22	6.0	9.1	0.50	12.5	7.3	0.32	0.48	6.5	-22.1	-8.8	n.a.	n.a.	-25.5	n.a.
Donggi	4095	35.23	98.65	35.0	7.9	0.70	0.8	4.7	0.07	0.20	8.8	-24.7	-5.8	n.a.	n.a.	n.a.	-13.1
GA-01	3485	34.24	102.33	0.8	9.7	0.14	12.2	35.9	0.22	0.62	4.0	-21.5	n.a.	n.a.	n.a.	n.a.	n.a.
LC-02	5001	29.79	92.39	4.9	7.3	0.04	8.0	5.3	0.15	0.47	6.6	-21.3	n.a.	n.a.	-9.9	n.a.	-19.3
LC-05	4050	29.81	94.43	38.0	8.0	0.01	1.4	5.8	0.06	0.40	6.1	-27.0	n.a.	n.a.	n.a.	n.a.	n.a.
LC-06	4132	29.83	94.46	23.0	7.0	0.01	4.9	10.4	0.06	0.41	7.9	-27.1	n.a.	n.a.	n.a.	n.a.	n.a.
LC-10	4431	29.65	96.72	0.5	7.7	0.11	1.2	6.6	0.14	0.64	4.1	-20.8	-15.4	-16.9	n.a.	n.a.	n.a.
MiY-21	4332	35.04	97.39	0.1	9.9	3.91	4.1	12.4	0.21	0.45	9.2	-19.4	-12.4	n.a.	n.a.	n.a.	n.a.
MiY-22	4341	35.05	97.39	0.4	9.9	2.80	3.7	10.0	0.11	0.28	4.7	-18.5	-8.3	n.a.	n.a.	n.a.	n.a.
MiY-28	4257	35.03	98.05	0.5	9.5	0.61	1.4	9.2	0.35	0.55	7.2	-18.0	-12.1	n.a.	n.a.	n.a.	n.a.
MiY-29	4256	34.99	98.08	0.3	10.1	3.60	0.9	7.8	0.25	0.32	6.8	-20.6	-14.7	n.a.	n.a.	n.a.	n.a.
MiY-30	4247	34.97	98.10	0.4	9.9	8.96	0.9	8.0	0.11	0.33	8.7	-20.4	-10.8	n.a.	n.a.	n.a.	n.a.
MiY-35	4241	34.74	98.11	0.2	10.2	1.81	13.1	27.9	0.20	0.66	5.4	-18.4	-6.0	n.a.	n.a.	n.a.	n.a.
MiY-38	4240	34.87	98.17	0.2	9.4	22.72	1.1	7.5	0.10	0.20	7.6	-21.3	-13.6	n.a.	n.a.	n.a.	n.a.
MiY-39	4581	33.99	97.46	0.4	10.5	1.85	10.4	22.4	0.04	10.5	6.6	-19.3	-7.4	n.a.	n.a.	n.a.	n.a.
MiY-40	4581	34.00	97.47	1.0	10.2	0.21	11.9	20.8	0.34	0.59	5.7	-19.6	-12.3	n.a.	n.a.	n.a.	n.a.
MiY-42	4617	34.03	97.55	0.5	10.4	0.21	13.2	23.3	0.07	0.50	5.1	-21.8	-16.1	-16.7	-17.7	-26.5	n.a.
MiY-44	4740	34.25	97.85	0.4	9.3	0.40	10.9	11.5	0.03	0.63	8.1	-24.6	-12.0	n.a.	-12.0	n.a.	n.a.
MiY-46	4233	34.68	98.06	0.5	10.8	0.59	2.9	9.8	0.35	0.39	4.6	-21.6	-11.3	n.a.	n.a.	n.a.	n.a.
MiY-53	4267	34.92	98.52	1.2	10.6	2.14	1.4	8.4	0.33	0.34	4.4	-21.4	-12.4	n.a.	n.a.	n.a.	n.a.
NB-01	4030	33.38	101.10	45.0	8.1	0.04	4.1	5.8	0.11	0.40	4.4	-24.6	n.a.	n.a.	n.a.	n.a.	n.a.
Qai-02	3205	37.04	100.58	7.0	9.2	41.30	11.5	17.1	0.31	0.12	11.3	-25.9	n.a.	n.a.	n.a.	n.a.	n.a.
Qai-06	2812	37.29	96.89	6.8	8.5	1.05	7.3	12.6	0.22	0.65	12.6	-20.2	n.a.	n.a.	n.a.	n.a.	n.a.
S-10	4066	33.23	101.02	28.9	7.8	0.05	3.0	8.7	0.05	0.39	8.0	-26.2	n.a.	n.a.	n.a.	n.a.	n.a.
S-13	4307	33.22	101.12	39.9	8.0	0.03	2.8	8.5	0.08	0.32	4.3	-28.1	n.a.	n.a.	n.a.	n.a.	n.a.
S-16	4220	31.11	99.76	36.7	8.1	0.05	5.0	8.5	0.09	0.52	4.7	-27.9	n.a.	n.a.	n.a.	n.a.	n.a.
S-22	4610	33.35	96.07	2.8	9.9	0.19	6.1	12.8	0.09	0.47	4.9	-20.0	-14.2	-9.7	n.a.	n.a.	-16.8
S-26	2668	36.18	100.11	0.3	9.8	1.97	1.1	8.1	0.12	0.38	5.5	-21.8	-16.6	-14.3	n.a.	-26.4	n.a.
SET 15	2189	26.49	99.92	3.2	8.6	0.24	15.3	14.0	0.25	0.35	5.8	-21.9	n.a.	n.a.	n.a.	n.a.	n.a.
SET 16	1967	25.92	100.12	5.0	9.0	0.21	23.7	16.6	0.52	0.60	6.5	-18.2	n.a.	n.a.	n.a.	n.a.	n.a.
SET 19	1620	25.68	100.65	9.7	9.3	0.24	0.5	5.0	0.35	0.32	7.0	-24.5	n.a.	n.a.	n.a.	n.a.	n.a.
SET 21	2746	27.73	100.74	0.5	7.3	0.11	5.9	13.6	0.15	0.57	4.5	-25.3	n.a.	n.a.	n.a.	n.a.	n.a.
SET 25	1500	27.82	102.29	12.7	8.4	0.25	1.4	6.5	0.18	0.37	6.4	-27.7	n.a.	n.a.	n.a.	n.a.	n.a.

Appendix 3: Location, limnologic, sediment and plant parameter of sampled lakes. n.a. = no sample available

A.4 *n*-Alkane concentrations in plants

lake	species	*n*-alkane [µg / g d.w.]																					sum
		C_{15}	C_{16}	C_{17}	C_{18}	C_{19}	C_{20}	C_{21}	C_{22}	C_{23}	C_{24}	C_{25}	C_{26}	C_{27}	C_{28}	C_{29}	C_{30}	C_{31}	C_{32}	C_{33}	
S-22	*Potamogeton*	0.3	0.3	0.6	0.7	1.8	1.2	6.3	1.7	24.4	2.0	14.1	1.2	9.2	0.7	5.1	0.5	1.3	0.0	0.0	71
S-22	*Myriophyllum*	0.4	0.5	0.7	0.7	1.1	1.1	3.3	2.4	18.4	6.0	11.9	1.1	3.0	0.5	1.3	0.0	0.0	0.0	0.0	53
S-22	*Chara*	0.3	0.6	1.2	1.3	1.9	2.3	3.7	2.1	8.2	1.9	6.4	1.1	5.1	0.9	1.8	0.0	0.0	0.0	0.0	39
S-26	*Potamogeton*	0.0	0.5	3.5	1.9	3.2	3.2	6.0	3.3	21.7	3.4	30.1	2.1	18.1	1.6	20.2	1.2	11.8	0.0	0.0	132
S-26	*Myriophyllum*	0.0	0.0	1.4	1.9	2.9	3.5	6.6	5.0	36.5	10.4	42.5	2.7	8.2	1.3	6.9	0.0	3.7	0.0	0.0	133
S-26	*Hippuris*	0.0	0.0	0.0	1.8	2.4	3.0	5.0	4.3	10.1	4.4	20.1	6.3	162.8	34.9	581.2	11.0	48.3	0.0	0.0	896
Kou-Cha	*Potamogeton*	0.2	0.7	2.0	2.0	5.2	2.8	9.1	3.2	51.8	3.8	30.8	2.5	15.0	1.9	12.7	1.3	5.2	0.0	0.0	150
Kou-Cha	*Hippuris*	0.0	0.0	1.3	1.8	2.3	2.2	2.4	1.5	5.3	2.3	12.9	3.6	116.7	14.2	324.9	3.8	28.0	0.0	0.0	523
Donggi	*Potamogeton*	0.0	0.2	0.7	0.7	1.3	2.0	5.2	2.0	39.0	1.7	23.8	0.6	10.8	0.5	10.1	0.0	4.3	0.0	0.0	103
CTP-35	*Potamogeton*	0.0	0.0	4.2	2.7	3.3	2.4	7.4	2.5	37.1	3.3	30.0	1.5	15.2	1.1	12.6	0.0	4.8	0.0	0.0	128
MiY-42	*Batrachium*	0.9	2.2	6.6	7.4	8.1	4.4	6.2	2.9	13.0	3.3	12.6	3.7	41.3	6.7	79.7	3.2	19.0	1.2	1.6	224
MiY-42	*Hippuris*	1.1	2.8	5.9	5.9	7.2	3.2	4.0	2.2	12.3	3.5	24.0	6.5	167.9	27.4	589.0	8.9	63.7	1.5	2.9	940
LC-10	*Potamogeton*	0.4	0.7	1.8	1.5	4.0	1.1	12.8	1.1	13.5	1.6	16.9	1.8	10.8	2.3	6.8	0.9	1.3	0.2	0.0	80
CTP-20	*Potamogeton*	0.3	0.3	0.8	0.7	0.8	0.4	2.3	0.6	12.1	0.9	11.8	0.4	3.2	0.3	2.8	0.2	1.2	0.1	0.0	39
Ga-01	*Chara*	0.0	0.0	2.0	2.2	3.2	4.6	6.5	4.0	11.2	4.0	11.1	3.1	13.5	2.7	6.2	0.0	0.0	0.0	0.0	74

Appendix 4: Concentrations of *n*-alkanes [µg/g d.w.] in macrophyte and macroalgae samples

A.5 *n*-Alkane concentrations in surface sediments

	n-alkane																			
lake	C_{15}	C_{16}	C_{17}	C_{18}	C_{19}	C_{20}	C_{21}	C_{22}	C_{23}	C_{24}	C_{25}	C_{26}	C_{27}	C_{28}	C_{29}	C_{30}	C_{31}	C_{32}	C_{33}	sum
CTP-02	0.02	0.03	0.05	0.03	0.04	0.03	0.14	0.05	0.43	0.05	0.35	0.05	0.26	0.05	0.33	0.03	0.29	0.02	0.09	2.3
CTP-15	0.01	0.02	0.08	0.03	0.02	0.01	0.02	0.02	0.05	0.05	0.13	0.05	0.20	0.05	0.43	0.05	0.61	0.02	0.20	2.1
CTP-19	0.05	0.09	0.19	0.09	0.08	0.04	0.05	0.04	0.07	0.04	0.09	0.04	0.21	0.07	0.56	0.06	1.16	0.05	0.54	3.5
CTP-20	0.04	0.07	0.13	0.07	0.06	0.05	0.17	0.08	0.50	0.04	0.46	0.03	0.28	0.04	0.53	0.05	1.00	0.05	0.31	3.9
CTP-25	0.07	0.06	0.18	0.07	0.12	0.18	0.74	0.56	1.74	0.27	1.31	0.13	0.75	0.09	0.74	0.07	0.78	0.05	0.19	8.1
CTP-35	0.35	0.34	0.85	0.37	0.53	0.53	2.12	1.27	6.05	1.42	6.53	0.91	4.40	0.79	9.14	0.81	15.07	0.49	3.62	55.6
CTP-39	0.02	0.03	0.10	0.05	0.07	0.09	0.31	0.27	0.96	0.27	0.95	0.27	1.06	0.24	1.59	0.12	1.16	0.07	0.33	8.0
Koucha	0.00	0.77	3.12	0.82	0.96	0.71	1.30	0.77	4.22	0.83	3.75	0.57	2.45	0.83	3.78	0.39	4.89	0.00	1.31	31.5
Donggi	0.06	0.10	0.08	0.04	0.06	0.05	0.26	0.10	0.33	0.11	0.34	0.10	0.51	0.10	1.10	0.09	1.64	0.00	0.49	5.6
GA-01	0.03	0.06	0.08	0.09	0.08	0.06	0.14	0.08	0.49	0.11	0.60	0.14	0.46	0.15	0.34	0.08	0.34	0.09	0.14	3.6
LC-02	0.08	0.17	1.17	0.29	0.55	0.47	2.47	0.79	4.30	0.78	4.96	0.82	4.56	0.74	5.44	0.59	5.00	0.66	2.01	35.8
LC-05	0.05	0.08	0.12	0.10	0.16	0.19	0.66	0.46	1.29	0.55	2.52	0.49	2.47	0.34	2.54	0.24	3.10	0.21	1.44	17.0
LC-06	0.15	0.26	0.44	0.26	0.58	0.85	3.13	0.99	5.49	1.06	7.23	1.06	7.71	1.04	8.25	0.88	9.73	0.72	4.01	53.8
LC-10	0.00	0.01	0.06	0.04	0.06	0.07	0.13	0.15	0.53	0.19	0.74	0.16	0.53	0.13	0.36	0.05	0.36	0.05	0.16	3.8
MiY-21	0.05	0.13	0.14	0.09	0.04	0.06	0.08	0.03	0.34	0.05	0.37	0.03	0.20	0.03	0.36	0.05	0.50	0.04	0.17	2.7
MiY-22	0.09	0.20	0.26	0.17	0.14	0.26	0.23	0.16	0.68	0.30	0.90	0.46	0.88	0.29	1.67	0.20	2.46	0.16	1.12	10.6
MiY-28	0.04	0.23	0.14	0.23	0.04	0.07	0.07	0.07	0.23	0.05	0.25	0.04	0.18	0.02	0.20	0.01	0.19	0.01	0.03	2.1
MiY-29	0.05	0.08	0.12	0.13	0.05	0.06	0.08	0.03	0.15	0.03	0.16	0.03	0.18	0.05	0.28	0.03	0.36	0.02	0.12	2.0
MiY-30	0.06	0.08	0.10	0.10	0.06	0.06	0.13	0.08	0.37	0.06	0.45	0.06	0.44	0.07	0.74	0.07	0.93	0.06	0.28	4.2
MiY-35	0.06	0.12	0.39	0.12	0.13	0.07	0.38	0.20	2.39	0.40	2.24	0.52	1.15	0.30	1.31	0.14	1.04	0.10	0.27	11.3
MiY-38	0.00	0.12	0.10	0.08	0.04	0.04	0.05	0.03	0.14	0.04	0.19	0.04	0.21	0.07	0.53	0.06	0.79	0.03	0.25	2.8
MiY-39	0.01	0.03	0.04	0.02	0.06	0.04	0.37	0.20	1.08	0.19	0.94	0.20	0.77	0.16	1.03	0.11	1.46	0.09	0.47	7.2
MiY-40	0.33	0.40	0.80	0.87	0.32	0.33	0.47	0.36	1.49	0.42	2.59	0.34	1.26	0.21	1.38	0.20	1.45	0.19	0.57	14.0
MiY-42	0.19	0.29	0.40	0.29	0.34	0.40	1.86	1.53	5.87	1.46	6.26	1.44	3.77	0.91	4.69	0.64	7.52	0.60	2.41	40.9
MiY-44	0.00	0.00	0.02	0.00	0.00	0.01	0.09	0.07	0.41	0.09	0.52	0.05	0.19	0.02	0.20	0.01	0.35	0.00	0.04	2.1
MiY-46	0.22	0.68	0.39	0.85	0.23	0.29	0.22	0.15	0.46	0.12	0.54	0.09	0.39	0.09	0.62	0.24	0.92	0.05	0.28	6.8
MiY-53	0.09	0.56	0.21	0.49	0.08	0.12	0.08	0.05	0.18	0.06	0.24	0.07	0.19	0.08	0.33	0.06	0.46	0.05	0.16	3.6
NB-01	0.07	0.12	0.13	0.15	0.14	0.11	0.34	0.25	0.76	0.28	0.99	0.29	1.17	0.31	1.18	0.18	1.47	0.19	0.54	8.7
Qai-02	0.40	0.71	1.36	0.28	0.22	0.11	0.12	0.11	0.23	0.10	0.38	0.03	0.83	0.16	2.04	0.14	2.36	0.07	0.47	10.1
Qai-06	0.12	0.29	0.57	0.41	0.36	0.25	0.49	0.33	3.71	0.22	3.29	0.19	1.81	0.28	2.32	0.14	1.47	0.05	0.31	16.6
S-10	0.02	0.03	0.02	0.03	0.03	0.06	0.14	0.08	0.35	0.08	0.57	0.09	0.72	0.07	0.63	0.07	0.79	0.06	0.28	4.1
S-13	0.12	0.15	0.12	0.12	0.15	0.14	0.45	0.32	0.91	0.47	1.27	0.54	1.39	0.39	2.01	0.25	2.61	0.16	0.85	12.4
S-16	0.06	0.09	0.12	0.10	0.19	0.27	0.91	0.49	1.80	0.62	2.26	0.56	2.14	0.34	1.91	0.26	1.83	0.20	0.66	14.8
S-22	0.06	0.12	0.35	0.12	0.14	0.16	0.64	0.53	2.36	0.72	2.57	0.62	1.96	0.62	2.32	0.29	3.27	0.09	1.03	18.0
S-26	0.04	0.09	0.16	0.09	0.07	0.04	0.14	0.06	0.45	0.18	0.73	0.22	0.71	0.15	1.11	0.09	0.82	0.04	0.23	5.4
SET 15	0.06	0.06	0.12	0.05	0.08	0.03	0.10	0.04	0.28	0.04	0.15	0.05	0.23	0.06	0.38	0.06	0.41	0.05	0.18	2.4
SET 16	0.10	0.05	0.31	0.16	0.34	0.09	0.11	0.05	0.35	0.07	0.71	0.08	0.51	0.08	0.47	0.04	0.23	0.12	0.10	3.9
SET 19	0.04	0.04	0.10	0.04	0.04	0.02	0.10	0.02	0.11	0.01	0.04	0.01	0.06	0.02	0.13	0.02	0.18	0.02	0.10	1.1
SET 21	0.05	0.06	0.14	0.07	0.09	0.08	0.23	0.19	0.90	0.34	1.14	0.24	1.11	0.18	0.86	0.12	0.67	0.11	0.35	7.0
SET 25	0.03	0.03	0.01	0.02	0.04	0.02	0.05	0.02	0.12	0.02	0.06	0.02	0.10	0.02	0.16	0.02	0.16	0.00	0.08	1.0

Appendix 5: Concentrations of *n*-alkanes [µg/g d.w.] in sediment samples

A.6 GC-MS spectra

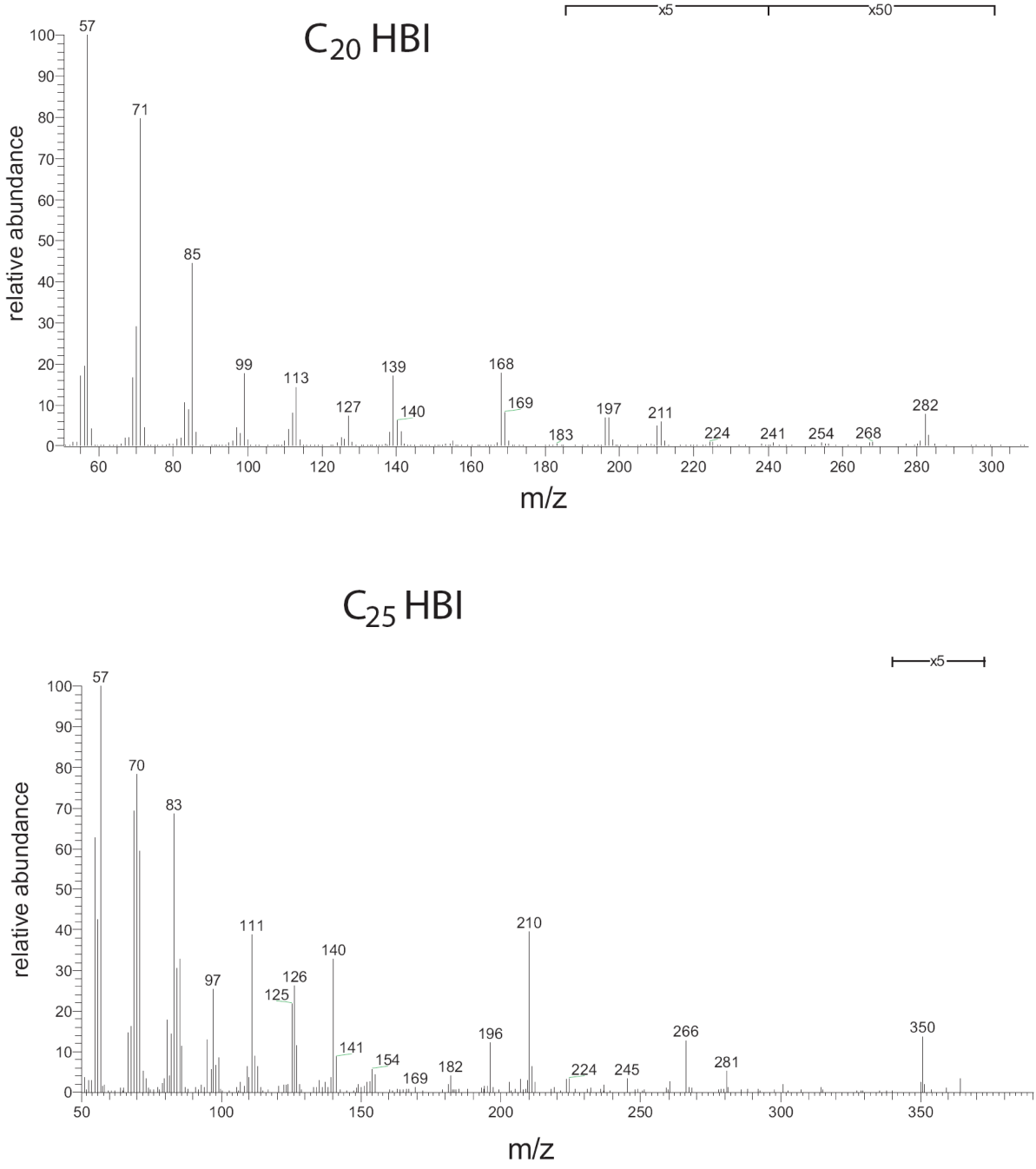

Appendix 6a) GC-MS spectra of C_{20} HBI and C_{25} HBI

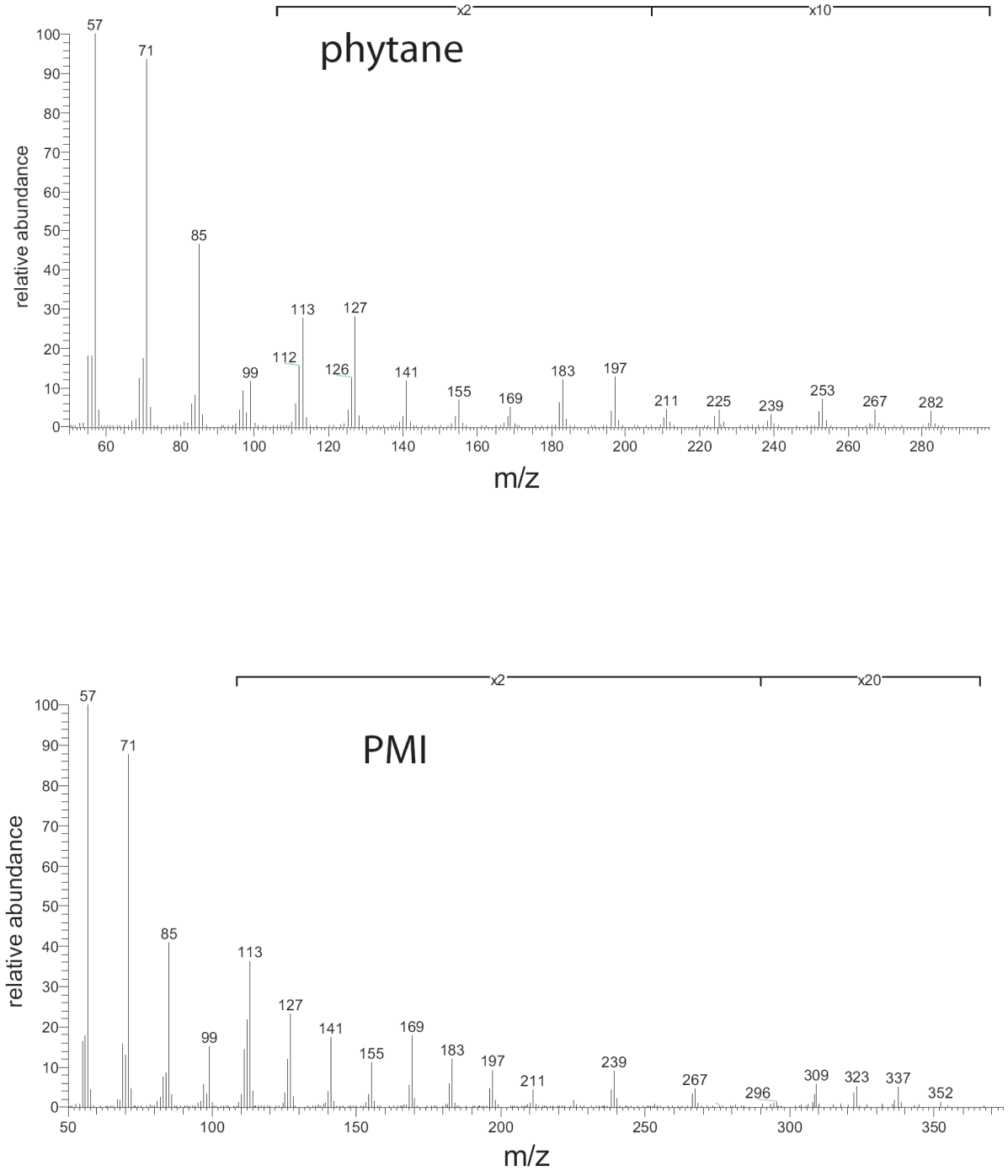

Appendix 6b) GC-MS spectra of phytane and PMI

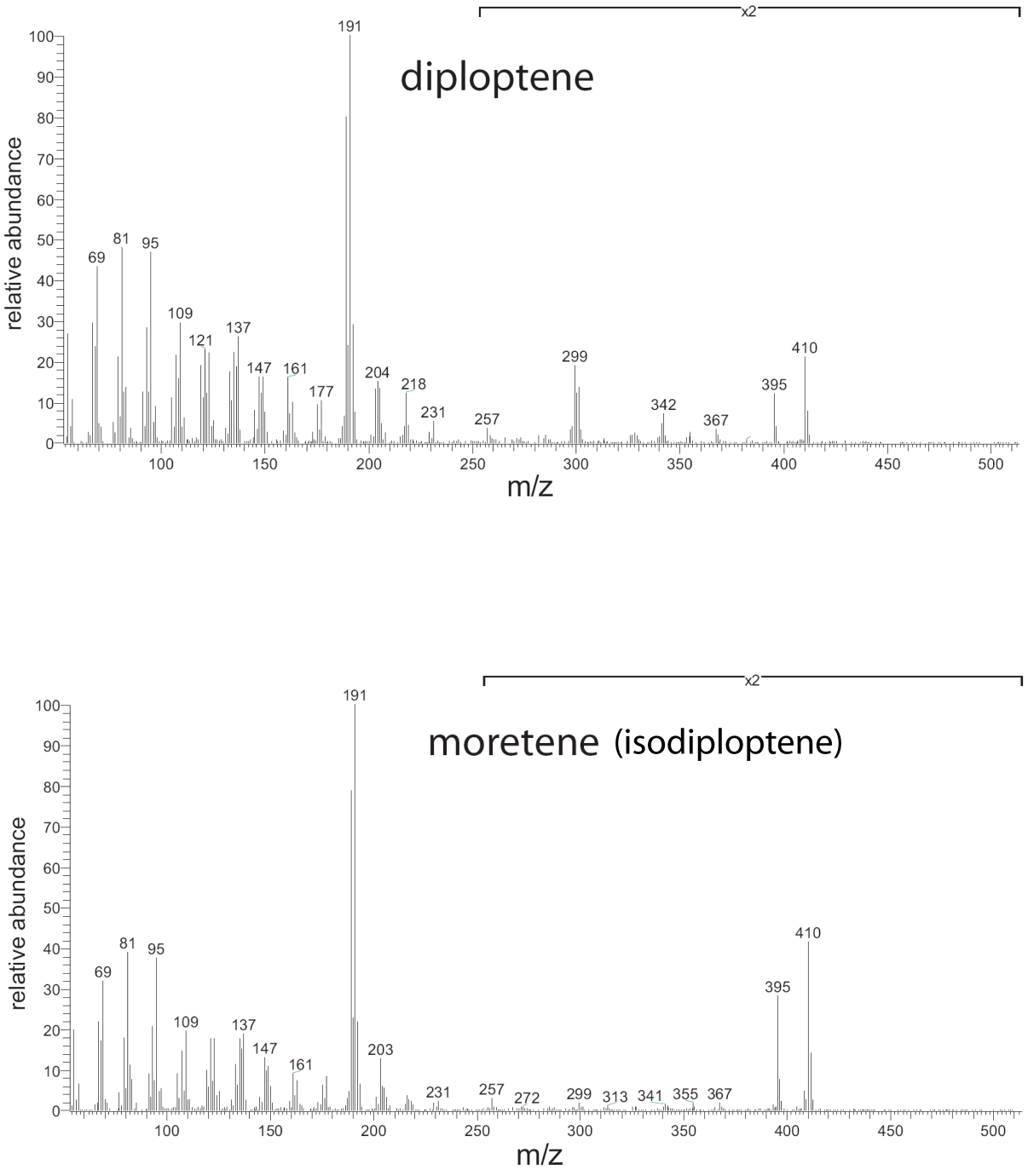

Appendix 6c) GC-MS spectra of diploptene and moretene

Acknowledgements

Finally I want to thank

- first of all my supervisors Prof. Dr. Ulrike Herzschuh at AWI Potsdam and University of Potsdam and PD Dr. Heinz Wilkes at GFZ Potsdam, who supported and guided me with their valuable motivation, constructive feedback and fruitful discussions during the time of research for this dissertation
- the head of the AWI Potsdam research department Prof. Hans-Wolfgang Hubberten for the opportunities to use the infrastructure of the institute and to attend national and international conferences, and for accommodating my PhD-project here at the institute
- the lab and administrative staff at AWI Potsdam for help in administrative, logistical and technical questions: Christine Litz, Kathrin Klein, Sigrun Gräning, Antje Eulenburg, Ute Bastian, Gerald Müller, Lutz Schoenicke, Heiko Gericke, Tobias Schmidt and Gabriela Schlaffer
- the lab and administrative staff of the Organic Geochemistry section of GFZ Potsdam, Anke Sobotta, Cornelia Karger, Kristin Günther, Michael Gabriel, Doreen Noack and Claudia Röhl for support and help with any kind of problem
- all people at the AWI Potsdam and the Organic Geochemistry section of GFZ Potsdam for the friendly atmosphere
- Steffen Mischke (FU Berlin), Kai Mangelsdorf (GFZ Potsdam), Dirk Sachse (FU Berlin), Bernhard Diekmann (AWI Potsdam), Hanno Meyer (AWI Potsdam), Andrea Vieth (GFZ Potsdam) and Ann-Kathrin Scherf (GFZ Potsdam) for scientific discussions and having an open ear to my questions
- Kirsten Rempel, Allison Bryan and Wang Yongbo for proof-reading
- my family and friends for helping me get my mind off and for support and encouragement
- Johanna Wittig for proof-reading, for 50,000 travel miles (approximately) during the last 3 years and for her overall support